PROGRESS IN BIOMEDICAL OPTICS

Proceedings of

Laser and Noncoherent Ocular Effects: Epidemiology, Prevention, and Treatment

Bruce E. Stuck
Michael Belkin, M.D.
Chairs/Editors

Abraham Katzir
Biomedical Optics Series Editor

10–11 February 1997
San Jose, California

Sponsored by
Air Force Office of Scientific Research
IBOS—The International Biomedical Optics Society
SPIE—The International Society for Optical Engineering

Volume 2974

REPORT DOCUMENTATION PAGE

Form Approved
OMB No. 0704-0188

1. AGENCY USE ONLY *(Leave blank)*	2. REPORT DATE	3. REPORT TYPE AND DATES COVERED

4. TITLE AND SUBTITLE
Laser and nonocoherent ocular effects : epidemiology, prevention, and treatment : proceedings.

5. FUNDING NUMBERS

6. AUTHOR(S)
Bruce E. Stuck and Michael Belkin, editors.
Abraham Katzir, Series editor

7. PERFORMING ORGANIZATION NAME(S) AND ADDRESS(ES)

8. PERFORMING ORGANIZATION REPORT NUMBER

9. SPONSORING / MONITORING AGENCY NAME(S) AND ADDRESS(ES)
Air Force Office of Scientific Research
IBOS - The International Biomedical Optics Society
SPIE - The International Society for Optical Engineering
Cooperating Organization - American Society for Laser Medicine & Surgery, Inc.

19. SPONSORING / MONITORING AGENCY REPORT NUMBER

11. SUPPLEMENTARY NOTES
San Jose, California , 10-11 February 1997
Series : Progress in Biomedial Optics, v. 2974

12a. DISTRIBUTION / AVAILABILITY STATEMENT
APPROVED FOR PUBLIC RELEASE : distribution unlimited

12b. DISTRIBUTION CODE

13. ABSTRACT *(Maximum 200 words)*

The spread of laser instruments to many fields of human activity and the potential of laser radiation to produce biological damage make certain that laser accidents leading to human injuries will occur. Laser radiation is especially liable to cause accidents since it may be projected over long distahces, is often used in the open space, and is sometimes invisible.

The potential of laser instruments to be harmful was realized quite early on in their development, and stringent rules were imposed in most countries to minimize injuries. Those regulations are obviously effective since laser injuries are as yet uncommon and the reported cases number only in the hundreds. However, more accidental laser-inflicted traumata are expected in the future as more people are potentially exposed.

The situation is especially grave in the military where lasers constitute parts of weapon systems to be used outdoors and are necessarily directed at other people. The hazards are even greater when the potential victims are using collecting optics. The facts regarding laser injuries are well known enough for some military planners to develop laser weapons aimed at producing visual incapacitation of the enemy. Some of these systems have been fielded and used. These potential weapons are based on the fact that the eye is the body organ most vulnerable to laser radiation, especially in the visible and near-infrared wavelengths. This vulnerability is a result of the eye's dioptric apparatus focusing the light on the retina, thus increasing the energy concentration many thousandfold. Consequently, almost all of the laser accidents reported thus far involved ocular, mainly retinal, damage.

14. SUBJECT TERMS	15. NUMBER OF PAGES
Biomedical optics, laser	232
	16. PRICE CODE

17. SECURITY CLASSIFICATION OF REPORT	18. SECURITY CLASSIFICATION OF THIS PAGE	19. SECURITY CLASSIFICATION OF ABSTRACT	20. LIMITATION OF ABSTRACT

Enclosure 3

PROGRESS IN BIOMEDICAL OPTICS

Proceedings of

Laser and Noncoherent Ocular Effects: Epidemiology, Prevention, and Treatment

Bruce E. Stuck
Michael Belkin, M.D.
Chairs/Editors

Abraham Katzir
Biomedical Optics Series Editor

10–11 February 1997
San Jose, California

Sponsored by
Air Force Office of Scientific Research
IBOS—The International Biomedical Optics Society
SPIE—The International Society for Optical Engineering

Cooperating Organization
American Society for Laser Medicine and Surgery, Inc.

Published by
SPIE—The International Society for Optical Engineering

Volume 2974

The papers appearing in this book comprise the proceedings of the meeting mentioned on the cover and title page. They reflect the authors' opinions and are published as presented and without change, in the interests of timely dissemination. Their inclusion in this publication does not necessarily constitute endorsement by the editors or by SPIE.

Please use the following format to cite material from this book:
Author(s), "Title of paper," in *Laser and Noncoherent Ocular Effects: Epidemiology, Prevention, and Treatment,* Bruce E. Stuck, Michael Belkin, M.D., Editors, Proceedings of SPIE Vol. 2974, page numbers (1997).

ISSN 0277-786X
ISBN 0-8194-2385-8

Published by
SPIE—The International Society for Optical Engineering
P.O. Box 10, Bellingham, Washington 98227-0010 USA
Telephone 360/676-3290 (Pacific Time) • Fax 360/647-1445

Printed in the United States of America.

Contents

Conference Committee

Conference Chairs

Bruce E. Stuck, Walter Reed Army Institute of Research
Michael Belkin, M.D., Tel Aviv University Goldschleger Eye Research Institute (Israel)

Program Committee

Donald A. Gagliano, M.D., Walter Reed Army Institute of Research
Randolph D. Glickman, University of Texas Health Science Center at San Antonio
James B. Sheehy, Naval Air Development Center
Harry Zwick, Walter Reed Army Institute of Research
Jon D. Masso, AOtec, Inc.
Elmar T. Schmeisser, University of Kentucky
David J. Lund, Walter Reed Army Institute of Research
David O. Robbins, Ohio Wesleyan University
David H. Sliney, U.S. Army Environmental Hygiene Agency
Steven T. Schuschereba, Walter Reed Army Institute of Research
Gary T. Forrest, SensorPhysics, Inc.
Joseph A. Zuclich, The Analytic Sciences Corporation
Penny J. Smalley, R.N., Technology Concepts International

Session Chair

Laser Safety in Medicine
Penny J. Smalley, R.N., Technology Concepts International

Introduction

The spread of laser instruments to many fields of human activity and the potential of laser radiation to produce biological damage make certain that laser accidents leading to human injuries will occur. Laser radiation is especially liable to cause accidents since it may be projected over long distances, is often used in the open space, and is sometimes invisible.

The potential of laser instruments to be harmful was realized quite early on in their development, and stringent rules were imposed in most countries to minimize injuries. Those regulations are obviously effective since laser injuries are as yet uncommon and the reported cases number only in the hundreds. However, more accidental laser-inflicted traumata are expected in the future as more people are potentially exposed.

The situation is especially grave in the military where lasers constitute parts of weapon systems to be used outdoors and are necessarily directed at other people. The hazards are even greater when the potential victims are using collecting optics. The facts regarding laser injuries are well known enough for some military planners to develop laser weapons aimed at producing visual incapacitation of the enemy. Some of these systems have been fielded and used. These potential weapons are based on the fact that the eye is the body organ most vulnerable to laser radiation, especially in the visible and near-infrared wavelengths. This vulnerability is a result of the eye's dioptric apparatus focusing the light on the retina, thus increasing the energy concentration many thousandfold. Consequently, almost all of the laser accidents reported thus far involved ocular, mainly retinal, damage.

The SPIE conference was a unique opportunity for people of all spheres of the laser world to exchange data and opinions in this multidisciplinary, rapidly expanding field. The conference focused its attention on the extent of the problem of laser-inflicted eye injuries, methods to minimize the occurrence of laser-related accidents, and developing currently nonexistent methods of therapy. Almost all relevant aspects were covered in the conference, including means of diagnosing and quantifying laser eye injuries, detailed descriptions of cases, the mechanism by which laser damage is produced, the sensory sequelae of the traumata, and the developing treatment of injuries using the new modality of neuroprotection. A new type of goggles that can potentially prevent laser injuries on the battlefield was presented. Other types of radiation which constitute eye hazards were described, as were the safety practices required in medical settings where many types of lasers are commonly used.

Michael Belkin, M.D.
Bruce E. Stuck

SESSION 1

Injury (Diagnostic)

Database structure for the Laser Accident and Incident Registry (LAIR)

James W. Ness, Stephen W. Hoxie,
Harry Zwick, Bruce E. Stuck, David J. Lund
USAMRD-WRAIR, Brooks AFB, TX 78235
Elmar T. Schmeisser
University of Kentucky, Lexington, KY 40536

ABSTRACT

The ubiquity of laser radiation in military, medical, entertainment, telecommunications and research industries and the significant risk of eye injury from this radiation are firmly established. While important advances have been made in understanding laser bioeffects using animal analogues and clinical data, the relationships among patient characteristics, exposure conditions, severity of the resulting injury, and visual function are fragmented, complex and varied. Although accident cases are minimized through laser safety regulations and control procedures, accumulated accident case information by the Laser Eye Injury Evaluation Center warranted the development of a laser accident and incident registry. The registry includes clinical data for validating and refining hypotheses on injury and recovery mechanisms; a means for analyzing mechanisms unique to human injury; and a means for identifying future areas of investigation. The relational database supports three major sections: (1) the physics section defines exposure circumstances, (2) the clinical/ophthalmologic section includes fundus and Scanning Laser Ophthalmoscope images, and (3) the visual functions section contains specialized visual function exam results. Tools are available for subject-matter experts to estimate parameters like total intraocular energy (TIE), ophthalmic lesion grade (Wolfe Grade), and exposure probability. The database is research oriented to provide a means for generating empirical relationships to identify symptoms for definitive diagnosis and treatment of laser induced eye injuries.

Keywords: laser-eye injury, database, laser-eye accident, laser safety, laser-ocular trauma

1. INTRODUCTION

The study of bioeffects resulting from laser eye exposure is concerned with the explanation and description of change in visual function and morphology subsequent to laser exposure. One method toward this end is to compare the visual function and morphological outcomes of subjects randomly assigned to conditions that are systematically varied along specified parameters. For example, analogues of laser eye exposure are developed through systematically varying laser exposure conditions and comparing subsequent visual function and morphology against control conditions.[1] In addition, aspects of visual function loss can be modeled by systematically augmenting or suppressing the visual system with various visual stimuli and comparing visual performance across treatment and control conditions.[2] These examples represent a nomothetic approach to discerning laser bioeffects. This approach emphasizes the treatment of subjects as groups in which individual differences are relegated

SPIE Vol. 2974 • 0277-786X/97/$10.00

to the status of error variance. The strength of this approach is in directly testing an *a priori* principle against rival positions. The extent to which the principle withstands the rigor of this method determines the generality of the principle. The weakness of the approach is in the conception of *a priori* principles in which to invest and in defining the parameters of the experiment in a manner that renders internally as well as externally valid results.

In contraposition to the nomothetic method is the evaluation of laser bioeffects through a comprehensive evaluation of visual function and morphologic change within each laser eye accident case. This is an idiographic approach to discerning laser bioeffects and is the focus of the US Army Laser Eye Evaluation Center.[3,4] This approach emphasizes the uniqueness of laser induced damage and repair processes within an individual. The emphasis on the contribution of individual differences to the outcome illuminates general principles through symmetries in the data across each case. The strength of this approach is in the rich description of naturally occurring laser induced damage and repair processes from which externally valid hypotheses can be derived. The weakness of this approach is in the lack of control over antecedent conditions. This lack of control over antecedent conditions diminishes the strength of relationships with consequent change in visual function and morphology. However, the richness of the idiographic approach in generating hypotheses in conjunction with the rigor of the nomothetic approach in testing hypotheses provides a formidable scientific method from which to study laser bioeffects.

Throughout the 20 year history of the Laser Eye Injury Evaluation Center a number of specialized visual functions tests and imaging technologies have been developed.[5,6] This effort has culminated in a comprehensive laser eye examination designed to evaluate the full extent of visual function and morphology in order to resolve abnormalities resulting from laser eye exposure and to distinguish them from other eye injury and disease. Since 1991, approximately 10 new acute laser eye accident cases have been evaluated per year (Figure 1). With a detailed accident interview, a precise description of the physics of the exposure circumstances, an ophthalmologic exam complete with fundus, scanning laser ophthalmoscope and optical coherence tomography images, a battery of specialized visual functions tests and data from follow-up evaluations, the complexity and extent of information can only be managed in a relational database format. The database constructed to store this information is the Laser Accident and Incident Registry (LAIR) which was created using *Microsoft Access* and attainable through the USAMRD-WRAIR Intranet.

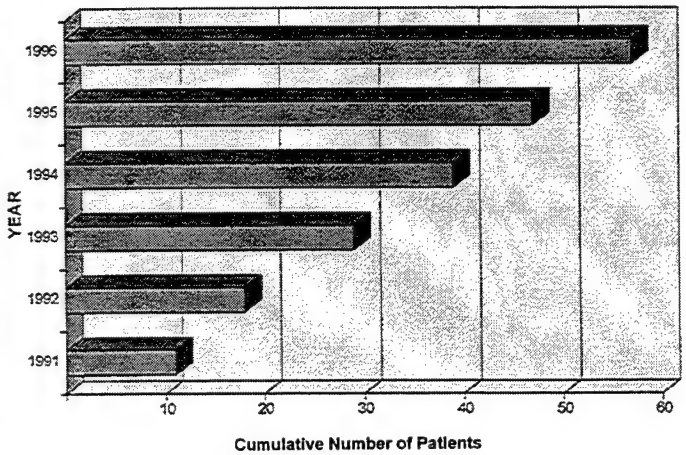

Figure 1. Cumulative number of acute laser eye accident cases referred to the Laser Eye Injury Evaluation Center, Brooks Air Force Base,TX.

2. LASER ACCIDENT AND INCIDENT REGISTRY

The purpose of the registry is to provide a research tool supporting the Laser Eye Injury Evaluation Center's idiographic methodology. As a research tool, the information within the registry must be empirical and reliable, and the registry must provide a facile means for manipulating the empirical information. The data within the registry are empirical in that the data sources for the registry yield observable and quantifiable results that are entered into the database in their original form. For example, the registry does not draw any conclusions about a contrast sensitivity curve such as reporting that the patient has a loss in low spatial frequency sensitivity. The registry simply presents the source of the data (CS-2000, dual Purkinje Eye-Tracker, Scanning Laser Ophthalmoscope), the patient's contrast sensitivity function, and a group mean function from clinically normal controls. The empirical nature of the database prevents the canalizing of the researcher's conclusions toward a particular end state. In this way, the registry is in contrast to a clinically oriented database which yields a reliable conclusion through a deliberate amalgamation of the empirical data into a syndrome.

The Laser Accident and Incident Registry consists of 25 tables with case identification as the primary table (Figure 2). This table contains a synopsis of the case, information about how to contact the patient, and information about who entered the data. The data entry information is used to estimate the reliability of the data entry process. Initially, the reliability for data entry will be based on 100% of the cases entered. Each case is entered independently by 3 data entry personnel. Percent agreement for each table is then evaluated by dividing the number of agreements for each dependent variable within a table by the number of disagreements plus the number of agreements and multiplying by 100 to yield a percent agreement score. The purpose of this reliability estimate is to insure the fidelity of the data entry process and to identify problems with the data entry forms that may facilitate data entry errors. Once the reliability estimate for a table is greater than or equal to 95%, reliability estimates for that table will be randomly sampled every fifth entry. Every fifth entry will be sampled unless a new data entry person has entered the data, the table has been changed, or the reliability estimate for a table drops below 95%. Any discrepancies in data entry will be reconciled with the original data source. This data entry reliability scenario optimizes entering the data in a timely manner with ensuring the reliability of the data entry process.

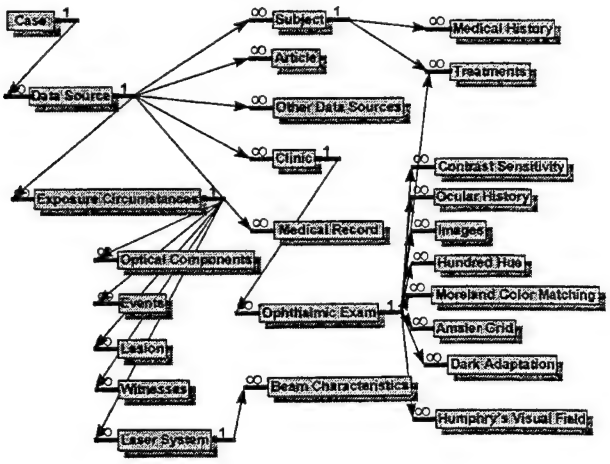

Figure 2. Data relationships in the Laser Accident and Incident Registry

Several tools are available for manipulating the empirical information within the registry. The obvious tools are links to the programs within the *Microsoft Office* suite. For example, the data for the various visual functions tests, like the contrast sensitivity functions, are stored in an

Excel spreadsheet that is directly accessible through the graph of the function within the database. Thus, the data are stored in a format easily exportable to a statistical package or statistics can be performed on the data using the functions available in *Excel*. Structured interviews are stored as *Word* files which can be parsed in any manner or searched for key words. In addition to the links to the programs within the *Microsoft Office* suite, there is an image analyzer that has tracing and area calculation functions. Total intraocular energy, probability of the injury as an actual laser induced injury and ophthalmic grade of lesions can be estimated through available algorithms which are based on standard laser safety and clinical estimates.[7,8,9]

3. RESULTS

Although not all of the laser accident and incident information from the US Army Laser Eye Injury Evaluation Center has been entered into the database, some potential research hypotheses have already been identified. For example, the database has revealed a nominal classification of laser eye injury that correlates with visual function.[10] Patients who were accidentally irradiated by neodymium Q-switched lasers show a range of ophthalmoscopically resolvable laser induced injury from similar retinal exposure. This range of damage suggested a classification based on the location of the injury (foveal or parafoveal), and on the degree of complication associated with the injury (uncomplicated, intermediate, or complicated). The degree of complication is based on the severity of secondary sequelae associated with the lesion (e.g.; scarring, traction and nerve fiber layer anomalies) (Figure 3). The classification system led to the hypothesis that there are separable contributions to visual function loss associated with laser induced retinal lesions. Part of the loss in visual function may be due to primary damage mechanisms and part of the loss may be attributable to secondary sequelae. This hypothesis was directly tested in a series of experiments using a dual Purkinje Eye-Tracker (Figure 4). Note that the contrast sensitivity function for the modeled visual

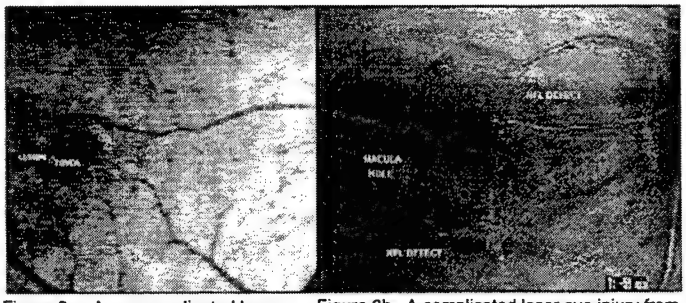

Figure 3a. An uncomplicated laser injury from an accidental Q-switched Neodymium laser exposure. The lesion is temporal to the fovea in the patient's right eye (20° SLO field). *Snellen acuity = 20/15*

Figure 3b. A complicated laser eye injury from an accidental Q-switched Neodymium laser exposure. The lesion is nasal to the fovea in the patient's right eye (20° SLO field). *Snellen acuity = 20/100*

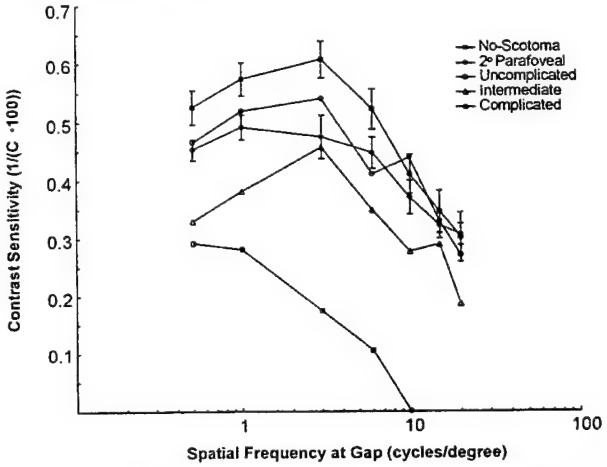

Figure 4. Landolt ring contrast sensitivity functions for clinically normal subjects under baseline and simulated parafoveal scotoma conditions compared with functions from three patients showing a range of complications associated with their parafoveal lesion.

field defect is concordant with that of the patient classified as uncomplicated and that concordance diminishes with complication. Data from a recent accident case and results from other nomothetic studies have supported the hypothesis.[6]

4. DISCUSSION

The Laser Accident and Incident Registry (LAIR) is a research tool with laser accident and incident information supplied by the US Army Laser Eye Injury Evaluation Center. The database has proven useful in directing investigations of laser bioeffects. As more accident case information is added to the database more subtle laser bioeffects may be revealed. The database is research oriented to provide a means for generating empirical relationships to identify symptoms for definitive diagnosis and treatment of laser induced eye injuries. Once reliable symptoms can be identified, a clinical database for acute exposure can be established which can be used as an expert system to facilitate diagnosis and treatment of acute laser induced eye trauma.

Referrals to the US Army Laser Eye Injury Evaluation Center are normally accident cases with ophthalmoscopically resolvable trauma and with the contingency certain that a laser induced the trauma. Therefore, the database is wanting in those cases in which the contingency is uncertain or in those cases where there is no ophthalmoscopically resolvable injury. To account for the contingency issue, at least in acute cases where the injury is ophthalmoscopically resolvable, the unit has developed a probability index of laser exposure.[8] This index is based on several factors including exposure geometry, feasibility of the patient's account of the incident, and the ruling out of disease or other trauma that could have caused the ophthalmoscopically resolvable anomaly.

Although the database captures the acute cases, it falls short on chronic low-level laser exposure cases. Chronic low-level effects are difficult to capture because visual function loss may not be allied with an ophthalmoscopically resolvable anomaly associable to laser radiation. Long-term vision problems could be experienced by persons subjected to the continuous viewing of low-level laser radiation, such as holography, ranging, pattern making, and other military, medical and industrial laser applications.[11] Laser ocular effects at or below ophthalmoscopically visible criteria may be a function of direct absorption of the energy in more superficial retinal layers. Moreover, repeated exposures may effect, in a cumulative fashion, the ability of the retina or visual system to recover.[12] In order to capture these effects, the database will have to be expanded to high risk occupations for chronic low-level laser exposure, such as soldiers on the battlefield,[13] as well as continuing to expand the database in animal analogue data on chronic low-level laser exposure.

5. REFERENCES

1. H. Zwick, D.J. Lund, R. Elliott, & S.T. Schuschereba. "Confocal spectral ophthalmoscopic imaging of retinal laser damage in small vertebrate eyes," In J. Parel, Q. Ren & K. Joos (Eds.), *SPIE Proceedings of Ophthalmic Technologies V*, Vol. 2393, pp. 182-188, 1995.

2. J.W. Ness, H. Zwick, & J.M. Molchany. "Modeling human laser eye injury on target recognition performance using simulated scotomas," *Military Psychology*, Vol. 8, 69-82, 1996.

3. H. Zwick, B.E. Stuck, J.M. Molchany, V.C. Parmley, D.J. Lund, J.J. Kearny, & M. Belkin. "Two informative cases of laser retinal injury," *Investigative Ophthalmology and Visual Science*, Vol. 31, No. 4, p.282, 1990.

4. H. Zwick, D. Gagliano, S. Ruiz & B. Stuck. "Utilization of scanning laser ophthalmoscopy in laser induced bilateral human retinal nerve fiber layer damage," In J. Parel, Q. Ren & K. Joos (Eds.), *SPIE Proceedings of Ophthalmic Technologies V*, Vol. 2393, pp. 189-193, 1995.

5. H. Zwick. "Visual functional changes associated with low-level light effect," *Health Physics*, Vol. 56, No. 2, pp. 657-663, 1989.

6. H. Zwick, J.W. Ness, & J. Loveday. "Optimization of visual-motor strategies in the presence of retinal scotoma," In B.E. Stuck & M. Belkin (Eds.), *SPIE Proceeding of Laser and Noncoherent Ocular Effects: Epidemiology, Prevention and Treatment*, Vol. 2974, in press, 1997.

7. B.E. Stuck, D.J. Lund & E.S. Beatrice. "Another look at the Ocular hazard from military lasers," *Proceedings of the Aerospace Medical Association Meeting*, pp. 224-225, 1981.

8. E. Schmeisser. "Laser Associated Injury Registry," Memorandum to B.E. Stuck, Director USAMRD-WRAIR, Brooks AFB., TX, 78235, 14 December 1993.

9. J. Wolfe. "Laser retinal injury," *Military Medicine*, Vol. 150, pp. 177-185, 1985.

10. J.W. Ness, H. Zwick, J.M. Molchany, & B.E. Stuck. "Modeling human laser eye injury using simulated scotomas," *Proceedings of the 20th Army Science Conference*, Vol. 2, pp. 727-731, 1996.

11. E.S. Beatrice, H. Zwick, D.I. Randolf, B.E. Stuck & D.J. Lund. "Laser hazards: Biomedical threshold level investigations," *Military Medicine*, Vol. 141, pp. 889-891, 1977.

12. H. Zwick, D.O. Robbins, S.B. Reynolds, D.J. Lund, S.T. Schuschereba, R.C. Long & M. Nawim. "Effects of small spot foveal exposure on spatial vision and ERG spectral sensitivity," In B. Drum, J.D. Moreland & A. Serra (Eds.), *Colour Vision deficiencies X* (pp. 581-597). Dordrecht, Netherlands: Kluwer Academic Publishers, 1991.

13. B. Ireland. "Tactical deployments of laser systems into low intensity conflicts," Paper presented at the *Lasers on the Modern Battlefield Conference*, San Antonio, TX February 1996.

The opinions and assertions contained are the private views of the authors, not to be considered as official or reflecting the views of the DoA or DoD. Investigators adhered to AR70-25 and USAMRMC Regulation 50-25 on the use of volunteers in research.

SESSION 2

Injury (Morphology)

Morphological evaluations of Q -switched Nd:YAG laser injury of human retina

David K. Scales[1], Steven T. Schuschereba [2], David J. Lund[2], and Bruce E Stuck[2]

(1) Wilford Hall Medical Center, Lackland AFB, TX and (2) U.S. Army Medical Research Detachment of the Walter Reed Army Institute of Research, Brooks AFB, TX

Abstract

Depiction of the cellular and immune responses in the human model is critical to design rational therapies preventing/limiting cellular destruction and ultimately functional visual loss following acute laser injuries. We report the light and electron microscopy histologic findings in a controlled ocular human laser exposure. Following informed consent, the normal eye of a patient scheduled to undergo exenteration for invasive carcinoma of the orbit was exposed to both continuous wave and Q-switched lasers. Four hours prior to exenteration, argon G lesions (514 nm, 280mW/100msec) were placed in the superior/temporal quadrant and Nd:YAG lesions (1064 nm, 1.2-2 mJ/20 nsec) were placed in the inferior/temporal quadrant. After enucleation, the retina was prepared for routine light and transmission electron microscopy. Histology of the argon G lesions showed primarily photoreceptor and RPE photocoagulation damage. Neutrophil adhesion was limited within the choroid and no neutrophils were observed in the subretinal space. In contrast, the 4 hr Nd:YAG lesions showed extensive retinal disruption, hemorrhage within subretinal and intraretinal spaces, neutrophil accumulation in the retina, and an extensive neutrophil chemotaxic and emigration response in the choroid. Severe laser injuries elicit a significant neutrophil response by 4 hr, suggesting that neutrophils should be an early stage therapeutic target.

Key Words: laser, injury, retina, photoreceptors, neutrophile, human, histology, argon, Nd:YAG

2. Introduction

Directed energies research is essential for the design and implementation of medical treatments for ocular laser injuries. Accurate depiction of human cellular and immune responses following laser exposure is critical to both design rational therapies and to avoid or limit cellular destruction, ultimately preventing or reversing functional visual loss. Information regarding human histologic tissue responses in acute laser injuries is difficult to acquire. Only one previous report on experimental non-macular Nd:YAG laser injury in humans has been reported and only one report with macular injury[2] exist. We report light and electron microscopy histology findings in a comparison series of controlled ocular human Q- Switched (Nd:YAG, 1064 nm) and Continuous Wave (Argon, 514 nm) laser exposures. Histologic analysis revealed that acute stage inflammatory responses are critical considerations in the early therapeutic management of these injuries.

3. Method

Following obtained informed consent, a normal human eye of a patient scheduled to undergo exenteration for an invasive morpheaform basal cell carcinoma of the medial canthal region was exposed

SPIE Vol. 2974 • 0277-786X/97/$10.00

to both visible continuous wave and near infrared Q-switched laser energy. Clinical Argon green (514 nm) and Nd:YAG (1064 nm) lasers were used. Four hours prior to exenteration the patient's eye was subjected to both continuous wave (CW) argon and Q-switched Nd:YAG pulses. The Argon G (280mW/100msec) 200 micron (200 micron slitlamp delivery via Volk Quadraspheric™ fundus contact lens) spots were placed in the superior/temporal quadrant above the patient's macula. The Nd:YAG (1064 nm, 1.2-2 mJ/20 nsec) spots were placed (via a macular Haag-Streit -64.5 diopter contact lens) in the inferior/temporal quadrant. After enucleation, the retina was prepared for routine light and transmission electron microscopy. Semi-serial plastic sections through the centers of the laser injuries were obtained and evaluated.

4. Results

4.1 Argon Light Microscopy

Light microscopy of the argon lesions at the choroid revealed vascular occlusion of the choriocapillaris. Neutrophil adhesion was limited to within the choroid and no neutrophils were observed in the subretinal space. The choroidal vasculature shows extensive polymorphonuclear cell (PMN) adhesion to the vascular endothelium and migration into the interstitial space. The choroidal vasculature revealed occlusion (Figure 1, A)

Light microscopy of the argon lesions in the RPE and outer retinal layers revealed significant heat-fixation of the photoreceptor and RPE layers. There was an artifactual separation of the RPE from the intact Bruch's' membrane with a zone of separation (edema and fluid accumulation) between the heat fixed mass of photoreceptors and the anterior outer nuclear layer. Serous exudate accumulated at the edge of the lesion. The inner retinal layers appeared histologically normal.

4.2 Argon electron microscopy

Electron microscopy of the choroid (Figure 1, B) revealed vascular endothelial cell (VEC) disruption. PMNs were adherent to the site of disruption and were noted to have emigrated beneath the VEC. Both PMNs and platelets were noted not to be degranulated. Disruption of VEC, elaboration of adhesion factors/integrins following injury leads to vascular permeability.

Electron microscopy of the outer nuclear layers (Figure 1,C) showed extensive destruction of the outer nuclear layer. The outer nuclear layer revealed nuclei in various stages of condensation, pyknosis, and fragmentation. The photoreceptor synaptic endings were also pyknotic and the inner segments were highly vacuolated. The overlying inner retinal layers were normal in appearance.

4.3 Nd:YAG light microscopy

Light microscopic histology of the lesions (Figure 2, A) at the level of the choroid revealed widespread PMN adhesion to the choroidal VECs in large numbers with PMN emigration from the choroidal vasculature into the choroidal interstitial space. Extensive platelet thrombi within the choroidal vessels were seen.

Light microscopic histology of the lesions within the RPE showed complete disintegration of the RPE near the lesion center. There were breaks in Bruch's membrane and the underlying choriocapillaris. These breaks together with the involvement of the underlying choriocapillaris lead to significant subretinal hemorrhage.

Figure 1, A: Light microscopy of the argon lesion.

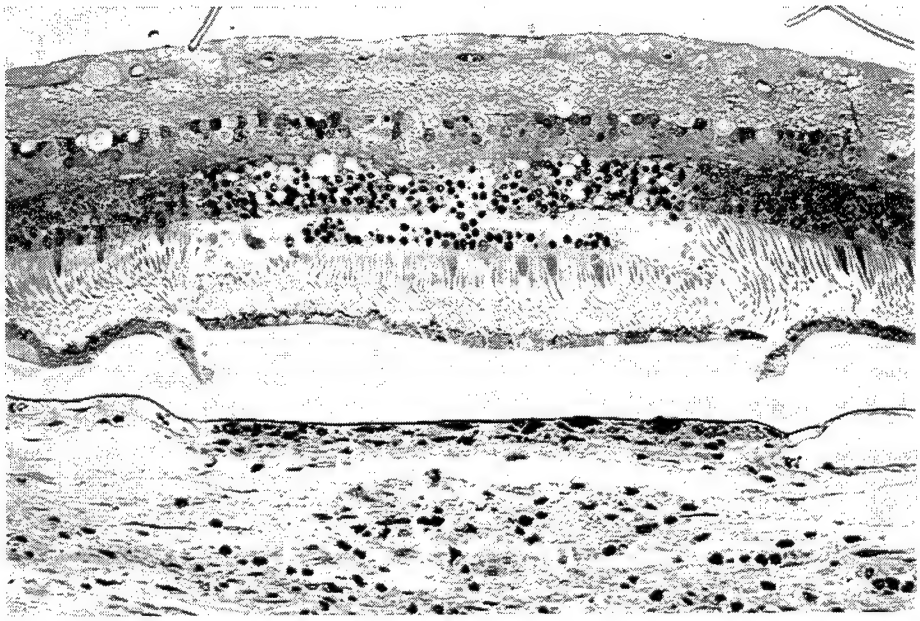

Figure 1, B: Electron microscopy of the choroid (argon).

Figure 1, C: Electronmicroscopy of the outer nuclear layer (argon).

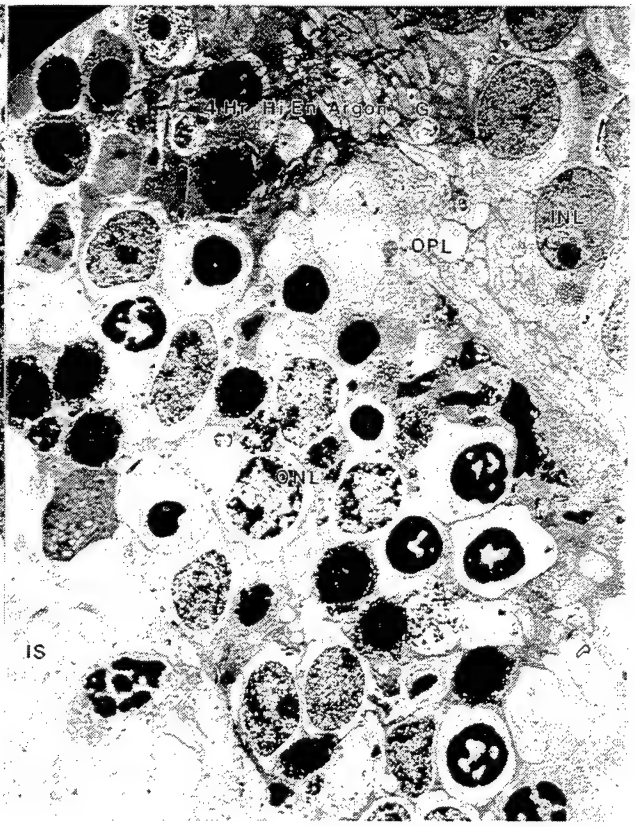

Figure 2, A: Light microscopy Nd:YAG lesion.

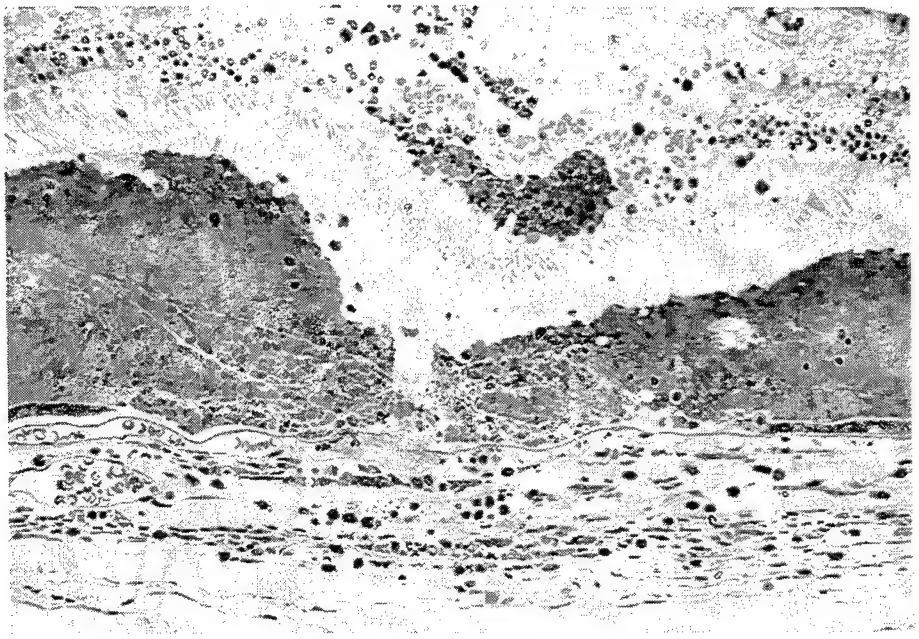

Figure 2, B: Electron Microscopy of RPE (Nd:YAG).

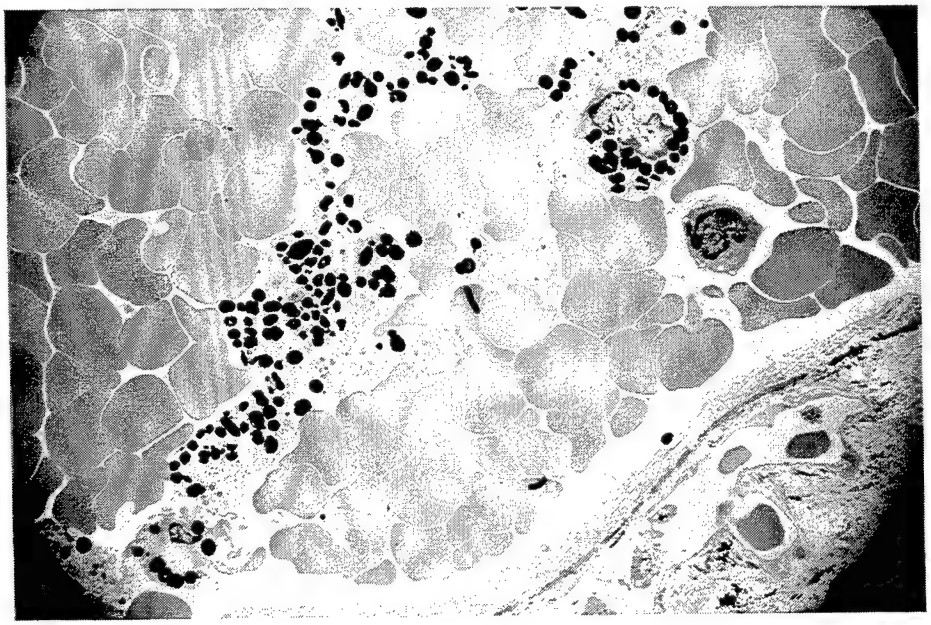

Figure 3, A: Electron microscopy of outer nuclear layer (Nd:YAG).

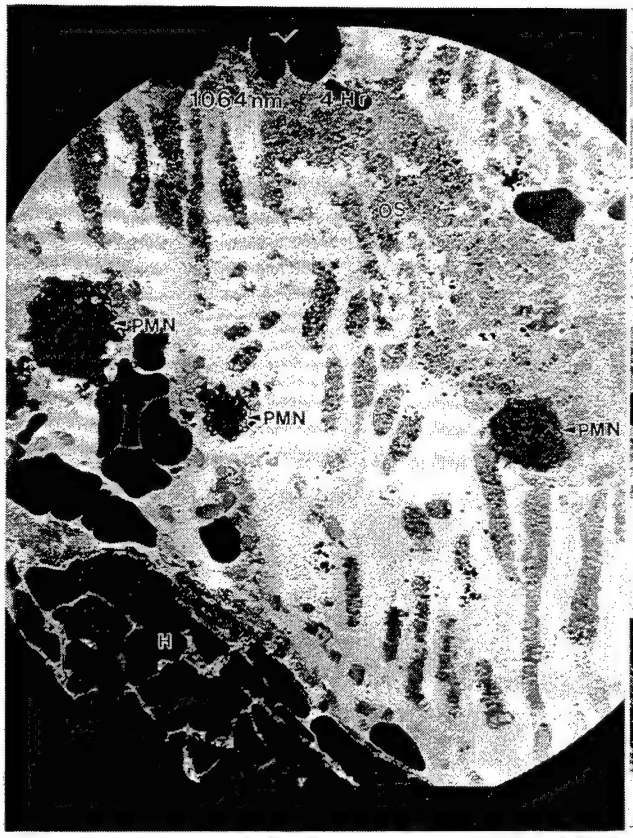

Figure 3, B: Electron microscopy of choroid (Nd:YAG).

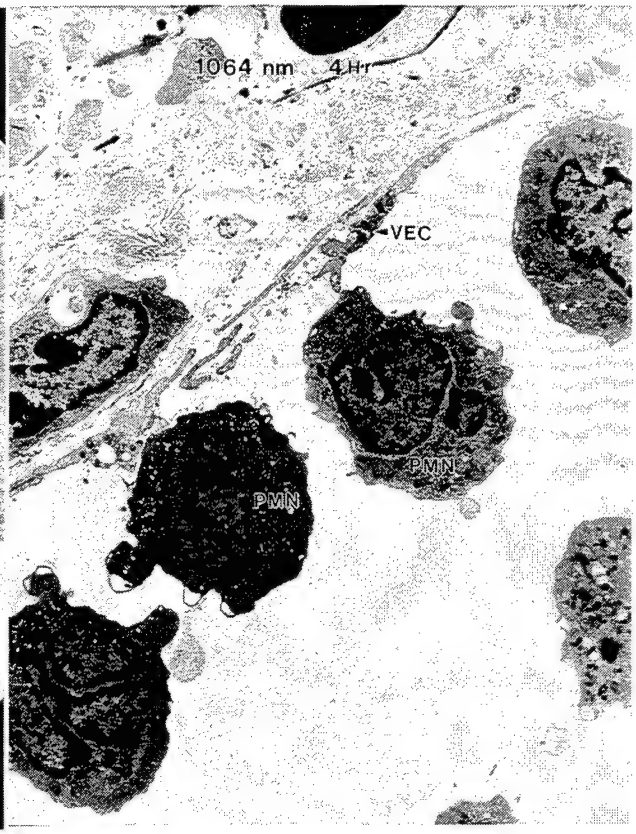

Figure 3, C: Electron microscopy of partially degranulated PMN in outer nuclear layer (Nd:YAG).

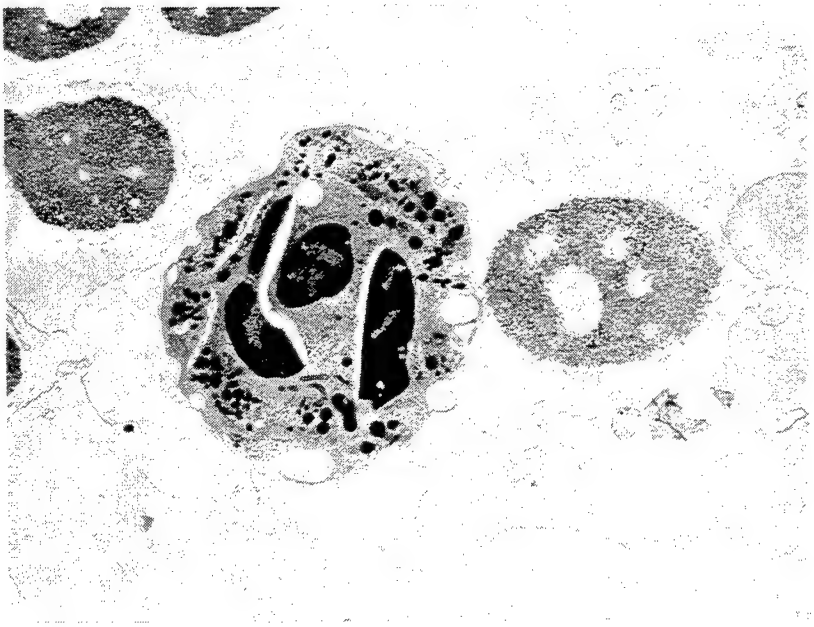

There was associated bleeding within the overlying retina with focal intraretinal hemorrhage as well. Whether this intraretinal hemorrhage was due to traumatic communication with the subretinal space or due to separate retinal vascular injury was not clear.

Light microscopic histology of the lesions (Figure 2, A) in the retina exhibited obvious intraretinal hemorrhage and breakdown of the "blood-retinal barrier". There were pyknotic nuclei dispersed along the lesion periphery. Fragmented nuclei were seen within the lesion center. Marked PMN infiltration into the outer retina was present by four hours following injury.

4.3 Nd:YAG electron microscopy

Electron microscopy revealed fragmented RPE (Figure 2, B) with dispersed melanin granules and PMNs in the subretinal space. There were fractured melanin granules in the subretinal space and these were noted to have been phagocytized melanin granules by monocytes. There were extensive infiltration of PMNs into the outer and inner segment zone (Figure 3, A). The choroid (Figure 3, B) showed PMNs lining up along the margins of a choroidal vessel. Several PMNs appear to be adherent to the damaged VEC. PMNs were also noted to have emigrated beneath the VEC into the choroidal interstitial space.. There were pyknotic nuclei within the outer nuclear layer. A serous exudate accumulated between the outer segments and within the subretinal space. The morphologic integrity of the outer segment was highly disrupted possibly due to: a) release of proteases, collagenases, elastases, and peroxidases from PMNs (Figure 3, C), b) products (free iron) from red blood cell degradation, c) ischemia from choroidal vascular occlusion and reperfusion injury (lipid peroxidation), and d) direct thermal and mechanical effects from the Q-switched exposure.

5. Discussion

Comparison of the light microscopy of the CW argon and Q-switched Nd:YAG reveal several interesting observations. The CW lesion resulted in heat-fixed RPE cells compared to the almost total disintegration of the RPE by the Q-switched exposure. The melanin granules were dispersed in the Q-switched injury. Light microscopy also revealed that the PMNs were markedly adherent and infiltrating the interstitial space of the choroid of the Q-switched injury. PMNs were also infiltrating the outer retina in the Q-switched exposures while they were not observed in the retina of the CW exposures.

The CW argon lesion resulted in a large area of coagulation within the choriocapillaris compared with very little to non-existent coagulation within the choriocapillaris of the Q-switched lesion. In the Q-switched injury, the deeper vasculature of the choroid was markedly invested with PMNs and platelet thrombi while the CW lesion was comparatively less involved. Subretinal and intraretinal hemorrhage with PMN infiltration was seen following the Q-switched pulse, while the CW lesion produced no visible hemorrhage at this power density. Subretinal hemorrhage seemed to be associated with the severity of the Q-switched lesion and the disruption of both Bruch's membrane and the vessel walls of the choriocapillaris.

Electron microscopy of the Q-switched lesion evidenced fragmentation of the melanin granules as a result of the laser exposure. This release of morphologically altered melanin and subsequent phagocytic

inclusion in such antigen presenting cells as the monocyte may lead to enhanced immune cell interaction and recruitment. The RPE of the CW injury were heat fixed. In the acute Q-switched exposure, PMNs were noted to be present in large numbers in the choroidal vasculature, as well as the subretinal space and intraretinally. The acute CW lesion had comparatively less PMN involvement and no leukocytic infiltration was seen subretinally or intraretinally. The large numbers of PMNs seen in the Q-switched injury reflects more extensive injury and may lead to enhanced tissue loss within primarily laser damaged layers and secondary damage to previously uninvolved or adjacent "bystander" cells in the retina.

6. Conclusion

We have documented human immune and histologic responses to acute continuous wave Argon 514 nm and Q- Switched Nd:YAG 1064 nm laser ocular injuries. Histologically, one of the earliest cellular responses in both CW and Q-switched injuries of the human eye consists of an intense acute inflammatory response consisting of neutrophiles. Q-switched Nd:YAG injuries are the most commonly encountered laser accidents.[3] The Nd:YAG induced injury reported here accurately modeled the typical ophthalmoscopic and morphologic appearance of accidental Q-Switched injuries seen at our institution and reported in the literature.[3,4] That the severe injury of the Q-switched pulse elicits a significant neutrophil response by 4 hr, suggests that neutrophils should be one of the primary therapeutic targets during the early stage of medical treatment. Therapies designed to interrupt these initial events may prevent secondary damage by PMNs, preserve tissue, and prevent functional visual loss.

7. References

1. Manning JR, Daviddorf FH, Keates Rh, Strange AE. "Neodynium:YAG laser lesions in the human retina: accidental/experimental" Contemp. Ophthalmic Forum Vol 4., pp. 86-91, 1986.
2. Marshall J, Hamilton AM, Bird AC. "Histopathology of ruby and argon laser lesions in monkey and human retina. A comparative study". Brit J. Ophthalmol Vol 59., pp. 610-630, 1975.
3. Rockwell Jr RJ. "Laser accidents: reviewing thirty years of incidents: what are the concerns-old and new?" J Laser Applications Vol. 6, pp. 203-211, 1994
4. Wolf JA. "Laser retinal injury." Military Medicine Vol. 105, pp. 150-177, 1985

The opinions or assertions contained herein are the private views of the authors and are not to be construed as official or as reflecting the views of the Department of the Army, Department of the Air Force or Department of Defense.

Human Volunteers participated in these studies after giving their free and informed voluntary consent. Investigators adhered to AR 70-25 and USAMRMC Regulation 50-25 on the use of volunteers in research.

Bilateral photic maculopathy after extracapsular cataract surgery - a case report

Steven Chalfin

Department of Ophthalmology
University of Texas Health Science Center at San Antonio
7703 Floyd Curl Drive, San Antonio, TX 78284-6230

ABSTRACT

A 42 year old Caucasian female underwent uncomplicated extracapsular cataract extraction with posterior chamber lens implantation in the left eye, using a Zeiss model OpMi-6 operating microscope. Her postoperative course was unremarkable and she achieved a corrected visual acuity of 20/15+3. A lesion consistent with a photoretinal injury was noted inferior to the fovea. Seven months later the patient underwent cataract extraction in the right eye. Special care was taken to minimize light exposure during the procedure, including reducing the microscope illumination, minimizing operating time, intraoperative pharmacologic miosis, and using a corneal light shield. Despite these precautions, the patient developed a photoretinal injury almost identical to that in the contralateral eye. Postoperative corrected visual acuity was 20/15+3. Recent studies have reported incidences of retinal photic injuries from operating microscopes between 0 and 28% of patients. Several risk factors have been identified, including light intensity, intensity of the blue light component, and exposure time. The occurrence of a retinal photic injury in this patient despite precautions, development of bilateral cataracts at a young age, and a strong family history of early cataracts may indicate an inherited susceptibility to light induced damage. The American National Standards Institute (ANSI) is developing a product performance standard which will be applicable to operating microscopes used in ophthalmic surgery. The as yet undetermined role of individual susceptibility to retinal photic injury should be considered in the formulation of this standard.

Keywords: phototoxicity, photic maculopathy, operating microscope, cataract surgery

1. INTRODUCTION

1.1 Historical perspective

Light-induced thermal damage to the retina as a consequence of solar exposure was first studied by Verhoeff, et al[1] in 1916. Noell, et al[2], in 1966, first described the phenomenon of nonthermal retinal phototoxicity. Ham, et al[3,4] later confirmed that the mechanism of retinal damage varied with wavelength. As illumination sources for ophthalmic instrumentation, particularly surgical microscopes, became more intense, iatrogenic clinical phototoxicity became inevitable. McDonald and Irvine[5] first reported this phenomenon in 1983. In the 1980s and 90s a number of authors published case series involving phototoxicity from operating microscopes used during cataract extraction[6-10].

1.2 Significance of this case

This is the first reported case of bilateral photic maculopathy following cataract surgery. The occurrence of a second retinal photic injury in this patient despite precautions, development of bilateral cataracts at a young age, and a strong family history of early cataracts may indicate an inherited susceptibility to light induced damage.

2. CASE REPORT

2.1 Patient history

A 42 year old Caucasian female presented with a history of painless, progressive visual loss in both eyes over a three to four year period. Her vision had worsened rapidly in the previous five months, and she complained of significant difficulty with glare. She was unable to perform her job as a secretary during that time. Her past ocular history was otherwise negative. Her family ocular history was significant for cataracts in her mother and an older sister, both requiring cataract extraction in their forties. Her past medical history was negative. She was not taking any medications, and had never been on steroids or photosensitizing medications. The patient denied past exposure to ionizing or non-ionizing radiation.

2.2 Physical examination

The general physical examination was within normal limits. Eye examination revealed best corrected visual acuity of 20/50 in the right eye and 20/50-2 in the left eye. Under normal ambient lighting, the visual acuity dropped to 20/200 in both eyes. External examination, ocular motility, and pupillary reaction were normal in both eyes. The anterior segments were normal in both eyes. Dilated examination showed moderately dense nuclear sclerosis and posterior subcapsular changes in the lenses of both eyes. Fundus examination showed normal optic nerves and vessels in both eyes. The maculae were 'blond', with minimal pigmentation of the retinal pigment epithelium. Laboratory studies failed to disclose an underlying metabolic etiology for this patient's cataracts.

2.3 Postoperative course

The patient underwent uncomplicated cataract extraction on her left eye. Her uncorrected visual acuity was 20/20-1 within six weeks following surgery, and her best corrected visual acuity was 20/15+3 with a refraction of -0.50-0.50x035. An oval area of pigment mottling and atrophy measuring approximately one disc diameter in size, consistent with the appearance of a photoretinal injury, was noted just below the inferior vascular arcade.

Seven months later, the patient underwent cataract extraction in the right eye. Because of the photoretinal injury to the left eye, the surgical technique was modified to minimize retinal light exposure. The patient's uncorrected visual acuity was 20/25 within seven weeks following surgery, and her best corrected visual acuity was 20/15+3 with a refraction of +0.50-1.00x160. As in the left eye, an oval area of pigment mottling and atrophy measuring approximately one disc diameter in size was noted just

below the inferior vascular arcade. Intravenous fluorescein angiography showed transmission and blocking defects in the area of pigment mottling as well as late staining, characteristic of a healed photoretinal injury.

3. METHODS

3.1 Surgical technique

The same basic technique was used for cataract extraction in each eye. The operating microscope used for the surgeries was a Zeiss model OpMi-6, equipped with a halogen fiberoptic central illuminator. UV and IR absorbing filters were installed, but no blue light filter was available for this microscope. 0.5% Mydriacil and 2.5% Neosynephrine drops were used for pupillary dilation. Anesthesia was achieved by retrobulbar injection of 3 to 5 cc of a mixture of 0.75% Marcaine, 2% Xylocaine, and 150 units of Wydase. A bridle suture through the superior rectus muscle was used to infraduct the eye. A superior conjunctival peritomy was performed, followed by a mid-limbal groove incision. A viscoelastic (Healon) was injected into the anterior chamber and an anterior capsulotomy was performed. The groove incision was opened with scissors and the lens nucleus was removed by expression. The wound was closed with interrupted nylon sutures and residual cortex was removed using an automated irrigation-aspiration handpiece. Additional viscoelastic was injected to inflate the lens capsule, and a Cilco model S2-B intraocular lens was placed into the capsular bag. Residual viscoelastic was removed with the irrigation-aspiration handpiece. The remainder of the wound was closed with interrupted nylon sutures. Conjunctiva was reposited over the wound. Subconjunctival injections of Gentamycin and Dexamethasone were given. The eye was patched with Maxitrol ointment.

For the surgery on the patient's second eye every effort was made to reduce retinal light exposure. The light output of the microscope was reduced to the minimum level necessary to visualize intraocular structures. A corneal light shield was in place for all portions of the procedure not requiring intraocular visualization. Immediately following lens implantation, Miostat was injected into the anterior chamber to achieve pupillary constriction.

3.2 Spectral irradiance measurements

Following the patient's second surgery, the spectral irradiance of the operating microscope was measured at maximum output, at the plane of the patient's pupil by Byrnes, et al[10]. Measurements integrated over several wavelength ranges are listed in Table 1. The total measured irradiance of the microscope at maximum output between 250 and 800 nm was 55.4 mW/cm^2. The illumination level used for the patient's second surgery was estimated to be 50% of maximum output.

3.3 Surgical times

Duration of exposure to microscope illumination was recorded on the operative report. The preimplantation exposure was calculated from the narrative portion of the operative report.

Table 1. Operating Microscope Spectral Irradiance

Wavelength (nm)	Irradiance (mW/cm^2)
250-320	<0.005
320-400	0.34
400-500	6.8
500-700	40
700-800	8.3

4. RESULTS

4.1 Exposure times

Total illumination exposure time and preimplantation exposure time are listed in Table 2:

Table 2. Exposure Times

	Total exposure (min)	Preimplantation exposure (min)
Left eye	80	40
Right eye	65	31

4.2 Photic maculopathy

Photic retinal injuries developed as a result of operating microscope light exposure in both eyes of this patient. Morphologically, the lesions were quite similar. Fortunately, in both eyes, their location was extrafoveal, and the patient's visual acuity was normal. This location was a result of the surgeon's customary practice of using an superior rectus bridle suture to infraduct the eye, combined with inferior angulation of the operating microscope 10 to 15 degrees[11].

5. DISCUSSION

5.1 Risk of photoretinal injury

Khwarg, et al[9], in a retrospective study of cataract surgery using the same model microscope, reported the incidence of photic maculopathy to be 7.4%. The most significant associated risk factor was mean total operating time (124 min in the maculopathy group vs. 73 min in the non-maculopathy group, $p<0.0001$). Byrnes, et al[10], in a prospective study of photic maculopathy using the same microscope used for this patient's surgery, reported the incidence of photic maculopathy to be 28%. In this series, the authors found, using stepwise logistic regression analysis, that the only statistically significant risk factor

for development of a photoretinal injury was the preimplantation exposure time (p=0.0099). In a later series[12], using a different model microscope with 40% lower irradiance, and with shorter operative times, none of 37 patients developed fluorescein angiographic evidence of photoretinal injury.

5.2 Predisposing factors

Using Byrnes' logistic model[10], the calculated risk of photoretinal injury based on this patient's preimplantation exposure times was 0.20 in the left eye and 0.13 in the right eye. Assuming no predisposition to photoretinal damage, the risk of developing lesions in both eyes would be 0.026.

Several studies have shown a higher prevalence of cortical and posterior subcapsular lens opacities in populations living in areas of high incident ultraviolet B radiation. While mechanisms of photochemical damage cannot be assumed to be the same in the lens and retina, it seems plausible that individuals susceptible to such damage would be so in both locations. This patient, her mother, and sister all developed significant, bilateral cataracts at a very young age without an identifiable predisposing factor (metabolic, pharmacologic, radiation, etc.). This familial predisposition to develop cataracts may be related to a susceptibility to ocular photochemical damage.

Several authors have noted similarities between photic lesions and those of age related macular degeneration (AMD)[4,8,13]. The higher prevalence of AMD in lightly pigmented populations is well known. This patient's skin was very lightly pigmented. She had blond hair and blue irides, and as noted previously, her fundi were also minimally pigmented. The role of iris pigmentation in susceptibility to retinal phototoxicity is controversial. Cavonius, et al[14] showed that blue eyed individuals required a 50% greater exposure to a Xenon arc source to produce a threshold lesion than dark eyed individuals. Byrnes, et al[10] found no relationship between iris color and microscope-induced photic maculopathy. The role of the retinal pigment epithelium (RPE), independent of iris pigmentation is also unclear. Whether the RPE functions primarily as a source of energy absorption and free radical production, as a free radical scavenger, or both is not known.

The microscope used for this patient's surgeries, while intermediate in irradiance, was brighter than seven of the ten operating microscopes measured by Sliney and Armstrong[15]. Blue light and eclipse filters were not available for this model microscope at the time of this patient's surgeries. Surgical times, although typical for standard extracapsular cataract extraction by a resident surgeon, were significantly longer than would be expected for small incision phacoemulsification performed by an experienced surgeon[12].

5.3 Recommendations

Foveal photic lesions frequently result in permanent visual loss. Awareness of the potential for photic retinal damage during ocular surgery is a key element in its prevention. The Food and Drug Administration of the US Department of Health and Human Services recently published a Public Health Advisory on retinal photic injuries from operating microscopes[16]. Additionally, several survey articles on retinal phototoxicity have recently appeared in the ophthalmic literature[17-19]. Reduction of the total energy delivered to the retina by reducing microscope illumination, appropriate IR, UV and blue light filtration, and shortening operating time are practical measures which should be employed in all cases.

Additionally, angulation of the microscope to avoid illumination of the fovea, use of non-coaxial illumination when practical, and eclipse filters or corneal light shields may mitigate phototoxic retinal damage.

The American National Standards Institute (ANSI) is developing a product performance standard for ophthalmic operating microscopes. When formulating this standard, the role of individual susceptibility to retinal photic injury should be considered.

6. ACKNOWLEDGMENT

This work was supported, in part, by an unrestricted research grant to the University of Texas Health Science Center at San Antonio Department of Ophthalmology from Research to Prevent Blindness, Inc., NY.

7. REFERENCES

1. F.H. Verhoeff, L. Bell, C.B. Walker. "Pathological effects of radiant energy on the eye," Proc. Am. Acad. Arts Sci. 51:629-818, 1916.

2. W.K. Noell, V. Walker, B-S. Kang, et al. "Retinal damage by light in rats," Invest. Ophthal. 5:450-473, 1966.

3. W.T. Ham, Jr, H.A. Mueller, D.H. Sliney. "Retinal sensitivity to damage from short wavelength light," Nature 260:153-155, 1976.

4. W.T. Ham, Jr, J.J. Ruffolo, H.A. Mueller, et al. "The nature of retinal radiation damage: Dependence on wavelength , power level, and exposure time," Vision Res. 20:1105-1111, 1980.

5. H.R. McDonald, A. Irvine. "Light-induced maculopathy from the operating microscope in extracapsular cataract extraction and intraocular lens implantation," Ophthalmology 90:945-951, 1983.

6. E.E. Boldrey, B.T. Ho, and R.D. Griffith. "Retinal burns occurring at cataract extraction," Ophthalmology 91:1297-1302, 1984.

7. S.G. Khwarg, M. Geoghegan, and T.A. Hanscom. "Light-induced maculopathy from the operating microscope," Am. J. Ophthalmol. 98:628-630, 1984.

8. W.H. Ross. "Light induced maculopathy," Am. J. Ophthalmol. 98:488-493, 1984.

9. S.G. Khwarg, F.A. Linstone, S.A. Daniels,et al. "Incidence, risk factors, and morphology in operating microscope light toxicity," Am. J. Ophthalmol. 103:255-263, 1987.

10. G.A. Byrnes, A.N. Antoszyk, D.O. Mazur, et al. "Photic maculopathy after cataract surgery," Ophthalmology 99:731-738, 1992.

11. R.D. Brod, K.R. Olsen, et al. "The site of operating microscope light-induced injury on the human retina," Am. J. Ophthalmol. 107:390-397, 1989.

12. G.A. Byrnes, B. Chang, I. Loose, et al. "Prospective incidence of photic maculopathy after cataract surgery," Am. J. Ophthalmol. 119:231-232, 1995.

13. M.O.M. Tso and B.J. Woodford. "Effect of photic injury on the retinal tissues," Ophthalmology 90:952-963, 1983.

14. C.R. Cavonius, S. Elgin, and D.O. Robbins. "Threshold for damage to the human retina by white light," Exp. Eye Res. 19:543-548, 1974.

15. D.H. Sliney and B.C. Armstrong. "Radiometric evaluation of surgical microscope lights for hazards analysis," Appl. Opt. 25:1882-1889, 1986.

16. D.B. Burlington. "Retinal photic injuries from operating microscopes during cataract surgery," FDA Public Health Advisory, October 16, 1995.

17. M. Michels and P. Sternberg, Jr. "Operating microscope-induced retinal phototoxicity: Pathophysiology, clinical manifestations, and prevention," Surv. Ophthalmol. 34:237-252, 1990.

18. B.L. Lee and P. Sternberg, Jr. "Phototoxicity of the macula," in Ophthalmology Clinics of North America 6:231-237, 1993.

19. P. Davidson and P. Sternberg, Jr. "Potential retinal phototoxicity," Am. J. Ophthalmol. 116:497-501, 1993.

Accidental macular burns caused by artillery laser rangefinder

Nikola Smiljanic, Branislav M. Djurovic

Military Medical Academy, Eye Clinic, Belgrade, Yugoslavia 11000

ABSTRACT

Authors present two cases of macular burn caused by artillery laser rangefinder. Both injuries resulted from improper use of laser device. One of them occurred during combat activities. Safety goggles were not used. Macular burns resulted in permanent loss of central vision and visual acuity reduced to less than 0.1.

Authors present results of clinical and functional tests made during long follow up period and comment similar published cases and ways of protection.

Keywords: eye injuries, military lasers, macular burns, accidents.

1. INTRODUCTION

Eye injuries by laser beam can occur by incidence during therapeutical procedure (fotocoagulation of the retina), as well as during laser use in other, nonmedical purposes: industry, research centers, military activities [1, 3, 4, 5].

Since 1960, when laser was invented, dozens of laser beam eye injuries, mostly accidental, have been reported. The first one was described by Rathkey in 1965. In 1985 Wolf [1] cited all reported injuries caused by laser from 1965 to 1985.

Injuries caused by lasers used for military purposes are relatively rare and are almost exclusively caused by laser rangefinders. In this study two cases of macular injury caused by laser rangefinder have been presented for the first time. One of them occurred during combat activities.

The aim of this study is to point out the dangers related to use of powerful lasers, the necessity to recognize clinical picture and course of this pathological condition, and particularly to emphasize the great importance of correct handling of laser devices and means of protection .

2. CASE REPORTS:

2.1. First case

P.S., 36 year old male, member of the army, injured his right eye while operating artillery laser rangefinder. The injury occurred during careless adjusting of laser device, during which he didn't wear safety goggles. The patient describes the moment of injury as a light blow, after which he noticed a "dense fog" in front of his right eye, and a few minutes later two vertical dark lines in the central visual field. The same day he was admitted to hospital. At admission visual acuity was 0.30.

Examination found out a preretinal cloudlike opacity in vitreous. A large hemorrhage, surrounded by edema was present in foveolar region. Other segments of right eye appeared normal. Left eye had normal visual acuity and no pathological findings.

SPIE Vol. 2974 • 0277-786X/97/$10.00

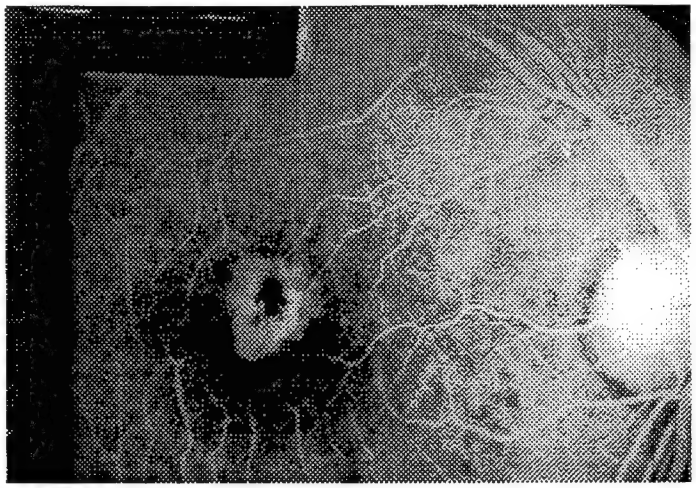

Photo. 1. Fluorescein angiography - patient P.S.

Clinical testing: visual field (kinetic perimeter - Goldmann) of the right eye showed absolute central scotoma 3^0 in diameter, with the surrounding, ringlike relative scotoma. (Fig. 1). Amsler net of the right eye: absolute central scotoma surrounded by zone of extensive metamorphopsia. (Fig. 2).

Fluorescein angiography, performed two weeks after the injury, showed profound perifoveolar spotlike fluorescence accompanied with dark fovea phenomenon (Photo. 1). Absence of primary adaptation was noted (Goldmann-Weekers adaptometer), while secondary was normal.

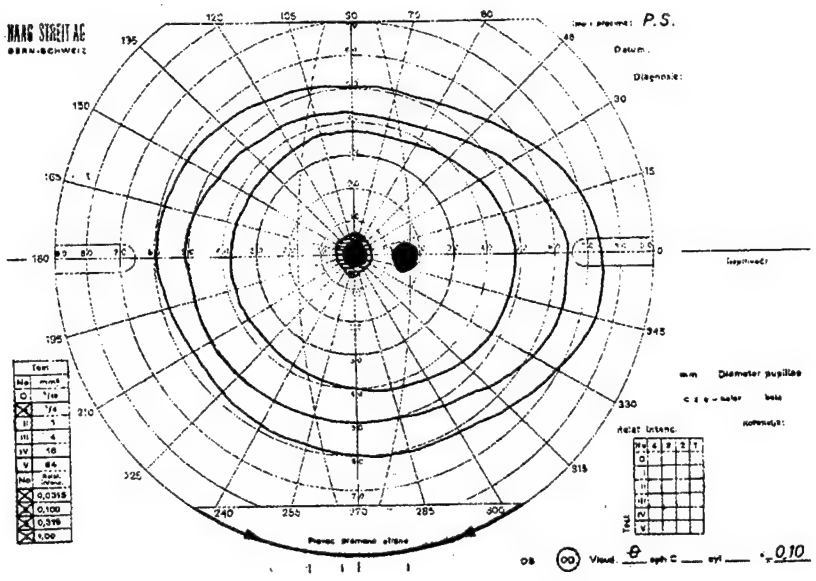

Fig. 1 Visual field - patient P.S.

Vitreous opacity has withdrawn during treatment, and both the foveolar hemorrhage and the surrounding edema have disappeared. A scar was formed which presented as a macular hole.

At dismissal from the hospital visual acuity of the right eye was 0.08. Patient f was followed for several years. The last control examination showed visual acuity 0.04. The foveolar scar is completely formed with the central hole and melanin and lipofuscin deposits at the edge.

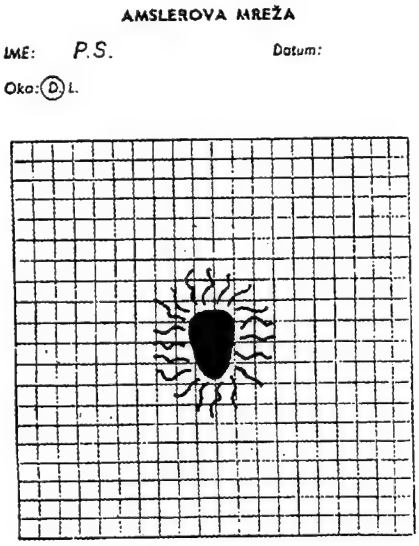

Fig. 2 Amsler net - patient P.S.

2.2. Second case

M.A. 27 year - old male, member of the army, was injured during combat activities while using ship artillery laser rangefinder. The injury occurred accidentally, while attempting to repair malfunction. At the moment of injury he felt a light blow into his left eye, and noticed a green membrane afterwards, which changed into black, and finally, after several hours, into a red spot. He was admitted to hospital 9 days after the injury. Visual acuity of the left eye at admission was 0.30. Examination showed grayish edema with centrally positioned spotlike hemorrhage of macula in regression.

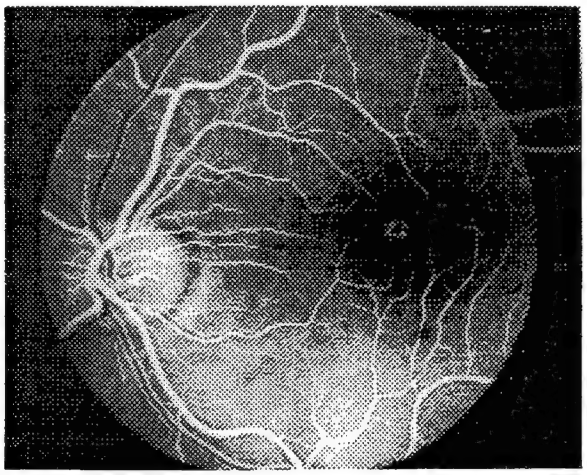

Photo. 2 Fluorescein angiography - patient M.A.

Clinical testing: visual field (kinetic perimeter-Goldmann) of the left eye showed central absolute scotoma 2^0 in diameter (Fig. 3). Amsler net showed absolute central scotoma with the surrounding metamorphopsia (Fig. 4). Fluorescein angiography: in arterio - venous phase punctate fluorescence in the injury zone could be noted. During venous phase those puncta conflated (Photo. 2). Adaptometry (Goldmann-Weekers) showed absence of primary adaptation , while secondary retained within normal values.

At the beginning of the second week visual acuity of the left eye was reduced to 0.10. The patient was followed for 3 years. The last examination showed visual acuity 0.06. The central macular scar was completely formed with formation of foveolar microhole.

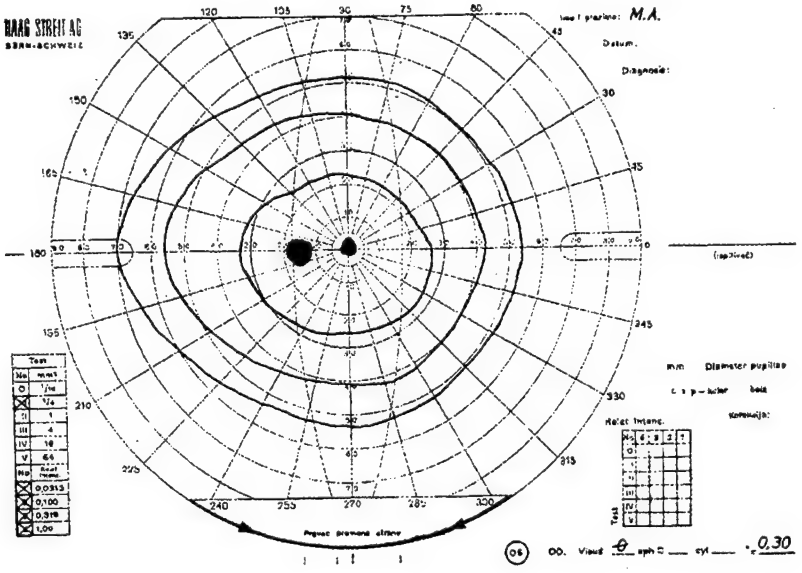

Fig. 3 Visual field - patient M.A.

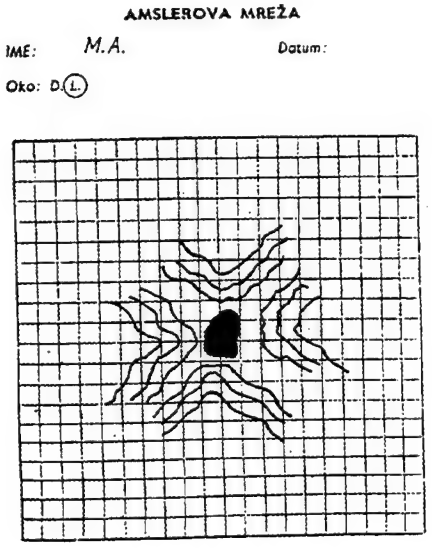

Fig. 4 Amsler net - patient M.A.

3. DISCUSSION

Accidental eye injuries by laser beam are relatively rare, considering widespread use of laser devices in almost all fields of human activity, including military purposes. Until 1985. there were 23 reports on laser eye injury and since then about 10 more. Only five of those were injured by lasers for military purposes, mostly rangefinders.

Laser beam damages retina either in a form of a burn (photocoagulators) or as disruption (pulse or Nd YAG lasers). The most common injury site was macula which was presented as a sudden and permanent reduction of central visual acuity under 0.10.

According to intensity, injuries could be graded as following:
1. retinal edema,
2. retinal necrosis,
3. subretinal and/or retinal hemorrhage,
4. vitreal hemorrhage and/or full thickness retinal hole.

Presented patients were injured by laser rangefinder which is used as a part of BOFI system to measure the distance between cannon and the target. The main principle used is to count the time (t), during which laser beam travels to target and back. The system then automatically calculates distance through formula D=ct/2, where "c" stands for speed of light in atmosphere.

Laser type is Nd YAG with wavelength of 1.06 microns, impulse power 90 mJ, impulse width 20 ns and frequency of repetition of 10 Hz.

Both patients were injured while carelessly operating the laser device without safety goggles. Distance from beam source was less than 1 meter and maximum range of this laser is 20.000 m. In both cases injury was located in central part of macula causing fourth degree damage. Injury resulted in reduction of central visual acuity to 0.1, absence of primary light adaptation, occurrence of metamorphopsia and central absolute scotoma.

Isolated cases of similar injuries were reported. [2,3,4,5].

The possibilities of treatment and protection are some of the topics initiated by this type of injury. Strictly following instructions for use and wearing safety goggles are cornerstones of protection.

Applied therapy (cycloplegics, corticosteroids, polivitamins...) was absolutely inefficient.

4. CONCLUSION

To our knowledge, this is the first paper presenting more than one patient injured by military laser device.
Injuries occurred solely from careless use and lack of protective gear.

There is no evidence that any form of therapy can be beneficial. The best and so far the only way to deal with this type of injury is prevention: insisting on strictly obeying instructions for use and wearing safety goggles.

5. REFERENCES

1. Wolfe, "Laser retinal injury," Military Medicine, Vol. 150, pp. 177-185, April 1980.
2. Zweng, "Accidental Q-switched laser lesion of human macula," Arch. Ophthal. Vol. 78. pp. 596-599, Nov. 1967.
3. Lang, G. Lang, O.H. G. Nauman, "Akzidentelle bilaterale asymetrische Rubin-Laser-Makulopathie," Klin.Mbl.Augenheilk.. Vol. 186, pp. 366-370, 1985.
4. Pramemer, J. Wiesflecker, G. Grabner, "Makula verletzung durch Festkorperlaser," Klin.Mbl.Augenheilk. Vol. 176, 1980.
5. Bleckmann, R. Zorn, "Akzidentalle laserkoagulation der macula," Klin.Mbl.Augenheilk.. Vol.179. pp. 38-40, 1981.

Macular pigmentary alterations after repeat viewing of argon laser trabeculoplasty

D.K. Scales[1], H. Zwick[2], D.J. Lund[2], M. Belkin [3], and J. Loveday[2]

(1) Wilford Hall Medical Center, Lackland AFB, TX, (2) U.S. Army Medical Research Detachment of the Walter Reed Army Institute of Research, Brooks AFB, TX, (3) Goldschlager Eye Institute, (Israel)

ABSTRACT

We evaluated retinal morphologic and visual functional changes in two individuals accidentally exposed to argon laser "flashback" from an incorrectly placed laser protective filter while viewing a routine argon laser trabeculoplasty. These exposures, measured in the absence of a patient's eye, are in the region of the maximal permissible exposure (MPE). The patients were followed with serial visual function testing, scanning laser ophthalmoscopy (CSLO) and chromatic contrast sensitivity. The first individual received 54 monocular exposures. Acute examination revealed inferior and central Amsler grid abnormalities. These distortions matched the CSLO evidence of pigmentary changes in the corresponding retinal field. Initial contrast sensitivity showed high spatial frequency loss which increased during the ensuing 1.5 months. Chromatic contrast sensitivity revealed high spatial frequency loss for long wavelength test targets ("yellow") and broad spatial frequency loss with short wavelength targets ("blue"). The second individual received fewer exposures (4-6) bilaterally. Both eyes showed foveal morphologic alterations with non-selective changes in Moreland anomaloscopic matches, indicative of macula edema. We have shown a correlation between ophthalmoscopic and functional measures of spatial vision. Progressive loss in contrast sensitivity and spatial chromatic functional loss were associated with the more severe exposure while minimal changes were observed with fewer exposures.

Keywords: laser, repetitive exposure, human, contrast sensitivity deficit, nerve fiber layer, scanning laser ophthalmoscopy,

1. INTRODUCTION

Human laser accidents have generally involved single acute exposures. Repeated exposure human laser accidents are relatively more rare. Concern has been raised regarding retinal injury from chronic repeated laser exposures in the routine use of ophthalmic lasers.[1] Previous work has demonstrated that multiple exposures at suprathreshold doses may result in severe morphologic alterations with both intraretinal and epiretinal scar formation and subsequent retinal hole formation, retinal tractional changes, and detachment.[2] Human laser accident cases with multiple foveal exposures have also been shown to affect both static and dynamic contrast sensitivity peaks.[2] Investigations into the morphologic and functional effects of repeated laser exposures at lower or non-thermal levels are lacking.

Single or more recently bilateral exposure effects at doses that produced no visible damage yet produced secondary effects have been documented. Non-human primate investigations have demonstrated the possibility of such effects.[3] Rhoades showed a discrete bullseye maculopathy which

developed after (time) that was associated with repeated Q-switched exposure at levels between the MPE and ED50 for burn in an animal model.[4] This maculopathy appeared prominently as a circular area of window defects during fluorescien angiography. These animals showed no change in the visual acuity measurements performed and further functional testing was not performed. Lower level laser exposure work showed prolonged functional effects with spectral sensitivity measurements.[5,6] Measurements of contrast sensitivity have required repeated Q-switched exposure to affect achromatic acuity and contrast sensitivity measures to any permanent degree. Morphological change has always been apparent first in these kinds of studies.

Prolonged, or repeated exposure effects represent an area of environmental laser impact that at present has not been well investigated. Early work on threshold effects in non-human primates suggests that repeated effects may induce lower thresholds. Prolonged repeated exposure to non-human primates demonstrated significant loss in visual spectral sensitivity.[5,6] Recent investigations in Q-switched pulses[4] demonstrated altered macular regions even though exposures were below threshold damage levels. Animal investigations have long suggested that prolonged exposure to both coherent and incoherent light can cause photoreceptor and morphologic alterations,[7] as opposed to others,[8] who have proposed that these low-level, non-thermal induced changes are resident in the melanin of the Retinal Pigment Epithelial cells. The possibility of such effects in humans has most recently been described by measurement of visual functional changes in ophthalmologists where chronic repeated low level exposure to clinical Argon laser photocoagulators may have induced such changes.[9]

In the present report we have examined two ophthalmic technicians who were accidentally exposed to multiple pulses from an incorrectly placed laser filter device while viewing argon laser trabeculoplasty. We have documented their progressive morphologic and functional changes following exposure.

2. Methods

Two unique cases of repeated accidental laser exposure occurred while two separate individuals were observing a routine argon laser trabeculoplasty (ALT) procedure as part of an ophthalmic introductory training program. The laser observation tube had been incorrectly placed in front of the laser filter allowing the observer tube to receive unfiltered laser energy as "flashback" energy from the procedure. These exposures, measured in the absence of a patient's eye, are in the region of the maximal permissible exposure (MPE). The first individual received 54 monocular exposures. The second individual received fewer exposures (4-6) bilaterally.

Both individuals were evaluated for visual field changes using Amsler Grid and Humphrey visual fields. Color vision was assessed with both the Farnsworth 100 hue and Raleigh and Moreland anomaloscopic matches. Contrast sensitivity was measured for sinewavegratings as well as Landolt ring test targets. Chromatic contrast sensitivity was measured against a "blue" or a "yellow" background. The luminance of the "yellow" background [1.83E-3 Iu/(cm2*ster)] was approximately 1 log unit higher than that of the "blue" background [2.64E-4 Iu/(cm2*ster)]. Contrast sensitivity was measured in the presence of each chromatic background for landolt ring targets varying in spatial frequency from 0.5 to 20 cycles per degree. All test targets were of the identical chromatic makeup as the backround used (i.e. "yellow" landolt rings on a "yellow' background). Serial confocal Scanning Laser Ophthalmoscopy images of the macular morphologic changes were obtained.

3. RESULTS

Figure 1. Acute CSLO picture and Amsler Grid recording from Case 1

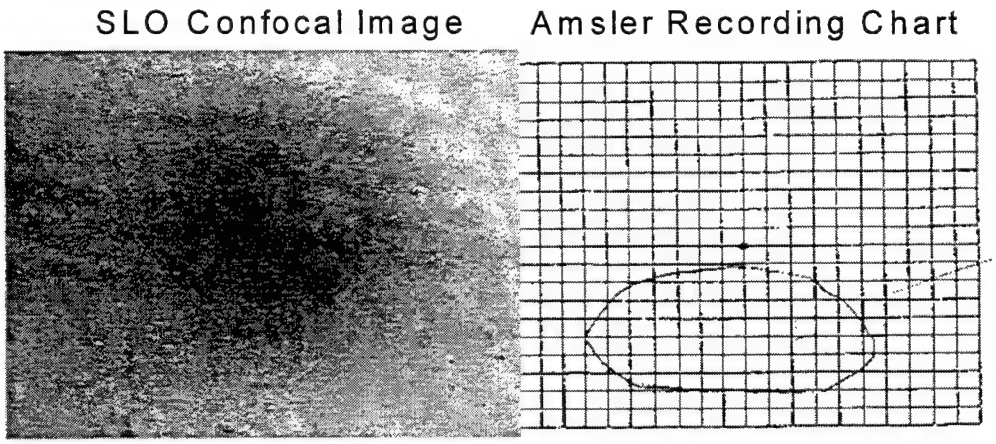

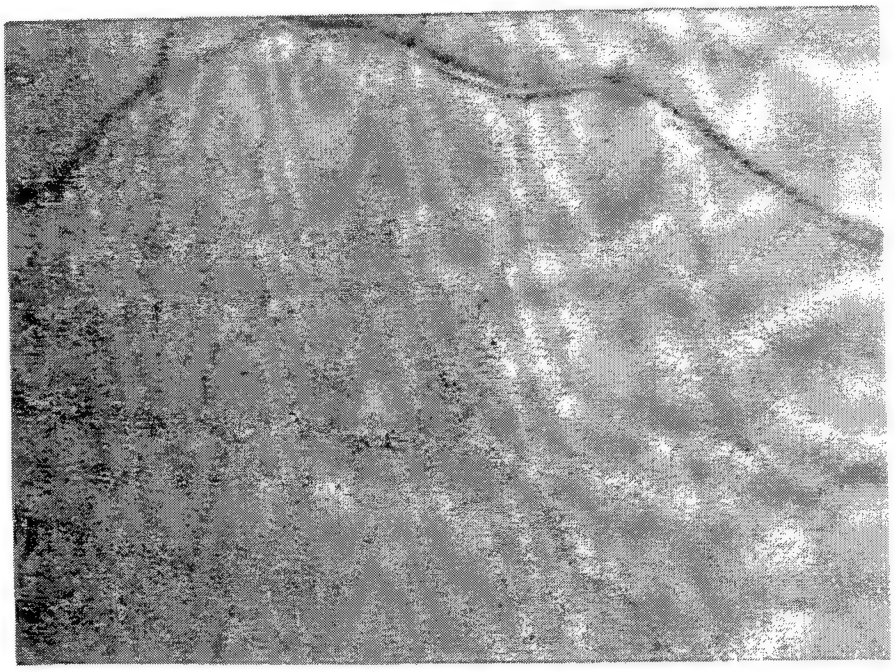

Figure 2. 3 month near IR CSLO image Case 1.

The first individual received 54 monocular exposures. Figure 1 shows a composite image of the macular region imaged with the CSLO short wavelength (488) Argon laser source and a corresponding Amsler grid measurement in this eye. An area of punctate pigmentary disturbance was observed in the superior and nasal regions of the macular pigment accompanied by inferior and central Amsler grid abnormalities with mild grid distortion. Snellen visual acuity measured 20/30 acutely but subsequently recovered to 20/20 after one week.

Clinical examination, performed acutely by an experienced vitreoretinal surgeon, both with the 90 diopter and direct macular contact lens biomicroscopy utilizing white, red-free, and cobalt blue light failed to reveal any morphologic foveo-macular alterations. Detection of acute and chronic ophthalmoscopic alterations were only possible with CSLO examinations. These were initially only observable in the inner retinal layers with the 488 nm imaging source, suggesting disturbance in the macula luteal pigment itself. Over an approximate 3 month time frame (87 days post exposure), CSLO imaging of the affected area appeared more profound and could be imaged in the outer retinal and retinal pigment epithelial layers with the near IR CSLO diode laser source(Figure 2). Near IR examination revealed increased reflectance in the previously affected supra foveo-macular area as well as a new demarcated area of reflectance in the superior-nasal macular region suggesting subsequent nerve fiber layer involvement.

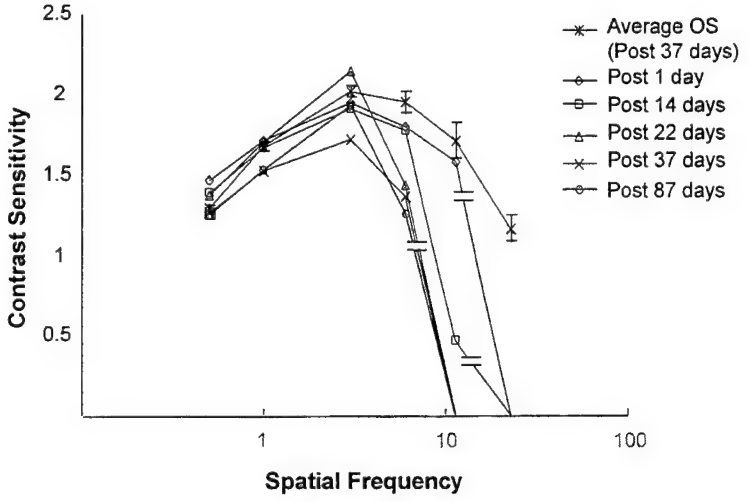

Figure 3. Sinewavegrating target contrast sensitivity case 1.

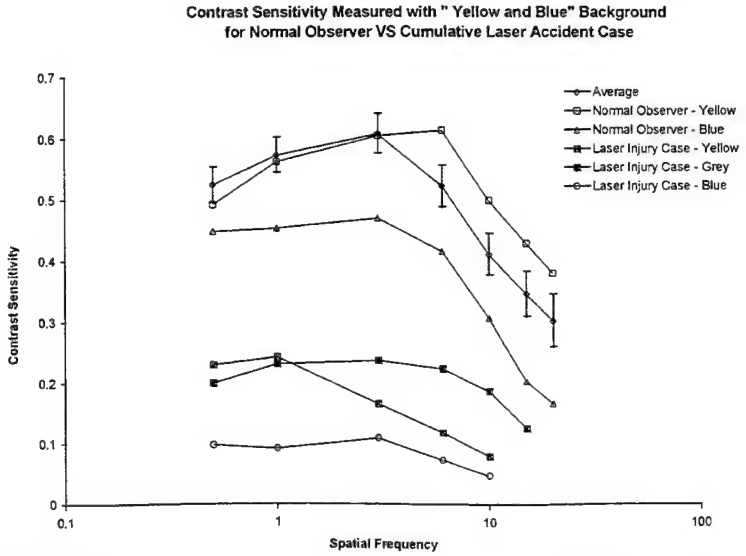

Figure 4. Chromatic spatial contrast sensitivity curves for normal and case 1.

During this time contrast sensitivity measured with sinewave grating targets (Figure 3) showed a selective loss of high to mid-spatial frequency sensitivity. This selective loss of the higher spatial frequencies was followed over time and revealed progressive loss in those involved frequencies. These changes appeared to stabilize in the higher spatial frequencies after 22 days post exposure but still showed some variability in the mid-

spatial frequencies. There were no observed changes in the sinewave grating contrast sensitivity in the unexposed contralateral eye. In case 2 the sinewave grating contrast sensitivity remained stable. Chromatic contrast sensitivity made in case 1 measurements made at 2 to 3 months post exposure showed significant loss relative to normal subjects measured under comparable conditions (Figure 4). Landolt contrast sensitivity measured against a uniform gray background was uniformly suppressed across all spatial frequencies. For normal observers tested against a yellow background the peak sensitivity shifts from 3 to 6 cycles/degree. This is contrasted by the patient's suppression curve in which the presence of the yellow background more severely affects the mid and high spatial frequencies, indicating a possible selective spectral laser effect in the long wavelength cones. This was contrasted by a relative lack of observed effect (relative to normals) when a blue background was used. Unlike the yellow, the blue background produces further suppression of the contrast sensitivity function but is relatively uniform across the spatial frequencies relative to the gray background. This is in the presence of lower overall luminance (dimmer) than either yellow or gray backgrounds. This suggests a non spatial chromatic interaction for the blue background in both the normal and the laser accident case. However, the lower sensitivity of the laser accident case relative to the normal for the blue background may indicate blue cone system loss independent of selective spatial frequency laser effect.

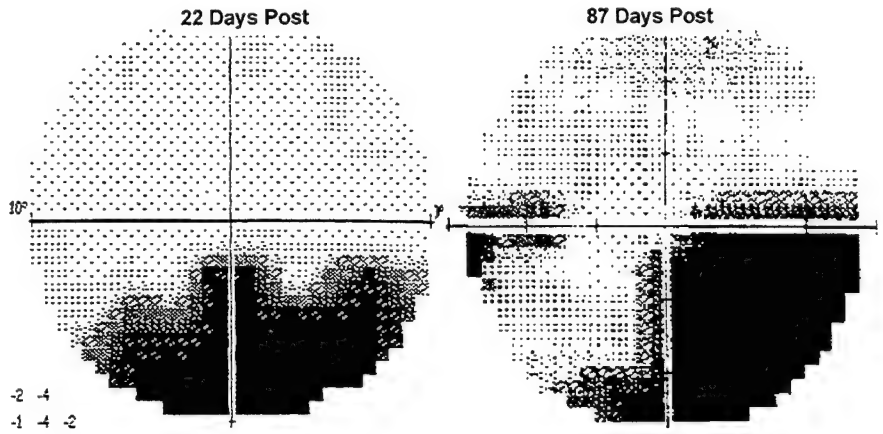

Figure 5. Serial Humphrey visual fields (10-2) case 1.

The Humphrey visual field (HVF 10-2) testing showed inferior field loss of sensitivity in the superior and nasal macular retinal region. (Figure 5) These changes, noted as early as 14 days after the exposure, were consistent and essentially non-progressive over the 3 months of observation. This early loss in the visual field confirms the early SLO observed alterations in the macular pigment and finding of mild grid distortion and partial scotoma noted in the Amsler grid evaluations. The persistence of the visual field deficits supports the functional visual loss also suggested by the loss of contrast sensitivity.

The second individual, receiving fewer exposures (4-6) bilaterally, was noted to have bilateral mild foveal morphologic changes in the 488 nm CSLO. Acute functional testing was normal (visual acuity, contract sensitivity) except for a vertical shift in the Moreland match indicating macular edema. This vertical shift in the Moreland match subsequently developed in the other eye at two weeks. The patient was asymptomatic and elected no further evaluations after that time.

4. Discussion

This report correlates progressive focal morphologic and selective functional changes for repetitive non-thermal laser exposures in two humans. Findings both morphologic and functional selectively progressed over the period of observation in case 1. Case 2 who received only several pulses bilaterally showed some change in the Moreland match that appeared to change over time as well. All tests correlated with other tests (convergent validity). Conventional clinical ophthalmologic examination techniques failed to identify these morphologic changes. Identification of the morphologic retinal changes was possible with the employment of spatial, confocal imaging techniques (CSLO). Layer specific involvement of the inner retinal (macular pigment) layer was present and this finding was maintained through out the period of observation. Later changes compatible with progressive changes in the nerve fiber layer were observed.

Differential, progressive, and selective loss in the higher spatial frequencies was noted without shifts in the peak sensitivity in the yellow (long wavelength cones) versus blue (short wavelength cones) background contrast sensitivity functions. The selective nature of the observed progressive functional changes in these repetitive non-thermal human exposures are similar in nature to previously reported non-human primate repetitive non-thermal exposure experiments performed at this institution.[10] Earlier work in diabetic clinical photocoagulation showed tritan defects that were presumed to be due not to the direct thermal effects but rather due to the non-thermal exposure associated with coherent scatter within the media during treatments.[11] The selectivity of the observed findings reflect the ascertainment that only specific layers of the retina appear to be involved in this type of injury. These progressive finding are consistent with a slow mechanism evolving over time following repetitive exposures. This slow mechanism may relate to subsequent nerve fiber layer loss in the papillomacular bundle reflecting changes in the long wavelength cone system.

These morphologic and functional findings suggest that damage due to repetitive and cumulative laser exposures at non-thermal levels may be present but not suspected or detected if conventional clinical examination techniques are used. Compete evaluations of suspected cases of repetitive and non-thermal laser injuries should employ specific spectral confocal imaging techniques and chromatic, spatial-selective visual function testing. Concerns for similar changes following repetitive environmental or occupational laser exposures[1,9] and subsequent progressive, cumulative changes in long wavelength cone system, nerve fiber layer, and papillomacular bundle are credible.

5. References

1 K. Gunduz, and G. B. Arden. "Changes in contrast sensitivity associated with operating argon lasers," Br. J. Ophthalmol. Vol. 73, pp. 241-146, 1989.

2 H. Zwick, B.E. Stuck, D. Gagliano, V.C. Parmley, J. Lund, J. Molchaney, J. J. Kearney, and M. Belkin. "Two informative Cases of Q-Switched laser Eye Injury" Letterman Army Institute of Research Report No. 463 Jul 1991

3 H. Zwick, D.A. Gagliano, J.A. Zuchlick, B.E. Stuck, D.J. Lund, and R Glickman. "Confocal scanning laser evaluation of repeated Q-switched laser exposure and possible retinal NFL damage" SPIE Proceedings Series Laser Tissue Interaction VI Vol. 2391 1995

4 J. W Rhodes, J.A Zuchlick, H. Zwick, D. A. Gagliano, P.V. Garcia, D. J. Lund, and B. E. Stuck. "Bullseye-Gap maculopathy associated with repeated large spot Q-switched laser exposure, " Investigative Ophthalmology and Visual Science, Vol. 34, p.1516
5 R. S. Harwerth and H. G. Sperling. "Prolonged color blindness induced by intense spectral lights in Rhesus monkeys," Science Vol. 174, pp. 520-523, 1978.
6 H. Zwick, B.E. Stuck, and E. S. Beatrice. "Low level laser effects on Rhesus visual function," Ocular Effects of Non-ionizing Radiation SPIE Vol. 229, pp. 55-62, 1980
7 J. Lanham. "The damaging effect of light on the retina, empirical findings, theoretical and practical implications," Survey o f Ophthal. Vol. 22, pp. 221-249, 1978.
8 W. T. Ham and H. A. Mueller. "The photopathology and nature of the blue light and near-UV retinal lesions produced by lasers and other optical sources," Ed. M.L. Wolbarsht, pp. 191-246, Plenum Publishing Corporation, N.Y., 1989.
9 T. A Berninger, C. R. Canning, K. Gunduz, N. Strong, and G. A. Arden. "Using argon laser blue light reduces ophthalmologist' color contrast sensitivity," Arch. Ophthalmol. Vol. 107, pp. 1453-1458, 1989.
10 H. Zwick, E. S. Beatrice, and T. A. Garcia. "Long-term and progressive changes in Rhesus spectral sensitivity after low-level coherent light (514 nm) exposure," Letterman Army Institute of Research: Color Deficiencies V: Chapter 1, pp. 52-60, 1980
11 A. E. Ariffin, J. Birch, P. J. Polkinghorne, and C. R. Canning. "Colour vision changes following pan-retinal photocoagulation with the dye laser," Khewer Acadamie Publishers, Colour Vision Deficiencies X, pp. 529-532, 1991.

The opinions or assertions contained herein are the private views of the authors and are not to be construed as official or as reflecting the views of the Department of the Army, Department of the Air Force or Department of Defense.

Human Volunteers participated in these studies after giving their free and informed voluntary consent. Investigators adhered to AR 70-25 and USAMRMC Regulation 50-25 on the use of volunteers in research.

Morphological and histological changes on skin induced by 1540 nm laser radiation.

Alexei V.Lukashev, Valery P. Solovyev(*), Boris I.Denker, Vadimir I.Kaz'min(*)

General Physics Institute, 38 Vavilov Str., Moscow 117942, Russia
Phn: (095)-135 3038, Fax: (095)-135 2055, e-mail: lukashev@kapella.gpi.ru
(*) Institute of Biophysics, 46 Zhivopisnaya Str., 123098 Moscow, Russia

ABSTRACT

The dose-response relationship for producing different grades of burns on skin produced by single Er-glass laser pulse(λ=1540 nm) were determined for energy densities within the range 0.5-35 J/cm^2 and pulse duration 100 ns and 2.5 ms. The persistent lesions on skin were subdivided into four morphologically different groups vs. radiant exposure of laser pulses. Histological investigation were made at 1- and 3- days post-exposure. Different methods of tissue preparation were tried to obtain better contrast of laser induced changes in skin tissue. At the 1-day post-exposure we observed on the histological samples coagulation of surface tissue, epidermis and dermis of skin depending on radiant exposure. 3-days histological samples revealed tearing of tissue detrit and active epitalization of damaged tissue.

Keywords: Medical applications of lasers, Er-glass laser, laser damage of skin.

1. INTRODUCTION

This work was a development of investigation on laser safety for skin using 1540 nm laser radiation[1]. The goal was to classify super-threshold modifications on skin such as surface damage, coagulation and ablation and estimate their possible medical applications.

Since Er-glass laser systems were oriented for military applications(range finders, laser radars, etc.) and had not been wideused in medical practice, it was very little information on its medical applications and especially for skin treatment. The absorption coefficient of water-contained tissue(cornea, skin ,etc.) at 1540 nm (α=10 cm^{-1}) is in between to that of at 1064 nm of Nd-laser(α= 0.4 cm^{-1}) and 2120 nm of Ho-laser(α=40 cm^{-1}). There are many works have been published so far on medical applications of Nd and Ho lasers. Intermediate tissue absorption at 1540 nm could be interesting for optimization of different skin modification made with Nd and Ho lasers. As a result of considerable progress in laser and crystal growth technologies Er-glass laser system both with flash lamp and diode pumping could be developed for medical applications.

The research reported was undertaken to receive experimental data on super-threshold interaction of 1540 nm laser radiation of an Er glass laser with skin in the wide range of laser energy fluences and pulse duration.

2. METHODS

2.1 Laser System

In experiments we used 1540 nm Erbium-glass laser radiation in a wide range of energy densities and pulse duration produced by an original laser system operating in both free-running and Q-switched regimes. The basic optical setup is presented in Fig.1a.

The active rods of the laser were made of Er-activated phosphate-based glass which was designed and produced in General Physics Institute[1]. In order to enhance its efficiency under flashlamp pump operation the glass was co-doped by chromium and ytterbium ions. The rods used in the laser system had diameter of 6-7 mm, length 85-90 mm and AR coatings of both ends. The single-lamp pump cavity had narrow (1-1.5 mm) channels for water cooling of Xe flashlamp and glass rod. Narrow channels are required to reduce pump radiation absorption by water in the spectral band of ytterbium absorption (0.85 - 1.05 micrometers). This peculiarity of laser cavity design has made it possible to avoid cooling of the laser head by deuterised water and thus to reduce the cost of the laser system.

In the free-running regime the laser head was supplied with a flat 65% reflectivity output mirror. The output energy reached 6-8 J in multimode and the plug efficiency - 1.5 - 2 %. The pulse duration was about 3 ms.

SPIE Vol. 2974 • 0277-786X/97/$10.00

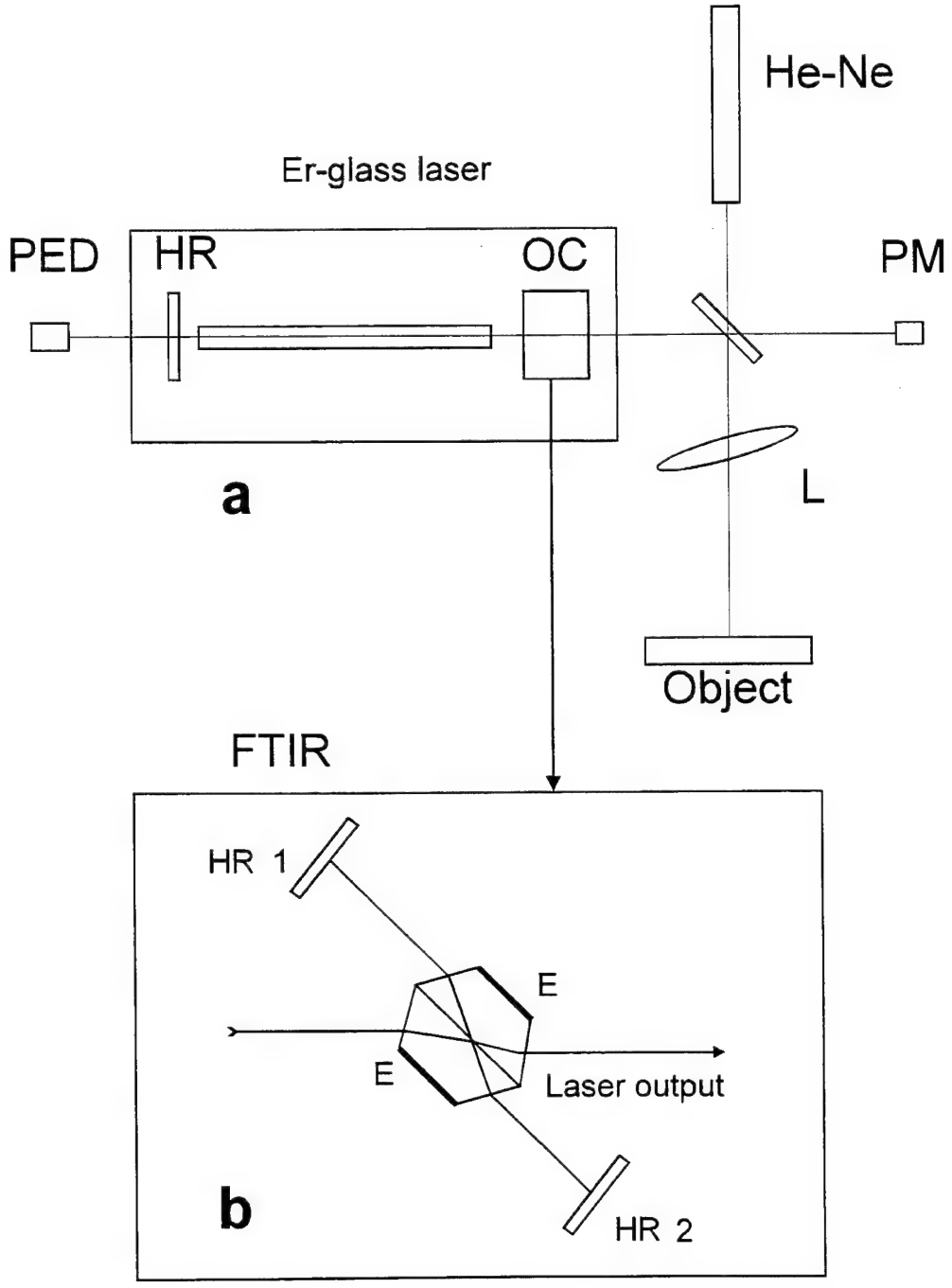

Fig.1. Experimental optical setup. HR-high reflecting mirror, OC-output coupler (a mirror for free running and FTIR modulator for Q-switching), PED- pyroelectric detector, PM-power meter, E-electrodes.

To obtain Q-switched regime the laser output mirror was substituted by a frustrated total internal reflection (FTIR) optical shutter in combination with two highly reflecting at 1.54 micrometers flat mirrors[2] (Fig.1b). This kind of shutters has been chosen due to its high optical damage threshold, low insertion losses in combination with low (100 V) driving voltage and insensitivity to laser beam polarization state. Our shutter consisted of a pair of truncated fused silica pyramids having a rigid connection with each other. The gap of about 0.5 micrometer wide between the pyramids can be rapidly collapsed to zero with the help of two piezoelectric cells mounted on the truncated facets of each pyramid. The output energy of Q-switched laser reached 0.5 J in multimode beam and pulse duration was about 100 ns. In experiments laser output parameters was monitored by pyroelectric detector PED(pulse duration) and by power meter PM (output energy)(Fig.1).

A tilted lens L is used to compensate non-uniformity of the pump and thermo-induced lens and astigmatisms in the laser rod. The density of the laser radiation on the target can be varied with the help of either pump variations or neutral filters, and also by changing the size of illuminated spot by varying the optical power of the focusing lens. The aiming and focusing of the laser beam on the target was made with the help of a pilot He - Ne laser beam coaxial with the Er-glass one. The beam shape on the object plane was round with diameter 2-10 mm for free running and 2-4.5 mm for Q-switched modes. The corresponding maximum energy fluence was up to 35 J/cm^2 for free running and 20 J/cm^2 for Q-switch modes.

2.2 Animals

In experiments we used white domestic pigs free of visible pigmentation. Pigs were selected because of histological resemblance of their skin to that of man. The pigs were 1.2-2 months old and weighted 8-16 kg.

One day before the experiment the bristle on the animal's back and sides was removed with hand clippers and then shaved. No visible skin reaction(reddening, cuts, etc.) was observed on the skin at the time of experiments because of hair removing. The depilated area was divided into a grid of squares about 15x15 mm in size. A side of the animal could have up to 90 cells.During experiments we did not used any anesthetic agents, since we assumed possible influence of anesthesia to the skin reaction.

2.3 Experimental procedure

The main task of the study was determination of lesion threshold and supra threshold effects on animal skin made during single pulse exposures and histological investigation of the damaged skin. The study included investigation both with free running and Q-switched laser pulses.

The experimental set was started up with preliminary estimation of the ranges and values of dose which produce visible lesions. We started with maximum energy fluence determined by laser output parameters and then decreased the dose by step of 0.5-1 J/cm^2 . Five cells on the animals were exposed by the pulses with the same dose.

The skin reaction data was obtained by visual examination the areas exposed at several minutes, one-hour and at 24 hours post exposure. In general, the one-minute reaction at a given radiant exposure level served as a guide in determining whether increased radiant exposure levels should be given. In general, a very mild erythematous reaction at one-minutes will probably fade at one-hour. This level would represent the lowest level to be used. A definite well demarcated erythematous reaction on the skin at one-minutes will probably be present at one-hour examination.

At one-hour post exposure, each area exposed was again visually controlled and photographed. The number of "reactions" (this could be erythema, papules, blanching, etc.) were determined at each exposure level. The burns were categorized independently by two investigators. A similar examination and photographs were done at 24 hours post-exposure. Experimental data were processed by the probit method of Litchfield and Wilcoxon[3]. This data, expressed as a percentage of the reactions observed at each exposure level, was plotted on probability scale and the radiant exposure at the 50 percent probability level was taken as the ED50 level.

In the subsequent experimental sets probability of specific skin response in the range of transient reaction was determined more accurately. To do this we exposed up to ten cells with the same fluence close to threshold range in order to have more accurate statistical data. To obtain truly data and estimate deviation of individual reaction we conducted experimental set on three animals and then the results were averaged.

3. RESULTS

3.1 Morphology

Clinical analysis of the skin damaged by 1540 nm laser radiation showed that laser radiation produced lesions of different grades of heaviness. We classified observable skin reaction into following five types, assuming that at minimum persistent lesions(no.2,3) only superficial epithelium structures of skin are damaged in the most of the cases.

1. Diffusive, transient erythema that appeared within a minute post exposure and usually extended beyond the limits of exposed area. Within several or dozen minutes(< 1 hour) the diffusive reddening decreased in size disappeared entirely. This was the functional reaction of blood vessels to laser action.
2. The persistent lesion(erythema) of round flat form(which does not come over the surface of the skin) and red color. Its size corresponded to the size of laser beam.
3. Erythema as described in the previous grade with infiltration(inflation). The nidus protruded over uninjured skin.
4. Coagulation of subepidermal layers of dermis. The round almost flat nidus of white color with the very thin red circle of inflammation.
5. Coagulation of deeper layers of dermis. The round nidus of white color with strong protruded inflammation.

In the first set of experiments(Free running, τ=2.5 ms, the spotsize diameter 5.5 mm) the radiant exposure ranged from 1.1 J/cm^2 to 23 J/cm^2.

ED50 at 1 hour post exposure was found to be 5.7±1.2 J/cm^2. 282 burns were processed. ED50 at 24 hour post exposure 6.5 J/cm^2.

The skin reaction No. 3(erythema with inflation) started at 8 J/cm^2.

The skin reaction No.4 (flat coagulation) - 13 J/cm^2.

Coagulation of dermis - 22 J/cm^2.

In the second set of experiments(Q-switch, τ=100 ns, the spotsize diameter 2.5-3.5 mm) the radiant exposure ranged from 1.7 J/cm^2 to 16 J/cm^2. ED50 at 1 hour post exposure for persistent erythema was found to be 3.0±1.1 J/cm^2. 266 burns was processed. ED50 at 24 hour post exposure 3.5 J/cm^2 .

We did not clearly distinguish burns described in the No.3 of skin reaction.

The flat coagulation was at 9 J/cm^2.

An example of skin damages is shown in the Fig.3. The deviation of individual sensitivity of animals and skin at different places (back, belly) in the both sets was within 15 % of obtained data..

3.2. Histology

Histological investigation was conducted at 1- and 3-days post-exposure. Different methods of tissue preparation and coloring was used. Classification of damage grades was done not only by estimation of deepness of the damage but also by the state of subepithelium blood vessels net.

Histological study at 1-day post exposure generally confirmed our classification of damaged skin. Analysis of histological samples at 3-days PE revealed fast epitalization of the damaged area. In the case of burns of III-degree(No.4 in skin reaction classification) it was found that new epithelium intruded from adjacent undamaged skin underneath the area of necrosis(showed by arrow in Fig.4b). We observed that epitalization developed not only from surface vicinity but also from inside, out of hear matrix. Thus hair-skin showed fast regeneration of damage.

4. DISCUSSION

The skin response resulting from exposure at 1540 nm is considered to be a result of temperature elevation of the tissue. The clinical description of skin burns at 1540 nm is fairly coincides with that of at 10.6 μm of CO_2 laser[4,5,6]. Histolological investigation also showed that morphological changes of skin exposed to 1540 nm laser radiation is similar to that of contact burn and exposure to 10.6 μm radiation. The geometry of the experiment and estimation of the cooling of the exposed volume suggests weak influence of heat dissipation in our experiments,

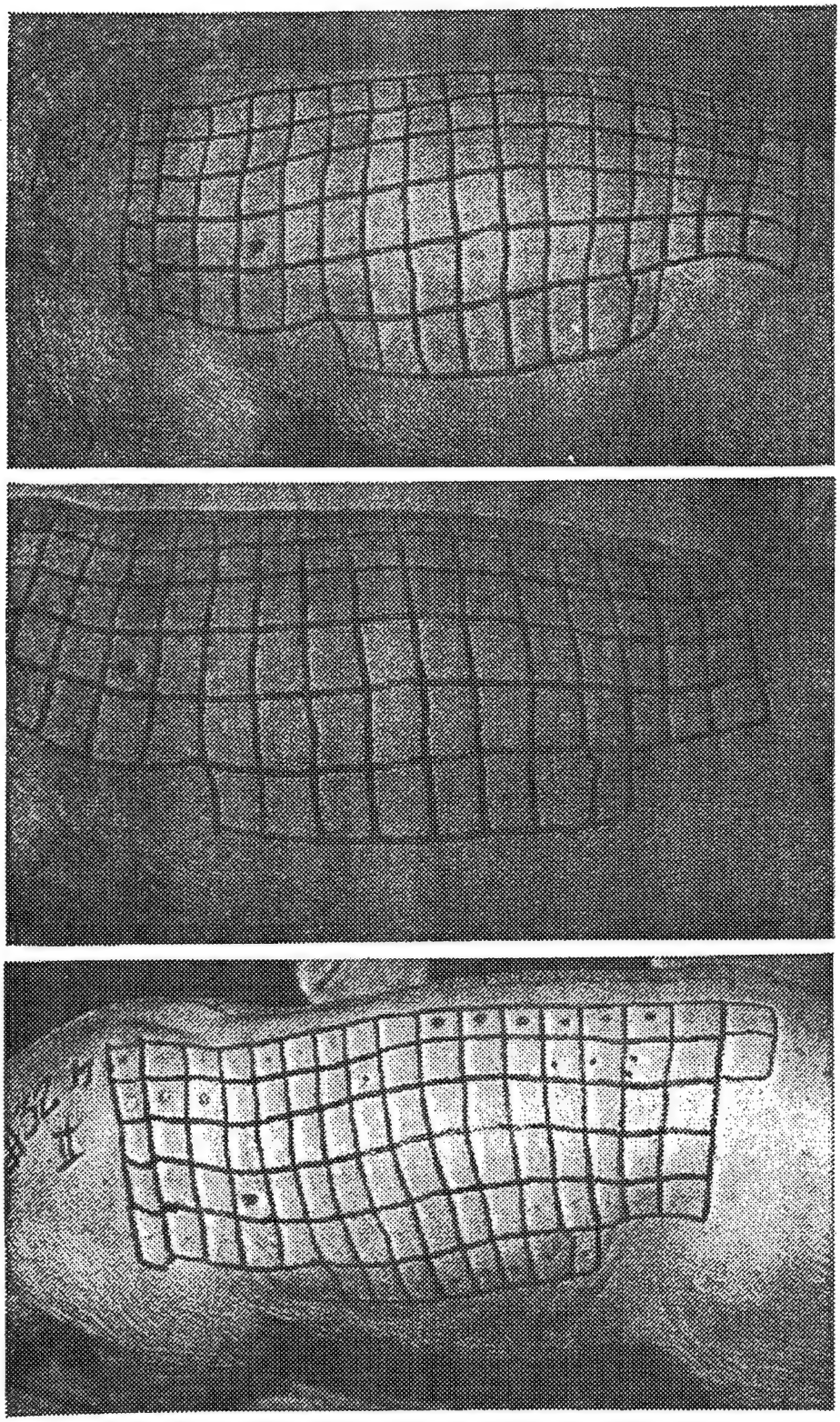

Fig.2 . A view of skin lesions caused by free running radiation of Er-glass laser. **a** - 5 minutes post-exposure (PE), **b** - 1 hour PE, **c** - 24 h PE.

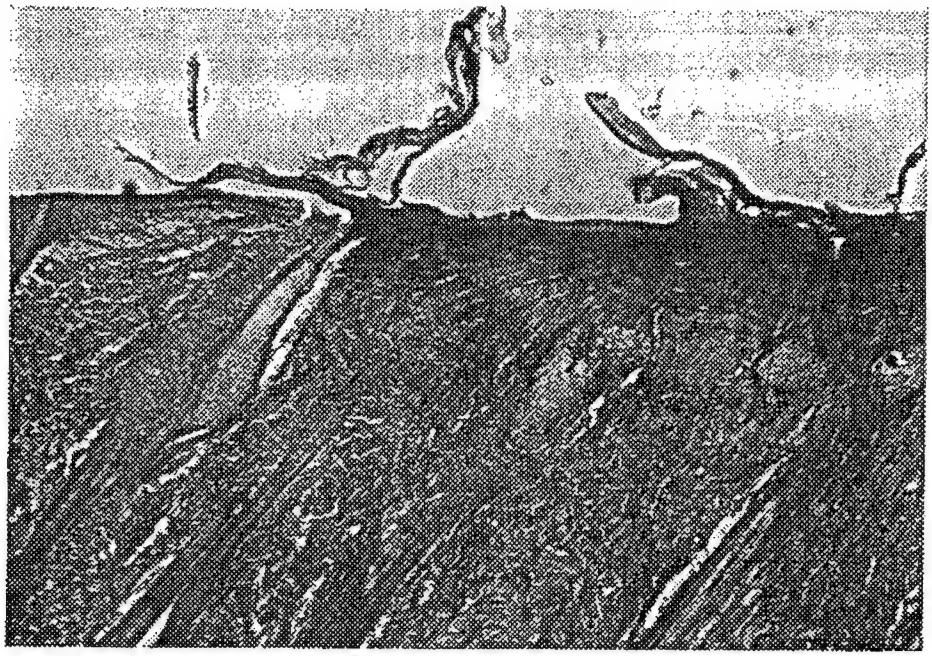

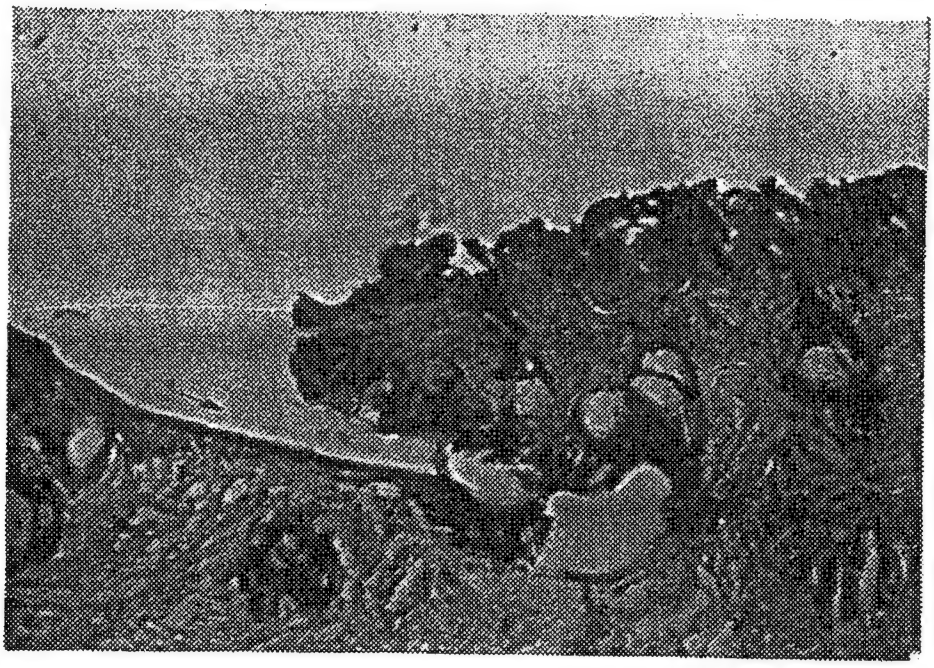

Fig.3. Histological cuts of the damaged skin. **a-** 24 hours post exposure, **b-** 72 h PE

especially for short pulses (< 1 μs) (Fig. 4). The penetration depth h of laser light at 1540 nm to water is about 1 mm(the absorption coefficient $\alpha \approx 10$ cm^{-1} [7,8], in the first approximation we consider that true for the skin too. The smallest laser beam diameter on skin was 2 mm and the largest 10 mm (long pulses: free running). Characteristic cooling time t_c of the layer thickness h could be estimated from formula $h \approx (\chi t_c)^{1/2}$, where χ- thermal diffusivity of water ($\chi = 1.4\ 10^{-3}$ cm^2/s). For water layer 1 mm thick which is equal to penetration of laser light into water t_c is equal 10 sec . The cooling time is much longer than pulse duration for both laser pulses(100 ns and 2 ms), only in the latter case some weak heat dissipation could be considered. If again to use water substance as a model for our experiment, the equivalent temperature rise $\Delta T = E_l/(Shc_p)$ is 8^0 C for short and 15^0 C for long pulses at ED50 dose; 20^{0}C and 34^{0}C respectively for coagulation. (E_l - laser energy, S - laser beam cross section, c_p - specific heat, $c_p = 4.2$ J/(Kcm^3)). Thus, the absolute temperature of the animal skin is higher than 42-43^0 C which is close to the temperature of protein denaturation. The greater value of ED50 for longer pulses we explained by the influence of heat dissipation during the laser pulse.

5. CONCLUSIONS

In this study we experimentally determined reaction of porcine skin(*in vivo)* to exposure by 1540 nm radiation of Er-glass laser. The persistent lesion of the skin in the range up to 35 J/cm^2 was classified. The ED50 value for minimal lesion was found to be 5.7 J/cm^2 for millisecond and 3.0 J/cm^2 for nanosecond laser pulses. The skin coagulation starts at 13 J/cm^2 for millisecond and 9 J/cm^2 for nanosecond pulses.

Histological investigation generally confirmed our classification of skin burns by 1540 nm radiation and proved thermal mechanism as the main of skin damage. It was found fast epitalization of damaged skin. The results of this work might be used for possible applications of 1540 nm radiation for surface skin operations(cosmetic surgery).

6. ACKNOWLEDGMENT

This work was partly supported under USAF Contract F61708-94-C-0008 arranged via European Office of Aerospace Research and Development(EOARD). Authors are grateful to Dr.N.Tankovich for the interest to this work and useful comments.

7. REFERENCES

1. Denker B.I., Maximova G.V., Osiko V.V., Sverchkov S.E., Sverchkov Yu.E. Lasing parameters of GPI erbium glasses. Solid State Lasers III. Ed.G.J.Quarles, Proc.SPIE 1627:37-41, 1992.

2. Denker B.I., Fefelov A.P., Kertez I., Khomenko S.I., Kroo N., Luk'yanov A.L., Osiko V.V., Sverchkov S.E., Sverchkov Yu.E. A compact FTIR Q-switched 1.54 μm erbium glass laser. p.99-101 in Laser in Engineering. Proc.11 Int.Cogress 'Laser 93', Springer-Verlag, 1994.

3. Litchefield J.T., Wilcoxon F., A simplified method of Evaluting Dose-Effect Experiments. J.Pharmacol.Exp.Ther. 96(2):99,1949.

4. Brownell A. S., Parr W. H., Hysell D. K., Dedrick R. S., CO_2 Laser induced skin lesions, Rep. 769, Research in Biomedical Sciences, DA Project No. 3A014501B71R USAML, Fort Knox, Kentucky 40121,1968.

5. Brownell A. S., Parr W. H., Hysell D. K., Skin and Carbon Dioxide Laser Radiation Arch. Environ.Health 18 :437-440, 1969

6. Brownell A. S., Stuck B.E. Ocular and skin hazards from CO_2 laser radiation, Joint AMRDC-AMC Laser safety team, Frankford Arsenal,Philadelphia, PI

7. Stuck B.E., Lund D.J., Beatrice E.S. Ocular effects of Holmium(2.06 μm) and Erbium (1.54 μm)laser radiation. Health Physics 40(6): 835-846, 1981.

8. Zolotarev V.M., Morozov V.N., Smirnov E.V. Optical constants of natural and technical substances, Handbook, Ed."Chemistry", Leningrad,1984.

SESSION 3

Injury (Mechanisms)

In vivo confocal scanning laser ophthalmoscopic characterization of retinal pathology in a small eye animal model

H. Zwick, R. Elliott, S.T. Schuschereba, D. J. Lund, B.E. Stuck

US Army Medical Research Detachment
Walter Reed Army Institute of Research
San Antonio, TX 78235

ABSTRACT

We have used confocal scanning laser ophthalmoscopy (CSLO) to evaluate acute laser retinal injury in a small eye animal model. The snake eye is optically unique, combining a high numerical aperture with a clear ocular media and a cornea covered with a hard dry *spectacle.* These optical qualities allow detailed resolution of photoreceptors, retinal nerve fiber, and retinal capillary blood cells in an intact vertebrate eye. We demonstrated that acute laser exposures capable of damaging the photoreceptor matrix may also alter blood flow at more anterior levels of the retina. Changes in photoreceptor density and orientation were indicated in the early post exposure seconds at high dose acute Argon laser exposures. An increase in photoreceptor reflectivity was observed in surviving photoreceptors and was enhanced with a near IR CSLO imaging source. Q-switched exposure failed to show this enhancement, possibly because of greater subchoroidal involvement associated with acoustic damage processes.

Keywords: laser, numerical aperture, small eye optics, confocal ophthalmoscopy, photoreceptors, blood toxicity.

1. INTRODUCTION

Numerous investigations have demonstrated significant damage to photoreceptors induced by laser exposure.[1] Acute human laser injuries that are definable by laser exposure generally involve penetration of the entire retina including subretinal choroidal vasculature.[2] Hemorrhage, retinal scar formation, and retinal nerve fiber layer damage are often associated with high dose acute laser injuries. Lower level exposures may be restricted to photoreceptor alteration or damage in the absence of injury to other layers. Recent evidence supports involvement of the vascular retinal network in mediating inflammatory products released by acute laser injury.[3] While the damage process may involve complex biochemical events leading to cell death, data suggest that reorganization of the photoreceptor matrix may play an important role in visual function recovery from acute laser exposure.[4]

For these reasons, we have employed a unique combination of imaging technology and animal model selection to clearly image the photoreceptor matrix *in vivo*. We have used confocal scanning laser ophthalmoscopy (CSLO) to evaluate acute laser injury to the retina in a small eye animal model. The snake eye is optically unique, combining a high numerical aperture with a clear ocular media and a cornea covered with a hard dry *spectacle*. These

SPIE Vol. 2974 • 0277-786X/97/$10.00

optical qualities allow detailed resolution of photoreceptors, retinal nerve fiber layer, and retinal capillary blood cells in an intact vertebrate eye.

2. METHODS

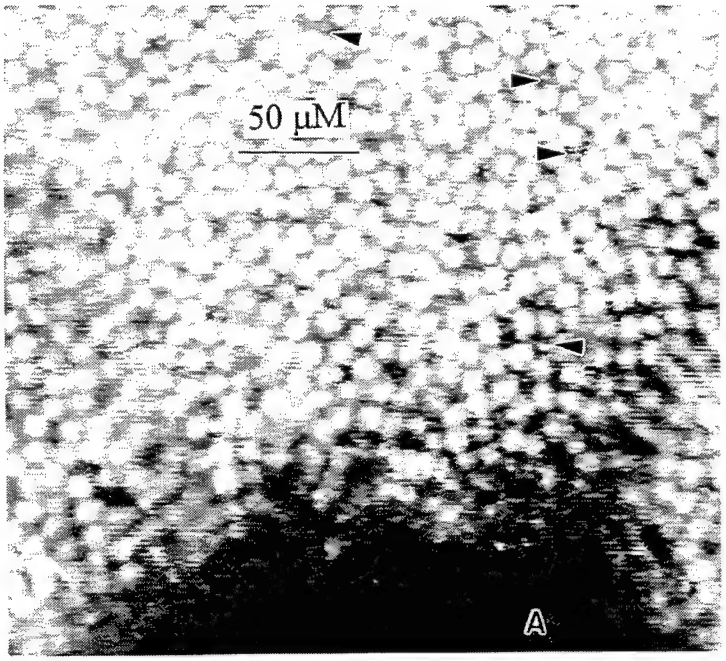

Figure 1a. CSLO image of Checkered Garter snake retina showing large, 7-9μ and small cones 2-4μ.

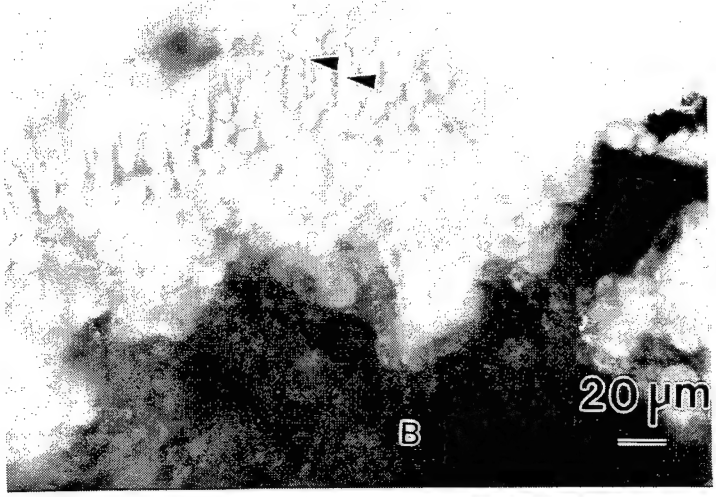

Figure 1b. Histological flat preparation of snake photoreceptors, 7-9μ.

Images of the Checkered Garter snake (*Thamnophis m. marcianus*), the Great Plains Rat Snake (*Elaphe guttata emoryi*) and the Western Coachwhip (*Mastcophis flagellum testaceous*) retinas were recorded and digitized from a Rodenstock confocal scanning laser ophthalmoscope (CSLO). The optical powers of these eyes are estimated at 445, 370, and 205 diopters, respectively. A 0.1 diopter change in these eyes corresponds to a 0.5, 0.7 and 5.0 micron shift, respectively, in focal depth at the retinal plane.[4] An air-cooled Argon laser (488 and 514nm) provided acute laser exposures ranging from 152 to 1000 μjoules Total Intraocular Energy (TIE) for 10-100msec pulse widths. A Q-switched Neodymium 532nm laser was used at energy levels from 6 to 18 μjoules. Retinal spot size was about 35 microns. Anesthesia was achieved with a combination of Ketamine and Xylazine in a ratio of 3.5:1.

3. RESULTS

Figure 1a is a CSLO view of the Checkered Garter snake retina imaged at the photoreceptor matrix showing large, small single, and small secondary cones. Large cones are about 7-9μ and small cones are about 2-4μ. A retinal flat mount from the Western Coachwhip is shown in Figure 1b. These cones are 7-9μ in diameter in the absence of their natural ocular optics. Outer segments of these

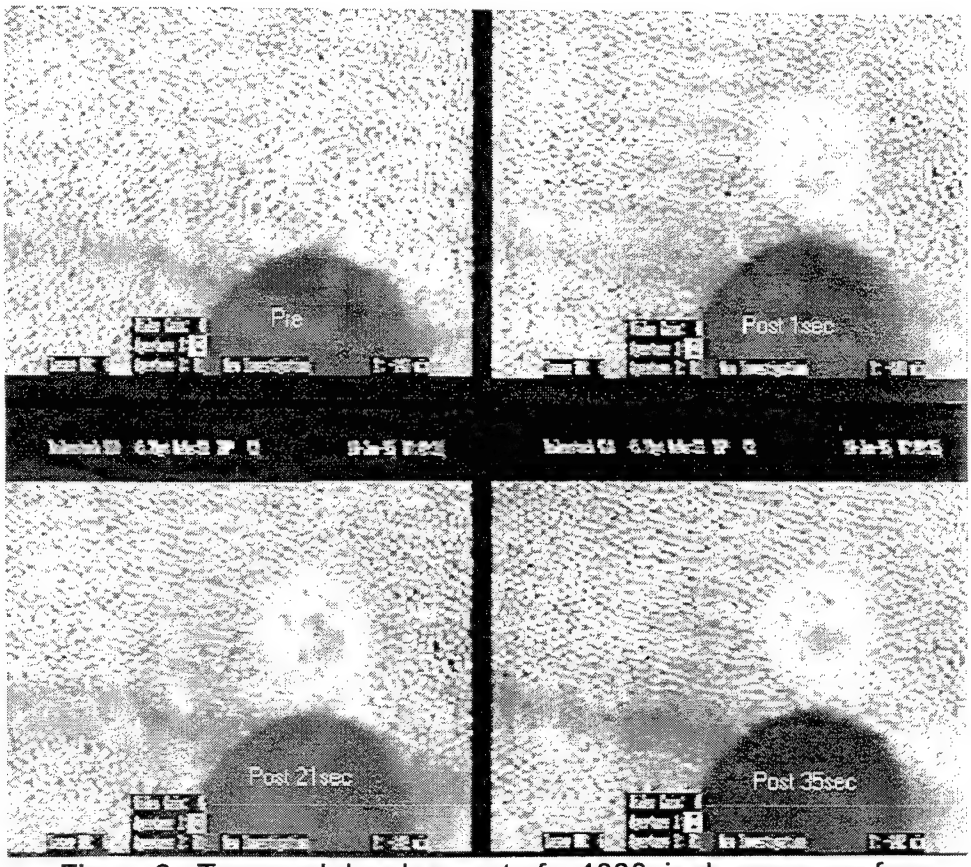

Figure 2. Temporal development of a 1000μjoule exposure from pre-exposure 1, 21 and 35 seconds post-exposure.

photoreceptors are displayed toward the top of this image where photoreceptors have been flattened in more sagittal position (arrows).

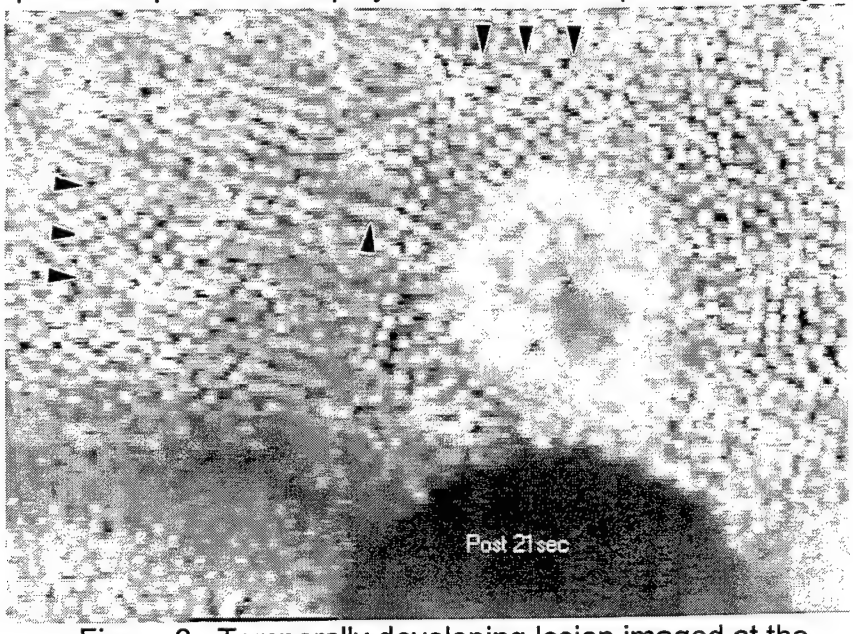

Figure 3. Temporally developing lesion imaged at the photoreceptor layer at 21 seconds post-exposure.

Figure 2 shows the temporal development of a 1000 μjoule exposure from pre-exposure 1, 21 and 35 seconds post-exposure. During this time period the exposed photoreceptor region developed an annulus of highly reflective photoreceptors, enlarged photoreceptors, as observed in the center of the lesion site, and alteration in photoreceptor orientation outside the lesion site, characterized by a "rope-like" appearance of some

regions of photoreceptors apparent at 35 seconds post exposure.

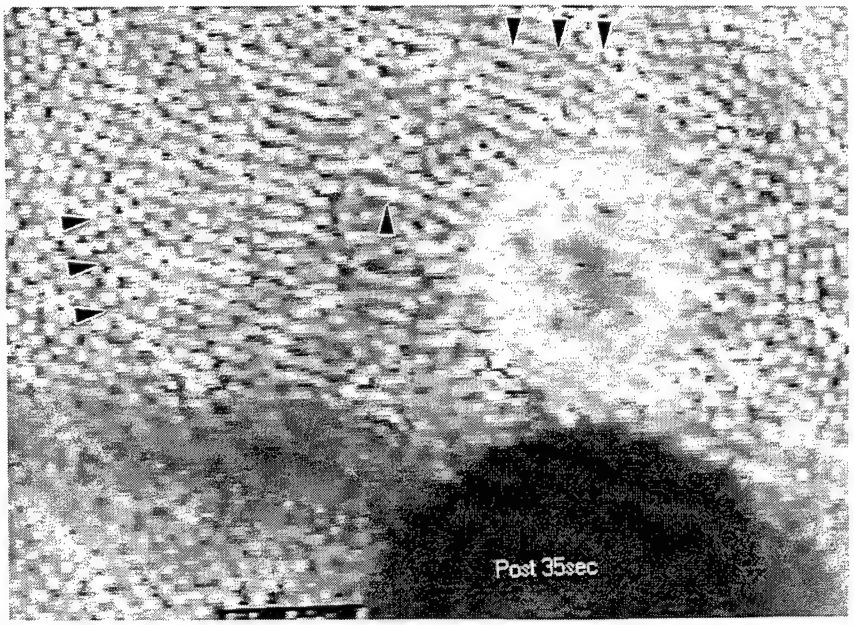

Figure 4. Temporally developing lesion imaged at the photoreceptor layer at 35 seconds post-exposure.

Figures 3 and 4 show fuller views of the photoreceptor images at 21 and 35 seconds post-exposure. The areas of suggested change in receptor orientation are indicated by arrows. Photoreceptors adjacent to the region of highly reflective photo-receptors appear as though they might be lying on their sides in a more sagittal than tangential position, as compared with comparable photoreceptor regions at 21 seconds post exposure. These changes in orientation are characterized by more subtle change in the photoreceptors superior and to the left of the developing ring of reflective photoreceptors, appearing as a more sagittal than transverse view of individual photoreceptors (see arrows).

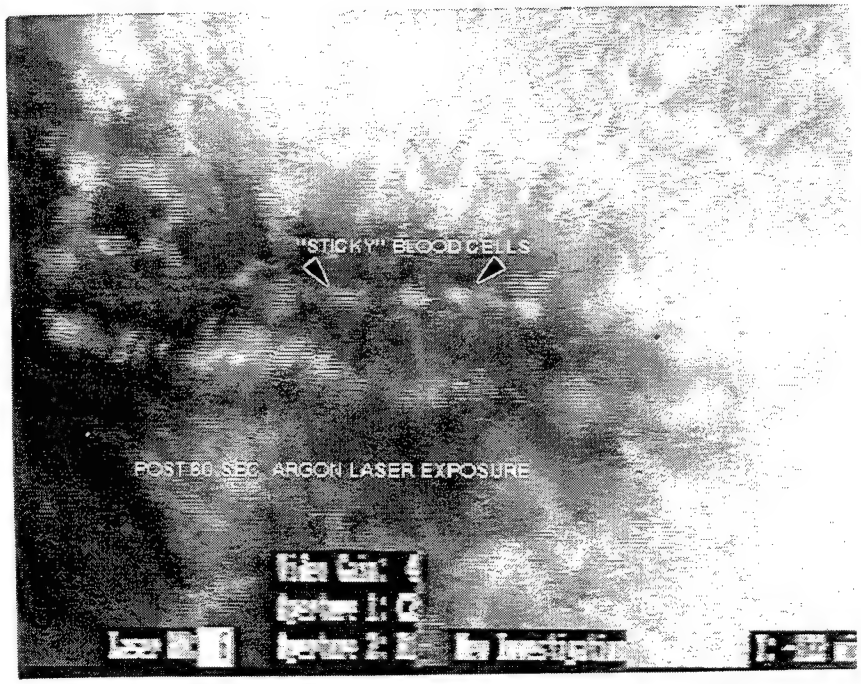

Figure 5. "Sticky" blood cells at 55 seconds post 1000μjoule exposure.

Figure 5 shows the corresponding effect of a comparable 1000 μjoule exposure imaged in the anterior vascular retinal layer. Blood cell flow through the optic disk of the snake (*Conus Papillaris*) showed immediate evidence of slower moving blood cells becoming very apparent at 55 seconds, where at least 5 blood cells were observed in very slow movement through the central vessel of the *Conus Papillaris.*

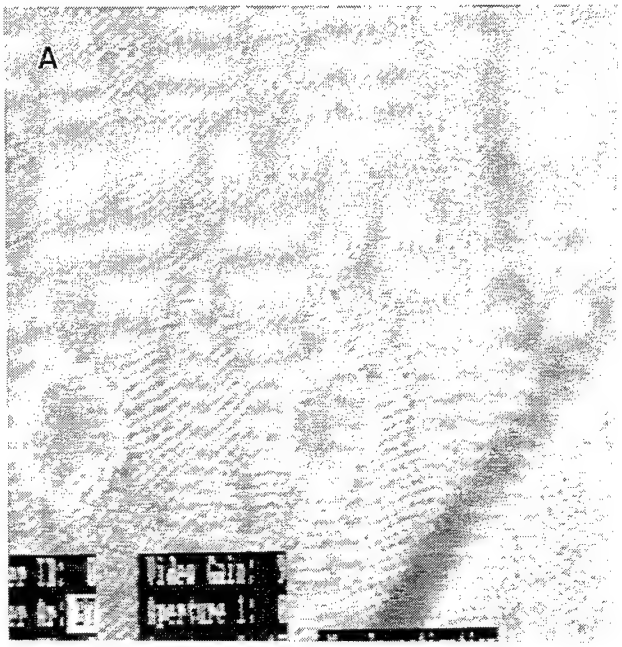

Figure 6a. Argon lesions imaged at 488nm

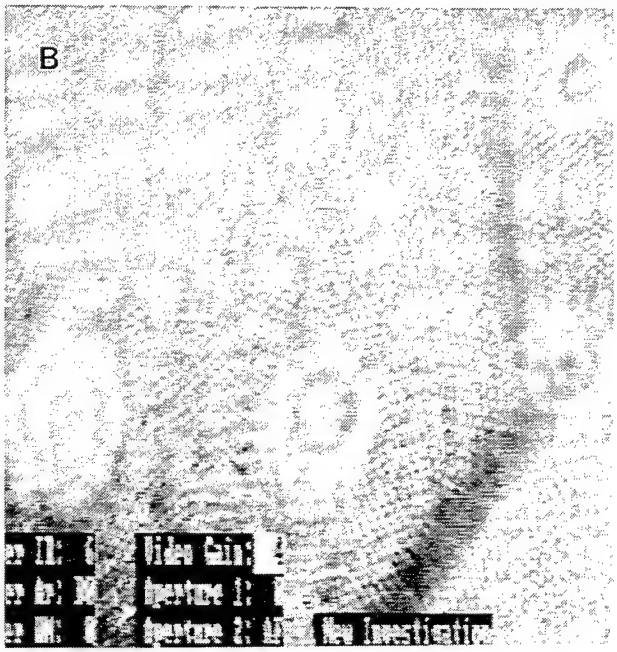

Figure 6b. Argon lesions imaged at 780nm

Figure 6a presents five exposure sites with annular rings of highly reflective photoreceptors, produced by equal energy lesions. Lesion diameter clearly decreases as energy is maintained constant at 500 μjoules by halving the power and doubling the duration of the exposure. The same five lesions were imaged with the 780nm laser diode (Figure 6b), revealing an increase in photoreceptor reflectivity within the central region as well as an increase in the number of reflective photoreceptors, observed in the upper two exposures of longer duration.

Figure 7a and 7b show a comparison of Q-switched 532nm and Argon (488 and 514nm) exposures in the same retina made about 15 minutes apart producing two different lesion sites as a function of imaging wavelength. The Q-switched lesion at the left was induced by a 12 μjoule Q-switched 532nm single pulse, while the Argon laser exposure was made at 500 μjoules. These figures show a differential relationship for photoreceptor reflectivity within the Argon and Q-switched Neodymium laser site. At 488nm, both lesion sites show similar reflectivity(7a). The Q-switched 532nm exposure site darkens and enlarges when imaged with the 780nm source(7b). A significant number of low reflecting and enlarged receptors are observable in this site.

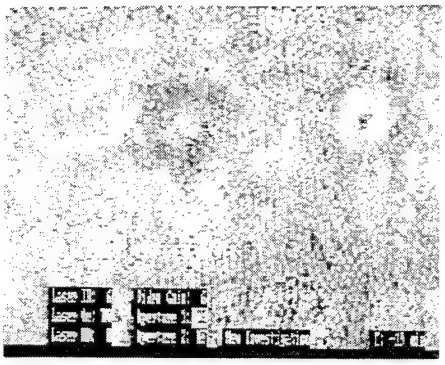

Figure 7a. Argon and Q-switched exposures imaged at 488nm.

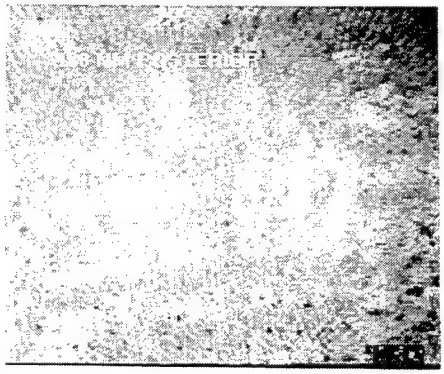

Figure 7b. Argon and Q-switched exposures imaged at 780nm.

4. DISCUSSION

We have demonstrated an enhanced capability to image *in vivo* laser-induced retinal cellular pathology in both the posterior and anterior retina by combining the high numerical aperture and high spatial resolution of the snake eye with the CSLO's ability to traverse retinal depth. We have observed a new type of lesion based on *in vivo* changes to the photoreceptor. The most characteristic feature of these changes is an increase in photoreceptor reflectivity in the annulus surrounding the center of the exposure site, where photoreceptors may have disappeared, become enlarged and at lower doses enlarged and reflective.[4] Moreover, when these exposure sites are imaged in the near IR (780nm) versus the visible (488nm) the number of reflective photoreceptors increases, suggesting that the higher absorption of retinal labile and non-labile pigments in visible light masks additional structural damage to the photoreceptor.

On the other hand we have shown in Figure 7, that Q-switched 532nm and Argon laser induced damage to the photoreceptors display differentially when imaged with visible (488nm) and near IR (780nm) laser sources. The enlarged darkened area shown for the Q-switched exposure may reflect deeper subretinal as well as damage to the photoreceptor structure revealed with visible imaging source. These differences are a consideration in comparing such lesion sites, as Q-switched exposures more easily penetrate the subretina and induce hemorrhagic effects because of acoustic shock wave properties.

Also unique to this investigation of laser induced retinal injury is the ability to image the damage process at anterior as well as posterior retina. We have shown alteration to the anterior blood cell flow following acute Argon laser exposure. While slowing of blood cell flow occurs within the first several seconds post exposure, it rapidly decreases, revealing blood cell "stickiness" after about 1 minute post exposure. Such effects may develop vascular blockages in areas of lesion sites visible several days post exposures as cells "sticking" to vessel walls.[4] The recruitment of "sticky" blood cells may induce secondary damage to the photoreceptors and neural elements by release of chemotoxic compounds associated with laser induced photoreceptor damage.[3]

In summary, we have demonstrated the ability to image *in vivo* laser induced retinal photoreceptor damage, showing unique changes in cellular reflectivity, and characterizes laser induced pathophysiology in the vascular system. These changes we see in living tissue may be absent in fixed histological preparations. Visualization of these dynamic cellular interactions are essential in understanding the morphological reorganization of the retina in response to acute laser injury or low level repetitive injury. Our understanding of how the receptor mosaic reestablishes itself after injury, if it does, and the role of blood cell behavior with regard to the induction of injury are essential in assessing the permanency of functional loss.

5. REFERENCES

1. D.O. Adams, E.S. Beatrice, and B.E. Bedell. "Retina: Ultrastructure alterations produced by extremely low levels of coherent radiation," *Science*, Vol. 31, pp. 9-13, 1972.

2. H. Zwick, S.T. Schuschereba, D.A. Gagliano, M. Silverman, D. Lund, S.B. Reynolds, B.E. Stuck. "Morphological and functional effects of induced laser retinal fibrosis," S.T. Melamed (Ed.), *Laser Applications in Ophthalmology, Europto Series, SPIE*, Vol. 2079, pp30-43, 1993.

3. M.F. Humphrey, Y. Chu, C. Sharp, S. Moore, K. Mann, P. Rakoczy, I.J. Constable. "Glial reactions to argon laser photocoagulation injury in rabbit and rat retinas." B.E. Stuck and M. Belkin (Eds.) *Laser Inflicted Eye Injuries, SPIE*, Vol. 2674, pp.98-106, 1996.

4. H. Zwick, D.J. Lund, R. Elliott, S.T. Schuschereba, P.R. Edsall. "Small eye confocal scanning laser ophthalmoscopy and assessment of retinal damage.", B.E. Stuck and M. Belkin (Eds.), *Laser Inflicted Eye Injuries, SPIE*, Vol. 2674, pp.80-88, 1996.

5. M.F. Land and A.W. Snyder. "Cone mosaic observed directly through natural pupil of live vertebrate." *Vision Research*, Vol. 25, pp. 1519-1523, 1985.

6. R.O.L. Wong. "Morphology and distribution of neurons in the retina of the American Gartertalis," *Journal of Comparative Neurology*, Vol. 283, pp. 587-601, 1989.

Variation of Retinal ED_{50} with Exposure Duration for Near-IR Sources

David J. Lund, Daniel R. Fuller, Stephen W. Hoxie and Peter R. Edsall

US Army Medical Research Detachment, Walter Reed Army institute of Research,
San Antonio, TX

ABSTRACT

A body of data relates the ED_{50} for laser-induced retinal damage to exposure duration for visible-wavelength laser exposure and for 1064 nm laser exposure. The data base, extending from sub-nanosecond exposures to kilosecond exposures, can for the most part, be fit to models based on thermal interactions, thermal-mechanical mechanisms, and photochemical processes. Exceptions to this fit occur between 1 and 100 microseconds where the damage mechanism transitions from exclusively thermal to thermal-mechanical. Disagreement exists as to whether this anomalous dip of ED_{50} is real or is an artifact of the data. We determined the laser-induced retinal ED_{50} in Rhesus monkey eyes for several exposure durations from 12 nanoseconds to 1000 milliseconds at 755 nm using a dye laser, an alexandrite laser, and a Ti:Sapphire laser. These data do not show a dip in ED_{50} in the microsecond time period

Key Words: Laser, retina, damage threshold, Ti:Sapphire, near infrared, time dependence

1. INTRODUCTION

In recent years, a number of tunable lasers have become available which in composite span the wavelength range from 700 nm to 1000 nm and the temporal range from femtoseconds to continuous operation. Interest in this spectral range has been driven by the fact that it includes the emission wavelengths of most semiconductor lasers and light emitting diodes (LEDs). Laser diodes and LEDs are so pervasive in commercial optoelectronic products that the probability for ocular exposure of any individual is near unity. One would assume that a predictable relationship between ED_{50} and wavelength would be documented for the visible and near-infrared based on early data and tissue absorption characteristics. Such is not the case. Lund reported variability in the relationship of ED_{50} to wavelength in the region between 700 nm and 900 nm. and showed evidence for nonlinear laser/tissue interaction mechanisms.

A body of data relates the ED_{50} for laser-induced retinal damage to exposure duration for visible-wavelength laser exposure and for 1064 nm laser exposure. Green-emitting (frequency doubled neodymium and argon) lasers and near infrared (neodymium) lasers show similar dependence of ED_{50} upon ocular exposure duration (**Figure 1**). The data, extending from femtosecond exposures to 1000 second exposures, can for the most part be fit to models based on thermal interactions, thermal-mechanical mechanisms, and photochemical processes. Exceptions occur, most notably for exposures in the 1 μs to 100 μs duration range where the damage mechanism transitions from exclusively thermal to thermal-mechanical. The data indicate that the ED_{50} may decrease as the exposure duration increases from 1 μs to 100 μs. Disagreement exists as to whether this anomalous dip of ED_{50} is real or an artifact

of the data. The purposes of this study were to determine the time dependence of ED_{50} for lasers emitting in the deep red spectral region, and to relate this data to ED_{50} vs. exposure duration data for green-emitting and 1064 nm lasers.

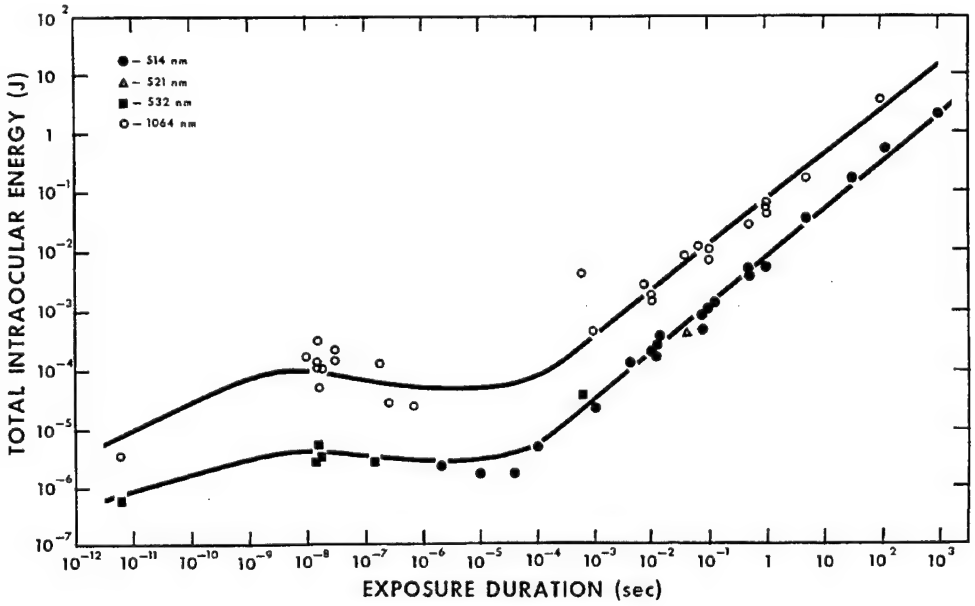

Figure 1. The ED_{50} for laser induced retinal damage in Rhesus monkey as a function of the exposure duration for visible and 1064 nm radiation. All data are for minimum retinal irradiance diameter exposure and 1 hour observation time.

2. MATERIALS AND METHODS.

2.1 Lasers

A number of lasers were used to span the time domain from 12 ns to 1000 ms

12 ns duration pulses were generated by a Molectron Model DL-18 dye laser pumped by the second harmonic output of a Molectron MY33 Nd:YAG laser

Three alexandrite lasers were used. The first emitted 200 ns pulses when operated in the Q-switched mode or 50 μs pulses in the non-Q-switched mode.. The second emitted pulses of 175 ns duration in the Q-switch mode. In the non-Q-switched mode, 6 μs pulses were obtained by using the pockel cell switch, as a shutter to gate the normal-pulse output duration. The third alexandrite laser emitted non-Q-Switched pulses of 350 or 750 μs duration, switch selectable. The first laser was tunable over the range from 730 nm to 780 nm. The wavelength of the other two was fixed at 755 nm.

10 ms to 1000 ms exposures were obtained from a Spectra Physics Model 3900 Ti:Sapphire laser pumped by the 514.5 nm output of a Coherent INOVA 100 argon laser.

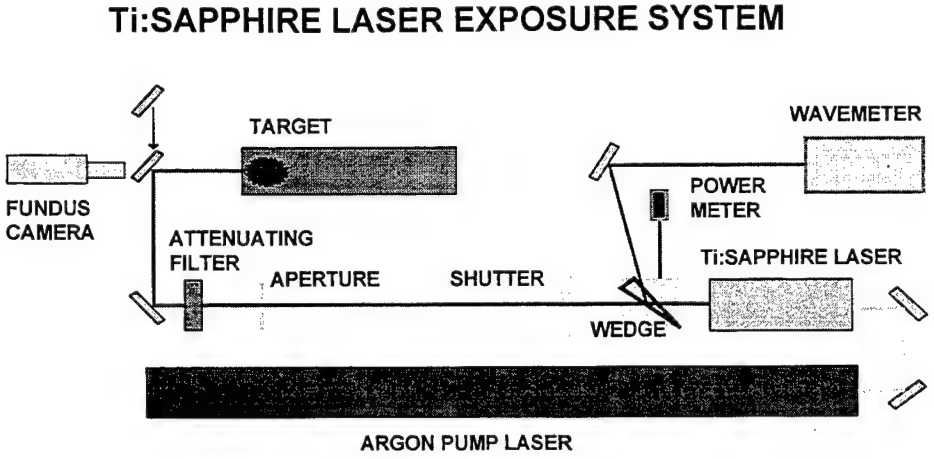

Figure 2: Schematic of laser exposure system employed to expose the rhesus monkey eyes. The argon laser pumped the Ti:Sapphire laser. An optical wedge directed a portion of the beam into a reference detector and a portion into a Wavemeter. A shutter controlled the exposure duration. After passing through attenuators, the beam was directed by mirrors into the target (animal eye or calibrated detector). The mirror in front of the fundus camera was translated to permit observation of the target retina.

2.2 Experimental Technique

Figure 2 is a representative exposure system. A portion of the laser output was directed by a beamsplitter into a Burleigh Model 4000 Wavemeter so that the laser could be accurately tuned to the desired wavelength and the wavelength could be continuously monitored. A shutter determined the exposure duration for continuous beam lasers or selected a single pulse from a pulse train for repetitive pulsed lasers. A beamsplitter deflected a constant proportion of the pulse energy into a reference detector while the remainder of the energy passed through attenuators and onto a mirror which directed the laser beam into the eye to be exposed. The mirror was mounted on a translation stage so it could be moved to permit observation and accurately repositioned for exposure. A fundus camera permitted observation of the retina and selection of sites for exposure. The fundus camera, mirror, and laser beam were aligned so that the laser energy reflected by the mirror passed through the center of the ocular pupil and struck the retina at the site corresponding to the crosshairs of the fundus camera viewing optics.

Before the rhesus monkey was positioned, a calibrated detector was positioned to directly receive the power that would normally enter the eye. The ratio of the power at this position to the power at the reference detector was obtained with the attenuator removed. Subsequently, when the eye was exposed, the power entering the eye for each exposure was determined by multiplying the power at the reference detector by the ratio previously determined and by the transmission of the attenuating filter chosen to give the desired power.

The alexandrite lasers emitted far more energy than was required for this study, and it was necessary to greatly attenuate the energy reaching the subject animal eye. The laser beam was expanded, recollimated, and apertured to limited the beam delivered to the eye. The laser beam diameter at the eye position was 4 mm for all exposures.

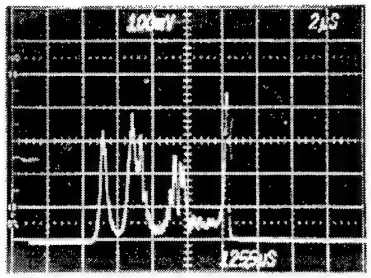

6 microsecond pulse

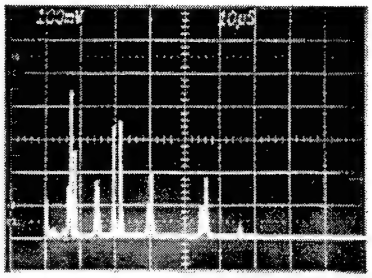

58 microsecond pulse

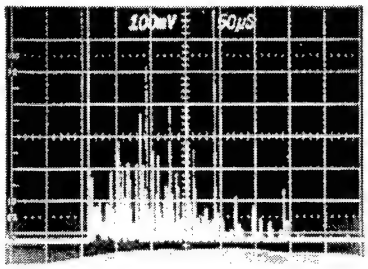

350 microsecond pulse

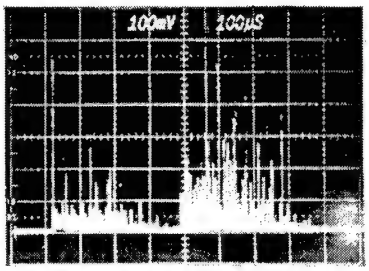

750 microsecond pulse

Figure 3. Representative oscillographs of alexandrite laser emission at 6, 58, 350, and 759 µs pulse duration. For each duration, the emission consists of a series of relaxation oscillations which vary from shot to shot within an envelope which is consistent in duration from shot to shot.

The beam divergence, and pulse duration were determined for each exposure condition. A silicon photodetector (EGG Lite-Mike) and an oscilloscope were used to record the pulse durations. The determination of pulse duration for the Q-switch pulses and the shuttered CW was straightforward, and the full-width-half maximum (FWHM) values are reported. The emission duration of the non-Q switched lasers required interpretation. **Figure 3** shows representative oscillograph traces of the emission durations used in this study. The number and shape of the individual pulses within the envelope for the non-Q-switch emission varied from shot to shot, but the envelope duration remained relatively constant. The duration of the exposure for these cases was defined to be the time from the first significant pulse to the last significant pulse (The criterion for significance was the judgment of the first author and was consistent throughout these measurements). For each non-Q-switched exposure duration, ten shots were recorded via oscillograph and the duration of each shot determined. The average duration of these ten is reported.

2.3 Experimental Subjects

Rhesus monkeys were sedated and anesthetized for exposure. Cycloplegia and full pupil dilation were pharmaceutically induced in both eyes, and the eye to be exposed was held open by a lid speculum. The cornea was periodically irrigated with physiological saline solution to maintain clarity. For each test, an animal was positioned and 30 exposures were placed in an array in the extramacular retina. The initial row of six exposures in each sequence were at a dose high enough to produce an immediate visible retinal burn. Subsequent exposures were at lower doses so that the range of doses in the array varied by about a factor of ten. The retina was photographed and the exposure sites marked on the photograph for subsequent identification. The exposure sites were examined via direct ophthalmoscope one hour after

exposure and the presence or absence of visible alteration noted for each site. The response at each site was correlated to the dose at that site. For each wavelength, the data obtained by exposure of four to six eyes were statistically evaluated to determine the ED_{50} and associated 95% confidence limits.

3. RESULTS

The ED_{50}s for retinal alteration in Rhesus monkeys were determined for 10 exposure duration at 755 NM. The criteria was the presence of an alteration visible via ophthalmoscope one hour after exposure. These data are presented in **Table 1** and **Figure 4.**

Table 1
ED_{50} FOR LASER INDUCED RETINAL DAMAGE IN RHESUS MONKEY AT 755 nm

PULSE DURATION	ED_{50} μJ	95% LIMITS μJ	SLOPE
12 ns	9.3	8.02-10.9	1.64
175 ns	11.5	10.1-13.0	1.49
200 ns	11.8	9.98-14.0	1.84
5.9 μs	35.9	31.1-41.5	1.75
58.1 μs	58.5	52.4-65.4	1.47
321 μs	118	107-127	1.40
761 μs	135	119-153	1.37
10 ms	440	431-449	1.10
100 ms	2470	2310-1650	1.21
1000 ms	11900	11030-13030	1.29

4. DISCUSSION

The 755 nm ED_{50} does not conform to the exposure duration dependency shown for the green and infrared laser exposures. Between 200 ns and 750 μs, the ED_{50} varies approximately as $t^{0.3}$ where t is the exposure duration . There is no evidence of a dip in the ED_{50} vs exposure duration curve between 1 and 100 μs. Rather, there is an orderly transition between a region of constant energy below 200 ns and a region above 1 ms where the ED_{50} varies as $t^{0.75}$. In attempts to explain the dip in the ED_{50} , it has been argued that in the region of transition between laser/tissue interaction mechanisms, energy might be dissipated in the weaker mechanism and not contribute to eventual tissue damage. The data of this study would support the argument that energy is not dissipated, but is conserved, and all the energy contributes to tissue damage regardless of which interaction mechanism it encounters.

The 755 nm data is compared to the ED_{50} data for green emitting lasers and 1064 nm lasers in **Figure 5**. The data for all three wavelength regions are similar for short exposures and for long exposures, and the ratio of ED_{50}s is consistent with predictions based on the optical properties of the Rhesus monkey eye

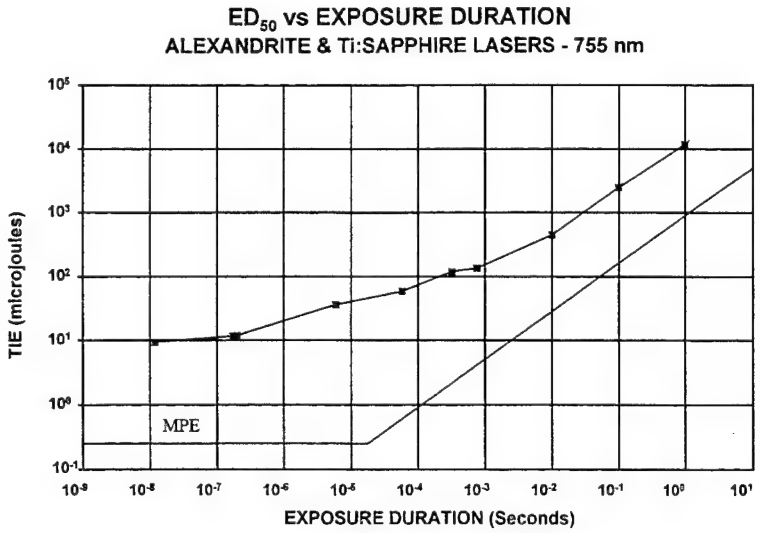

Figure 4. The ED_{50} for laser-induced retinal damage in Rhesus Monkey retina are plotted for 10 exposure durations. The ED_{50} is given as the Total Intraocular Energy (TIE) which is the total energy incident at the cornea within the ocular pupil diameter. The laser sources were a dye laser, 3 alexandrite lasers and a Ti:Sapphire laser, all operating at 755 nm., These data are compared to the MPE at 755 nm.

The lines of **Figure 5** through the visible and 1064 nm data simply connect constant ED50 to constant slope. These data do not preclude an orderly transition as exhibited by the 755 nm data. Neither do they necessarily support such a transition.

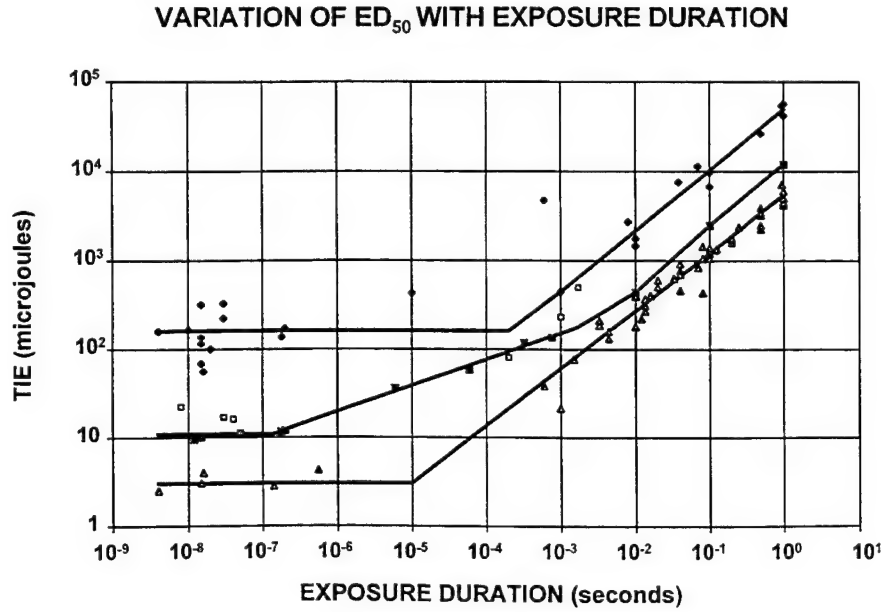

Figure 5. The ED_{50} for laser-induced retinal damage in Rhesus Monkey retina at 755 nm (squares) is compared to the ED_{50} s for exposure to green-emitting lasers (diamonds)and 1064 nm lasers (triangles).. The ED_{50} is given as the Total Intraocular Energy (TIE) which is the total energy incident at the cornea within the ocular pupil diameter.

This study used a wavelength of 755 nm because that is the wavelength of the nontunable alexandrite lasers used to obtain some of the exposure durations. **Figure 6** Shows the variation of $ED_{50}$with wavelength in the near-infrared for two of the lasers used in this study. The ED_{50} is relatively constant with wavelength around 755 nm. Other intervals show rapid changes of ED_{50} with small changes of wavelength. The data for 15 ns exposure and 100 ms exposure strongly suggest nonlinear interaction mechanisms at 860 nm. While the data of this study is valid for 755 nm exposure, it may not be representative of the time dependence of ED_{50} for other near-infrared wavelengths

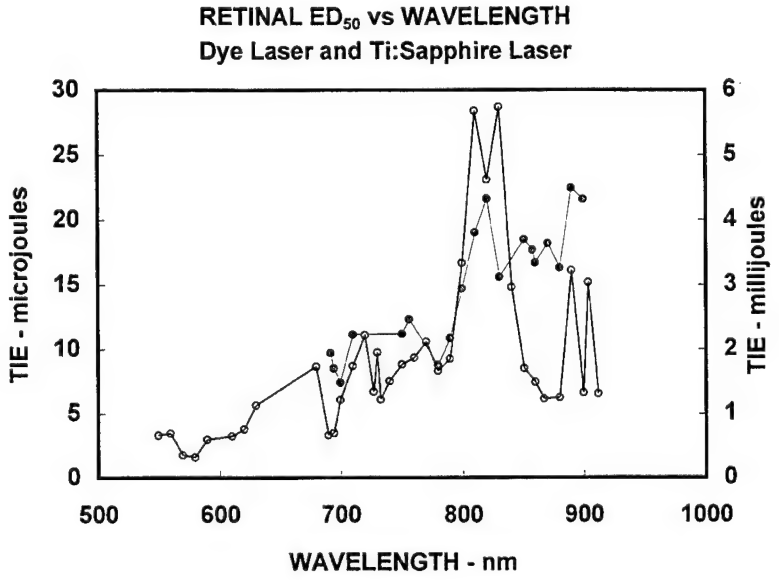

Figure 6. The ED_{50} for laser-induced retinal damage in Rhesus Monkey retina as a function of wavelength in the near infrared for 15 ns dye laser exposure (open circles, left scale) and 100ms Ti:Sapphire laser exposure (closed circles, right scale). The ED_{50} is given as the Total Intraocular Energy (TIE) which is the total energy incident at the cornea within the ocular pupil diameter. The ED_{50} is relatively constant in the region near 755 nm . Nonlinear laser/tissue interaction is suggested at 870 nm.

5. CONCLUSIONS AND RECOMMENDATIONS

The data of this study do not show a minimum of ED_{50} for laser induced retinal damage at 0.1 to 10 μs exposure duration. Rather, the ED_{50} at 755 nm increases as $t^{0.3}$ for exposure durations from 0.2 μs to 750 μs. The transition from thermal damage mechanisms to thermal/mechanical damage mechanisms appears to be energy conservative in that all the energy contributes to tissue alteration for all distributions of energy into the two interaction mechanisms. Comparison of these data to the MPE (Figure 4) show that the standards are certainly adequate and are probably conservative in the 1 to 100 μs time frame for 755 nm laser exposure. In other studies we have demonstrated evidence for nonlinear interaction mechanisms at some NIR wavelengths (**Figure 6**). Nonlinear interaction mechanisms might dramatically alter the ED_{50} vs exposure duration relationship. Further research of the time dependence of ED_{50} is recommended for other NIR wavelengths.

6. DISCLAIMER

In conducting the research described in this report, the investigators adhered to the "Guide for the Care and Use of Laboratory Animals,", as promulgated by the Committee on Revision of the Guide for Laboratory Animal Facilities and Care, Institute of Laboratory Animal Resources, National Academy of Sciences - National Research Council.

The opinions or assertions contained herein are the private views of the authors and are not to be construed as official or as reflecting the views of the Department of the Army or the Department of Defense.

Citation of trade names in this report does not constitute an official endorsement or approval of the use of such items.

7. REFERENCES

1. WT Ham, Jr., AM Clarke, WJ Geeraets, SF Cleary, HA Mueller, and RC Williams, "The eye problem in laser safety," *Arch Env Health*, 20:156- 160, 1970.

2. ES Beatrice, DI Randolph, H Zwick, BE Stuck, and DJ Lund, "Laser hazards: biomedical threshold investigations," *Mil Med*, 14(11):889-892, 1977.

3..DJ Lund,, PE Edsall, DR Fuller, and SW Hoxie. Ocular hazards of tunable continuous-wave near-infrared laser sources. In: Laser-inflicted Eye Injuries: Epidemiology, Prevention, and Treatment. Bruce E. Stuck, Michael Belkin, and Abraham Katzir, Editors. SPIE 2674:53-61;1996

4. DJ Lund and ES Beatrice , "Near Infrared laser ocular bioeffects." *Health Physics*; 56(5): 631-636. 1989

5. RG Allen, SJ Thomas, RL Harrison, JA Zuclich, and MF Blankenstein. "Ocular effects of pulsed Nd laser radiation: Variation of threshold with pulsewidth". *Health Physics*; 49:5: 685-692. 1985

6. DG Odom, DJ Lund, and ST Schuschereba. "Histopathology of suprathreshold retinal lesions produced by the Alexandrite laser." *Lasers in the Life Sciences*; 2(2): 113-124. 1988.

7. DH Sliney and ML Wolbarsht, *Safety with Lasers and Other Optical Sources*, New York: Plenum Publishing Corp., 1980.

8. DJ Finney, *Probit Analysis*, New York: Cambridge University Press, 1971

9 ANSI (American National Standards Institute), *Safe Use of Lasers, Standard Z-136.1*, Cincinnati: Laser Institute of America, 1993.

10. US Department of the Army, AR40-46: *Control of Health Hazards from Lasers and Other High Intensity Optical Sources*, Headquarters, Department of the Army, Washington, DC, 15 November 1978.

11. US Department of the Army, *TBMED 524: Control of Hazards to Health from Laser Radiation*, Headquarters, Department of the Army, Washington, DC, 30 June 1985.

Ultrashort Laser Pulse Retinal Damage

Benjamin A. Rockwell, William P. Roach[*], Dale Payne, Paul Kennedy, Jeffrey Druessel, Rodney Amnotte, Brent Eilert, Shana Phillips[†], David Stolarski[+], Gary Noojin[+], Clarence Cain[+] and Cynthia Toth[*]

Air Force Armstrong Laboratory, AL/OEOP, 8111 18th Street, Brooks Air Force Base, TX, 78235-5215

[*]Air Force Office of Scientific Research, AFOSR/NL, 110 Duncan Ave, Bolling AFB, DC 20332

[†]Air Force Armstrong Laboratory, AL/OEV,2509 Kennedy Circle, Brooks Air Force Base, TX, 78235-5118

[+]TASC, 4241 Woodcock Dr., Suite B-100, San Antonio, TX, 78228-1330

[*]Duke University Eye Center, P.O. Box 3802, Durham, NC 27710

ABSTRACT

Recent studies of retinal damage due to ultrashort laser pulses[2,3] have shown that less energy is required for retinal damage for pulses shorter than one nanosecond. Laser minimum visible lesion (MVL) thresholds for retinal damage from ultrashort (i.e. < 1 ns) laser pulses are produced at lower energies than in the nanosecond (ns) to microsecond (μs) laser pulse regime. We review the progress made in determining the trends in retinal damage from laser pulses of one nanosecond to one hundred femtoseconds in the visible and near-infrared wavelength regimes. We have determined the most likely damage mechanism(s) operative in this pulse width regime and discuss implications on laser safety standards.

Keywords: eye, laser, nonlinear optics, retinal damage, safety

2. INTRODUCTION

Lasers are currently proliferating which produce sub-nanosecond laser pulses in the visible and near infrared spectral regions. These wavelengths easily propagate through the eye and can

SPIE Vol. 2974 • 0277-786X/97/$10.00

result in retinal damage and functional vision loss if appropriate laser protective measures are not used. Unfortunately, there exists no current Air Force or national laser safety standard which specifies allowable exposures for pulses shorter than 1 ns in duration. In recent works by Cain, et al. [1,2,3] MVL threshold data for ultrashort single laser pulses show a decrease in the amount of pulse energy needed to cause observable retinal damage below 1 ns and LIB was shown to influence those thresholds below 150 fs for the visible wavelength regime. According to the growing sub-nanosecond single-pulse MVL data base, one can conclude that extending the current microsecond to nanosecond constant-corneal-fluence-regime ANSI standard to shorter pulse durations may prove to be imprudent and possibly that the current guidance to use constant power may be overly conservative.

In this study we review the nonlinear optical phenomena considered in previous studies and the influence of these phenomena on the amount of energy required for retinal damage, here defined to be the MVL threshold. We will consider recent near infrared (NIR) MVL studies and their impact on determining new damage mechanisms. In general it should be noted that the single-pulse MVL data shows three broad trends. For exposures longer than 20 μs there is a region where near constant irradiance (W/cm^2) is required for retinal damage. For pulses from 1 ns to 20 μs, diffusion of heat is negligible during the exposure and the fluence (J/cm^2) required for retinal damage is nearly constant. The third regime occurs for pulse durations shorter than one nanosecond where the data shows that it takes less energy to create retinal damage than for longer pulses.

3. NONLINEAR OPTICAL EFFECTS

There are several nonlinear optical properties which may have an affect on the mechanism of retinal damage or its variation with spot size, wavelength or pulse duration. In previous analyses of ocular damage, propagation effects were seldom cited as having an effect on retinal damage, except for chromatic aberration effects on spot size. We have considered several nonlinear optical phenomena and their plausible effects on retinal damage[4,5].

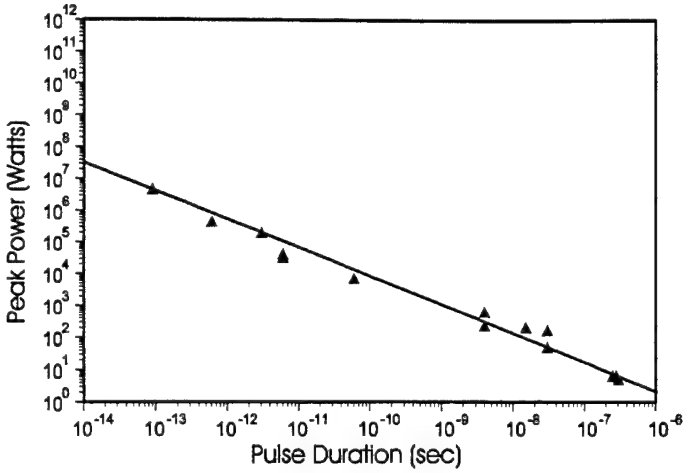

Figure 1. Plotted is the sub-microsecond, single-pulse, visible MVL data available for rhesus monkeys versus pulse peak power. A linear trend is evident across the range from the microsecond to femtosecond regime. The lines are a guide to the eye to emphasize the linear trend in the data.

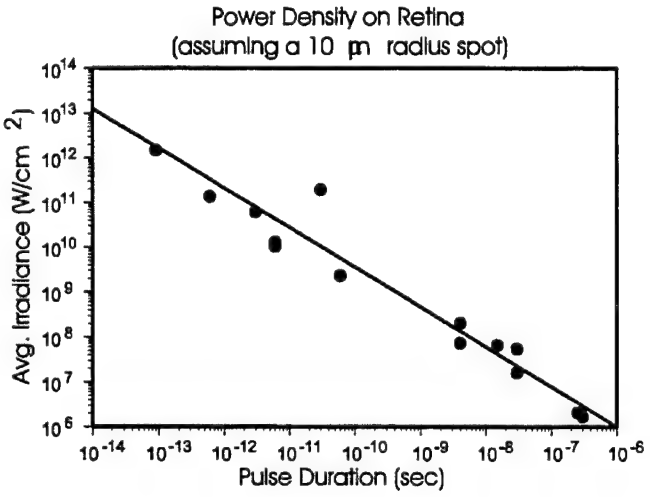

Figure 2. The same data as in Figure 1 is plotted versus average irradiance at the retina assuming a 10 μm spot size on the retina. The lines are a guide to the eye to emphasize the linear trend in the data.

Figure 1 shows a trend in MVL data when they are plotted versus peak power (peak power = energy per pulse/ pulse duration) for visible wavelengths below one microsecond. We see the MVL threshold scales with power in a near linear fashion on this log-log scale. If we assume a retinal spot size radius of 10 μm, we can then plot pulse duration versus average irradiance at the retinal plane. This is shown in Figure 2.

In a previous paper[3] we showed that various nonlinear optical phenomena may influence the spot size, wavelength, bandwidth or pulsewidth that impinges the retina. In long pulse MVL exposures, the spot size on the retina can be defined by knowledge of the wavelength, divergence angle and spot size on the cornea, but nonlinear propagation phenomena also effect the retinal beam characteristics after propagation through the eye. Pictured in Figures 3 and 4 are the

regimes where different nonlinear propagation effects may effect the retinal beam characteristics. We see that self-focusing may affect the spot size for pulses in the femtosecond regime and LIB may affect the MVL threshold for 150 fs and below in the visible.

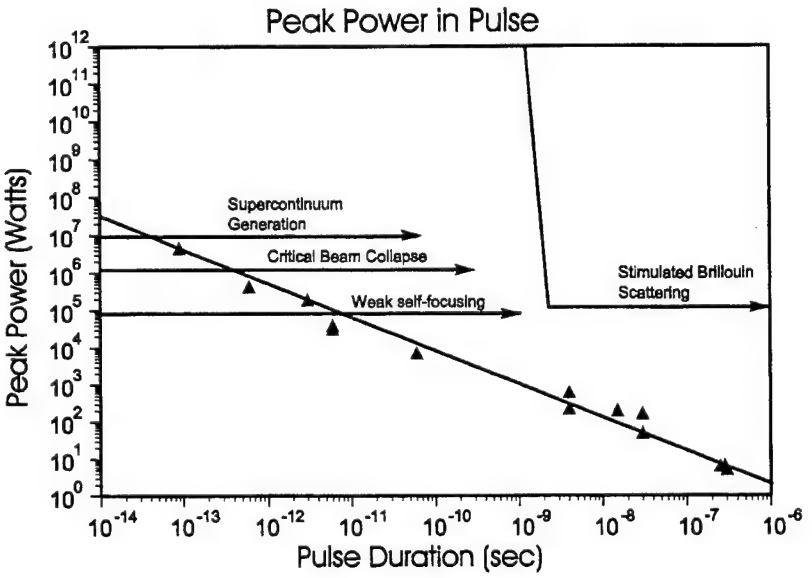

Figure 3. Pictured is the peak power for MVL data (triangles) with an outline of the peak power required for various nonlinear optical effects in the geometry of the eye.

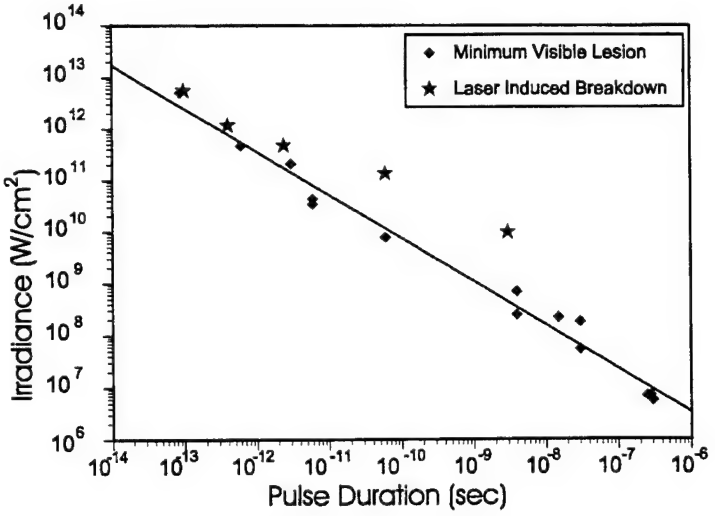

Figure 4. Pictured is the retinal irradiance for MVL points (diamonds) and the threshold for laser induced breakdown (stars) for various pulse widths.

4. CONCLUSIONS

Self-focusing and LIB have been found to be possible factors for subnanosecond MVL thresholds for visible wavelengths. To extend these arguments into the NIR, one needs to consider that NIR wavelengths focus behind the retina[6]. Neither self-focusing nor LIB should be a player for these longer wavelengths, as they both are phenomena related with the focal plane which is behind the RPE for NIR wavelengths. This is true except for LIB which can extend up the beam path for much higher energies, much higher than the MVL threshold for these arguments.

As reported by Cain et al.[7], the NIR MVL data follow the same trend as the visible MVL's. If the decrease in MVL threshold for the visible pulses was due to self-focusing, one would not expect to see the same trend in the NIR data because of the light focusing well behind the retina. Since the data show similar trends, it is suspected that melanin mediated phenomena have an effect on reducing the MVL threshold for ultrashort laser pulses.

The increasing use of ultrashort lasers emphasizes the fact that defining an appropriate maximum permissible exposure limit is necessary. Use of ultrashort laser pulses offers the possibility of unique solutions to many optical problems as well as unique explanations for retinal damage. Studies are continuing to determine the interplay between the nonlinear processes mentioned and melanin mediated effects. The combination of these studies should generate an important biophysical understanding of retinal damage in many pulse and wavelength regimes.

5. ACKNOWLEDGMENTS

This work was supported by the Air Force Office of Scientific Research (2312A103) and Armstrong Laboratory. This research was conducted while Dale Payne held an NRC-Armstrong Laboratory Postdoctoral Research Associateship.

6. REFERENCES

[1] The animals involved in this study were procured, maintained, and used in accordance with the Federal Animal Welfare Act and the "Guide for the Care and Use of Laboratory Animals," prepared by the Institute of Laboratory Animal Resources -- National Research Council.

[2] C. P. Cain, C. D. DiCarlo, B. A. Rockwell, P. K. Kennedy, G. D. Noojin, D. J. Stolarski, D. X. Hammer, C. A. Toth, and W. P. Roach, *Retinal Damage and Laser-Induced Breakdown Produced by Ultrashort-Pulse Lasers*, Graefe's Archive for Clinical and Experimental Ophthalmology **234**: suppl. 1, S28-S37 (1996).

[3] C. P. Cain, C. D. DiCarlo, G. D. Noojin, R. E. Amnotte, B. A. Rockwell and W. P. Roach, *In-Vivo Laser-induced Bubbles in the Primate Eye with Femtosecond Pulses*, in Laser-Tissue Interaction VII, Steven L. Jacques, Ed., Proc. SPIE **2681A**, 382-388 (1996).

[4] B.A. Rockwell, P.K. Kennedy, R.J. Thomas, W.P. Roach and M.E. Rogers, *The Effect of Nonlinear Optical Phenomena on Retinal Damage*, in Laser-Tissue Interaction VI, Steven L. Jacques, Editor, Proc. SPIE **2391**, 89-99 (1995).

[5] C.P. Cain, C.A. Toth, C.D. Stein, G.D. Noojin, D.J. Stolarski, B.A. Rockwell, S.A. Boppart and W.P. Roach, *Femtosecond laser threshold: retinal damage versus induced breakdown mechanisms*, in Laser-Tissue Interaction V, Steven L. Jacques, Ed., Proc. SPIE **2134A**, 22-27 (1994).

[6] B.A. Rockwell, D.X. Hammer, P.K. Kennedy, R. Amnotte, B. Eilert, J.J. Druessel, D. Payne, S. Phillips, D.J. Stolarski, G.D. Noojin, R.J. Thomas, and C.P. Cain, *Retinal Spot Size with Wavelength*, in Laser-Tissue Interaction VIII, Stephen L. Jacques, Editor, Proc. SPIE **2975**, paper 21 (1997).

[7] C. P. Cain, G. D. Noojin, R. E. Amnotte, B. A. Rockwell, *Near-infrared single laser pulses for visible lesion thresholds in the primate eye*, in Laser-Tissue Interaction VIII, Stephen L. Jacques, Editor, Proc. SPIE **2975**, paper 19 (1997).

Investigation of nonlinear ocular media using femtosecond laser pulses

M. J. Potasek[1] and A.E. Paul[2]

[1,2]Air Force Armstrong Lab, Mathematical Products Division
2503 Gillingham Dr., BLDG 175E, Brooks AFB, TX 78235-5102
and
[1]Department of Applied Physics, Columbia University, NYC,NY 10027

[2]Courant Institute of Mathematical Sciences, New York University, NYC, NY

ABSTRACT

The recent development of ultrafast laser systems in the visible and near infrared spectral regions requires detailed knowledge of the material properties of ocular media. Different physical mechanisms play competing roles and give rise to new phenomena as the femtosecond laser pulse propagates in ocular media. We investigate the relative importance of radial diffraction and material dispersion for a wide range of wavelengths for femtosecond laser pulse propagation. Because no analytical solution exists which can fully explain the laser-material interaction, we use numerical techniques. The numerical technique will be described in detail.

Keywords: ultrashort pulses, lasers, self-focusing, dispersion, nonlinear propagation, ocular media

2. INTRODUCTION

Currently, the study of spatiotemporal effects of laser propagation is of significant interest[1-17]. For intense continuous optical waves (cw), the interaction of nonlinearity and diffraction can lead to self-focusing and, for sufficiently intense pulses, to critical collapse where (in principle) the laser beam waist approaches zero and the beam intensity becomes infinite.[1,11] For temporally as well as spatially pulsed optical beams, the nonlinearity couples the spatial and temporal behavior leading to complex dynamical behavior. In a nonlinear dispersive medium, the study of propagating optical pulses have combined the effects of diffraction, Kerr nonlinearity and group velocity dispersion (GVD)[4-9]. The relative sign of the Kerr nonlinearity and the GVD plays a significant role in the dynamics of the light matter interaction. In most studies, a positive Kerr nonlinearity is assumed and used in conjunction with either a negative GVD (anomalous dispersion) or a positive GVD (normal dispersion).

In the negative GVD, it is suggested that a stable light bullet forms.[3] The situation in the positive GVD region is more complex. In the normal dispersion region, the optical pulse broadens along the time axis but compresses (positive Kerr effect) in the transverse direction. This spatiotemporal interplay leads to the splitting of the pulse in both space and time. In the case of weak GVD, the pulse can achieve a high degree of spatial compression before splitting into several subpulses.[4-9]

Nonlinear effects, such as self-focusing, may be responsible for some of the experimental observations for laser eye damage.[18-25] It was recently proposed[2] that normal group velocity dispersion (GVD) increases the peak input power required for two-dimensional self-focusing of ultrashort pulses. Several researchers have examined the effects of weak GVD on self-focusing for picosecond (ps) pulses [4-9]. Normal GVD affects self-focusing by spreading the pulse along the propagation direction. Because cross sections of the light pulse differ in power, those possessing powers that exceed the critical power self-focus at different rates.

Additional experiments [10] showed the presence of light-induced breakdown (LIB) and a propagation model was developed to incorporate LIB [12]. This theory solved a Drude model for the electron density generated by LIB coupled to the paraxial wave equation for the propagating electromagnetic field. This model includes GVD, nonlinear self-focusing, multiphoton absorption, and absorption and defocusing due to the electron plasma.

The recent advent of femtosecond visible and infrared lasers prompts the extension of the interaction of nonlinear, dispersive and diffractive to be extended to new reals. This is because as the optical pulse becomes temporally shorter, the dispersive effects

SPIE Vol. 2974 • 0277-786X/97/$10.00

grow in importance. Previous studies assumed an instanteous (electronic) Kerr nonlinearity. However, in many materials, the Kerr nonlinearity consists of both instantaneous as well as time-delayed components (i.e. Raman terms). This time-delayed component becomes significant for ultrashort temporal pulses and was experimentally observed in optical fibers.

As the temporal pulse with decreases, higher order dispersive effects, beyond the GVD, can make significant contributions to the optical beam propagation. These effects include self-steepening in addition to the time-delayed Kerr effect. In this paper we examine theses effects for a femtosecond optical beam propagating in a Kerr nonlinear, dispersive medium. These results can play a role in ultrashort laser propagation in biological media, such as the vitreous humor, and in bulk media, including solids, liquids and gases.

3. FEMTOSECOND DISPERSION AND DIFFRACTION

The polarization can be written as

$$P(r,t) = \varepsilon_0 \int_{-\infty}^{\infty} \chi^{(1)}(t-t')E(t-t')dt' + \varepsilon_0 \int_{-\infty}^{\infty}\int_{-\infty}^{\infty}\int_{-\infty}^{\infty} \chi^{(3)}(t-t_1,t-t_2,t-t_3)E(r,t_1)E(r,t_2)E(r,t_3)dt_1dt_2dt_3 \quad (1)$$

where E is the electromagnetic field and P is the polarization vector. and (r,t) = (x,y,z,t). We are concerned with the effects of the third-order nonlinearity governed by $\chi^{(3)}$.

$$\chi^{(3)}(t-t_1,t-t_2,t-t_3) = \chi^{(3)}R(t-t_1)\delta(t-t_2)\delta(t-t_3) \quad (2)$$

The nonlinear part of the polarization can be written in terms of the dielectric constant,

$$P_{NL}(r,t) = \varepsilon_0 \varepsilon_{NL} E(r,t) \quad (3)$$

The dielectric constant can be approximated by

$$\varepsilon = (n_0 + \Delta n)^2 \cong n_0^2 + 2n_0\Delta n \quad (4)$$

where n_0 is the linear index of refraction and

$$\Delta n = n_2 |E|^2 \quad (5)$$

and n_2 is the coefficient of the nonlinear index of refraction, $k_0 = \omega_0/c$, and α_K is the coefficient for K photon absorption.

However, the third-order susceptibility includes both resonant and nonresonant (incoherent) intensity-dependent effects and the nonlinear part of the polarization vector can be written as

$$P_{NL}(r,t) = \varepsilon_0 \chi^{(3)} E(r,t) \int_{-\infty}^{t} R(t-t_1) |E(r,t)|^2 dt_1 \tag{6}$$

The response function, R(t) includes both the electronic (instantaneous) and vibrational (time-delayed) terms,

$$R(t) = \alpha' \, \delta(t) + (1-\alpha') f(t) \tag{7}$$

where $\acute{\alpha}$ is the fraction of the response that is instantaneous and f(t) can be obtained from the measured Raman gain curve.

3.1 Theory

The electric field can be written in terms of the rapidly varying part and an envelope function,

$$E(r,t) = \frac{1}{2}(A(r,t)e^{-i(\omega_0 t - k_0 z)} + c.c.) \tag{8}$$

where A(r,t) is the envelope function and ω_0 is the central or carrier frequency of the electromagnetic field. For femtosecond pulses we obtain,[13,14]

$$\left[i\left(\frac{\partial}{\partial z} + k^{(1)}\frac{\partial}{\partial t}\right) + \left(\frac{1}{2k_0} - \frac{k^{(1)}}{2k_0^2}\frac{\partial}{\partial t}\right)\nabla_\perp^2 - \frac{k^{(2)}}{2}\frac{\partial^2}{\partial t^2} - i\frac{k^{(3)}}{6}\frac{\partial^{(3)}}{\partial t^{(3)}}\right] A$$

$$+ \frac{n_2\omega_0}{c}\left(1 + \frac{i}{\omega_0}\frac{\partial}{\partial t}\right) A \int_0^\infty R(t') |A(t-t')|^2 dt' = 0 \tag{9}$$

where $k^{(n)} = d^n k/d\omega^n$ evaluated at ω_0 and $\nabla_\perp$ represents the transverse spatial derivative.

An incident pulse of the form is assumed

$$A(0,x,y,t) = A_0 e^{-\frac{x^2+y^2}{2r_0^2}} e^{-\frac{t^2}{2\tau_0^2}} \tag{10}$$

where r_0 is the spatial beam waist, τ_0 is the temporal width of the pulse and A_0^2 is the peak incident pulse intensity. For simplicity we will now let the transverse coordinates, x ,y be represented by r ($r^2 = x^2 + y^2$).

In order to examine the physics in more detail, we define the length scales

$$L_{DF} = \pi n_0 r_0^{\,2} / \lambda_0 \qquad \text{Diffraction Length}$$

$$L_{DS} = \tau_0^{\,2} / k^{(2)} \qquad \text{Dispersion Length}$$

$$L_{NL} = \lambda_0 / 2\pi n_2 A_0^{\,2} \qquad \text{Nonlinear Length}$$

As the length scale decreases for a particular effect, the more dominant it becomes relative to the other effects. Therefore, if $L_{DF} \ll L_{DS}$, the dominant effect is diffractive; whereas, if $L_{DS} \ll L_{DF}$ the dominant effect is dispersive. Similarly, if $L_{NL} \ll L_{DF}$, the effect is nonlinear.

In many cases the nonlinear terms can be simplified by expanding the field in a Taylor series to obtain

$$\left[i\left(\frac{\partial}{\partial z} + k^{(1)}\frac{\partial}{\partial t}\right) + \left(\frac{1}{2k_0} - \frac{k^{(1)}}{2k_0^2}\frac{\partial}{\partial t}\right)\nabla_\perp^2 - \frac{k^{(2)}}{2}\frac{\partial^2}{\partial t^2} - i\frac{k^{(3)}}{6}\frac{\partial^{(3)}}{\partial t^{(3)}}\right] A$$

$$+ \frac{n_2\omega_0}{c}|A|^2 A + i\frac{n_2}{c}\frac{\partial}{\partial t}\left(|A|^2 A\right) - \frac{n_2\omega_0 T_R}{c}\left(A\frac{\partial |A|^2}{\partial t}\right) = 0 \tag{11}$$

where $T_R = \int_0^\infty t' R(t')dt'$.

3.2 Transformations

Assuming the nonlinear diffractive effect is dominant, we define the transformations

$$Q = \frac{A}{A_0}, \qquad \rho = \frac{r}{r_0}, \qquad \xi = \frac{z}{L_{DF}}, \qquad \tau = \frac{(t - k^{(1)}z)}{\tau_0} \tag{12}$$

and obtain the nondimensioned equation

$$\left[i\frac{\partial}{\partial \xi} + \frac{1}{4}\left(1 - \sigma\frac{\partial}{\partial \tau}\right)\nabla_\perp^2 - \frac{\gamma}{2}\frac{\partial^2}{\partial \tau^2} - i\frac{\delta}{6}\frac{\partial^{(3)}}{\partial \tau^{(3)}}\right] Q$$

$$+ ap\{|Q|^2 + i\sigma\left(2Q^*\frac{\partial Q}{\partial \tau} + Q\frac{\partial Q^*}{\partial \tau}\right) - \tau_R\left(\frac{\partial |Q|^2}{\partial t}\right)\}Q = 0 \tag{13}$$

where

$$a=\left(\frac{1.22\pi}{4}\right)^2, p=\frac{1}{a}\frac{L_{DF}}{L_{NL}}, \gamma=\frac{r_0^2 k^{(0)} k^{(2)}}{2\tau_0^2}, \delta=\frac{r_0^2 k^{(0)} k^{(3)}}{2\tau_0^3},$$

$$\sigma=\frac{1}{\omega_0 \tau_0}, \tau_R=\frac{T_R}{\tau_0} \tag{14}$$

4. NUMERICAL PROCEDURE

The numerical solution is solved in the form

$$\frac{\partial Q}{\partial \xi}=(D_{DS}+D_{DF}+N)Q \tag{15}$$

where D_{DS}, D_{DF}, and N are operators given by

$$D_{DS}=-\frac{i\gamma}{2}\frac{\partial^2}{\partial \tau^2}+\frac{\delta}{6}\frac{\partial^3}{\partial \tau^3}$$

$$D_{DF}=\frac{i}{4}\left(1-\sigma\frac{\partial}{\partial \tau}\right)\nabla_\perp^2 \tag{16}$$

$$N=ap\left\{i|Q|^2-\sigma\left[2Q^*\frac{\partial Q}{\partial \tau}+Q\frac{\partial Q^*}{\partial \tau}\right]-i\tau_R\frac{\partial |Q|^2}{\partial \tau}\right\}$$

Equation (15) can be solved using the symmetric split-step method[14]

$$Q(\xi+\Delta\xi)=e^{\frac{\Delta\xi}{2}D_{DF}}\ e^{\frac{\Delta\xi}{2}D_{DS}}\ e^{\int_\xi^{\xi+\Delta\xi} d\xi'\, N(\xi')}\ e^{\frac{\Delta\xi}{2}D_{DS}}\ e^{\frac{\Delta\xi}{2}D_{DF}}\ Q(\xi) \tag{17}$$

where the exponential operators are defined by their Taylor series expansion. The problem is solved in three separate parts. The linear dispersion operator, D_{DS} is solved in the Fourier domain using the fast Fourier transform (FFT) method. The nonlinear operator, N, is solved in the time domain using the trapezoid rule and iterated until the algorithm converges,

$$\int_{\xi}^{\xi+\Delta\xi} d\xi'\ N[Q(\xi')] = \frac{\Delta\xi}{2}\{N[Q(\xi)] + N[Q(\xi+\Delta\xi)]\} \tag{18}$$

where the first iteration N[Q(ξ+Δξ)] is set equal to N[Q(ξ)] to obtain a guess for Q(ξ+Δξ) which is used for N[Q(ξ+Δξ)] and the process is repeated until convergence is reached. The terms are evaluated using a discrete space and time grid given by

$$\tau \to \tau_i, \xi \to \xi_n, \rho \to \rho_j$$

Therefore $$Q(\xi,\rho,\tau) \to Q(\xi_n,\rho_j,\tau_i) = Q_{ij}^n$$

Then the nonlinear operator can be written as

$$N(\xi_n) = ap\left\{\left|Q_{ij}^n\right|^2 - \sigma\left[2Q_{ij}^{n*}\left(\frac{Q_{i+1,j}^n - Q_{i-1,j}^n}{2\Delta\tau}\right) + Q_{ij}^n\left(\frac{Q_{i+1,j}^n - Q_{i-1,j}^n}{2\Delta\tau}\right)^*\right]\right\}$$
$$- iap\tau_R\left\{Q_{ij}^{n*}\left(\frac{Q_{i+1,j}^n - Q_{i-1,j}^n}{2\Delta\tau}\right) + Q_{ij}^n\left(\frac{Q_{i+1,j}^n - Q_{i-1,j}^n}{2\Delta\tau}\right)^*\right\} \tag{19}$$

where the "leap frog" method is used to evaluate the derivatives.

The third part involves solving the linear diffraction operator D_{DF}, which is equivalent to

$$\frac{\partial Q}{\partial \xi} = \kappa(\omega)\nabla_\perp^2 Q(\xi,\rho,\omega) \tag{20}$$

where $$\nabla_\perp^2 = \frac{1}{\rho}\frac{\partial}{\partial\rho} + \frac{\partial^2}{\partial\rho^2},$$

and $$\kappa(\omega) = \frac{1}{4}(i - \sigma\omega). \tag{21}$$

Equation (20) is solved using the finite difference scheme,

$$\frac{\partial Q}{\partial \xi} = \frac{Q_{ij}^{n+1} - Q_{ij}^{n}}{\Delta \xi} \tag{22}$$

and

$$\frac{\partial Q}{\partial \rho} = \frac{1}{2}\left\{ \frac{Q_{i,j+1}^{n+1} - Q_{i,j-1}^{n+1}}{\rho_{j+1} - \rho_{j-1}} + \frac{Q_{i,j+1}^{n} - Q_{i,j-1}^{n}}{\rho_{j+1} - \rho_{j-1}} \right\} \tag{23}$$

and using the Crank-Nicholson scheme, and assuming equal spacing in ρ,

$$\frac{\partial^2 Q}{\partial \rho^2} = \frac{1}{2}\left\{ \frac{Q_{i,j+1}^{n+1} - 2Q_{i,j}^{n+1} + Q_{i,j-1}^{n+1}}{(\Delta\rho)^2} + \frac{Q_{i,j+1}^{n} - 2Q_{i,j}^{n} + Q_{i,j-1}^{n}}{(\Delta\rho)^2} \right\} \tag{24}$$

Equqtions (22)-(24) are used in Eq. (20) for $0 < \rho_j < \rho_{max}$. Assuming a cylindrically symmetric system,

$$\frac{\partial Q}{\partial \rho} = 0 \quad at \quad \rho = 0$$

Eq (20) becomes (i.e. j=0)

$$\begin{gathered} \left(1+\phi(\omega_i)\right)Q_{i,0}^{n+1} - \phi(\omega_i)Q_{i,1}^{n+1} - \left(1-\phi(\omega_i)\right)Q_{i,0}^{n} - \phi(\omega_i)Q_{i,1}^{n} = 0, \\ \phi(\omega_i) = \frac{2\Delta\xi\,\kappa(\omega_i)}{\rho_1^2} \end{gathered} \tag{25}$$

For the maximum radial value, ie $\rho = \rho_{max} = \rho_N$, Eq. (20) becomes

$$\begin{gathered} \theta(\omega_i)Q_{i,N-1}^{n+1} + \left[1-\theta(\omega_i)\right]Q_{i,N}^{n+1} + \theta(\omega_i)Q_{i,N-1}^{n} - \left[1+\theta(\omega_i)\right]Q_{i,N}^{n} = 0, \\ \theta(\omega_i) = \frac{\Delta\xi\,\kappa(\omega_i)}{2\rho_N(\rho_N - \rho_{N-1})} \end{gathered} \tag{26}$$

Using Eqs. (22)-(26), Eq. (20) can be written in the form

$$\Xi_1(\omega_i)\bullet\bar{q}_i^{n+1}=\Xi_2(\omega_i)\bullet\bar{q}_i^{n},$$

$$\bar{q}_i^{n}=\left(Q_{i,0}^{n},\ldots..,Q_{i,j}^{n},\ldots..,Q_{i,N}^{n}\right) \tag{27}$$

and Ξ_1 and Ξ_2 are tridiagonal matrices. The matrix Ξ_1 is composed of the subdiagonal, diagonal and superdiagonal elements,

$$\bar{a}(\omega_i)=\left[0,\ldots,\frac{\Delta\xi\kappa(\omega_i)}{\rho_{j+1}-\rho_{j-1}}\left\{\frac{1}{2\rho_j}-\frac{1}{\rho_j-\rho_{j-1}}\right\},\ldots,\theta(\omega_i)\right],$$

$$\bar{b}(\omega_i)=\left[1+\phi(\omega_i),\ldots,1+\frac{\Delta\xi\kappa(\omega_i)}{(\rho_{j+1}-\rho_{j-1})}\left(\frac{1}{\rho_{j+1}-\rho_j}+\frac{1}{\rho_j-\rho_{j-1}}\right),\ldots 1-\theta(\omega_i)\right], \tag{28}$$

$$\bar{c}(\omega_i)=\left[-\phi(\omega_i),\ldots,-\frac{\Delta\xi\kappa(\omega_i)}{\rho_{j+1}-\rho_{j-1}}\left(\frac{1}{2\rho_j}+\frac{1}{\rho_{j+1}-\rho_j}\right),\ldots,0\right]$$

and matrix Ξ_2 is composed of the subdiagonal, diagonal and superdiagonal terms,

$$\bar{d}(\omega_i)=\left[0,\ldots,-\frac{\Delta\xi\kappa(\omega_i)}{\rho_{j+1}-\rho_{j-1}}\left\{\frac{1}{2\rho_j}-\frac{1}{\rho_j-\rho_{j-1}}\right\},\ldots,-\theta(\omega_i)\right],$$

$$\bar{e}(\omega_i)=\left[1-\phi(\omega_i),\ldots,1-\frac{\Delta\xi\kappa(\omega_i)}{(\rho_{j+1}-\rho_{j-1})}\left(\frac{1}{\rho_{j+1}-\rho_j}+\frac{1}{\rho_j-\rho_{j-1}}\right),\ldots 1+\theta(\omega_i)\right], \tag{29}$$

$$\bar{f}(\omega_i)=\left[\phi(\omega_i),\ldots,\frac{\Delta\xi\kappa(\omega_i)}{\rho_{j+1}-\rho_{j-1}}\left(\frac{1}{2\rho_j}+\frac{1}{\rho_{j+1}-\rho_j}\right),\ldots,0\right]$$

We can solve a tridiagonal system for each angular frequency, ω_i or construct a super-matrix to solve for all frequencies simultaneously. Using these three methods, Eq.(17) is used to numerically propagate the electromagnetic field in the nonlinear dispersive medium. In the limiting case of the nonlinear Schroedinger equation, the numerical results agree well with analytic solutions.

5. ACKNOWLEDGMENTS

This research was supported in part by the Air Force Office of Scientific Research, Armstrong Laboratory and the Office of Naval Research.

6. REFERENCES

1. J. H. Marburger, "Self-focusing: Theory", Prog. Quant. Electr. 4, 35 (1975).
2. D. Strickland and P.B. Corkum, "Short pulse self-focusing" Proc. Soc. Photo-Opt. Instrum. Eng. 1413, 54 (1991).
3. Y. Silberberg, "Collapse of optical pulses", Opt. Lett. 15, 1282 (1990)
4. P. Chernov and V. Petrov, "Self-focusing of light pulses in the presence of normal group velocity dispersion", Opt. Lett. 17, 172 (1992).
5. J. Rothenburg, "Pulse splitting during self-focusing in normally dispersive media", Opt. Lett. 17, 583 (1992).
6. A.B. Aceves and C. DeAngelis, "Spatiotemporal pulse dynamics in a periodic nonlinear waveguide", Opt. Lett. 18, 110 (1993).
7. G. Luther, J.V. Moloney, A. Newell and E. Wright, "Self-focusing threshold in normally dispersive media", Opt. Lett. 19, 862 (1994).
8. G. Luther, A. Newell and J. Moloney, "The effects of normal dispersion on collapse events", Physica D 74, 59 (1994).
9. G. Fibich, V. Malkin, G. Papanicolaou, "Beam self-focusing in the presence of small normal time dispersion", Phys. Rev. A, submitted.
10. P. K. Kennedy, S.A. Boppart, D.X. Hammer, B.A. Rockwell, G.D. Noojin and W.P. Roach, "A First-Order model for computation of laser induced breakdown thresholds in ocular and aqueous media: Part II-code description and comparison to experiment", IEEE J. Quant. Electron., 31, 2250 (1995).
11. M. Landman, G. Papanicolaou, C. Sulem and P. Sulem, "Rate of blowup for solutions of the nonlinear Schroedinger equation at critical dimension", Phys. Rev. A 38, 3837 (1988); and references therein.
12. Q. Feng, J.V. Moloney, A.C. Newell, E.M. Wright, K. Cook, P.K. Kennedy, D.X. Hammer and C.R. Thompson, "Theory and simulation of laser-induced breakdown and self-focusing of ultrashort focused laser pulses in water", preprint.
13. M.J. Potasek, "Femtosecond solitons in optical fibers", J. Appl. Phys. 65, 941 (1989); and references therein.
14. G.P. Agrawal, Nonlinear Fiber Optics (Academic Press, NY, 1989); and references therein.
15. X.D. Cao, G.P. Agrawal and C.J. McKinstrie, "Self-focusing of chirped optical pulses in nonlinear dispersive media", Phys. Rev. A 49, 4085 (1994).
16. A.T. Ryan and G.P. Agrawal, "Pulse compression and spatial phase modulation in normally dispersive nonlinear Kerr media", Opt. Lett. 20, 306 (1995).
17. L. Berge, J. J. Rasmussen, E. A. Kuznetsov, E. G. Shapiro and S. K. Turitsyn, "Self-focusing of chirped optical pulses in media with normal dispersion", J. Opt. Soc. Am. B, 13, 1879 (1996)
18. G.H. Bresnick, et.al., "Ocular effects of argon laser radiation I. Retinal damage threshold studies", Invest. Ophthalmol. 9, 901 (1970)
19. R. Birngruber,C. A.Puliafito, A. Gawande, W. -Z. Lin, R.J. Schoenlein and J.G. Fujimoto , IEEE J. Quant. Electron. QE-23, 1836 (1987).
20. R.G. Allen, S. J. Thomas, R.F. Harrison, J.A. Zuclich,and M.F. Blankenstein,"Ocular effects of pulsed Nd laser radiation: variation of threshold with pulsewidth", Health Phys. 49, 685 (1985).
21. W. P. Roach, C.A. Toth, C.D. Stein, G. D. Noojin, D. J. Stolarski and C. P. Cain, "Minimum visible lesions from pico- and femtosecond laser pulses", Proc. SPIE, Laser-Tissue Interaction V, 2134, 10 (1994).
22. J. Taboada and W. D. Gibbons, "Retinal tissue damage induced by single ultrashort 1064 nm laser light pulses", Appl. Opt. 17, 2871 (1978).
23. A.P. Bruckner, J.M. Schurr, and E.L. Chang, "Biological damage threshold induced by ultrashort 2nd and 4th harmonic light pulses from a mode-locked Nd:glass laser", USAF SAM-TR-80-47 (1980).
24. A. J. Goldman, W.T. Ham, and H.A. Mueller, "Ocular damage thresholds and mechanisms for ultrashort pulses of both visible and infrared laser radiation in the Rhesus monkey", Exp. Eye Res., 24, 45 (1977).
25. W. P. Roach, C. D. DiCarlo, G.D. Noojin, D.J. Stolarski, R. Amnotte, A.B. Smith, M.E. Rogers and C. P. Cain, "Retinal threshold studies for nanosecond and picosecond visible laser pulses", SPIE, OE-LASE-95, to be published.

Optimization of neural retinal visual motor strategies in recovery of visual acuity following acute laser induced macula injury

H. Zwick, J.W. Ness, J. Loveday, J. Molchany & B.E. Stuck

US Army Medical Research Detachment
Walter Reed Army Institute of Research
San Antonio, TX

ABSTRACT

Laser induced damage to the retina may produce immediate and serious loss in visual acuity as well as subsequent recovery of visual acuity over a 1 to 6 month post exposure period. While acuity may recover, full utilization of the foveal region may not return. In one patient, a superior/temporal preferred retinal location (PRL) was apparent, while a second patient demonstrated significant foveal involvement and contrast sensitivity more reflective of foveal than parafoveal involvement. These conditions of injury were simulated by using an artificial scotoma technique which optically stabilized a 5° opacity in the center of the visual field. The transmission of spatially degraded target information in the scotoma was 0%, 5% and 95%. Contrast sensitivity for the 0% and 5% transmission scotoma showed broad spatial frequency suppression as opposed to a bipartite contrast sensitivity function with a narrow sensitivity loss at 3 cycles/degree for the 95% transmission scotoma. A PRL shift to superior temporal retina with a concomitant change in accommodation was noted as target resolution became more demanding. These findings suggest that restoration of visual acuity in human laser accidents may depend upon the functionality of complex retinal and cortical adaptive mechanisms.

Keywords: Human laser injury, primary and secondary damage, pseudofovea, contrast sensitivity, artificial scotoma

1. INTRODUCTION

Laser induced damage to the macula region of the human retina causes immediate and serious loss of visual acuity.[1] Remarkably, many of these investigations of either human or non-human primate photic macular damage report either a complete or partial restoration in visual acuity, with restoration generally requiring several months. One potential mechanism for such recovery, proposed by Tso,[2] suggests that damaged photoreceptors are removed and replaced by normal photoreceptors adjacent to the damage site. Tso based this suggestion on sequential studies of non-human primates having laser induced macula damage. Animals examined histologically within the first week post exposure showed damaged and missing photoreceptors in the macular area; histological examination at six months post exposure revealed normal macula with apparent restoration of the photoreceptor densities within the central retina. Other studies have demonstrated a change in the Stiles Crawford effect with

macula disease, suggesting that normal photoreceptor orientation within the macula region is another photoreceptor consideration in the recovery of visual acuity in addition to number of photoreceptors and photoreceptor packing density.[3]

Alternatively, retinal sites of equivalent sensitivity and receptor densities might exist in areas adjacent to the macula region. Shifting target placement away from damaged areas to these sites would also explain recovery in visual acuity after laser induced damage to the macula. In clinical investigations of macular disease alternative retinal sites appear with acuity recovery.[4] In more recent investigations utilizing artificial scotomas, we have demonstrated that superior/temporal retina may be a preferred retinal location (PRL) especially as target recognition size becomes small requiring foveal like receptor resolution.[5,6]

Although the above mechanisms are involved in recovery of visual acuity, recovery may also involve alteration in primary visual cortical neural mechanisms. In previous investigations, we have shown that Q-switched induced laser macular injury is represented in the striate cortex.[7] Neurophysiological investigations suggest that exposure to visible laser sources can alter central nervous system visual receptive field characteristics in vertebrate[8] and mammalian receptive fields.[9] Such mechanism could compensate for peripheral signal alterations induced by acute laser injury by expansion of central neural coverage of weaker peripheral input from non-existent or damaged retinal photoreceptor systems. Such neural modulation by higher visual centers could play a significant role in restoration of high spatial frequency visual function (i.e., visual acuity).

In the present paper, we have evaluated two patients that demonstrated visual acuity recovery following serious laser induced macular damage. One of these patients, treated with high dose steroids, showed significant recovery within 8 weeks from 20/100 to 20/15 Snellen acuity and significant recovery of contrast sensitivity. A second patient, presented with 20/100 after similar laser induced damage,[10,11] where Snellen acuity recovered to 20/17 within 6 weeks and has remained stable for over 3 years. No pharmacological treatment was given. Detailed contrast sensitivity measurements were made under ophthalmoscopic conditions in these two patients and compared with normal observers whose contrast sensitivity functions and PRLs were measured under analogous artificially induced central retinal scotoma conditions.

2. METHODS

A dual Purkinje Eye-Tracker (Version 5) was used to provide eye-movement data to control an artificial scotoma. The eye-movement data was in the form of vertical and horizontal output voltages that were used to control the position of the scotoma. The scotoma was generated with a combination of three image processing boards that provided an image plane, an insert plane for placing information within the scotoma, and a scotoma mask plane which allowed manipulation of scotoma size, shape and location in the visual field. Absolute scotomas were created by displaying a black or gray field uniformly over the insert plane. The field was produced by setting the pixel gray level to a value between 0 and 256. A very dark or "black"

5° central scotoma was used to effectively mask the entire macula region. Relative scotomas were produced by placing a spatially degraded image of the displayed image in the insert plane at a fixed value of the recognition threshold for each Landolt test target. All degraded images were produced by band-passing the Fourier spectrum at 9 cycles/degree with a Butterworth half maximum band-pass of about 4 cycles/degree. The insert target was set at either 5% or 95% of the recognition threshold for each Landolt target presented in the image plane. All scotomas were 5° and centered in the subject's visual field.

Visual recognition sensitivity functions were measured for standard Landolt ring test stimuli over a spatial frequency range from 0.5 to 20 cycles/degree. Contrast for the presented stimuli was increased by 0.1% increments every 500msec beginning at 0% contrast (gray field). Contrast was defined as the absolute value of the target luminance minus the background luminance divided by the luminance of the target plus the luminance of the background. Landolt ring contrast sensitivity measured in a Rodenstock Confocal Scanning Laser Ophthalmoscope (CSLO) was measured using an identical recognition threshold test paradigm with targets modulated into the SLO raster pattern so that target placement could be observed simultaneously with retinal lesion sites in human laser accident cases.[12] Contrast sensitivity measurements were made in two laser eye injury cases. Both had bilateral accidental induced Q-switched exposure. FC(OS) recovered while FC(OD) remained at 20/100 and exceeded 20/200 after macular hole surgery.[11] Patient AG had high does steroid therapy initiated within 4 hours of laser injury. Visual acuity in both OD and OS returned to 20/15 within 4 to 6 weeks. FC(OS) and AG(OD) are compared in CSLO contrast sensitivity in this paper.

3. RESULTS

Figure 1. FC(OS)(left image) and AP(OD)(right image) CSLO images showing preferred retinal location in superior/temporal retina.

Figure 1 shows CSLO images of FC(OS) and AP(OD). Target placement conditions are indicated by Landolt "C". FC(OS) PRL is just superior and temporal to the dark temporal streak shaped lesion laterally traversing the foveal region and is consistent with previous similar estimates of FC(OS)'s PRL.[10] The estimated PRL for AP(OD) is also superior but less temporal and may frequently center on the superior white lesion area. It is also most often detected at this site for the highest spatial frequency Landolt targets. Figure 2 shows FC(OS) CSLO contrast sensitivity functions measured at 19 months post-exposure, similar to AP(OD) at 3 days and reflect parafoveal contrast sensitivity dominance indicated by both having peak sensitivity at <1cycle/degree. AP(OD) at 2 months shows an increase in mid and high spatial frequency contrast sensitivity indicating an increase in more central retinal function. Figure 3 compares chromatic contrast sensitivity functions measured under short wavelength ("blue" test against "blue" background) chromatic adaptation. FC(OS) shows a significant peak as well as a greater overall sensitivity relative to one normal observer and AP(OD).

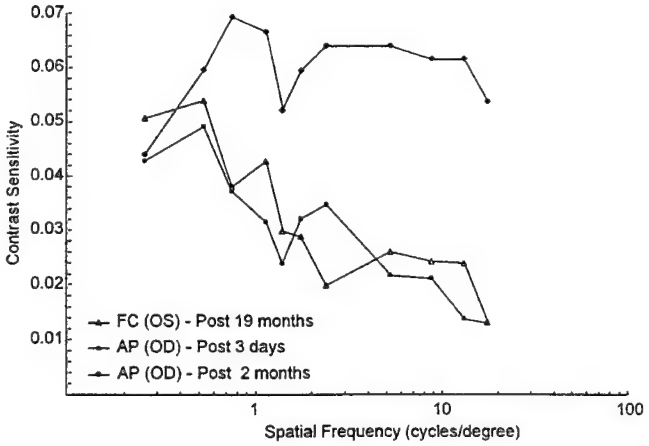

Figure 2. CSLO post-exposure functions for FC(OS) and AP(OD)

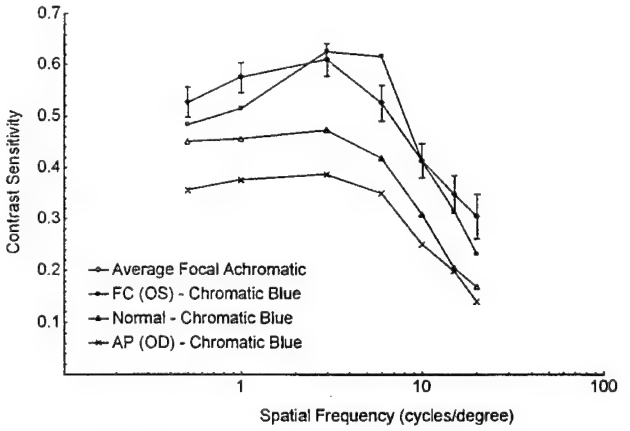

Figure 3. Chromatic contrast sensitivity functions ("blue" background & test target) for FC(OS), AP(OD), and a normal subject compared to baseline achromatic function.

In Figure 4, the mean contrast sensitivity function for five normal human subjects is shown relative to the contrast sensitivity function measured in the presence of a central 5° absolute "black" scotoma. The suppression in sensitivity appears across the entire spatial frequency axis with a maximum loss at 3 cycles/degree. In addition, the suppressive sensitivity effects for the 95% and 5% relative scotoma conditions are shown. While both functions show a broad loss in contrast sensitivity across spatial frequency, the 95% scotoma, which passed maximum information, shows a notch at 3 cycles/degree. In Figure 5, we have drawn two smooth functions through the 95% function with peaks at 1 and 4 cycles/degree suggesting the presence of two broadly tuned spatial frequency channels.

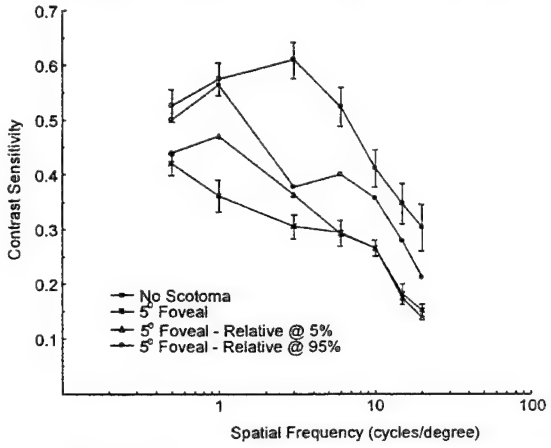

Figure 4. Contrast sensitivity functions for absolute and relative simulated scotomas

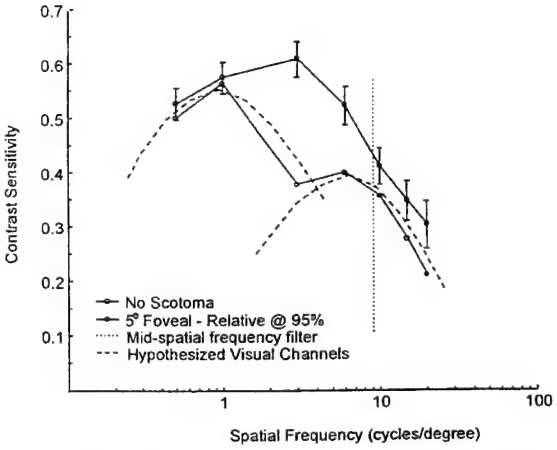

Figure 5. Hypothesized spatial frequency channels as indicated by relative scotoma function.

Figure 6 shows the shift in the preferred retinal location (PRL) for absolute and two relative scotoma conditions and the no-scotoma condition. All scotoma conditions caused a shift in the target PRL into superior retina and a small shift (not shown) into temporal retina. The maximal shift is obtained at the highest spatial frequencies for the absolute scotoma condition. The absolute scotoma shows a 0.8° higher placement into superior retina than either relative scotoma. Even though information content differs significantly

between the two relative scotoma conditions, they are nearly identical in their change with spatial frequency.

Figure 7 shows a corresponding change in fourth purkinje voltage with spatial frequency and scotoma condition. An increasing negative DC voltage is amplified with scotoma size over all spatial frequencies with the exception of the highest where an abrupt switch in voltage polarity appears. This relationship suggests an alteration in accommodation that is signaled by loss of local retinal neural output resulting from artificial spatial occlusion.

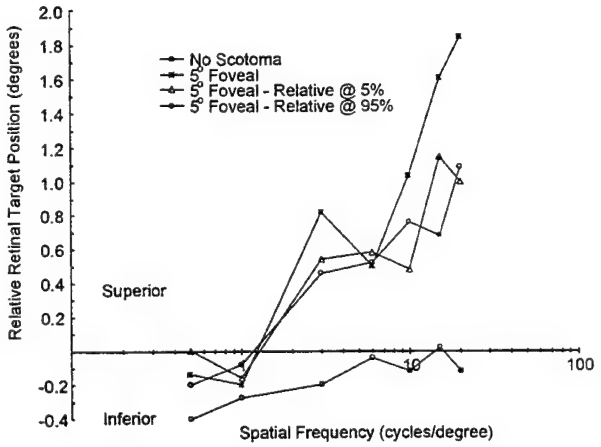

Figure 6. Preferred retinal location shifts as a function of spatial frequency for absolute and relative scotomas.

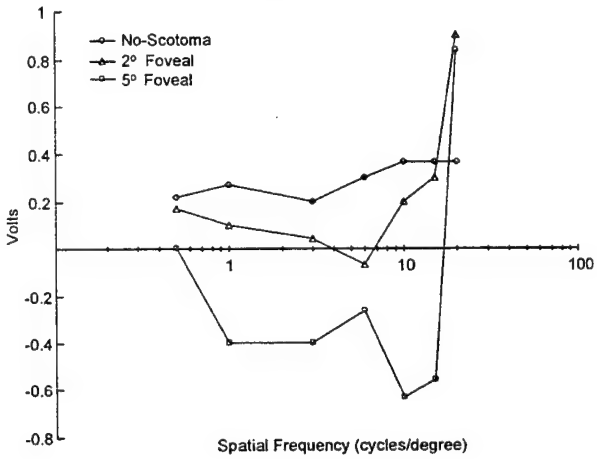

Figure 7. DC shift in 4th purkinje plotted against spatial frequency for no-, 2°, and 5° scotoma conditions.

4. DISCUSSION

We have shown in these two human laser accident cases a significant resiliency in the restoration of normal visual acuity following acute Q-switched laser induced damage to the macula. The restoration of acuity in these cases suggests that regardless of treatment regime, the injury process itself initiates a restoration mechanism capable of restoring visual acuity to normal levels. In explanation of this recovery, one could invoke the histological observations of Tso suggesting that photoreceptors adjacent to the damaged macula passively repopulate the macula, restoring its photoreceptor density sufficient for maximal restoration of visual acuity. However direct observations of small target placement measured under CSLO conditions suggest that a shift in the PRL away from the macula has occurred to superior/temporal retina. While some believe that superior retina may be developmentally close to the macula, morphologically it does not appear to have the packing density required for fine visual resolution. Thus, selection of a new PRL in itself is not solely sufficient for maximal acuity restoration.

The absolute degree of injury to the fovea may play a significant role. AP(OD) presented initially with bilateral relative central scotomas. High dose steroid treatment may have minimized the deleterious effects of injury even more by minimizing free radical formation and intra-retinal scar formation. Contrast sensitivity suppression measured in the CSLO for AP(OD) are indeed very comparable to contrast sensitivity suppression for the analogous

simulated relative scotoma condition. Both the patient and simulated relative scotoma function show a bipartite function over the spatial frequency scale, suggesting the presence of at least low and mid to high spatial frequency mechanisms.

On the other hand, only the low spatial frequency system is apparent in FC(OS). It is possible that higher spatial frequency mechanisms are indeed active but not well reflected because of a more peripheral PRL than that of AP(OD), or that a stronger influence of peripheral retinal suppression from parafoveal receptor systems is effecting high spatial frequency mechanisms. Figure 4 compares the "blue" chromatic adaptation function of FC(OS) with a normal human subject and that of AP(OD). FC(OS) presents with maximum sensitivity shifted to a peak at 10 cycles/degree. This shift is not evident in the normal human subject of AP(OD). We suggest that this function reflects an increased spatial resolution of superior/temporal retinal receptors with increased high spatial frequency resolution, possibly due to morphological alteration to superior/temporal packing densities and receptor orientation. Such alterations in receptor packing densities and receptor orientation are requisite conditions for restoration of maximal acuity and development of a pseudofovea. We speculate that the observed link demonstrated in artificial scotoma experiments between the suppression of the retinal output signal to higher visual centers and servo control from these centers of local accommodative processes may alter local image formation in the pseudofovea, while higher order central receptor fields may expand their areas of spatial integration to compensate for asymmetrical neural input from the central retina.

In summary, we have discussed the oculomotor and neural mechanisms that could underlie the development of a pseudofovea. We have reviewed two human laser accident cases where a partial and more complete pseudofovea developed. In both cases, full restoration of visual acuity occurred. Artificial scotoma experiments demonstrated the existence of several mechanisms that might explain pseudo or partial pseudofoveal development. The presence of a central artificial scotoma, whether absolute or transmissive (relative scotoma), arbitrarily shifts the contrast test target into superior and slightly temporal retina. Relative scotomas that allow some information transmission through the scotoma, produce a suppression in the contrast sensitivity function that reveals a low and high spatial frequency contrast system. Both low and high spatial processing systems are required for restoration of visual acuity and may be retained by either maintaining as much foveal function as possible or by alteration of receptor density and orientation. A mechanism for the latter appears to exist in artificial scotoma experiments involving scotoma modulation of the accommodative process. We suggest similar process along with alteration in cortical magnification for development of a functional pseudofovea capable of restoration of visual acuity as reported in the presented cases.

5. REFERENCES

1. H Zwick, "Visual function changes associated with low-level light effects," Health Physics. Vol. 56, pp. 657-663,1989.

2. M. TSO. "Photic maculopathy in the rhesus monkey," *Investigative Ophthalmology*. 12, 17-34 (1973).

3. J.M. Enoch and H.E. Bedell. "The Stiles-Crawford Effects," In J.M. Enoch and F.L. Tobery, Jr. (Eds.), *Vertebrate Photoreceptor Optics* (pp. 86-126). Springer-Verlag, Berlin: 1981.

4. J. Guez, J. Le Gargasson, F. Rigaudierre and K. O'Regan. "Is there a systematic location for the pseudo-fovea in patients with central scotoma?," *Vision Research*, Vol. 33, pp. 1271 -1279, 1993.

5. J. Ness, H. Zwick, J. Molchany "Preferred retinal location induced by macular occlusion in a target recognition task," B.E. Stuck and M. Belkin (Eds.), *Laser inflicted Eye Injuries, SPIE*, Vol. 2674, pp. 131-135,1996.

6. H. Zwick, J. Ness, J. Molchany and B.E. Stuck. "A comparison of artificial and accidental laser induced macular scotomas on human contrast sensitivity," B.E. Stuck and M. Belkin (Eds.), *Laser Inflicted Eye Injuries, SPIE*, Vol. 2674, pp. 136-142, 1996.

7. H. Zwick, S.T. Schuschereba, D.A. Gagliano, M. Silverman, D. Lund, S.B. Reynolds, B.E. Stuck. "Morphological and functional effects of induced laser retinal fibrosis," S.T. Melamed (Ed.), *Laser Applications in Ophthalmology, Europto Series, SPIE*, Vol. 2079, pp. 30-43, 1993.

8. Zwick, D.O. Robbins and T. Westgate. "Nonselective changes in receptive field by laser irradiation," *Letterman Army Institute of Research Laboratory Note No. 86-62*, pp. 1-10, 1986.

9. Gilbert and T.N. Wiesel. "Receptive field dynamics in adult primary visual cortex," *Nature*, Vol. 356, pp. 150-152, 1992.

10. Zwick, D.A. Gagliano, S. Ruiz, B.E. Stuck. "Utilization of scanning laser ophthalmoscopy in laser induced bilateral human retinal nerve fiber layer damage." J.M. Parel and Q. Ren (Eds.), *SPIE Proceedings of Ophthalmic Technologies V*, Vol. 2393, pp. 189-193, 1993.

11. P.H. Custis, D.A. Gagliano, H. Zwick, S.T. Schuschereba, C.D. Regillo. "Macular hole surgery following accidental laser injury with a military range-finder." B.E. Stuck and M. Belkin (Ed.) *Laser Inflicted Eye Injuries, SPIE*, Vol. 2674, pp. 166-173.

12. Zwick, D.J. Lund, D.A. Gagliano, and B.E. Stuck. "Functional and ophthalmoscopic observations in human laser accident cases using scanning laser ophthalmoscopy." J.M. Parel and Q. Ren (Eds.), *SPIE Proceedings of Ophthalmic Technologies V*, Vol. 2393, pp. 144-153.

The opinions and assertions contained are the private views of the authors, not to be considered as official or reflecting the views of the DoA or DoD. Investigators adhered to AR 70-25 and USAMRMC Regulation 50-25 on the use of volunteers in research.

Strategies for eye positioning after laser-related loss of central vision.

J.H. Bertera[1]

Adaptive Medical Systems, Inc., Boston, MA
and
Department of Psychology, Northeastern University, Boston MA

ABSTRACT

Loss of foveal vision from exposure to laser light or retinal disease can seriously impair visual functions like reading and visual search. Central scotomas produce large losses in visually guided performance because central vision has the best visual resolution, compared to more peripheral retina, and is also important in the normal reflexive pattern of eye movement. Relatively small central field scotomas can produce significant impairments in visual search if tasks require a high degree of foveal vision such as seeing fine detail or discriminating similar contours or letters. Subjects faced with the task of adapting to the loss of central vision sometimes position their eyes in ways which are either asymmetrical, not optimum, or seem to generate abnormal eye movements, even after extensive practice. Discussion includes oculomotor drift, error fixations, hyper-eccentric fixations and remedial eye positioning strategies.

Keywords: scotoma, macular disease, laser injury, eye slaved, eye movement, simulator

1. INTRODUCTION

Loss of foveal vision from disease or accidental exposure to bright light seriously impairs visual functions like reading and visual search. Typical human scotomas, areas of retina which become relatively insensitive to light, are associated with retinal diseases like macular degeneration, retinal detachments, infection or Stargardt's disease, to name a few. Such scotomas are produced by injury or death of receptors or neuronal pathways and are often permanent The widening use of lasers for sighting, range finding, and communications also poses a threat to human vision in the form of scotomas from retinal exposure aftereffects, either from permanent tissue damage, or bleaching and long lasting afterimages. The visual impairments of laser induced foveal scotomas may limit visual functioning as much as an advanced disease process, and, have been identified as a significant and evolving problem[2,3,4,5] during military operations and training. A third form of visual loss is the simulated scotoma which is produced artificially in the laboratory by slaving rapid display changes to eye position signals from a sensor and can be used to analyze some of the adaptive processes associated with visual loss, hopefully leading to improvements in the speed and optimization of adaptation.

Central visual field scotomas produce losses in visually guided performance because central or foveal retina has the best resolution compared to more peripheral retina[6], and central retina is also important in

[1] Further author information: ., 4 Longfellow Place, Suite 3011 A.D.1, Boston, MA 02114.
e-mail: amsi@tiac.net Voice & fax: 617-742-1007

SPIE Vol. 2974 • 0277-786X/97/$10.00

the normal reflexive pattern of eye movement which brings targets detected in the periphery to the central retina for recognition. After loss of foveal vision some subjects may spontaneously employ eccentric viewing to position targets of interest outside of the central scotomatous region. Foveal vision is normally distributed around the visual scene in pauses called eye fixations at about three per second. Each fixation is followed by a flicking eye motion called a saccade, or saccadic eye movement, which delivers fovea to a new visual filed location. Eccentric viewing is implemented by adapting the eye fixation position and the length of some saccades to avoid landing targets in the scotoma. The optimum unaided eccentric viewing adaptation is to translate the landing position of the eye for each movement by making peripheral to peripheral saccades, instead of the normal fovea to fovea saccades, while maintaining a normal saccade length or saccade gain. The target viewing time can be expressed as a percentage of total time a target is present, where eccentric viewing positions the target outside the scotoma boundary. Eccentric viewing is not easy and most subjects still make mistakes even after extensive practice, mainly by reflexively fixating the target with the unresponsive fovea.

The radius of a circular symmetric scotoma determines the minimum distance from fovea for targets to be projected just outside of the scotoma boundary, i.e. the optimum eccentric viewing position. Since the density of receptors falls off into the periphery, the larger the scotoma radius, the greater degree of eccentricity for optimum eccentric viewing and the lower the visual resolution available for detecting and recognizing targets. However, the speed or accuracy of visually guided performance is also determined by the demands of a given task. Loosing even a small portion of the central retina might be expressed on a continuum from an aesthetic impairment or mere inconvenience that does not affect performance or oculomotor control to an information blockade that may bring performance to zero.

In this paper I wish to draw a distinction between an adaptation to loss of central vision and an impairment. The reason for making this distinction is for improving the rationale for design of countermeasures or remediation of the effects of foveal loss. Under some circumstances what might be considered errors in eye positioning, or incomplete or non-optimum activity may have strategic value to the subject in adapting to a scotoma, especially if the scotoma is changing rapidly. Five processes were identified from clinical and experimental examination that could control target viewing time and eccentricity from fovea: 1) Asymmetric eye fixation positions, 2) Reflex foveations (scotoma fixations), 3) Scotoma nystagmus, 4) Hyper-eccentric eye positions, and 5) Compromise in eye position.

2. SCOTOMA CHARACTERISTICS

The variety of retinal lesions can make experimental analysis difficult by introducing such extraneous variables as duration of injury, depth of lesion (absolute v. relative), and the scotoma spatial characteristics: size, position, and shape. Simulating a retinal scotoma can be used with visually normal human subjects to establish control over these variables. One disadvantage is that the subject with a simulated scotoma cannot have the long history of visual loss and adaptation potentially represented in the clinical population. The simulated scotoma is closer in abrupt onset to the injury that might be expected in an accidental exposure to laser light, however. The same retinal injury can be simulated in different subjects or different injuries in the same subjects, improving the control over experience, motivation and other individual differences.

In the simulation, eye position data is linked to an obscurant area through a computer algorithm and the imagery within the scotoma boundary is either erased, replaced or distorted (See Figure 1). The targets within the boundary can be eliminated leaving a "black hole", an averaged luminance background, or replaced with a lower contrast version. Metamorphopsia associated with displacements in the retinal layers can also be introduced into the scotoma boundary by distorting the target images or background. The accuracy and linearity of the eye position sensor data is important especially for simulating foveal scotomas where small errors in scotoma positioning are clearly visible to the subject as an offset from foveal center.

Some disease processes and laser exposure can produce a sharp fall off in acuity, yielding a sharp edged scotoma, while the visual function loss from a long lasting afterimage may be better represented by a graded edge scotoma. The graded edge scotoma may reduce the spatial transient signals as its boundary crosses targets, i.e. the targets gradually disappear, making it more difficult for the subject or an examiner to assess the exact extent of the functional loss at the edge. A sharp edged scotoma is likely to supply better information about the spatial extent of the scotoma for use by adaptive processes. By changing the scotoma algorithm the central symmetric scotoma can be compared to an annulus which will block peripheral information rather than central. This allows a comparison of the contribution of central v. peripheral information to the visual performance. Previous work demonstrates the much greater effect of a small central scotoma compared with even very large annular obscurant blocking information in the peripheral field. The reason is plainly that much less information is being retrieved from the peripheral field.

The results of several different tasks will be used to describe the adaptations and impairments associated with scotomas. The simplest is a steady eccentric fixation task in which a single stationary target placed in the center of a visual display is instructed for eccentric viewing across a set of conditions with different scotoma sizes. To increase the task demands, sometimes a rapidly changing series of numbers is displayed in the single 0.3-2.0 degree window and the subject must recognize a target number(s). In a free visual search task, a matrix of acuity targets are presented on a raster display and the subject is free to search until a target gap is detected. A variant task is search for an instructed target letter among an array of alpha numeric elements which are scattered randomly over the display surface. The third task type is referred to as instructed scanning, including both single line text reading and a saccade alternation task. In saccade alternation two target positions (1-15 degree separation) are fixated alternately, with different target separations and scotoma sizes. Smaller separations and larger scotomas yield conditions under which both targets are obscured unless the subject takes a third eccentric fixation position, requiring a compromise in looking position.

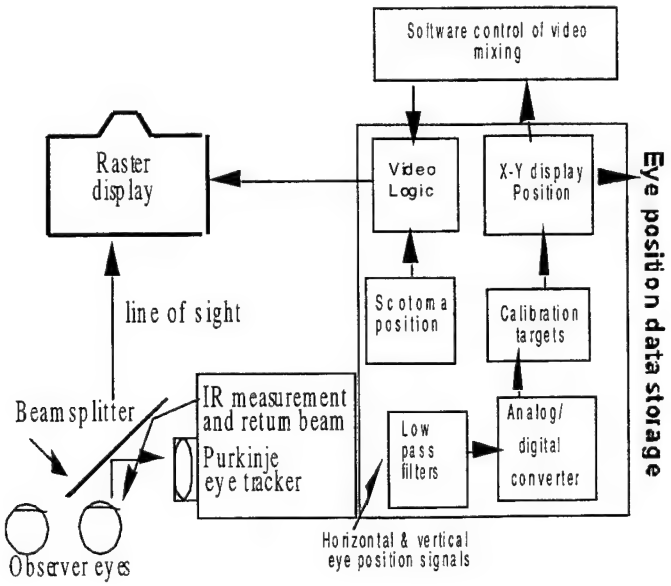

Figure 1. Schematic diagram of eye position sensor (Dual Purkinje tracker), analog data filter, analog to digital conversion, and eye position controlled video display. The subject's right eye movements are measured and the analog, filtered outputs for horizontal and vertical eye movements are fed to a software calibration look-up table to index display positions in minarc. Scotoma movements are programmed from settings for scotoma radius, offset (if any) from fovea, and shape and contrast. Visual targets and the scotoma are presented on the same visual display. A disadvantage of the Purkinje eyetracker is the use of a dental mold to steady the head and non-linearities and track loss problems.

3. IMPAIRMENTS AND ADAPTATIONS

Adaptation is triggered by detection of loss of vision. The subject must endure a sufficient period of loss of vision and make enough error eye movements which obscure the target to plot the boundary of the scotoma. The next step is to discover the best method of eccentric viewing. In addition, if the scotoma is dynamic, such as a fading afterimage where the scotoma may be shrinking in size, the subject must periodically overreach the current optimum eccentricity to discover that it is possible to bring the target closer to fovea. Of course, some conditions can be created which make the presence of a scotoma undetectable. For example, when the background in the visual display closely matches the perceived color and luminance in a bright flash afterimage. The afterimage boundary may be invisible until a target disappears inside it. Therefore, to trigger adaptation and to maintain a good degree of adaptability more eye movements and mistakes must be made than would be considered optimum for fixed conditions.

For two dimensional displays, a variety of oculomotor changes show the sensitivity of the system in responding to loss of central vision. For example, the duration of eye fixations generally increase with scotoma size as much as 15%. The number of error fixations which is initially very high also decreases rapidly as adaptation proceeds. Saccade lengths change depending on conditions with a simulated scotoma. The accuracy of eye fixations adapts to a much better degree than saccades.[22] Error fixation position can range from the scotoma center on the target (scotoma fixation) to the scotoma edge just covering the target (error fixation). Both error types can mask the target completely and bring the flow of visual information to zero. There may be an increase in contrast sensitivity thresholds.[7,8] It should be noted that artificial scotomas positioned across the foveal region of the retina are accompanied by a reduction in the motor component of convergence and divergence,.[9,10] although this is not of immediate concern to the present approach.

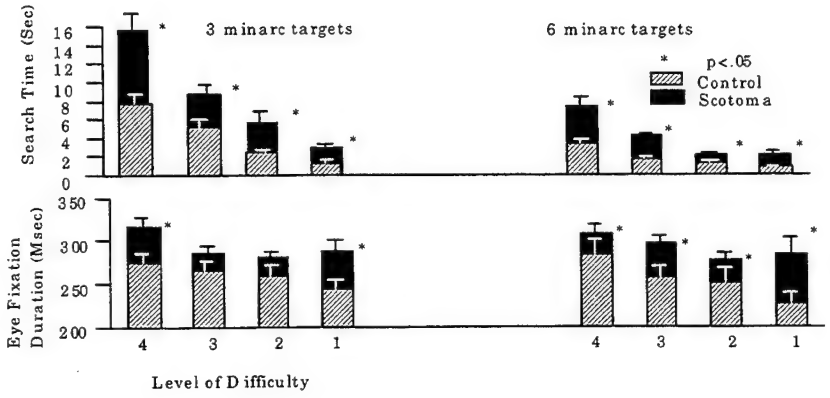

Figure 2

Visual search time and eye fixation duration for acuity targets with 3 or 6 minarc gaps. The level of difficult was a combination of search element density and relative contrast. The most difficult task (level 4) was to search for a small (3 minarc) gap of low contrast in a dense display (99 non-target elements). The large impairments in search and significant increases in eye fixation duration were found even though the simulated scotoma was only 20 minarc in diameter. (N=23)

Scotoma size and fixation duration

The most salient characteristic of the scotoma is its size. Simulated loss of a small (20 minarc) area of the central visual field was associated with a doubling in the search time and under some conditions significant (15%) increases in eye fixation duration (See Figure 2). This supports the idea that relatively small central field scotomas can produce large impairments in visual search if tasks require a high degree of foveal vision.[11] During reading single lines of text (See Figure 3) where the eye movement path is very well defined,

as scotoma size increases from 0 to 5.6 degrees in diameter, eye fixation duration increases from about 200 msec to over 400msec[12]. It appears that task conditions which require more foveal vision, such as fine detail or letters, are more sensitive to the impairing effects of a foveal scotoma. If foveal vision is not critical to a task, a foveal scotoma has very little effect, e.g. in visual search for targets with relatively large gaps, high contrast and with small scotomas.[11]

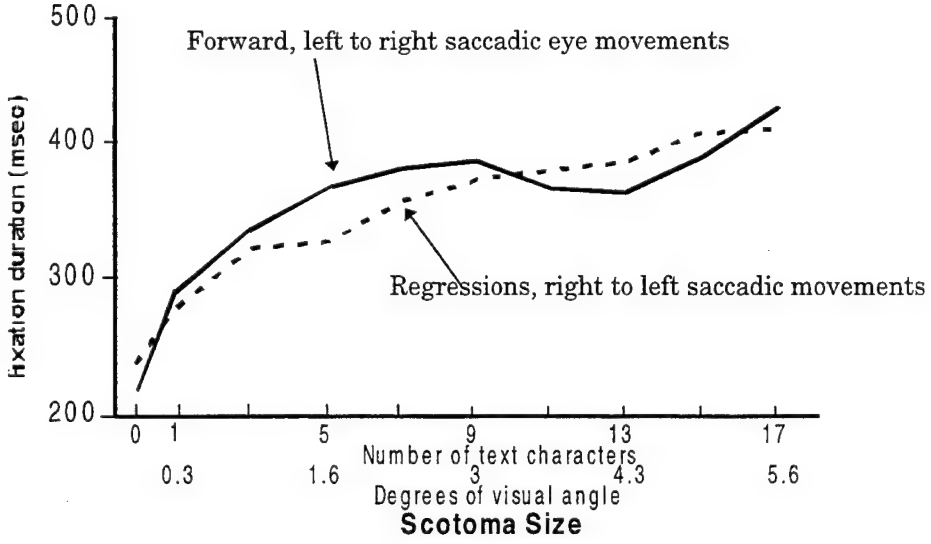

Figure 3

Reading lines of text with scotoma. Increases in scotoma size produce an increase in average eye fixation duration from 200 msec to 430 msec, as scotoma size increases up to 5.6 degrees (diameter). Reading time increased, comprehension (number of recalled words) declined, and saccade length decreased-until it appeared that the subjects were decoding letter by letter. Reading text differs from steady eccentric fixation in that the information acquired in reading English is generally considered to be from the right of fixation, but during steady fixation tests subject preferred to take information from the left of fixation. (N=4)

Asymmetry in preferred viewing position

Subjects faced with the task of adapting to the loss of central vision sometimes position their eyes in ways which are either asymmetrical, not optimum, or seem to generate abnormal eye movements even after extensive practice. There are preferences in viewing position in patient populations with clinical scotomas in which the eccentric viewing adaptation has had years to develop. Cummings et al[13] found that 72% of patients with a central visual loss had developed a single, strongly preferred viewing position outside of the scotoma. Timberlake, et al[14] also determined that patients with long standing macular disease tend to use an area adjacent to the scotoma for eccentric viewing, called a preferred retinal locus (PRL). However, their PRL was not necessarily as close as possible to the foveola, i.e., their strategy did not maximize resolution. White and Bedell[15] further determined that macular disease scotomas of 5, 10, or 20 degrees were associated with a preferred fixation area but re-referencing of eye movements to these areas was incomplete.

In a study of spontaneous adaptation to a simulated scotoma in six normal subjects, there was a marked preference to consistently position the scotomatous fovea out of the way to the upper right relative to the target (See Figure 4) even when subjects were free to look anywhere they choose. The subjects were required to hold the stationary target in clear view with a 2.5 degree scotoma across their fovea which moved over background grid lines. This consistent, preferred fixation position translates into maintaining the

target on the superior temporal retina and as close to the scotoma border as possible, i.e. in the highest available resolution retina. It is probably no coincidence that clinical reports indicate that patients are much more likely to notice deficits in vision when laser treatment or disease creates visual loss on the superior retina. This makes sense since the superior retina receives much more input from below the horizon field where there are more visual signals for daily activities. However, there are many asymmetrical functions and cellular architectures across the retinal[16] that might be used to explain the left right asymmetry, such as, left-right biases from reading habits, cerebral hemisphere asymmetries for input and spatial attention, and the position of the optic nerve.

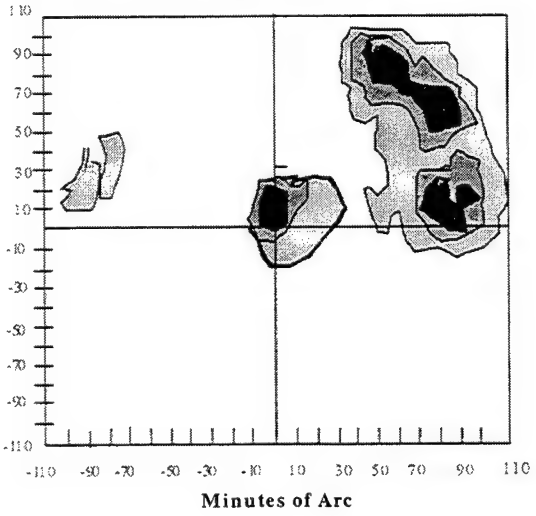

Figure 4
Composite map of eye position samples for six subjects. The subjects attempted to keep a central target cross (located at intersection of lines) in clear as possible view for a total of about 300 sec with a 2.5 degree simulated scotoma across their fovea. Density of crosshatching indicates increasing % fixation positions. An asymmetry is obvious in the scatter of eye positions which were freely chosen by these naive subjects. All subjects claimed that the upper right fixation position "felt" easier than anywhere else. Clusters of eye positions near the center represent the most common error: fixating the target with the scotoma. Darker areas show greater total fixation time. (N=6)

Scotoma nystagmus and drift.

During adaptation to a foveal scotoma, stable eccentric fixation and prolonged eye fixation durations may set the stage for the onset of drift or the slow phase of scotoma nystagmus (See Figure 5 & 6). These slow movements during eccentric viewing range from drift movements, some lasting 15 seconds, to repeated nystagmus-like movements consisting of drift with a saccadic return, called scotoma nystagmus. Unlike other forms of nystagmus (optokinetic or vestibular) this scotoma "nystagmus" can be interrupted with verbal instructions to make saccades. The significance of such movements is that they redefine the eccentric viewing position as a track.

Steinman and Cunitz[17] detected such drift eye movement while two subjects used eccentric viewing with a physiological scotoma and implicated them in the fluctuating visibility of targets first noticed by Simon.[18] They suggested that the drift movements were directed towards a target disappearance point and that the drift mechanism is guided by some retinal architecture or normal motor habit for fixation control. Whittaker, Budd and Cummings[19] found drift eye movements with scotomas in three more subjects and showed that drift slow phase can be consistently towards other directions than the target, i.e., the normal fixation locus. Whether drift was target directed or not was idiosyncratic.

Bertera[20,21] measured eye movements during the early scotoma adaptation period and found repeated drift movements with normal subjects with simulated scotomas. Five subjects emitted drift eye movements with saccadic returns, but only after the initial period of adaptation when error saccades were minimized and the eccentric viewing position "settled down" to a stable vantage point. All the subjects showed periods exclusively of drift which brought the scotoma edge near an optimum position to the target followed by saccade returns, similar to jerk nystagmus. The target directed drift movements were strategic since they often ended before the scotoma actually obscured the target. The subject in Figure 5 shows a typical drift

amplitude of about one degree. The drift velocity ranged from 20 to 120 minarc/s. Drift was a significant portion of the total viewing time, averaging 58%.

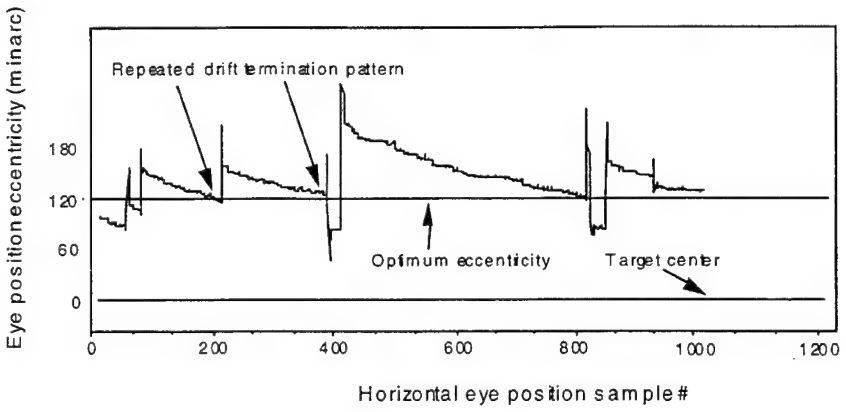

Figure 5

Eye drift and eccentricity from target (minarc). At 120 minarc, the optimum eccentricity, the target is visible. Repeated termination of drift as the scotoma boundary approaches the target generates a jerk nystagmus pattern. To avoid covering the target the subject must estimate the distance from fovea to target (or from scotoma edge to target). The subject learns the extent of the scotoma boundary when a target disappears inside it.

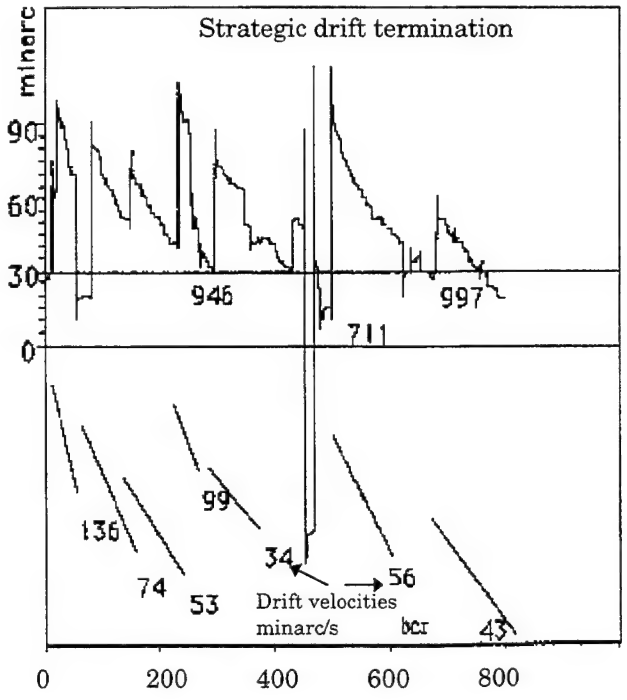

Figure 6

Eye drift track and drift velocities show a form of "scotoma nystagmus". Horizontal eye drift stops as target approaches the 30 minarc scotoma boundary (line at 30). Drift is strategic since it terminates about 10 minarc before the scotoma boundary crosses the target. The drift appears to be under enough control to be used to limit error fixations at the end of saccadic eye movements. Estimation of the distance from the scotoma boundary to the target may be made with previous feedback from boundary crossings and target disappearance or spatial mapping on retina. There are still residual error saccades but most are too short to bring the scotomatous fovea near the target. The drift velocity is 20 to 80 minarc/s, compared to some fast phase saccade velocities at around 1000 minarc/s. A higher drift velocity was typical early in a 2 minute trial. (N=1)

Hyper-eccentric viewing with drift, steady fixation and saccades.

The drift or scotoma track moves the average viewing position away from fovea towards more peripheral or hyper-eccentric retina with poorer acuity. A drift or nystagmus track of 60 minarc would position the eccentric viewing point 60 minarc farther from the target than necessary, for example, with a 120 minarc radius scotoma. Hyper-eccentric adaptation to scotomas has the effect of enlarging the scotoma so that the spot size on the retina is an underestimate of the impairment. It is well known that the ophthalmoscopically visible area of injury on retina may not be the full extent of the area of visual dysfunction. It appears that scotoma nystagmus may serve also to expand the functional scotoma beyond the tissue damage dimensions.

There are at least two possibilities for enlarging the functional scotoma by adjusting the eccentric viewing position, so that targets fall farther than needs be from the scotoma boundary. The first is through the scotoma nystagmus shown above, through the return saccades that reset the eye position for another drift towards the target. The second hyper-eccentric adaptation could to be due to overestimate of the scotoma size (See Figure 7) along with a lack of exploration of the scotoma boundary. Such overestimates could be associated for example with a shrinking scotoma caused by recovery from bleaching and the fading of a light afterimage. On the other hand, underestimating the scotoma size could be associated with an emerging scotoma, developing from increasing retinal edema.

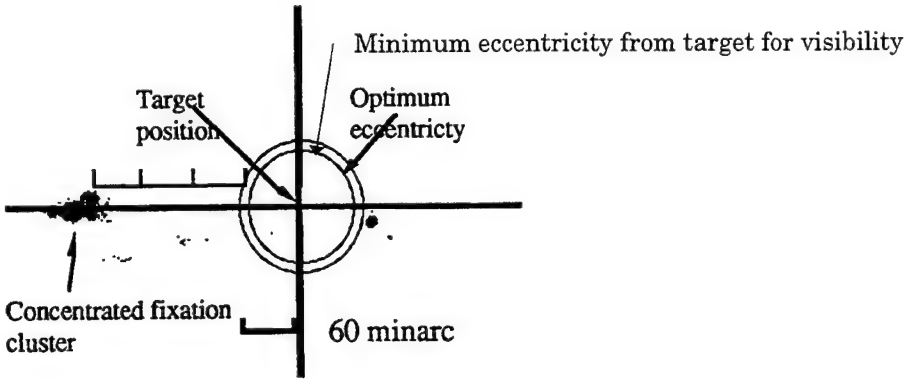

Figure 7

This subject's eye positions show paradoxical hyper-eccentric fixations -- while the scotoma is only 60 mm radius the main fixation cluster is approximately 3 times farther from the target than necessary. This subject was given a larger scotoma on previous trials and had very stable fixation position. When the scotoma became smaller the subject did not adapt because no feedback indicated that the eccentric fixation position should be adjusted inwards to optimize the viewing position Verbal instructions that the scotoma is smaller produce fast correction to paradoxical eccentric fixation.

Saccades and steady fixation are affected quite differently by a scotoma. If a subject tries to fixate a single stationary target in peripheral vision there are two processes which must be accounted for. Adjusting the eye position in small trial and error increments until the target is visible near the scotoma edge is required as the first step. Once an alignment to the target has been achieved the subject may need only to inhibit the reflexive tendency to fixate the target with the scotomatous fovea. However, if the target is moving, either smoothly or in jumps, the subject must update their eye position with saccades to maintain an optimum eccentric viewing position.

When the target moves, e.g. once per second, the subject is required to make a series of saccades to keep the target on an eccentric viewing position. At each landing or fixation the subject must detect the new target position, program a saccade of the right length depending on the current eye position, and finally land and check to see if the target is outside of the scotoma boundary. This problem was examined in an animal

model[22] by ablating fovea bilaterally in monkeys. When required to maintain a steady eccentric view to a single stationary target, adaptation of fixation position was rapid and the animal was able to maintain the target outside of the scotoma boundary, much like the human subjects with a simulated scotoma. However, in a second saccade tracking task, the target shifted around the display requiring repeated saccades to maintain the target in view outside of the scotoma. Here the subjects showed little adaptation and continued to make foveations with the scotoma area.

Compromises in eye positioning

It seems that fixation adapts but saccades do not. The reason probably lies in the processes of computing a landing position in the periphery and in defeating the reflex to land with fovea, which must be accomplished just before the saccade starts. However, the recorded eye positions below (See left panel) show that subjects are able to orient their saccades to two targets and achieve a position which makes both targets visible from a single eccentric vantage point. However, these scotoma saccades are not accurate enough to position targets on the optimum spared retina.

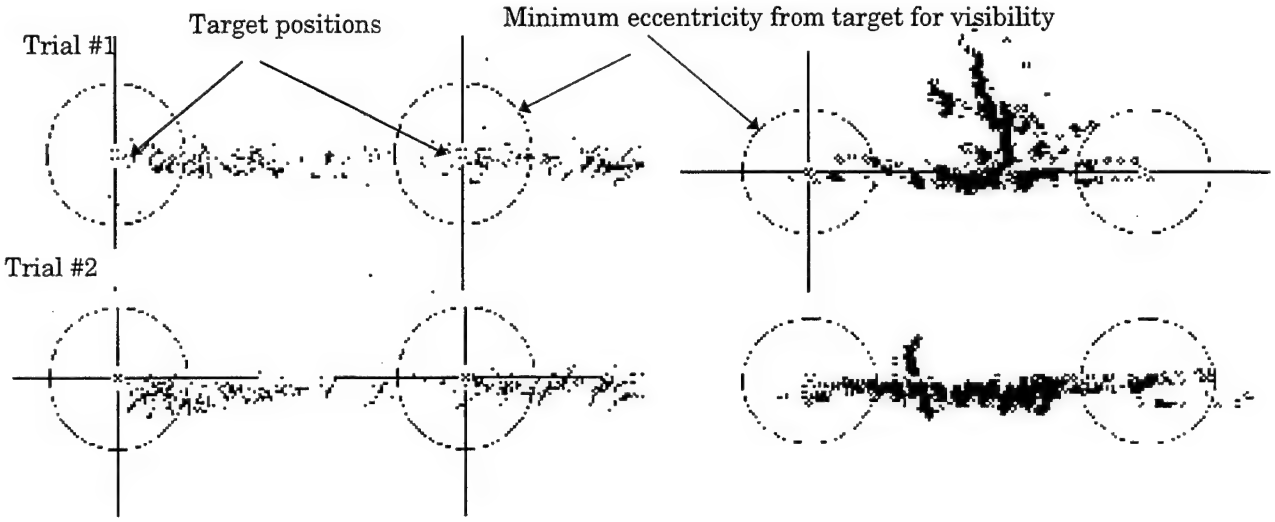

Figure 8. Instructed eccentric fixation positions with a 120 minarc scotoma. Subject was instructed to look to the right of the targets in a two saccade pattern (left panel) or on the inner side of the targets (right panel). This back and forth motion produced an inaccurate scatter of eye positions. Minimum eccentricity from target for target visibility places fovea (and scotoma center) on dotted circle line.

4. STRATEGY FOR EYE POSITIONING AND VISUAL AIDS

Five processes were presented above that are present during the adaptive response to a central scotoma and may contribute to controlling target viewing time and eccentricity from fovea. They were: 1) Asymmetric eye fixation positions, 2) Reflex foveations (scotoma fixations), 3) Scotoma nystagmus, 4) Hyper-eccentric eye positions, and 5) Compromise in eye position. These processes can be viewed as residual deficits or as the active capacity for change in the oculomotor system. Viewed as active processes, it should be expected that any strategy for compensating for the loss should address them, and ideally, employ whatever advantages possible by incorporating them. The objective is to increase viewing time and optimum eccentricity.

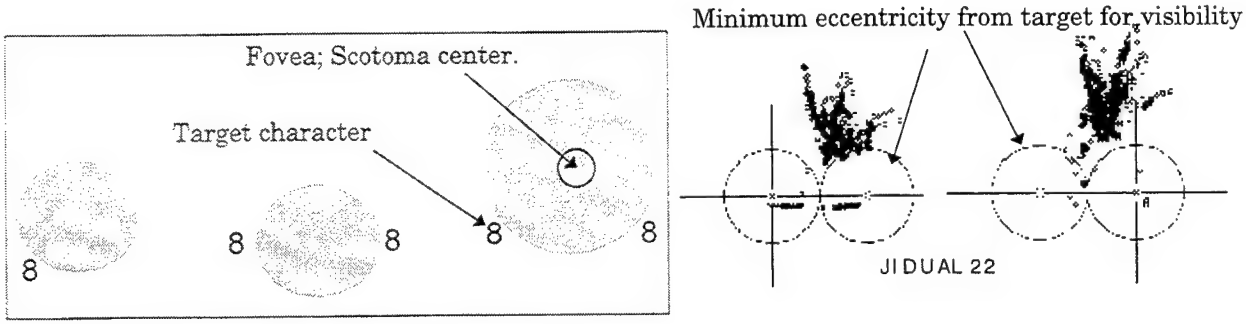

Figure 9. Panel Left-Three vantage points for steady eccentric fixation depending on target configuration. Single target with grayed image of scotoma. Middle: Two targets with scotoma sized to "fit" between them so both are visible. Right: Two targets with large scotoma; to make both visible; eccentric fixation point must be shifted upwards, a compromise position. Panel Right-Examples of eye positions with two target compromise positions, making both targets visible.

Saccade braking and image shifting are two strategies that could be of value in adaptation to visual loss. Both employ limited, voluntary saccadic eye movements to discover the scotoma boundary, and to minimize reflex foveations, drift, and hyper-eccentric fixations. The effect of saccade braking, first described generally by Dell'Osso, relies on the mutual incompatibility of voluntary saccades and drift. By making periodic voluntary saccades the subject prevents drift and retains more control over the oculomotor system. In image shifting, the portion of the central visual field corresponding to the scotoma is copied into a computer memory and is rapidly re-displayed on the highest resolution peripheral retina outside of the scotoma area. The following functions can be implemented within a presently attainable hardware-software system: copy the current image under the scotoma, save it, and shift and re-display the image at a peripheral location, then, replace the image to its true location and erase the shifted copy, after an eye movement moves the scotoma to a new location (See Figure 10.). Image shifting uses the normal pattern of peripheral attention to foveal fixation as a designator to direct the electronic image shift system. Instead of trying to break up or inhibit the normal reflexive pattern of eye movement that brings peripheral targets to fovea, the image shift method employs the reflex to designate the targets of interest.

An important variable in selection of the peripheral area for the image transplant area is the relationship between the size of the scotoma image and the size of the anticipated targets. Scotomas smaller than a target image would require mutilation of the target image in an image transplant operation if only the scotoma area were copied and shifted to peripheral retina. A partial remedy for such image truncation may be found in an image shift system which transplants as large an image as feasible to the periphery no matter what the scotoma size. The choice of the position for the transplant area is the preferred viewing asymmetry described above, i.e. the stereotyped lower right visual field relative to fovea.

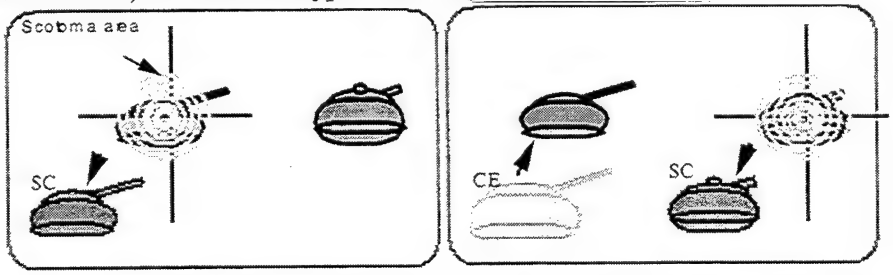

Figure 10. Image shifting between two alternately fixated targets. Panel Left: An eye fixation to the left target obscures it requiring the target to be shifted graphically to a preferred eccentric viewing position. Panel Right: An eye fixation to the right target, obscures it, requiring another image shift to the PRL, but also a replacement of the shifted left target image.

There are several advantages to an automated image shifting method over unaided eccentric viewing to compensate for central visual loss. First, there is consistency in maintaining reflexive pattern of eye movement that brings peripheral targets to fovea; the image shift method employs the reflex to designate the targets of interest. After an area of interest has been designated, a computerized graphic controller can then rapidly re-display the area in a position outside of the scotoma. A zero delay between eye position change and image shift, the ideal, is only possible in a case of true retinal lesion or with an afterimage from strong light sources. While such a close linkage of eye movement and image jumps might be useful, repeated image jumps could stimulate the visual motor and information processing systems with many temporal transients.

ACKNOWLEDGMENTS

This work was supported in part by the U. S. Army Medical Research Acquisition Activity Contract No. DAMD17-94-Z-4068

REFERENCES

[2] P. A. O'Mara, D. A. Stamper, , Lund, J. D., and Beatrice, E. S. Chromatic strobe flash disruption of pursuit tracking performance. Letterman Army Institute of Research, Report No. 88, November, 1980. p1-18.

[3] B. Stuck, Ophthalmic Effects of Lasers - Research knowledge. Medical (Ophthalmic) Surveillance Symposium, U.S. Army Environmental Hygiene Agency, Aberdeen Proving Ground, M.D,.1982, 21-31.

[4]A.R. Menendez, and P.A. Smith, Model for predicting the effects of laser exposures and eye protection on vision, School of Aerospace medicine, Interim report, January, 1990, 1-14.

[5]R.P. Green, R.M. Cartledge, F.E. Cheney and A.R. Menendez, Medical management of combat laser eye injuries: School of Aerospace Medicine, Brooks, AFB, Final Report, Oct 1986-October 1988, 1991

[6]E. Ludvigh, Extrafoveal acuity as measured with Snellen test letters. Am J Ophthalmol, 1941, 24, 303-310.

[7] D.H. Kelly Photopic contrast sensitivity Optics Letters, 2:79, 1978.

[8] K.E. Higgins, R.C. Caruso, N.J. Coletta and F.M. de Monasterio. Effect of artificial central scotoma on the spatial contrast sensitivity of normal subjects. Investigative Ophthalmology and Visual Science, 24:1131-1138, 1983.

[9] A.E. Kertesz and D.R. Hampton, Fusional response to extrafoveal stimulation. Investigative Ophthalmology and Visual Science, 21:600-605, 1981.

[10] D.K. Boman and A.E. Kertesz, Horizontal fusional responses to stimuli containing artificial scotomas. Investigative Ophthalmology and Visual Science 26:1051-1056, 1985.

[11]JH. Bertera Effects of simulated scotomas on visual search in normal observers. Investigative Ophthalmology and Visual Science. 1988, 29:470-475.

[12] K. Rayner, K. & J.H. Bertera Reading without a fovea. Science, 1979, 206, 468-469.

[13]RW Cummings, SG Whittaker, GR Watson, and JM Budd, Scanning characters and reading with a central scotoma. Am J Optom Physiol Optics, 1985, 62, 833-843.

[14]GT Timberlake, MA Mainster, E Peli, RA Augliere, EA Essock and LA Arend: Reading with a macular scotoma I. Retinal locus of scotoma and fixation area. Invest Ophthalmol Vis Sci 27:1137, 1986.

[15]JM White and HE Bedell,: The oculomotor reference in humans with bilateral macular disease. Invest Opthalmol Vis Sci 31:1149, 1990.

[16]W.K. Estes and G.L. Wolford, 1971, Effects of spaces on report from tachistosopically presented letter strings. Psychonomic Science, 1971, 25, 77-8.

[17]RM Steinman, and RJ Cunitz. Fixation of targets near the absolute foveal threshold. Vision Res 1968; 8:277-286.

[18]R. Simon, Uber fixation im Dammerungssehen. Z. Psychol. Physiol. Sinnesorg. 1904, 36, 181-189. Referenced in Steinman and Cunitz, 1968.

[19]SG Whittaker, J Budd, RW Cummings. Eccentric fixation with macular scotoma. Invest Ophthalmol Vis Sci 1988; 29:268-278.

[20]JH Bertera. Preferred retinal loci and drift direction with simulated scotomas in normal subjects. Investigative Ophthalmology & Visual Science. 1990, 31, 598.

[21]J.H. Bertera, Blindness simulation in normal subjects and target position effects. Computer Simulation Society, Summer Simulation Conference, Baltimore, MD, 1991.

[22]SJ Heinen, and AA Skavenski Adaptation of saccades and fixation to bilateral foveal lesions in adult monkeys. Vision Research, 1992, 32, 365-373.

Visual Acuity Changes in Rhesus Following Low Level Q-Switched Exposures

David O. Robbins, Harry Zwick, Bradley D. Bearden, Brenda S. Evans, Bruce E. Stuck

Department of Psychology, Ohio Wesleyan University, Delaware, OH 43015 and United States Army Medical Research Detachment, Walter Reed Army Institute of Research, Brooks AFB, TX 78235-5138

ABSTRACT

Previously we have shown that visual deficits can be produced by long (msec) duration pulses at or slightly below traditional threshold levels for retinal injury. Initially the deficits produced were only transient shifts in baseline acuity that lasted less than 30 min, but successive exposures over a period of days at these same power levels were shown to be cumulative and their impact on visual acuity lengthened and became permanent. The present investigation extended these exposures to Q-switched, 532 nm Nd/YAG pulses presented to awake, task-oriented nonhuman primates performing Landolt ring discriminations. At and above the ED_{50}, single pulses of minimal spot diameter (50 μ) produced only minor, transient shifts in visual acuity while repeated exposures produced significant shifts in acuity that became permanent over time. At lower energies (10X below the ED_{50} level), minimal spot, single-pulsed exposures again produced little observable consequence until either retinal spot sizes or number of pulses were increased. At these lower energy levels, however, no permanent functional loss was observed. Hence, the functional impact of single Q-switched pulses was more difficult to assess than longer time domain exposures. Multiple, low level Q-switched pulses, and/or larger spot sizes produced visual deficits similar to those observed for msec time domain exposures, suggesting both temporal and spatial summation at energy levels where no permanent effects have been noted.

Keywords: laser irradiation, functional deficits, visual acuity, rhesus monkeys, transition zone, flash blindness, visual loss

1. INTRODUCTION

Traditional fundoscopic and histological studies have provided clear evidence for the presence and location of morphological insult that results from relatively intense retinal exposures.[1, 2] These studies typically have been used to derive laser damage thresholds for single or multiple exposures. These thresholds are most applicable to those exposure situations in which the energy is presented over a very limited time period. Somewhat ignored in these traditional standards for laser safety has been the consequences that relatively low level energy exposures might produce if they were repetitively presented over a period of days, weeks, or months and if their impact was assessed using a functional rather than morphological criterion. Previously we have demonstrated the importance of using a functional measure even when presenting brief, spatially discrete CW exposures at or near the MPE. In these studies significant visual deficits were observed for energy densities below the ED_{50} that were of both a transient and prolonged nature. Single-pulsed, minimal spot diameter, Q-switched exposures produced more elusive functional results and failed to demonstrate any significant permanent functional deficit even at power densities above the ED_{50}. Increasing the area of retinal involvement either by using multiple pulses or larger diameter spots, however, has resulted in prolonged functional deficits of the type observed using CW lasers.[3] For example, we have demonstrated that daily exposure to power densities at or below a transition zone between temporary and permanent functional loss become additive resulting in longer recovery times for each successive exposure at the same power level. The additivity of successive exposures at the transition zone was most easily observed when relatively large-diameter (>100 μ), prolonged CW (100 msec) retinal exposures were made. When relatively small diameter (<50 μ) Q-switched (15 nsec) exposures were presented, significant decreases in acuity were less detectable even with relatively intense exposures presented as single or multiple pulses with or across test sessions.[4]

Different damage mechanisms have been proposed to explain variations in the severity and location of the elicited damage. Generally, a thermal model has been attributed to those changes resulting from relatively long duration, low energy exposures to long wavelength coherent light. On the other hand, mechanical damage mechanisms have typically been

SPIE Vol. 2974 • 0277-786X/97/$10.00

associated with extremely high energy, short duration (Q-switched) pulses. As morphological techniques for detecting minimal retinal alterations have been refined, the energy levels necessary to produce threshold damage have decreased. Furthermore, the site of minimal damage has shifted to examinations of the fine structure of the photoreceptor outer segments.[5, 6, 7] Since the site of morphological disruption observed is the location where the initial transduction of light energy to electrochemical energy occurs, it is also important to consider the behavioral (functional) consequences of any induced physical change. Obviously, changes in the functional capacities of the retina have specific legal, medical, and ultimately practical consequences especially when considering how much human behavior is based on accurate visual assessments of the physical world.

Less frequently examined are the more subtle changes associated with repeated low energy exposures at power levels well below those in which either thermal or mechanical disruptions would be predicted. In these cases it has been proposed that laser irradiation might produce photoreceptor and/or photopigment damage which ultimately could affect the receptor transduction process and even the viability of the receptor cell itself.[8, 9, 10] It might be expected that functional changes associated with these more subtle retinal alterations would be a more sensitive measure of the adverse effects of low level laser irradiation since these types of physical changes in retinal morphology and/or photochemistry would be extremely difficult to detect in an intact retina.

The development of behavioral techniques to rapidly assess altered retinal functioning and the added ability to expose awake, task-oriented animals further extended explorations of the transition zone between permanent and temporary shifts in visual acuity. These techniques[11] eliminated the need to anesthetize the subject for the reliable placement of foveal exposures. Any use of anesthesia delays the opportunity for postexposure testing by as much as 24 hours, eliminating any attempt to explore the transient or initial effects of laser irradiation both above and below the energy levels necessary to produce a permanent alteration. Furthermore, the need to use anesthesia as a method to reliably isolate laser exposures on the retinal mosaic seriously curtails the exploration of any cumulative consequences of repeated exposures, since frequent administration of anesthesia in the same animal is medically inadvisable. In the past only wide field laser irradiation could be chronically employed without anesthesia since it was difficult to predict the amount and location of light exposure in an awake animal with relatively free head and eye movements. When using relatively small diameter exposures (less than 500 μ) that more closely simulate real life exposure conditions, however, it was necessary to develop this behavioral paradigm to condition animals to voluntarily restrict their eye and head movements and fixate on a known portion of their visual field. Exposures outside an animal's fovea should produce little or no shift in maximum photopic acuity since such exposures would allow the animal the ability to "look around" the exposure site(s) and use other, equally or more sensitive, retinal regions to make the required discriminations. Therefore, this method was critical for producing foveal exposures necessary to assess immediate postexposure photopic acuity in a behaviorally active animal.

We have previously shown that acute exposures can produce both transient and prolonged shifts in visual acuity immediately following laser irradiation. Below the transitional zone daily laser exposures normally produce predictable temporary degradations in acuity which vary little from one exposure to another. At higher exposure energies within the transitional zone, however, we have shown that the performance decrements produced by successive pulses become additive and ultimately lead to permanent shifts in visual acuity. These effects were primarily observed with CW laser pulses of relatively long duration. Earlier work with Q-switched pulses at and below the ED_{50} has failed to demonstrate any significant loss in visual function. We have previously shown that repetitive high energy Q-switched pulses over time produce a significant visual loss that is relatively long lasting.[4] However, these visual losses were likely compounded by retinal edema produced by these laser pulses. The present study characterizes the time course of acuity deficits and recovery for low level Q-switched pulses at levels below those that would be expected to create either an ophthalmic lesion or retinal edema.

2. METHOD

A reliable behavioral technique was developed to expose awake, task-oriented animals. This method required animals to maintain central fixation for prolonged periods of time during the test session. The impact of random and voluntary eye movements was further reduced by using relatively brief duration exposures that were presented while the animal was

actively engaged in a threshold visual discrimination task that required fixation on known critical features of the visual targets.

Subjects and Apparatus. Adult male rhesus monkeys with normal vision were used as subjects. The animals were housed in traditional primate cages and were tested in a portable restraint apparatus. This device [12] was also used to transport the animal to and from the housing colony. A custom fitted helmet molded from high impact plastic and equipped with an inner, high density foam liner with an inflatable air bladder allowed for stability of the animal's head without undue force or discomfort. An opaque facemask with an adjustable iris diaphragm was aligned with the animal's line of sight. This required the animal to voluntarily align its pupil with an artificial pupil in order to successfully avoid an aversive stimulus and to complete the visual discrimination task. Animals were quickly trained using positive reinforcement to voluntarily leave their home cages and enter the restraint apparatus without resorting to drugs or unnecessary force.

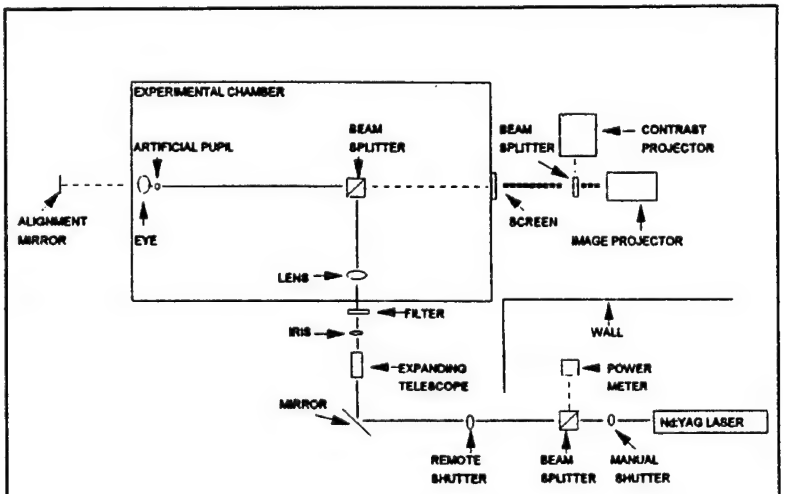

Figure 1. Diagram of the laser and image optical system. The laser beam from Q-switched Nd/YAG laser was presented using a Maxwellian view and was coaxial to the gap in a threshold Landolt ring. The number of Q-switched pulses, energy per pulse, and the diameter and position of the beam on the retina was controlled outside the test chamber.

Discrimination Task. Animals immobilized in the restraint device were trained to press a lever when they detected the presence of a Landolt ring ("C") which was randomly positioned within a series of equally sized gapless rings ("O"). Individual rings were successively projected onto a rear projection screen placed one meter in front of the artificial pupil that was mounted onto the animal's head restraint. The animal's failure to press the lever to the Landolt ring when presented (miss), or lever pressing during the presentation of a gapless ring (false alarm), resulted in the presentation of a brief discriminative tone, and on a variable reinforcement schedule, the administration of a brief electrical shock. Threshold acuity was derived using a tracking technique. In this technique, if the subject correctly detected the Landolt ring (hit) by pressing a lever, the next series of Landolt rings and gapless rings were 10% smaller while incorrect detections of the Landolt ring (miss) produced the presentation of rings 10% larger. The critical feature of Landolt ring that distinguished it from a gapless ring varied from 0.25' to 30' visual angle and was always positioned in the same location on the viewing screen. By varying the payoff matrix used during training, the number of false alarms was remarkably low (<10%) and animals maintained a stable acuity for periods in excess of 45 minutes of testing. In well trained animals, baseline visual acuity varied from Snellen acuity of 20/25 to 20/15 depending upon the parameters of the viewing conditions. Darkened rings of various diameters were projected onto different wavelength and intensity backgrounds to determine any differential color, contrast, or brightness acuity effects. In a series of comparative tests, the baseline visual acuity of rhesus and human subjects was remarkably similar which supports the use of rhesus as a prototype for predicting human performance following laser irradiation. [13,14]

Laser Exposures. A Nd/YAG pulsed laser was positioned on an optical bench outside the test chamber. The laser beam was first directed through several neutral density filters and a manual safety shutter before passing through an electronic shutter and beam splitter. A portion of the attenuated beam was incident upon an absorbing disc calorimeter for monitoring exposure energy. The transmitted portion of the beam was diverted by a front surface mirror and passed through a variable beam expander and a convex lens placed in front of the animal's pupil. A coated pellicle beam splitter placed 5 cm in front of the lens was positioned at the intersection of the diverging laser beam and the light beam from the viewing screen. The laser beam was positioned such that it was presented to the animal coaxial with a line between the artificial pupil and the gap in a specified, threshold Landolt ring, or in the case of off-axis exposures, was positioned one degree above the gap in

the specified Landolt ring. (Figure 1). Beam diameter could be varied from less than 50 μ to greater than 500 μ on the retina. The number of pulses presented to an animal was controlled by an remote electronic shutter placed in the beam pathway. Varying the duration of the shutter opening from less than 50 msec to greater than 250 msec resulted in the presentation of one to six pulses within the exposure session. Longer duration exposures were avoided to eliminate any impact voluntary eye movements might have on the position of the energy on the retina.

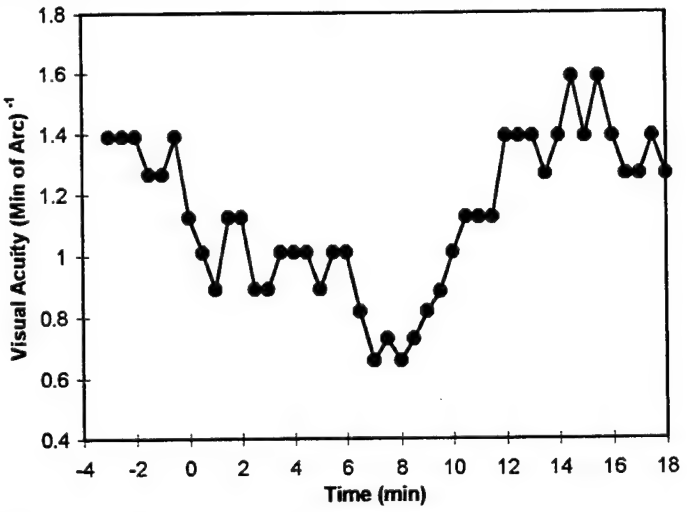

Figure 2. Sample raw data demonstrating the immediate drop in visual acuity following laser exposure. The ordinate indicates the various sizes of the gaps in presented Landolt rings. The scale is measured in discrete steps. The abscissa represents the presentation of the Landolt rings; corresponding times (in minutes) for representative trials are indicated relative to exposure. Two, 0.1 μJ Q-switched pulses of 300 μ diameter were used.

All exposures were presented while the animal was tracking its threshold visual acuity and immediately after the animal had correctly detected a minimal gap in the Landolt ring. Observations of animals working under these conditions have shown that they normally maintain their fixation on the screen for several seconds following lever pressing. Normally animals were exposed only once per day and only after their pre-exposure baseline was reliably established. Prior to any exposures, complete baseline acuity measurements were obtained for both the experimental and control eye. Postexposure acuity measurements continued until the animal regained its pre-exposure acuity or the elicited deficit had stabilized (see Figure 2). All behavioral testing including laser exposures were made under monocular viewing conditions.

3. RESULTS

When single Q-switched pulses of small diameters (50 to 150 μ spots on the retina) were presented, there was relatively little decrement in visual acuity noted regardless of the energy of the pulse. With larger diameter (>150 μ) exposures the adverse impact of single pulses on visual acuity was more evident and generally the same as the transient deficit produced by small diameter exposures presented multiple times in close succession. With either exposure condition, immediately after exposure, the animal's baseline acuity dropped and remained depressed for some time before postexposure acuity gradually returned to its pre-exposure baseline. Both magnitude and duration of the observed visual deficits were related to the amount of retinal area involved (exposure spot size) and to the number of Q-switched pulses presented. Increasing the power density of the exposure for the small diameter exposures or for single pulses produced little visible impact on the animal's visual acuity. With larger spot sizes, however, the energy of the pulses clearly influenced the duration of the deficit as well as the likelihood of full recovery within the remaining time of the test session.

The impact that multiple Q-switched pulses had on the animal's performance on the visual acuity task is shown in Figure 3. In this example, the animal was exposed to a series of 5-6 low-level energy pulses within a 250 msec window. Each pulse created a 500 μ spot on the retina and was presented coaxial with the gap in a Landolt ring. The exposure was triggered as soon as the animal responded to its threshold Landolt ring, while the ring was still displayed on the viewing screen. Postexposure acuity was measured using either high or low luminance targets. The animal's pre-exposure acuity in the high luminance condition (bright screen) was approximately 1.2 $(\text{min of arc})^{-1}$ or a Snellen acuity of 20/17 while this same animal's pre-exposure acuity derived under the low luminance condition was approximately 0.65 $(\text{min of arc})^{-1}$ or a Snellen acuity of 20/31. In this figure and those that follow, average postexposure acuity for each two minute interval after exposure is plotted as a function of pre-exposure acuity and is displayed as a percent deficit. Our animals' pre-exposure acuity varied little from session to session and was extremely consistent within a testing session when no exposure was

made. In Figure 3, the animal's acuity dropped approximately 40% within the first six minutes after the exposure and remained depressed before gradually recovering to its pre-exposure level in approximately 14 minutes. Little difference was noted in either the magnitude or the duration of the deficit when using targets of differing luminances. Similar results demonstrating consistent deficits for both high and low luminance targets were observed for other exposure conditions where spot size and number of pulses were varied. The magnitude of the deficit and its duration were related to the exposure conditions employed. Another consistent result for low energy exposures noted in this figure was the "rebound" effect in acuity during the later stages of the recovery function. Typically after the animal's postexposure acuity deficit recovered, the animal's acuity became temporarily enhanced for several minutes before gradually returning its normal pre-exposure level. In this figure the animal's transient enhancement was approximately 20% better than its baseline, an increase in visual acuity to 1.44 (min of arc)$^{-1}$ or a Snellen acuity of 20/14. This enhancement lasted approximately five to seven min before the animal's acuity returned to its pre-established baseline.

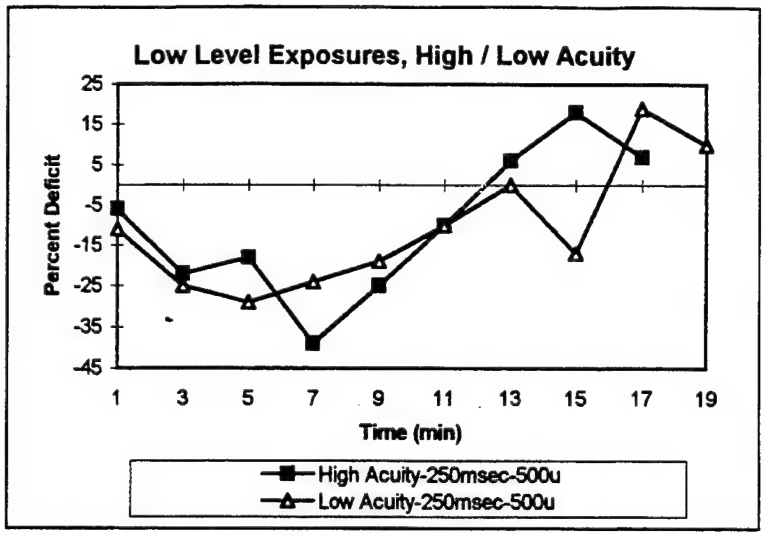

Figure 3. Effects of high and low luminance targets on post-exposure acuity. In this figure the animal was exposed to 5 Q-switched pulses of 0.1 μ J presented coaxial with the gap in a specified Landolt ring. Each exposure was approximately 500 μ on the retina. Postexposure acuity was measured for 20 minutes after each exposure using different targets projected onto white light backgrounds of different luminances.

A comparison of the impact that position of the exposure on the retina had on visual acuity is shown in the next two figures. In these figures the beam was positioned either coaxial with the gap in a threshold Landolt ring (on-axis) or positioned approximately one degree above the critical feature of the target (off-axis). When positioned within the critical feature of the target, a foveal exposure would be expected as long as the animal maintained its central fixation immediately after detecting the presence of a threshold gap. Positioning the beam away from the gap should expose areas of the retina outside the central fovea. In Figure 4, two Q-switched pulses of low energy (0.1 μJ) from a Nd/YAG laser were presented either on- or off-axis. A relatively large retinal spot (500 μ) was employed. The off-axis exposure produced no immediate or delayed acuity deficit. The animal maintained its pre-exposure acuity and, if anything, slightly improved during the course of the 20 minute postexposure session. When an on-axis exposure was made, however, the animal's visual acuity immediately dropped to approximately 25% of its pre-exposure acuity (resulting in a Snellen acuity of 20/24) and remained depressed for several minutes before

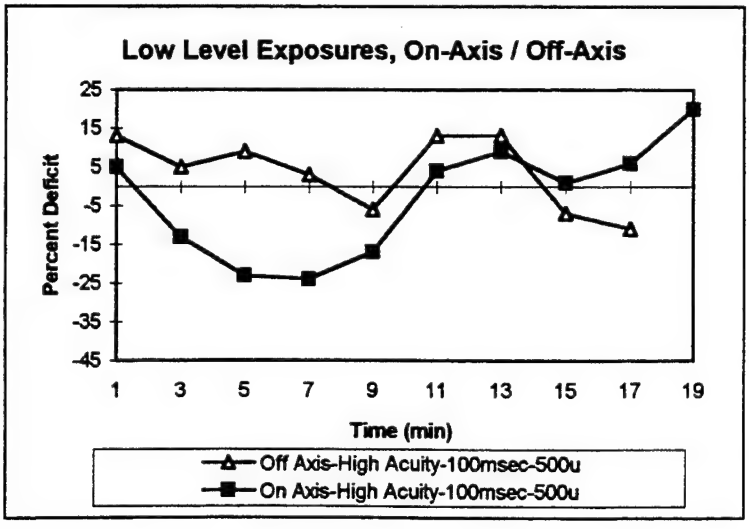

Figure 4. On- and off-axis exposures to low level, Q-switched pulses from a Nd/YAG laser. Two Q-switched pulses were presented within a 100 msec window either coaxial with or temporal to the gap in a threshold Landolt ring. The energy per pulse was 0.1 μJ and the beam diameter on the retina was approximately 500 μ.

gradually returning to its pre-exposure level in approximately 12 minutes. Similar to the previous example, the animal's visual acuity actually improved beyond its pre-exposure level during the final stages of postexposure testing. This acuity level appeared consistent with that observed for the off-axis exposure during its postexposure recovery. In Figure 5, the same comparison of on- and off-axis exposures is made except in this example the number of Q-switched pulses presented was increased from two to four within a 200 msec exposure window. Again for the off-axis exposure, little if any deficit was noted during the twenty minute postexposure session but the on-axis exposure produced an immediate significant drop in visual acuity. The initial postexposure deficit was over 40% (Snellen acuity of 20/28) and the animal's acuity remained depressed for approximately 10 minutes before returning to its pre-exposure acuity level. Similar to the previous examples, the elicited visual deficit was followed by a brief, but significant enhancement in acuity before the animal's acuity stabilized at its pre-exposure level. The initial drop in acuity for the on-axis exposures was greater for four pulses than for two pulses but the total recovery times were approximately the same. The off-axis curves for two and four pulses were virtually identical and demonstrated no significant drop in acuity when laser exposures were presented away from the central fovea.

Variations in the energy per Q-switched pulse did have some impact on the nature of the visual deficit but these differences were most evident for relatively large spot sizes. Single Q-switched exposures of minimal spot size (<50 μ) produced little observable change in postexposure acuity even for exposures at or slightly above the ED_{50}. Increasing the area of retinal involvement by increasing the spot size and/or by increasing the number of isolated Q-switched pulses in a moving eye, however, did produce immediate and transient changes in the animal's

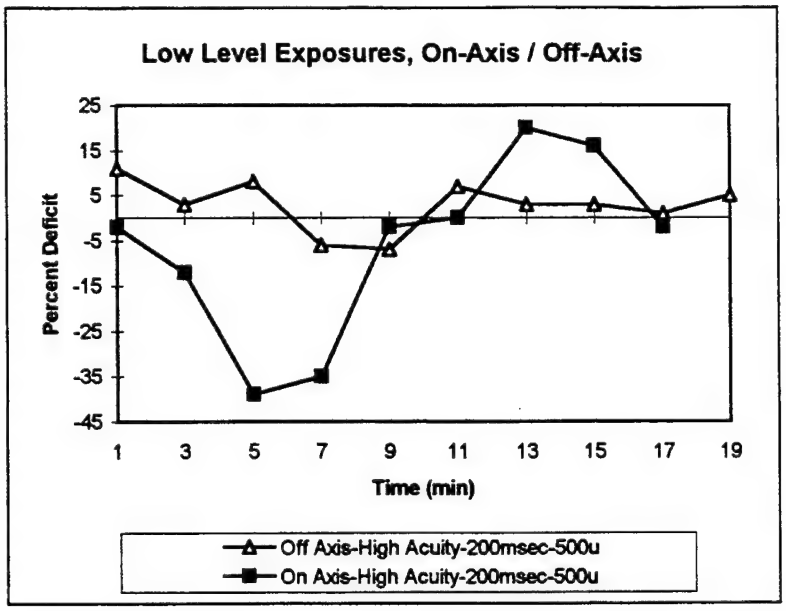

Figure 5. On- and off axis exposures to low level, Q-switched pulses from a Nd/YAG laser. Four Q-switched pulses were presented within a 100 msec time interval either coaxial with and temporal to the gap in a threshold Landolt ring. The energy per pulse was 0.1 μJ and the beam diameter on the retina was approximately 500 μ.

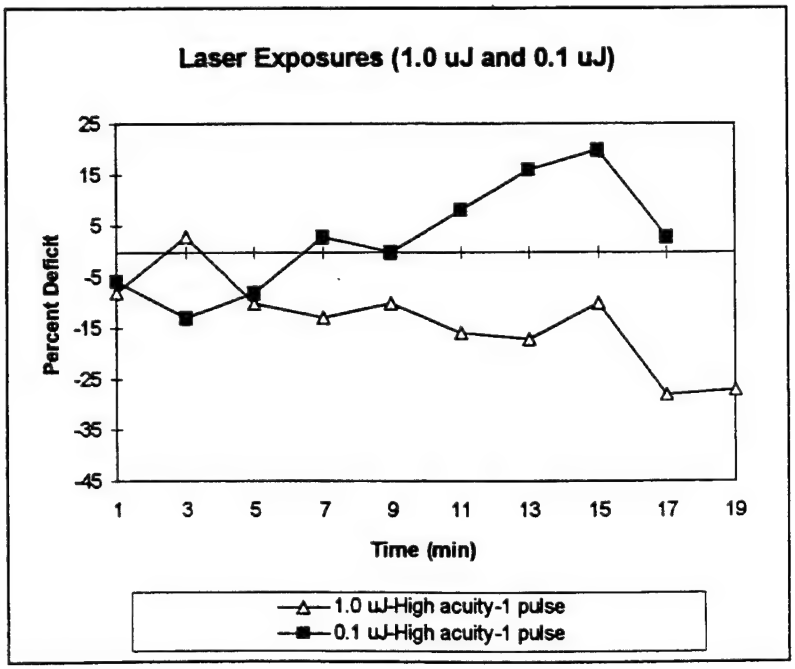

Figure 6. Comparison of a single Q-switched pulse exposure at two different energy levels. Single pulses at 1.0 μJ and 0.1 μJ are presented. Both exposures on made on-axis and the exposure produced a retinal spot size of 500 μ. Postexposure acuity was measured using high luminance targets.

postexposure acuity. In the next two figures the recovery functions for large spot exposures (500 μ) are shown at two different energy levels: 1.0 μJ (ED_{50} for small spot exposures) and 0.1 μJ (one log unit below the ED_{50}). In Figure 6, the animal was exposed on separate sessions to a single Q-switched pulse at both of these energy levels. In Figure 7, the animal was exposed to 3 Q-switched pulses within a 150 msec time interval at these same energy levels. All exposures were presented on-axis and the animal's postexposure acuity was examined using high luminance targets. When exposed to a single, low level Q-switched pulse, the animal's postexposure acuity dropped only slightly for a brief period before returning to its pre-exposure level within approximately eight minutes. This curve demonstrates little initial impact of this exposure on the ability of the animal to maintain a consistent postexposure threshold. However, during the later portions of this postexposure test session the animal demonstrated the same type of enhancement in visual performance that had been noted previously for those exposures where an immediate deficit was observed. In this example, the initial deficit elicited was less than 15% (Snellen acuity of 20/20) and was very transient in nature. The enhancement in postexposure acuity, on the other hand, was somewhat more pronounced and less transient in nature although by the end of the twenty minute test session, the animal's postexposure acuity had returned to its pre-exposure baseline. At a higher power density (1.0 μJ) per Q-switched pulse, again there was no significant immediate visual deficit in comparison to those transient deficits previously noted for the low energy exposures. As time passed, however, the animal demonstrated a gradual but significant drop in visual acuity that lasted for the duration of the test session. Within the twenty minute postexposure session, visual acuity had dropped by approximately 25% and no enhancement effect was noted. The next day the animal's acuity had recovered to its pre-exposure baseline level and remained at this level for the next several days. No additional exposures were presented to this animal during this recovery period.

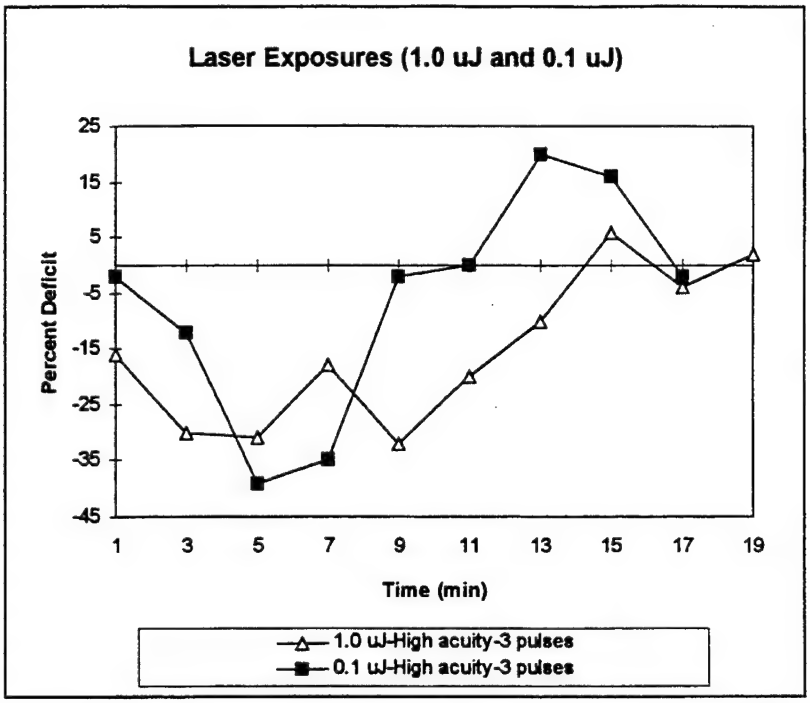

Figure 7. Comparison of three Q-switched pulses at two different energy levels. Three pulses at 1.0 μJ and 0.1 μJ were presented within 150 msec window. Both the high and low energy exposures on made on-axis and the exposure produced a retinal spot size of 500 μ. Postexposure acuity was measured using high luminance targets.

In Figure 7 the same exposures conditions as presented in Figure 6 are shown except in this figure the number of Q-switched pulses were increased from one pulse to three pulses. These three Q-switched pulses were presented within a 150 msec window. When this trio of relatively low energy pulses were presented, the animal's visual acuity decreased by as much as 40% to a Snellen acuity of 20/28. This deficit was not sustainable and within 10 min the animal's acuity had returned to its pre-exposure baseline before again "rebounding" to a heightened Snellen acuity of 20/14. By the end of the twenty minute postexposure session the animal returned to its pre-exposure level and remained at this level over the next several days. When the energy of the three pulses was increased to 1.0 μJ, the initial deficit did not increase over that observed for the low energy condition although the elicited deficit produced lasted longer and no enhancement effect was noted. In this case, the animal appeared to fully recover from the exposure within 16 minutes of the exposure. No lingering effects beyond this initial exposure session was evident and the animal's daily acuity was consistent with that observed prior to any exposure.

Differences in the diameter of the laser exposure on the retina were shown to affect the size of the deficit elicited. For very small diameter retinal exposures the deficits produced were often very small and transient, while larger spot sizes produced

a larger and more sustainable visual deficit. In figure 8 the comparison of two different spot sizes are shown. In this figure the animal was exposed on separate occasions to two Q-switched pulses of low energy light that generated a 400 μ and a 100 μ diameter spot on the retina. The exposure was presented on-axis and visual acuity was measured using high luminance targets. In both cases there was a significant decrease in the animal's visual acuity immediately after exposure. For the 100 μ diameter spot, the initial visual deficit leveled off after 4 min and remained at this level for approximately 12 min before gradually returning to its pre-exposure level in 16 min. The average deficit elicited during this time period was 15%. For the 400 μ diameter spot the animal's visual acuity also immediately dropped and within 6 minutes had reached its maximum deficit of 45%. The animal's deficit remained at this level for approximately the same length of time as the 100 μ diameter spot exposure before gradually returning to its pre-exposure baseline in 18 min.

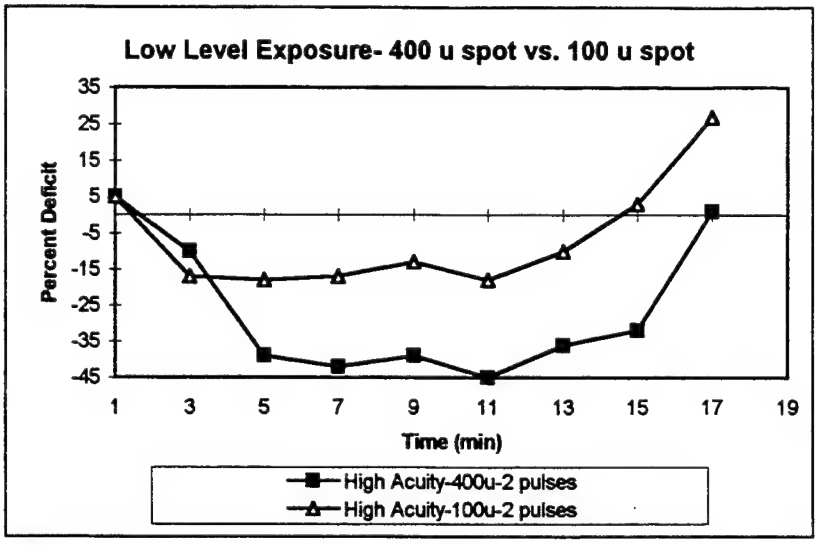

Figure 8. Comparison of spot size on the magnitude and duration of the visual deficit. Two, low energy, Q-switched pulses were presented. Each pulse produced either a 100 μ or 400 μ diameter spot on the retina. The beam was presented on-axis and only one exposure (two pulses) were presented per day. Acuity was measured using high luminance targets.

4. DISCUSSION

The visual deficits elicited by Q-switched pulses that were reported in this study are consistent with the notion that the experimental paradigm developed to expose awake, task-oriented animals did produce reliable placements of the exposures onto the retina. Movement by the laser beam by as little as one degree from its coaxial position within the gap in a threshold Landolt ring had a significant effect on postexposure acuity. Only those exposures that were presented coaxial with the critical feature of the discriminanda produced a conspicuous acuity deficit that was long lasting. Exposures presented off-axis produced little or no observable visual deficit as might be expected in an animal with an intact, functional central fovea.

Single and multiple Q-switched pulses at the energy levels used in this study produced no permanent visual deficit regardless of their repetition rate or retinal spot size. Most exposures, however, did temporarily impede the ability of the animal to maintain its baseline acuity. While large diameter exposures and more pulses per exposure produced larger and more sustainable visual deficits, neither condition alone or combined produced a permanent deficit in our animals' visual acuity. A relatively wide range of different retinal spot sizes (50 μ to 500 μ) were employed in this study which did produce somewhat varying initial deficits. Typically, the larger the spot size, the greater the initial visual deficit and, to some extent, the longer the time required for full recovery. The same relationship was generally true for number of Q-switched pulses. Single, 15 nsec pulses normally had only a minimal impact on the ability of the animal to maintain its pre-exposure baseline unless the spot size was large (greater than 150 μ). Multiple Q-switched pulses even for these small spot sizes, on the other hand, typically elicited more sizable deficits that required a longer postexposure recovery time. Multiple pulses that produced larger spot sizes on the central fovea produced even larger visual deficits that lasted longer and required more time for full recovery.

Increasing the power density of individual pulses generally produced longer recovery times, and in some cases, exposures at the ED_{50} produced prolonged deficits that extended beyond the test session. In no case, however, did single or multiple

pulses of any spot size produce a visual deficit that remained obvious 24 hours after exposure. In several cases where multiple, large diameter pulses were employed the animal's postexposure acuity on subsequent days was less consistent than normal but this condition was difficult to quantify and did not extend beyond several days. In these examples the power density per area was below the ED_{50} for the small spot condition.

Unlike our previous results with CW exposures, no cumulative effect across exposure sessions was noted for the energy parameters employed in this study. The lack of any corresponding cumulative impact of multiple exposures within or between exposure sessions leading up to a permanent visual acuity loss is noteworthy. While these exposures often revealed transient acuity shifts, they suggest that for the smallest spot exposures that are very brief, the functional criterion is limited in defining a permanent effect even when minimal physical damage may have been present. The transient effects observed in this study at energy levels below the ED_{50} and below those that might cause edema suggest that single, isolated Q-switched pulses can have a significant impact on an observer's immediate postexposure acuity even if the consequence is not permanent. Still unresolved is the possibility that with repeated exposures under slightly different exposure conditions, the effects of successive pulses might become additive and eventually permanent as we have previously reported with longer duration, CW exposures. Over time these transient deficits could blossom into a significant permanent functional loss with minimal initial warning that could only be observed if visual functioning is carefully tracked.

Of particular interest is the consistent enhancement effect noted for low energy exposures. Measurements of postexposure acuity to single and multiple Q-switched pulses at 0.1 μJ demonstrated an initial visual deficit that was then followed by a sometimes equally apparent enhancement, which like the preceding deficit was not sustainable. The cause of this acuity enhancement is difficult to discern, but it might be significant that it was only obvious with on-axis exposures and with exposures that were below the ED_{50} where overall recovery was more rapid than with higher energy exposures. A similar enhancement effect might not be expected in the off-axis exposure since the animal's central foveal would be unaltered by the off-axis exposure. Exposing the fovea to intense light might eventually disinhibit the areas within and around the central fovea by fatiguing the retina's lateral inhibitory mechanisms. The sensitivities and recovery times for this neural inhibitory mechanism and that of the photochemical process in the receptor cell could be different and could account for this apparent enhancement.

The threshold for producing immediate visual deficits using the Q-switched domain in this study is even lower than those that we previously reported for exposures within the 100 msec time domain.[4] These energy differences could be the result of the higher peak powers that would occur with Q-switched pulses than would occur with the more homogenous, lower energy density, but longer duration exposures that we have employed using CW lasers. The higher peak powers characteristic of Q-switched pulses can create acoustic damage, in addition to a thermal component, when it interacts with the retina. In comparison to longer duration exposures, this acoustic or mechanical insult may be sufficient to rupture tissue membranes at much lower energy levels than is possible in msec pulse domains. In relation to the function of retinal tissue, Q-switched pulses are deposited within the layers of the retina prior to the normal neural ability of the photoreceptor to respond. As we have previously speculated, this rapid delivery of light energy could temporarily short circuit the full response of the photoreceptor system and bypass its normal adaptation function. However, because the pulse is still sufficient to cause morphological damage, alterations in visual function might still occur. Because of both their limited temporal and spatial domains, it appears that repeated exposures are required to affect large enough areas necessary to produce a significant overall functional effect. For exposures in the msec time domain, larger spot sizes were normally employed and were made even larger due to the increased impact that involuntary eye movements had on the smearing of these pulses across larger retinal regions. Hence, with longer duration exposures, the immediate functional consequences at and below the transition zone were more obvious than those observed in the Q-switched time domain.

While we have not demonstrated a cumulative damage process occurring near or below the pre-established ED_{50} in this present study even after prolonged daily exposure, we have noted significant initial effects and possibly subtle longer term changes in discrimination errors especially when multiple, large punctate exposures within the fovea were made. These less conspicuous effects could possibly reflect more global dysfunctions when briefly presented discriminable targets fall on these "altered" regions. The consequences of repeated exposures within these transitional zones may appear particularly important in understanding these changes. The demonstration of any transitional zone between temporary and permanent functional changes for the Q-switched domain similar to that found for the CW domain would suggest the possibility of

cumulative processes within the retina. Such a phenomenon would most likely increase the susceptibility of the exposed tissue to permanent damage, especially in those situations in which repeated exposures may occur.

Our data continues to support the value of a functional approach to assess laser effects on the visual system and the notion that the nature of the required visual task can significantly influence one's detection of visual deficits. While there are clear differences between the recovery from Q-switched and CW laser exposures especially within the transitional zone between temporary and permanent visual function loss, the current study demonstrates that flash effects may be produced by low level Q-switched pulses even at levels where no tissue damage or edema would be expected. These results suggest, in addition to tissue damage, that photochemical and neural processes may also play an important role in predicting the safety of those working around lasers.

5. REFERENCES

1. E.T. Ham, W.J. Geeraets, H.A. Mueller, R.D. Williams, A.M. Clarke, and S.F. Cleary. "Retinal burn thresholds for the helium-neon laser in the rhesus monkey." *Arch. Ophthal.* Chicago. pp. 797-809, 1970

2. J.O. Powell, K.G.H. Bresnick, M. Yanoff, G.D. Frisch, and J.E. Chester. "Ocular effects of laser irradiation. II. Histopathology of chorioretinal lesions." *Amer. J. Ophthal.* Vol. 71, pp. 1267, 1971.

3. Zwick, H., Robbins, D.O., Nawim, M. Transient visual effects of prolonged small spot foveal laser exposure. *Proceedings Laser Surgery: Advanced Characterization, Therapeutics, and Systems. SPIE, Vol. 1066, 295-302* (1989).

4. D.O. Robbins and H. Zwick. "Subthreshold functional additivity occurring at the transition zone between temporary and permanent laser-induced visual loss. *Proceedings Laser-Inflicted Eye Injuries: Epidemiology, Prevention, and Treatment, SPIE*, Vol. 2674, pp. 44-52, 1996.

5. M.O.M. Tso, B.S. Fine, and L.E. Zimmerman. "Photic maculopathy produced by the indirect ophthalmoscope. A clinical and histopathologic study." *Amer. J. Ophthal.* 73, pp. 686, 1972.

6. M.O.M. Tso. "Photic maculopathy in rhesus monkey, a light and electron microscope study" *Invest. Ophthal.* 12, pp. 17, 1972.

7. D.O. Adams, E.S. Beatrice, and R.B. Bedell. "Retina: Ultrastructure alterations produced by extremely low levels of coherent radiation" *Science*, 31, 9-13, 1972.

8. D.O. Robbins and H. Zwick. "Changes in spectral acuity following brief laser (647 nm) exposure." *Colour Vision Deficiencies V* Chapter 2. Adam Hilger Press, Ltd. England, 1980.

9. H. Zwick, R.B. Bedell, K.R. Bloom. "Spectral and visual deficits associated with laser irradiation." *Modern Prob. Ophthal.* 13, pp. 299, 1974.

10. H. Zwick. "Visual function changes associated with low-level light effects." *Health Physics*, Vol. 56, pp. 657-663, 1989.

11. D.O. Robbins, H. Zwick, and G.C. Holst. "A method for producing foveal retinal lesions." *Behav. Res. Meth. Instr.* Vol. 5, pp. 457, 1973.

12. D.O. Robbins, H. Zwick, M. Leedy, and G. Stearns. "Acute restraint device for rhesus monkeys." *Laboratory Animal Science*. 1986.

13. C.R. Cavonius and D.O. Robbins. "The relationship between luminance and visual acuity in the rhesus monkey." *J Physiol.* (London), Vol. 232, pp. 239-246, 1973.

14. H. Zwick and D.O. Robbins. "Is the rhesus protanomalous?" *Modern Problems in Ophthal.*, Vol. 19, pp. 238-242, 1978.

Notes:

In conducting the research described in this report, the investigators adhered to the "Guide for the Care and Use of Laboratory Animals," as promulgated by the Committee on Revision of the Guide for Laboratory Animal Facilities and Care, Institute of Laboratory Animal Resources, National Academy of Sciences - National Research Council.

The opinions or assertions contained herein are the private views of the authors and are not to be construed as official or as reflecting the views of the Department of the Army or the Department of Defense.

Citation of trade names in this report does not constitute an official endorsement or approval of the use of such items.

Evaluation of Vernier Acuity near Healed Retinal Laser Lesions

Elmar T. Schmeisser, Ph.D.

Dept. of Ophthalmology
E-318 Kentucky Clinic
University of Kentucky
Lexington, KY 40536-0284

ABSTRACT

Seven Cynomolgus fasciculata who had graded laser lesions placed in one eye 6 years previously were evaluated for their vernier acuity by electrophysiologic recording techniques. In these experiments, 95% contrast vernier acuity targets were presented at high luminance levels to anesthetized primates. Visual evoked potentials were recorded by conventional means from scalp electrodes through hospital grade amplifiers. All animal testing was performed under IACUC approved protocols. The single q-switched pulses from a neodymium-YAG laser had produced lesions of 4 types: no visible change, minimal visible lesions, "white dot" lesions (localized circumscribed retinal blanching) and "red dot" lesions (contained retinal hemorrhage) in the eye at the time of placement. Single exposures had been made in four locations: 5 degrees superior, inferior and temporal to the fovea, and one foveally. Vernier recording proved somewhat successful in smaller animals with less than contained retinal hemorrhage lesions in the fovea. Initial analyses demonstrated a significant decrease of the pattern response signal/noise in the experimental eye overall, and an apparent relative loss of vernier signal in some lesioned eyes. Animals with the more severe lesions have somewhat degraded small pattern responses and no recordable vernier response. Apparent lesser losses produced less effect.

Keywords: laser, retina, lesion, vernier, VEP, monkey

1. INTRODUCTION

Vision, and visual compromise due to retinal burns caused by laser exposure, has been evaluated and measured in many different ways. Visual field effects, changes in grating acuity, gray scale contrast sensitivity and chromatic sensitivity have all been measured in the attempt to quantitate a very complex sense system. In some cases, the interest was in very acute changes, while in many others, only longer term studies were possible.[1-17]

This experiment specifically investigates the ability of the visual system to make localization judgments, i.e. vernier or hyperacuity, as opposed to pattern resolution judgments, e.g. grating or letter acuities.[18] The ability of an observer to correctly judge the offset of 2 dots or line elements is quite resistant to optical degradation and is significantly different in its response to pathology.[19-20] Additionally, this ability is critical to aiming and tracking tasks common to many activities, including simply driving down the road between the lines and parking a vehicle. Visual evoked potential correlates of hyperacuity have been obtained in humans.[21-23] These studies show that the hyperacuity VEP in humans scales linearly with log offset and thus can permit estimation of the psychophysical hyperacuity threshold by extrapolation to signal amplitude extinction. However, vernier acuity

falls off with retinal eccentricity even faster than resolution acuity or contrast sensitivity.[24]

The animals used in this study have had graded laser lesions placed 6 years previously by the native collimated beam from a pulsed Nd-YAG laser emitting 1062 nm light without expansion or focusing by any lens system other than that of the eye itself. Placement and severity of these lesions was governed by attempts to produce "Wolfe grade" equivalent effects[4] with single Q-switched exposures. Four lesions had been placed in the right eye of each animal, the left eye serving as a normalizing control with no laser exposures. The exposure energy (and thus lesion type) was counterbalanced across both locations and animals for severity and only four exposures were made in the right eye of each animal. The acute effects of these lesions on acuity as measured by the sweep VEP technique have been previously reported.[17]

Summarizing the 7 animals in this experiment, at the foveal site there are 2 animals which were labeled with no visible change at the time of exposure, 2 with a "minimal visible lesion" (MVL, or Wolfe Grade 1B[4]), 2 with "white dot" lesions (retinal blanching, grade IIB) and 3 with "red dot" lesions (contained retinal hemorrhage, grade IIIB). At the parafoveal locations, there are 11 sites with no visible change at the time of exposure, 4 sites with MVL (IA), 6 sites with a white dot lesion (IIA), and 4 sites with a red dot lesion (IIIA).

Since the VEP falls off with eccentricity due to both cortical magnification and to the topographic mapping of the visual field on the cortex, the signal to noise ratio of the VEP will fall off drastically in any attempt to record a response from the periphery with noninvasive methods.[23] Accordingly, this report is limited to the examination of the vernier VEP responses when the stimulus is placed on the foveal area itself. The consideration whether isolated peripheral lesions have any additional effect to that of the foveal exposure must await a further study with different animals, although some indications are presented here.

2. METHODS

2.1 Subjects: The decision of a suitable species was driven by 3 considerations: the animal must be a primate, it must have high luminance, high acuity color vision, and its retina must have a fovea. These requirements arise from the need to model the human visual system organization (anatomy and function) both retinally and cortically in order to generalize the results of this study to human visual performance. The lowest species that would therefore be used was the cynomolgus monkey (Macaca fascicularis). Further, the recording methods are noninvasive and routinely used with human patients. All procedures were pre-approved by the university IACUC and followed the guidelines of both ARVO and the NIH.

2.2 Procedure: The animal was sedated with ketamine (10 mg/kg) supplemented with ace-promazine (1 mg/kg) IM, and then brought to the laboratory. The animal was anesthetized with pentobarbital IV (10 mg/kg) and muscularly relaxed with pancuronium bromide IV (0.025 mg/kg) as bolus doses. The pupils were dilated with 1% tropicamide and 1% neosynephrin drops. The animal then was intubated and wrapped in a warming blanket on a padded rotating stage. Temperature, ECG and pCO2 were monitored, and ventilation and blanket temperature were adjusted to maintain stable physiologic values. EEG and ECG were monitored for signs of discomfort and the anesthetic level adjusted with backup doses as needed. The fovea of one eye was

aligned in front of the fundus camera and the other eye patched closed. Each animal had been individually refracted for the stimulus distance previously and had keratometry performed to specify the appropriate contact lens parameters. This individually fitted corrective contact lens was placed on the cornea over artificial tears and the retina visualized through it. Figure 1 shows the optical layout and alignment system.[25]

After an experimental session, the animal was allowed to recover from the muscular immobilizing agent. When it could breathe unassisted, it was extubated, removed to the transfer cage and then returned to the colony under the supervision of the veterinary staff.

2.3 Stimuli, Recording and Data Processing: The hyperacuity (vernier) stimuli were produced on a square high resolution (1024 pixels squared) monochrome monitor (VisionProbe (tm)) measuring 8.35 degrees of visual angle at the eye. The stimulus was constructed of five black vertical bars 2.63 degrees tall on a white background (78 Foot-Lamberts) whose center third was horizontally offset and subsequently realigned 694 msec later (0.72 Hz), following the method of Levi *et al.*[21] A gap of 2 pixels (0.97 arcmin) was placed between each third. Each bar measured 9 pixels (4.4 arcmin) in width and was separated from its neighbors by a further 9 pixels producing an overall pattern width of 81 pixels (0.66 deg). Contrast was measured at 99.6%. The offset was counterphased between 0 and (in turn) 27, 18, 9, 4, and 2 pixels to evoke the VEP, thus covering a range from a maximum of 13.2 arcmin (approx 0.24 degrees) down to 0.98 arcmin. The VEP was recorded from bilateral occipital scalp electrodes over the foveal visual cortex individually referenced to the eyebrows (the central scalp served as signal common) in response to the each stimulus until the step size used evoked no recognizable response (generally around the 9 pixel shift size). In order to avoid any time locked activity that might obscure the signal, a random 500 msec dither was introduced between each 1 second stimulus epoch. In most cases, at least 800 sweeps acquired over multiple runs had to be averaged together and the 2 cortical channels from each animal combined in order to get a response with sufficient signal under these anesthetic and recording conditions. In addition, a set of control recordings with 8 shift/sec counter-phasing 99.6% contrast checkerboard stimuli at 1, 3 and 10 cycles/degree filling the entire monitor were used to estimate the overall visual response from each eye.

The steady state (8 Hz) checkerboard VEPs were underwent Fourier analysis and the strength of the 8 Hz component was recorded. This power spectral density, being bounded at 0, was log transformed into a normal distribution before the analysis of variance (repeated measures ANOVA by CSS Statistica, Statsoft Inc., Tulsa, OK). Signal to noise ratios (s/n) were constructed from the power of the peak pattern response divided by the average power in the 2 neighboring frequency bins. Since these ratios are bounded at 0, they were log transformed before analysis. Next, in order to create a standard comparison template, all vernier evoked potentials were normalized to the individual animal's control eye base recording (the 27 pixel shift). The averaged normalized vernier VEPs were evaluated by cross correlation limited to the time region in which the vernier component occurred (between 186 ms to 250 ms, containing the nominal P200-N220 response) both to this average template, and also between each eye for each animal. The strongest positive correlation coefficient (a Pearson's r) at the closest offset (tau) to the template response was chosen to characterize the response, i.e the closest local maximum r to tau=0. Additionally, the correlation coefficient at tau=0 was also noted. Since

correlation coefficients are not normally distributed, they also had to be transformed via the equation (known as a Fischer's transformation[26]):

$$x(r)=0.5 \ln ((1+r)/(1-r)). \quad (1)$$

From this, means and standard deviations based on the variable x can be determined, since x is approximately normally distributed. These transformed values were then compared by repeated measures ANOVA and the effects of the lesions extracted. For graphical purposes, normal ranges can be obtained with these values (e.g. +/- 2 S.D.), and then back transformed to provide normal boundaries on a graph of r vs tau (the lead/lag amount) via the inverse of equation 1 as follows:

$$r=1-2/(\exp(2x)+1). \quad (2)$$

These equations coupled with the cross correlation analysis provides an relatively objective method of statistically determining the presence of any reliable response (i.e. the VEP), rather than having to judge which "squiggle" is the actual response component.

3. RESULTS

One of the animals (12043, a large male) had pattern VEPs in the control eye which at the base stimulus (1 c/d checkerboard) were too small to be useful; this animal's data was eliminated. Further, two other animals (1209 and 12029) had no reliable vernier VEPs even to the largest offset in the control eye (correlation coefficients with the template were consistently negative), and so were dropped from the vernier analyses. In order to attempt a statistical analysis with the remaining few animals, the experimental eyes were grouped roughly as those with no lesions to minimally visible foveal lesions (2 animals), and those with severe or scarring foveal lesions (2 animals). All comparisons were made against their paired control eye (repeated measures ANOVA). Both the x(r) at tau=0 and the x(r)max with the coupled tau at x(r)max as a covariate were analyzed as a function of lesion class (minimal vs white or red dot) with both eye and offset as the repeated measures. More quantitative characterization of the lesions will have to await fluorescein angiography, topographic retinal response mapping by ERG, detailed scanning laser ophthalmoscopy and postmortem histology.

Fig. 2 shows the normalized summed averages series of VEP responses from the normal control eyes (OS) and from all the fellow laser exposed eyes (OD) elicited by 3 checkerboard stimuli of differing check sizes. As can be seen, the lesioned side has pattern VEP responses down to 10 cycles per degree that appear similar to the control eye. Despite the small number of animals, statistical analysis of the signal to noise ratios derived from the power spectral densities of the steady state pattern VEPs showed that as a class, the more severely exposed eyes have lower log(s/n) than the normal eyes (P=0.036); however overall response power itself was not significantly different as a function of either eye, or exposure class (see fig. 4). There was a tendency towards more severe effects with more severe lesions, but this did not attain significance (p=0.27). Spatial frequency was as expected a significant factor (P=0.005) with the lowest spatial frequency demonstrating a stronger response than the smaller patterns.

Fig. 4 shows foveal vernier VEP responses from one animal, demonstrating that even with large offsets, the response decreases in the lesioned eye while remaining recordable from the control eye. Analysis of the maximum crosscorrelation results (with the corresponding tau set as a covariate) demonstrated no significant effects due to eye, class or vernier offset, even though the trends were as expected (lower correlation with smaller offsets, in the lesioned eye and with more severe lesions). For example, comparison of the data between exposure classes (minimal vs white or red lesions) in the experimental eye demonstrated a tendency towards more severe losses of correlation with the more severe lesion, but the effect did not attain significance ($p=0.152$). In contrast, examination of the correlation results with no offset in time (fig. 5) showed an interaction effect between lesion class and eye ($p=0.041$). Looking at only the exposed eye and analyzing for the effect of lesion class across all vernier offsets, the more severe lesion was significantly more effective in dropping the response ($p=0.033$). Finally, there is a tendency for the interocular correlation to drop with the more severe lesions, but this did not attain significance in this small sample ($p=0.13$).

Off-axis burns (5 degree) did not seem to affect vernier acuity in these particular long term animals, e.g. one animal with an apparent MVL in the fovea but with white and red dot lesions in periphery has vernier VEP responses that are equivalent between the 2 eyes.

4. DISCUSSION

The decrease in signal to noise ratio in the relatively large field pattern VEPs without a concomitant loss of absolute response power in intriguing. Does an abnormal fovea actually increase the visual system's noise as opposed to simply removing its contribution to the response? This type of masking or interference may have functional consequences that extends beyond the apparent lesion diameter, and would need to be separately considered. On the other hand, the data presented here does not support the inverse idea, viz. that damaged peripheral retina has a significant ability to affect foveal function as measured by pattern VEP.

The comparison between the responses to checkerboard stimuli and vernier stimuli of a comparable size indicates that the vernier response is probably even more sensitive to retinal disruption, a finding in opposition to that noted with optical compromise. This might be expected, since the pattern VEP responses were obtained with stimuli that covered normal as well as abnormal retina, but the localized vernier stimuli may not have impinged on unexposed retina, and in the case of the most severe lesions, may not extend outside a presumed local scotoma. Topographic mapping studies using electroretinography[27] are in progress and should clarify the extent of these effects. Other data exists that implicates retinal ganglion cells as being the limiting factor in vernier resolution.[28] While this data was obtained in cats rather than primates, if the physiological mechanism holds across species, the apparent damage to vernier acuity with the current laser lesions implies that the cortex may not be able to compensate for these retinal signal losses, unlike the image filling in or illusory border completion that can occur with more extended patterns.[29] In summary, the vernier VEP analyses imply that for any offset size, including those well above normal vernier threshold, 1) there tends to be a drop due to any foveal exposure, and 2) this drop appears to be more severe with greater lesions.

It should be reiterated that not all animals produced recordable vernier VEPs with this protocol, even from their normal eyes. This tended especially to be the case for the larger (male) animals and may be an artefact of their greater skull thickness and head musculature combined with the small size of the signal when recorded by surface (either subcutaneous needle or scalp cup) EEG electrodes. In order to improve this situation, implantation of chronic electrodes to record from at least the dural surface probably would be required.[30] Finally, an exhaustive perilesional mapping protocol in order to maximize any vernier signal by placing it just outside of a (presumed) lesion scotoma was not undertaken. Behavioral studies which would allow the animal to adopt individual compensatory strategies (such as off axis viewing with alternate preferred retinal loci) might be more appropriate to determine the final functional consequences of discrete retinal lesions such as those in this study.

5. ACKNOWLEDGMENTS

This work was supported in part by funds under USAMRMC Contract No. DAMD17-95-C-5038, Ft. Detrick, MD, by funds from The Analytic Sciences Corporation, Reading, MA, equipment from the Armstrong Laboratories and from the US Army Medical Research Detachment (WRAIR), both of Brooks AFB, TX, and by an unrestricted departmental grant from Research to Prevent Blindness, Inc.

6. REFERENCES

1. Moshos M. ERG and VER findings after laser photocoagulation of the retina. Metab Pediatr Ophthalmol 6:101 (1982).

2. Fowler BJ. Accidental industrial laser burn of the macula. Ann Ophthalmol 15:481 (1983).

3. Boldrey EE, Litle HL, Flocks M, Vassiliadis A. Retinal injury due to industrial laser burns. Ophthalmol (Rochester) 88:101 (1981).

4. Wolfe JA. Laser retinal injury. Mil Med 150:177 (1985).

5. Stuck BE, Lund DJ, Beatrice ESW. Repetitive pulse laser data and permissible exposure limits. Presidio of San Francisco, CA: Letterman Army Institute of Research. Institute Report No. 59 (1978).

6. Gibbons WD, Allen RG. Retinal damage from suprathreshold Q-switch laser exposure. Health Phy 35:461 (1978).

7. Allen RG, Thomas SJ, Harrison RF, Zuglich JA, Blankenstein MF. Ocular effects of pulsed Nd laser radiation: variation of threshold with pulsewidth. Health Phy 49:685 (1985).

8. Merigan WH, Pasternak T, Zehl D. Spatial and temporal vision in macaques after central retinal lesions. Invest Ophthalmol Vis Sci 21:17 (1981).

9. Callin GD, Devine JV, Garcia P. Visual compensatory tracking performance after exposure to flashblinding pulses: I, II, III. USAF School of Aerospace Medicine, Brooks Air Force Base, TX: Reports SAM-TR-81-3, -7, -8 (1981).

10. Randolph DI, Schmeisser ET, Beatrice ES. Grating visual evoked potentials in the evaluation of laser bioeffects: twenty nanosecond foveal ruby exposures. Am J Optom Physiol Opt 61:190 (1984).

11. Schmeisser ET. Flicker electroretinograms and visual evoked potentials in the evaluation of laser flash effects. Am J Optom Physiol Opt 62:35 (1985).

12. Schmeisser ET. Laser flash effects on laser speckle shift VEP. Am J Optom Physiol Opt 62:709 (1985).

13. Schmeisser ET. Laser flash effects on chromatic discrimination in monkeys. USAFSAM TR-87-17, Brooks Air Force Base, TX (1987).

14. Previc FH, Blankenstein MF, Garcia PV, Allen RG. Visual evoked potential correlates of laser flashblindness in rhesus monkeys. I. Argon laser flashes. Am J Optom Physiol Opt 62:309 (1985).

15. Previc FH, Allen RG, Blankenstein MF. Visual evoked potential correlates of laser flashblindness in rhesus monkeys. II. Doubled neodymium laser flashes. Am J Optom Physiol Opt 62:626 (1985).

16. Glickman RD, Previc FH, Cartledge RM, Schmeisser ET, Zuglich JA. Assessment of visual function following laser lesions. USAFSAM Protocol # 7757-02-82 (Contract F33615-84-C-0600) (1986).

17. Schmeisser ET. Acute laser lesion effects on acuity sweep VEPs. Invest Ophthalmol Vis Sci, 1992; 33:3546-3554.

18. Westheimer G. Visual acuity and hyperacuity: resolution, localization, form. Am J Optom Physiol Opt 64:567-574 (1987).

19. Enoch JM, Williams RA. Development of clinical tests of vision: Initial data on two hyperacuity paradigms. Percept Psychophys 33:314-322 (1983).

20. Enoch JM, Essock EA, Williams RA. Relating vernier acuity and Snellen acuity in specific clinical populations. Doc Ophthalmol 58:71-77 (1984).

21. Levi DM, Manny RE, Klein SA, Steinman SB. Electrophysiological correlates of hyperacuity in the human visual cortex. Nature 306:468-470 (1983).

22. Steinman SB, Levi DM, Klein SA, Manny RE. Selectivity of the evoked potential for vernier offset. Vis Res 25:951-961 (1985).

23. Srebro R, Osetinsky MV. The localization of cortical activity evoked by vernier offset. Vis Res 27:1387-1390 (1987).

24. Enoch JM, Williams RA, Essock EA, Barricks M. Hyperacuity perimetry. Assessment of macular function through ocular opacities. Arch Ophthalmol 102:1164-1168 (1984).

25. Blankenstein MF, Previc FH. Approximate visual axis projection for the rhesus monkey using a fundoscope and alignment laser. Vis Res 25: 301-305, (1985).

26. Kendall MG, Stuart A. The advanced theory of statistics, Vol 1. Hafner Publ Co., New York, NY, pp 390-392 (1963).

27. Bearse MA Jr, Sutter EE. Imaging localized retinal dysfunction with the multifocal electroretinogram. J Opt Soc Am A 13: 634-642, (1996).

28. Shapley R, Victor J. Hyperacuity in cat retinal ganglion cells. Science 231: 999-1002, (1986).

29. Ringach DL, Shapley R. Spatial and temporal properties of illusory contours and amodal boundary completion. Vis Res 36: 3037-3050, (1996).

30. Schmeisser ET. Laser induced chromatic adaptation. Am J Optom Physiol Opt, 65: 644-652 (1988).

7. FIGURES

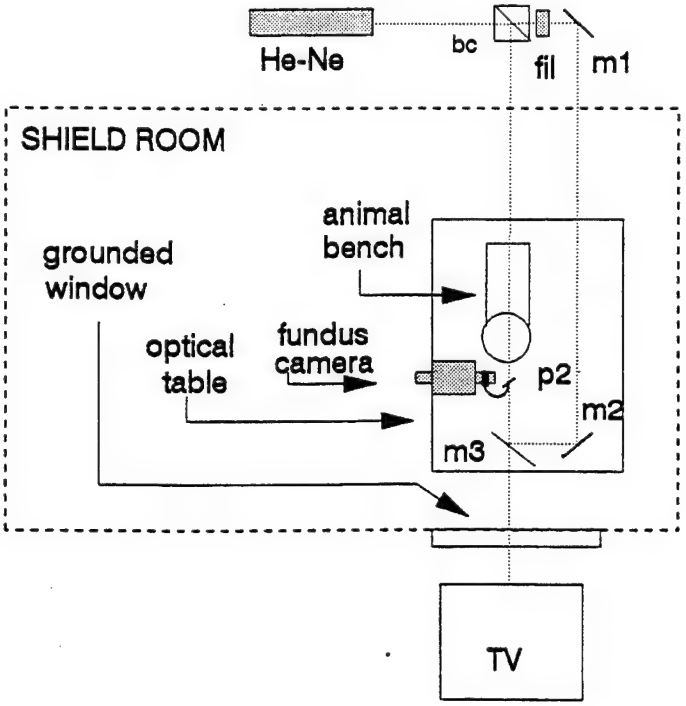

Fig. 1: Layout of the optical alignment system used in this study. He-Ne: alignment laser; bc: beam splitter cube; m1, m2 & m3: mirrors (m3 can be moved from the line of sight); p2: removable 80% reflecting pellicle.

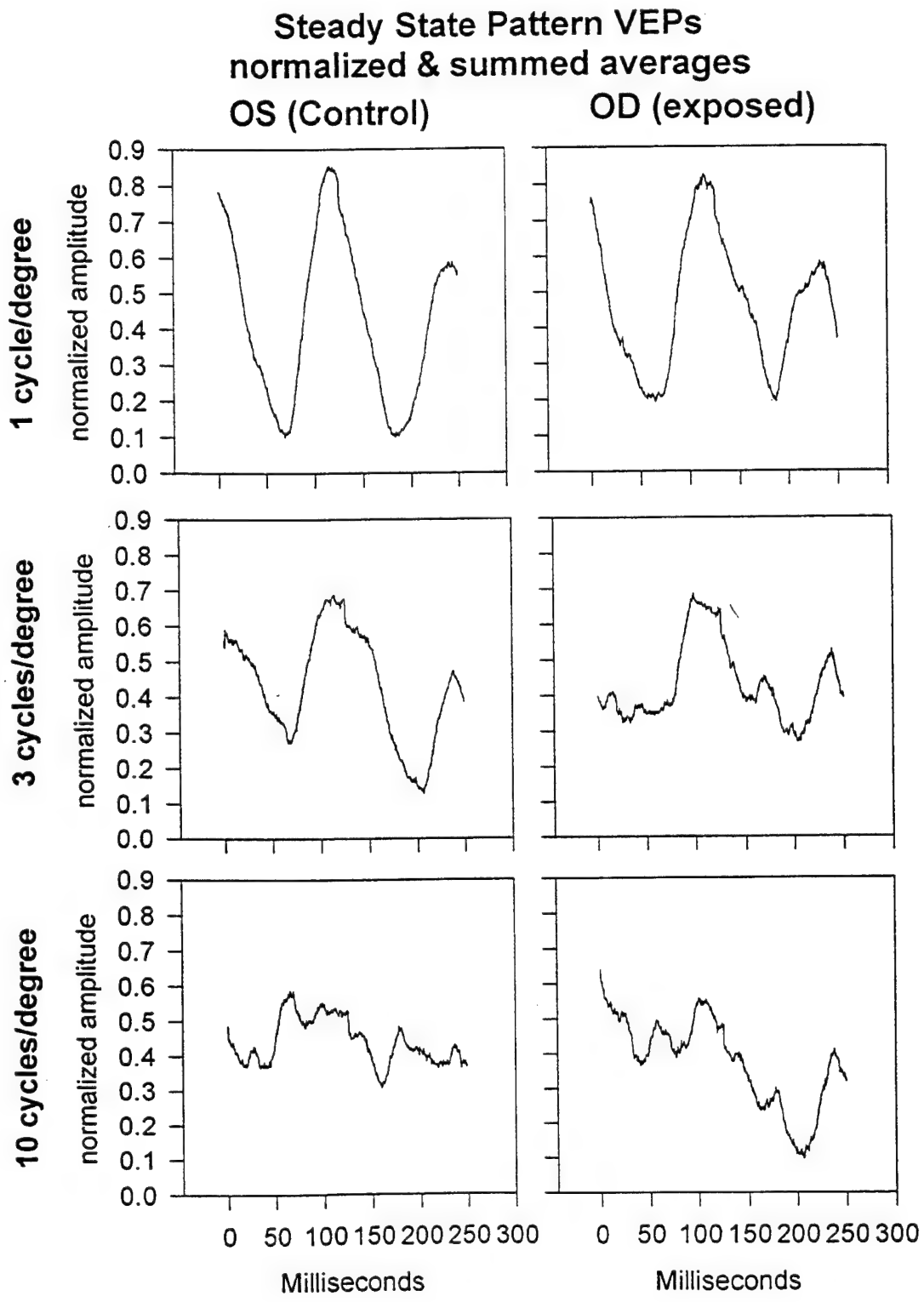

Fig. 2: Summed and averaged VEPs from checkerboard stimulation. Data combined across all animals.

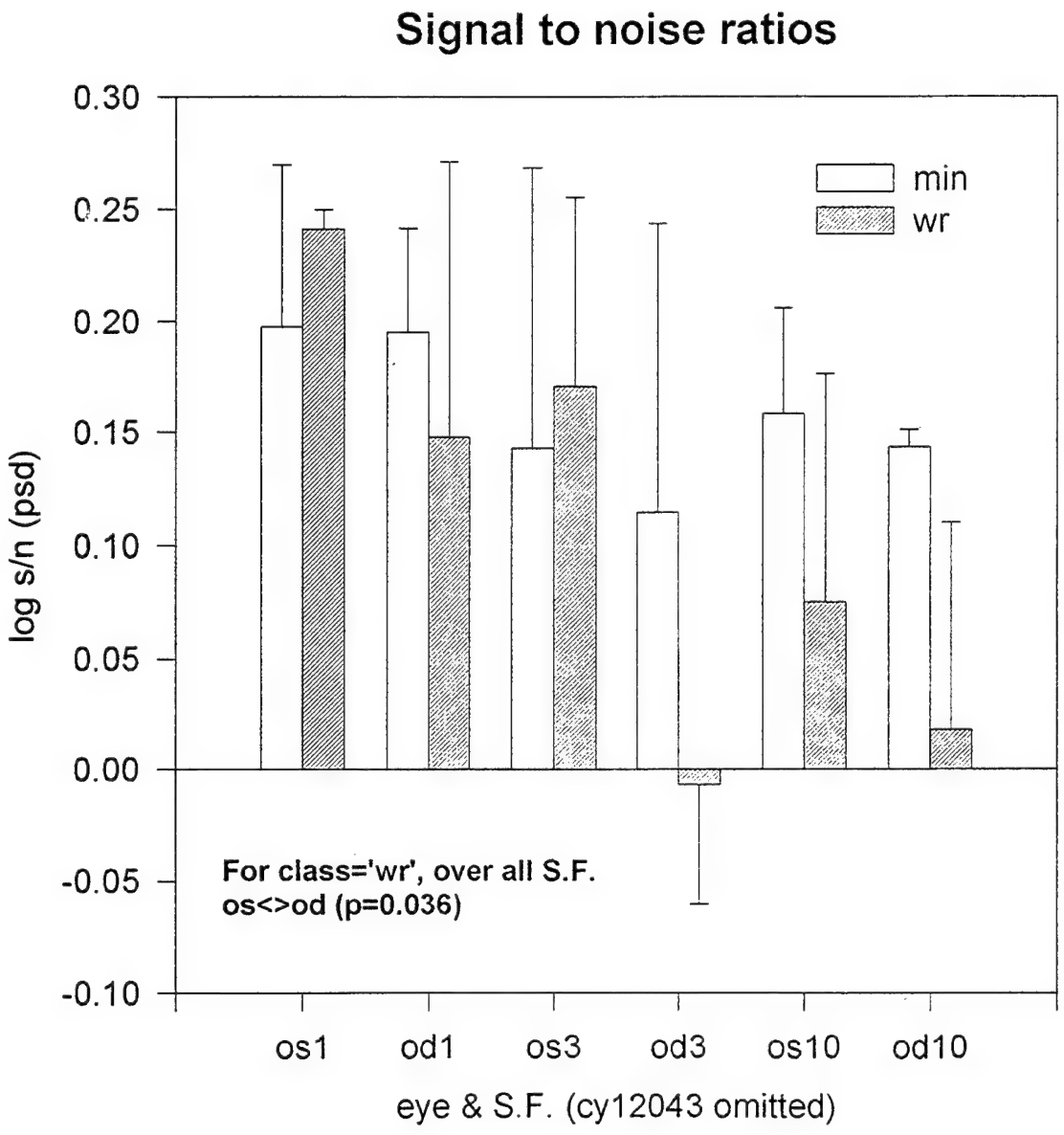

Fig. 3: Data graph of signal to noise ratios as noted in text. For those animals with white or red dot lesions, the exposed eye has a significantly worse s/n than the control eye (p=0.036).

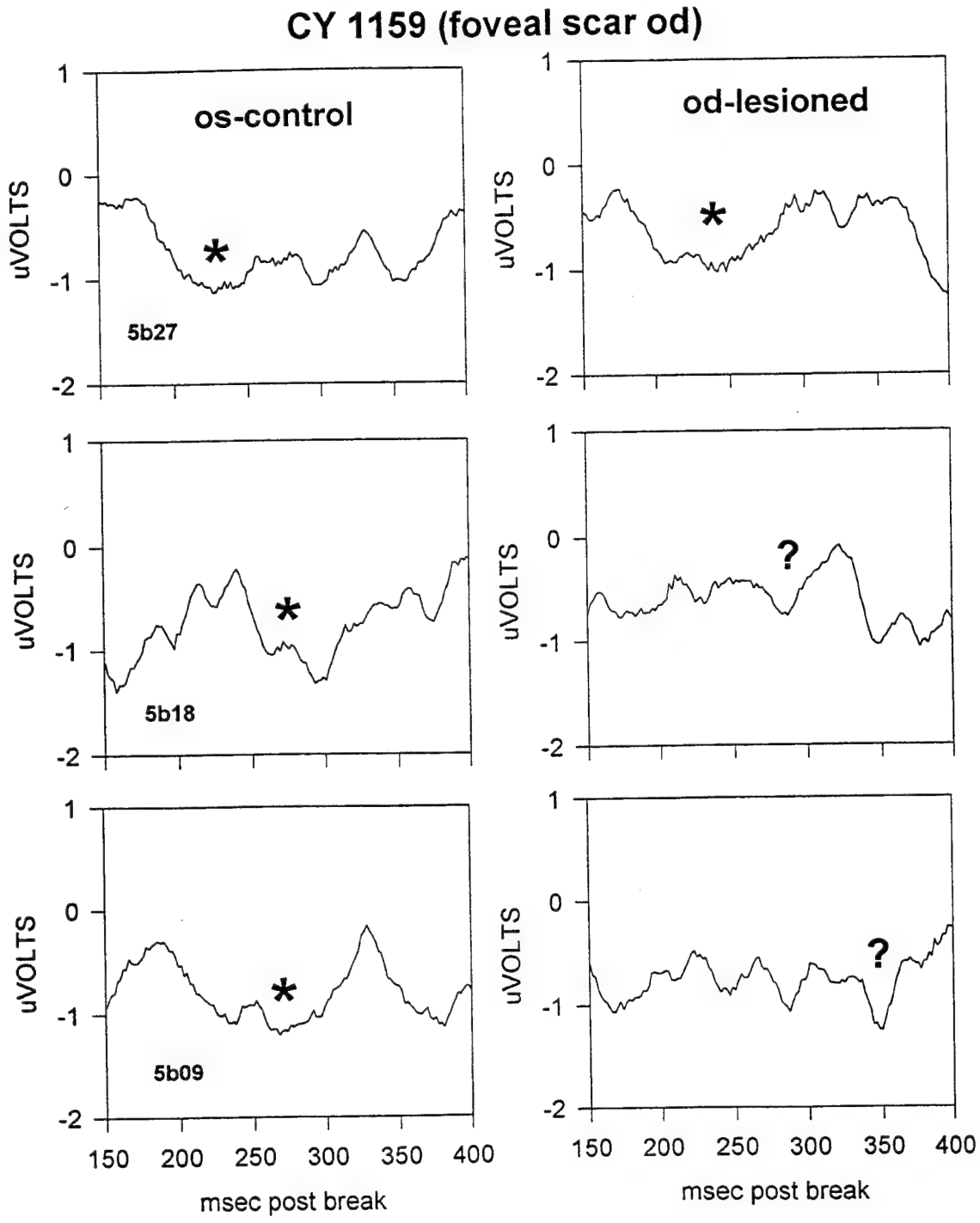

Fig. 4: VEPs from vernier stimulation for animal cy1159, which has a foveal bridging scar OD.

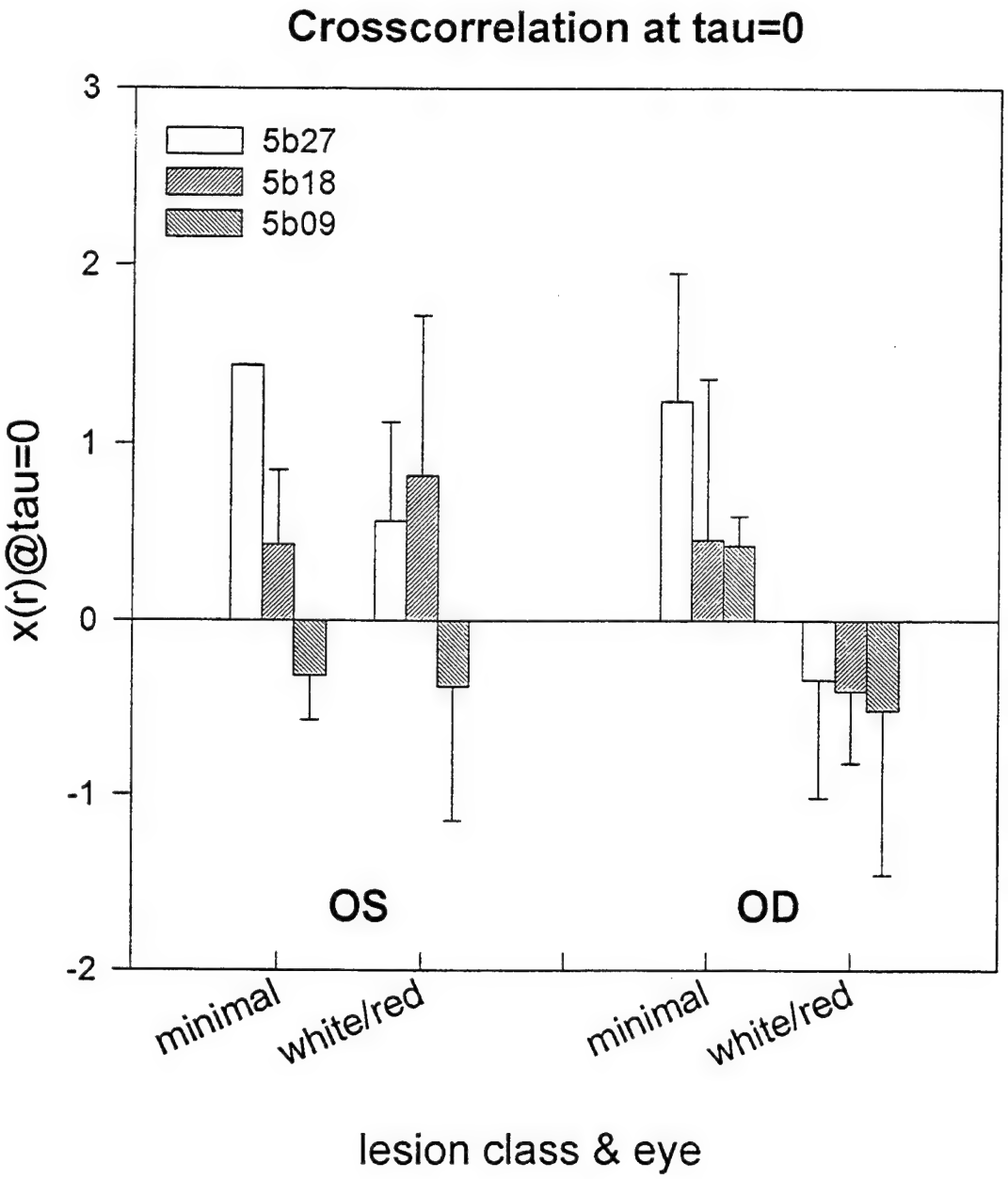

Fig. 5: Data graph of cross correlation results with no time offset against the 5b27 OS template. For those animals with white or red dot lesions, the exposed eye has a significantly lower correlations than the control eye (p=0.033).

Transient disruption of human pursuit tracking performance for laser exposures below permissible exposure limits

David A. Stamper, David J. Lund, Jerome W. Molchany and Bruce E. Stuck

US Army Medical Research Detachment of the Walter Reed Army Institute of Research,
Brooks Air Force Base, TX 78235-5138

ABSTRACT

The proliferation of lasers for medical care, laser displays, industrial applications and audio-visual presentations (e.g., pointers) has increased the potential for accidental intrabeam exposure to visible laser radiation . The output of these laser devices may be limited to below permissible exposure limits, but they are perceived as bright and can affect performance. The disruption experienced while viewing a laser is related to factors that include the retinal irradiance level, wavelength, ambient light level and mode (continuous wave (CW) and repetitively pulsed (RP)). This report describes studies where these factors were varied to assess the effects of laser light on tracking performance in a laboratory simulator and in a field study. Disruption was determined by measuring maximum error (the deviation from the center of a target expressed in milliradians) and total time off target. Performance disruption increased as irradiance levels increased and ambient light levels decreased. Under dawn/dusk conditions relatively low-level laser energy produced performance disruption. Green laser light at the peak of the photopic sensitivity curve was more disruptive than red laser light. Increased error scores during CW and RP trials were attributed to average rather than peak power effects. More than 1500 laser exposures at levels up to MPE/2 have been given to volunteers. Despite transient performance disruption comparison of the pre and post-laser visual performance tests and fundus evaluations were unremarkable.

Key words: Lasers, psychomotor performance, vision, glare, human.

1. INTRODUCTION

Recently there has been a proliferation of lasers for use in medical treatment, displays, industry and as pointers for audio-visual presentations. In addition to performing their primary function(s) these devices are capable of disrupting optical sensors (including eyes). The amount of disruption experienced is related to factors which include retinal irradiance levels, ambient light levels, wavelength and mode. The results of exposure to relatively high levels of laser radiation can produce damage to the retina or cornea. At intermediate levels temporary flashblindness effects can be present after the laser is turned off. These include the appearance of a scotoma or disruptive afterimage lasting from seconds to minutes At relatively low irradinace levels a veiling glare is present when the laser is turned on, but the visual disruption ends when the laser is turned off. The effects of high levels of laser energy on visual performance, where damage has occurred, is more easily predicted than at low or intermediate levels. Because the human eye is more sensitive to some wavelengths than others, individuals viewing visible wavelength lasers will experience different degrees of disruption depending on the wavelength. Lasers which produce green light are perceived as being brighter than red or blue lasers at comparable irradiance levels since they operate near the peak of the photopic spectral sensitivity curve. Ambient light level can alter the apparent brightness of the laser light. The disruptive effects are greater under mesopic conditions where the sensitivity of the eye is greatly increased due to a larger pupil, a shift of photopigments in the retina, and an increase in perception of intraocular scatter. However, under photopic conditions, intrabeam viewing of visible wavelength lasers will produce an intense colored light on a small retinal area which may not completely obscure the visual field. During bright-light conditions under irradiance levels that are safe for viewing, unlike non-laser light sources which can produce a full field flash, visible lasers because they are a point source will produce an intense colored light which may not completely obscure the entire visual field. The visible area outside the bright center can provide added information which can reduce the amount of visual disruption. Because lasers can generate high irradiance levels, the appearance of persistent afterimages and scotomas scattered across the visual field as a result of eye movements made to the adversive stimulus can produce greater disruption than a full-field flash despite the reduced area of the retina affected by the laser light. Finally, at comparable energy levels, the disruptive effects of a continuous wave (CW) laser which provides a constant glare source may be different than a repetitively pulsed laser which appears to be strobing.

Data that describes the effects of lasers on visual performance will be of greatest value if it can be used to predict performance on a variety of tasks. Pursuit tracking is a common test which has been extensively studied (1) and can be applied to many psychomotor tasks where aiming is required. For example, if someone attempts to keep a flashlight on a moving object or the crosshairs of the site on a target, they are performing a pursuit tracking task. Our work in the field (2) and in the laboratory (3) has studied the effects of lasers on pursuit tracking performance.

The purpose of this paper is to present the results of a series of studies that were conducted in a laboratory simulator and in a field study setting. These studies have evaluated the effects of laser irradiance levels, wavelengths, ambient light levels and presentation mode on pursuit tracking performance. The irradiance levels used in these studies were presented at sub-maximum permissible exposure levels (MPE) that were specified in the ANSI-Z-136.1 standards (4). To insure the visual health of all volunteers pre- and post-laser exposure eye examinations were given.

2. METHODS

2.1 Volunteers All of the studies were reviewed by Human Use and Scientific Review Committees. The conduct and progress of the project was monitored by an ophthalmologist. Ages of the volunteers ranged from 19 to 50 yrs. Each volunteer was given a preliminary ophthalmic screen and fundus evaluation to insure good ocular health prior to beginning the study. The tests performed were: the Snellen visual acuity, the Amsler Grid for central field deficits or macular disease, the Spectrum Color Vision Meter 712, and the Farnsworth-Munsell 100 Hue test. Slit-lamp fundoscopy was performed by the responsible physician. At the conclusion of each study the visual battery was repeated. All volunteers signed a Privacy Act and Subject Informed Consent Statement acknowledging that the purpose and all hazards associated with the study had been explained to them.

2.2 Apparatus

2.2.1 Field tests The field test were conducted using a ground mounted Tube-Launched, Optically-Tracked, Wire-Guided (TOW) missile launcher which had been electronically modified. The TOW unit was interfaced with a 386 NEC laptop computer with an expansion chassis containing a National Instruments 16-bit Analog-to-Digital (A/D) board. The single-ended signal for pitch and yaw from the TOW's missile guidance unit was routed to the A/D board which provided the signal for determining horizontal and vertical aiming error scores and for on-line data processing and storage. The TOW missile launcher was positioned in an overlook position 1500 -2000 m from the target vehicle.

The target vehicle, a High Mobility Multipurpose Wheeled Vehicle (HMMWV) had an M-70 infrared (IR) training source mounted center-of-mass on the passenger side which provided the reference point for the error detection system. With the IR source attached to the passenger side of the HMMWV collection of tracking data was limited to movement in the left-to-right direction. The angular speed of the target was 5 mrad/sec for the 30-sec tracking epoch. An Optronics Lab Imaging Spectrophotometer was used to obtain luminance measurements of the target and scene. The luminous contrast was calculated to be 18-20 %.

The green line (514.5 nm) for an argon ion laser and the red (632.8 nm) line of the HeNe laser were used as the flash sources in these studies. For the repetitively pulsed trials (RP) a mechanical chopper was used to create the desired pulse rates and widths. The laser light was introduced into the optics of the TOW via a fiber optic cable that was connected to a box mounted on the TOW sight. This box contained optics that re-collimated the beam before it passed to the objective of the sight. A shutter, preset for the desired exposure duration was activated by the investigator during the laser exposure trials. To preclude any possible injuries due to "knob twiddling," the laser was operated at full power and a neutral density filter was permanently placed in the optical pathway to limit the laser light to the desired irradiance level. The irradiance levels were calculated based upon the maximum permissible exposure (MPE) levels provided in the ANS-Z-136.1 standards. A radiometer was used to ensure that the laser energy was within the specified range. Power for the laser and the TOW unit was provided by two portable generators.

Measurement of the ambient light level indicated the average luminance to be approximately 4000 cd/m^2. The dawn/dusk trials, created by inserting a 0.1% transmitting neutral density filter over the front of the TOW collecting optics, reduced the ambient light level to $\cong$ 4 cd/m^2. During these reduced illumination trials a black cloth covered the upper torso of the person and the eye piece of the TOW, which significantly restricted the light reaching the eye except for the amount coming through the ocular, while allowing the person tracking to adjust to the lower ambient light level. A five-min adaptation period was given to each person to allow them to adjust to the simulated dawn/dusk conditions.

2.2.2 Laboratory tests The laboratory portion of these studies were conducted in the "BLASER" simulator. The BLASER simulator consists of a 26 x 30 ft terrain board which depicts a desert-like scenario. A computer station for data collection and an 8 x 8 ft bunker, which contains an in-house constructed viscous damped, dual pistol handle, monocular eyepiece tracking device were located adjacent to the terrain board. The tracking device with its' mechanical and optical enhancements provided tracking data appropriate for a 2 km distance and visually simulated a 10x sight at that distance. An infrared light-emitting diode (IR LED) located in a center-of-mass position on the target was imaged by a television camera mounted coaxially with the optics of the tracking device. The IR LED was invisible to the operator. The IR signal provided a reference point for the microprocessor and associated software to determine and store aiming error data at frame rate.

The target, a 1/35th scale Russian T-72 tank was track-mounted and traversed an arc on the terrain at the simulated distance of 2 km. It was driven alternately in the left-to-right and then right-to-left direction at a constant angular velocity of 5 mrad/sec for 15 sec. Luminance measurements of the camouflaged tank and background were taken with an imaging Spectrophotometer. The calculated contrast of the target to the background was 23%.

The laser sources for the flash trials was again an Argon ion or HeNe laser as described in the field study section. The laser light was introduced into the optics of the tracking device using a fiber optic cable and reflected into the eyepiece through a 50/50 mirror. Again a shutter was activated by the investigator during the preselected laser exposure trials. As in the field, the laser was operated at full power and with a neutral density filter permanently placed in the optical pathway which limited the laser light to the intended irradiance level. A radiometer was used to ensure that the laser energy was within the specified range.

The terrain luminance was 430 cd/m^2. The dawn/dusk condition was simulated by inserting a Neutral Density (ND) filter with an optical transmission of 1% (2 OD) that reduced the terrain luminance to 4.3 cd/m^2. The bunker light was turned off during the dawn/dusk condition trials and no light entered the bunker except through the optics of the tracking device. As with the field study, a five-min adaptation period was given to each person to allow them to adjust to the simulated dawn/dusk conditions.

2.2.3 Procedure All volunteers received identical training in the field and in the simulator which was conducted over a two-day period. The first training day consisted of twenty-two 1-min. trials, 11 under the bright ambient light condition and 11 under the dawn/dusk ambient light condition. Each trial was initiated by the commands "READY" and "GO". Because the length of the tracking periods (30 sec for the TOW and 15 sec for BLASER) one complete round trip (i.e., two, 30 sec tracks) was required in the field and two round trips in the simulator (i.e., four, 15 sec tracks) to complete each of the 1-min training trials. The volunteers were aware of the number of round trips and continued to track the target until it stopped. The data that was used to assess the progress of training and provide feedback on the first training day was taken during the first 30 sec of each trial in the field and during the first 15 sec of each trial in the simulator. During the second training day each volunteer performed 15 trials in the bright light and 15 in the dawn/dusk condition. During the second day the duration of the trials in the field and the simulator were of their standard length (i.e., 30 sec for TOW and 15 for BLASER). Percent time on target (TOT) and standard deviation (SD) error scores were announced to the person tracking after each trial as feedback to assist in their training. This training schedule was found to be the most efficient and produced performance levels which best matched the longer five-day schedule used in our earlier work (5).

On the test day the volunteers were told they would periodically receive a brief flash of laser light that was bright, but safe for viewing. One flash presentation schedule was used for all volunteers. The six flash trials in the field and in the six in the BLASER simulator were presented at a rate of one/five trials and the flash presentation within each group of five trials was random. The flash was initiated at the same location along the course. The order of the flash presentation was unknown to the volunteers. During both bright light and dawn/dusk trials the veiling glare completely obscured the target vehicles. Each volunteer was told to preserve their vision as best as possible since this would enable them to quickly reacquire the target. They were told that they must continue to use the same eye and could not switch eyes after the flash.

2.2.4 Statistical analyses The terrain in the field and in the BLASER simulator was essentially flat and required little change in the vertical tracking component. Visual inspection of the vertical tracking data was unremarkable and showed almost no change in tracking error across all trials. Therefore, the results will include only the horizontal tracking data. The first 2 sec and the last 2 sec of each trial were not used, to eliminate the effects of start-up and stopping. Maximum

absolute error scores (MAE), which represented the largest excursion in either direction from the center-of-mass aiming point, were calculated for all TOW and BLASER trials. Total time-off-target (TTOT) scores were computed for all flash trials (note that these are total-time-off-target scores as compared to TOT scores given to volunteers for feedback). The criterion for being off-target was an error larger than +/- one mrad on the horizontal axis. The target was judged to be reacquired when the horizontal error was < 1 mrad for a 2-sec. period. This criteria was selected since complete recovery to the pre-flash steady-state level is rarely attained within the short recovery periods used in these studies (approximately 25 sec for the TOW unit and 12 sec for the laboratory simulator). However, an aiming error < +/- 1 mrad for 2 sec indicated that they could see the target and cross hairs well enough to make the minor adjustments necessary to stay on the target vehicle and were not simply passing by chance through that area. Analysis of Variance (ANOVA) appropriate for each respective study was run based on the design of each study. Post hoc tests were performed and the 0.05 level was used for determining significance.

3 - RESULTS

3.1 Study 1 - HeNe laser (632.8 nm) exposures in the BLASER laboratory simulator. The first of the human on-axis laser exposure studied was conducted in the BLASER tracking simulator using relatively low levels of HeNe laser energy. This was done to insure the safety of the volunteers since this was the first purposeful on-axis exposures made using humans in a non-clinical setting. Table 1 presents the dosimetry for the twelve exposure conditions. Levine et al. used a 0.5 mW HeNe laser to present four different irradiance levels during bright light (≅ 250 nits) and simulated dawn/dusk conditions (0.8 nits) for 1, 3, and 5 sec. The four irradiance levels were 0.047, 0.47, 4.7, and 47 $\mu W/cm^2$. The MPEs for exposure duration's of 1, 3, and 5 sec are 1800, 1370, and 1200 $\mu W/cm^2$ respectively.

TABLE 1

BLASER HeNe EXPOSURE CONDITIONS/DOSIMETRY

CORNEAL IRRADIANCE (E_e)	CORNEAL RADIANT EXPOSURE (H_e)*		
	1 - sec	3 - sec	5 - sec
47.0	47.0 (1/38)**	141.0 (1/29)	235.0 (1/25)
4.7	4.7 (1/380)	14.1 (1/290)	23.5 (1/250)
0.47	0.47 (1/3800)	1.41 (1/2900)	2.35 (1/2500)
0.047	0.047 (1/38000)	0.141 (1/29000)	0.235 (1/25000)

*Total Dose: $H_e = E_e t$. Where t = exposure duration

**Ratio of exposure dose to the maximum permissible exposure (MPE).

During the bright light trials the MAE scores were essentially unchanged (Fig.1) except for the highest irradiance level. For the dim light trials off-target excursions were found for all exposure duration's and irradiance levels except for the one sec exposures at 0.047 $\mu W/cm^2$. Significance tests for MAE scores were not reported. However, as seen in Fig 1 when ambient light level decreased, laser irradiance level increased and exposure duration became longer, MAE scores clearly increased.

3.2 Study 2- HeNe laser exposures in the field. To validate and extend the results obtained in the BLASER tracking simulator work we conducted a field study using the modified TOW system. A 5 mW HeNe laser was used as the flash

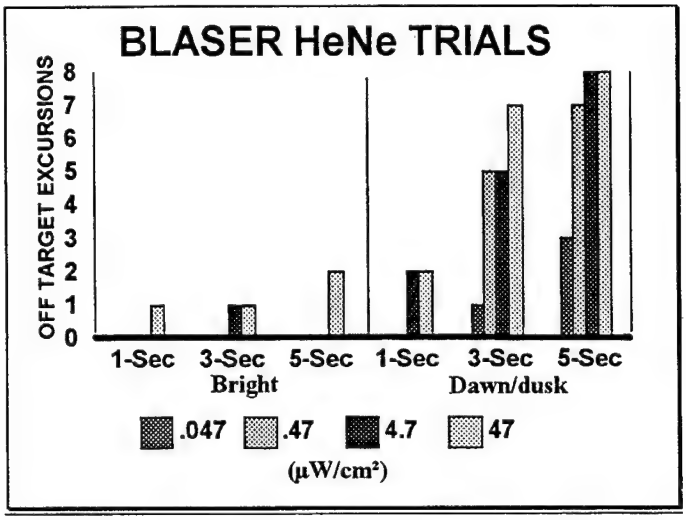

Fig 1. - Off target excursions (i.e., +/- 2 mrad for the center of the target) for each flash condition under bright ambient light condition.

source. In this study the number of irradiance levels was reduced from four to two (i.e., 12 and 120 $\mu W/cm^2$) which was equal to $1/100^{th}$ and $1/10^{th}$ of the MPE respectively (Table 2). Two flash duration's of 3 and 5 sec were used during bright and dawn/dusk ambient light levels. In response to requests for data to assess possible differences between a CW and a RP lasers, a 20 Hz, 280 μsec pulse duration exposure condition was created by placing a mechanical chopper in the optical pathway.

TABLE 2

TOW HeNe EXPOSURE CONDITIONS/DOSIMETRY

MPE Level	CW	Repetitive Pulse Peak	Repetitive Pulse Average
MPE	1200 $\mu W/cm^2$	13,900 $\mu W/cm^2$	78.0 $\mu W/cm^2$
MPE/10	120 $\mu W/cm^2$	1,390 $\mu W/cm^2$	7.8 $\mu W/cm^2$
MPE/100	12 $\mu W/cm^2$	130 $\mu W/cm^2$	0.78 $\mu W/cm^2$

The MAE scores for the bright light trials are presented in Fig. 2. The results of the Analysis of Variance of the MAE scores indicated that only the mode factor was significant. These tests indicated that with the exception of the CW 1/100

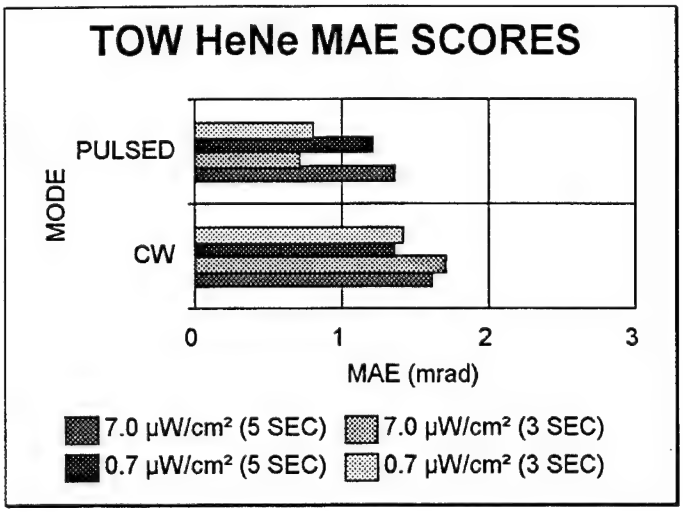

Fig 2 - MAE scores following exposure to 1/10 Th. and 1/100 Th. MPE levels of CW and RP HeNe laser light for three or five sec.

MPE, 3 sec and the RP 1/10 MPE, 5 sec trials, all of the CW trials were significantly higher than the RP trials. During the dawn/dusk trials the flash effects were dramatic. Statistical evaluation of these data was not performed since most of the MAE scores went beyond the range of measurement of the system and the recovery times extended beyond the length of the trials (i.e., 25 sec) for all but the RP 1/100 MPE trials. As with the laboratory study laser flashes presented during reduced ambient illumination produced substantially larger MAE scores.

TABLE 3

TOW HeNe ANOVA RESULTS

Source	df	MS	F	P
Mode (A)	1	5.21	8.94	0.02
Error	7	.58		
Irradiance (B)	1	.61		
Error	7	.32		
A X B	1	.22		
Error	7	.18		
Duration (C)	1	.81		
Error	7	.81		
A X C	1	1.34		
Error	7	1.27		
B X C	1	.16		
Error	7	.19		
A X B X C	1	.06		
Error	7	.39		

3.3 Study 3 - Argon laser (514.5 nm) exposures in the BLASER laboratory simulator. The photopic sensitivity curve of the human eye is approximately three times as sensitive to light in the green region of the visible light spectrum as it is to red or blue light. When assessing the potential disruptive effects of laser light on visuo-motor performance it would be expected that green laser light such as the 514.5 nm line from an Argon laser would be more disruptive than light from a HeNe laser operating at 632.8 nm. To test this hypothesis we presented volunteers with Argon laser flashes in the BLASER tracking simulator. As in the earlier TOW field study the irradiance levels were $1/10^{th}$ and $1/100^{th}$ of the MPE and a CW and RP condition was created by inserting a mechanical chopper into the optical pathways of the laser beam creating a string of 20 Hz pulses for 3 or 5 sec. Table 4 presents the dosimetry for each of the conditions and Fig 3 visually depicts the bright light trials.

TABLE 4

BLASER ARGON EXPOSURE CONDITIONS/DOSIMETRY

MPE Level	CW	Repetitive Pulse Peak	Repetitive Pulse Average
MPE	1200 $\mu W/cm^2$	13,900 $\mu W/cm^2$	78.0 $\mu W/cm^2$
MPE/10	120 $\mu W/cm^2$	1,390 $\mu W/cm^2$	7.8 $\mu W/cm^2$
MPE/100	12 $\mu W/cm^2$	130 $\mu W/cm^2$	0.78 $\mu W/cm^2$

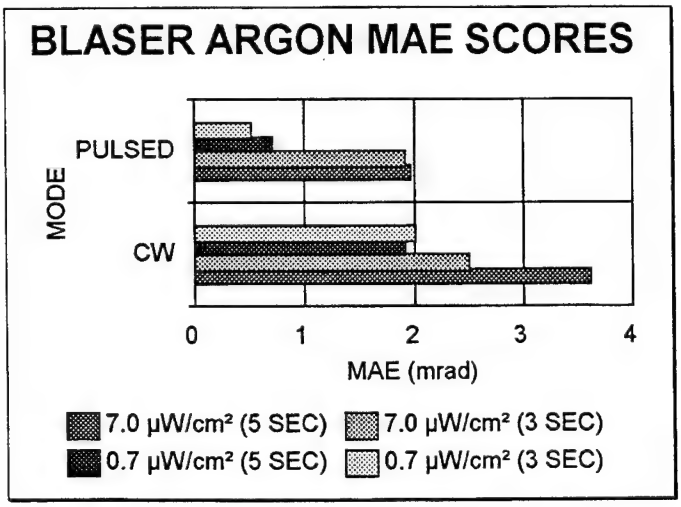

Fig 3 - MAE scores following exposure to $1/10^{th}$. and $1/100^{th}$. MPE levels of CW and RP argon laser light for three or five sec.

Inspection of Fig. 3 indicates that the CW trials produced larger error scores than did the RP trials and the $1/10^{th}$ MPE condition produced larger error scores than did the $1/100^{th}$ MPE trials. Additionally, 5 sec flash duration's trials produced larger error scores than did the 3 sec trials. The results of the ANOVA of the bright light MAE scores (Table 5)

TABLE 5

BLASER ARGON ANOVA RESULTS

Source	df	MS	F	P
Mean Error	1	7.94	13.56	0.00
Mode (A)	1	11.19	183.73	0.00*
Irradiance (B)	1	11.43	131.26	0.00*
A X B	1	2.56	58.89	0.00*
Duration (C)	1	.44	9.81	0.02*
A X C	1	0.00	0.00	0.99
B X C	1	0.09	1.15	0.31
A X B X C	1	0.62	12.22	0.01*

confirms what is shown in Fig 3. Mode was again found to be significant and additionally, irradiance level, flash duration, and the three-way interaction of mode, irradiance level, and flash duration were all significant. During the dawn/dusk trials many of the MAE scores were, as with the HeNe TOW study presented above, beyond the limits of the system and the recovery times extended beyond the length of the trial.

3.4 Study 4 - Argon laser light (514.5 nm) exposures in the field. This field study was conducted to provide answers to several questions. The first purpose was to validate the results found in the BLASER study using the Argon laser in a field study setting. Next, we intended to demonstrate a post-flash daylight effect could be achieved by increasing the irradiance level to 0.4 MPE. Finally, we increased the RP rate to 30 Hz to determine if this higher repetition rate, which is closer to the flicker fusion rate, would reduce the difference between the RP and CW conditions. The laser source was a 20 mW Argon ion laser with a mechanical chopper that provided a 30 Hz string of pulses with a 245 μsec pulse width. Table 6 presents the dosimeter for all laser exposure conditions.

TABLE 6

TOW ARGON EXPOSURE CONDITIONS/DOSIMETRY

MPE Level	CW	Repetitive Pulse Peak	Repetitive Pulse Average
MPE	1200 $\mu W/cm^2$	6520 $\mu W/cm^2$	33.4 $\mu W/cm^2$
MPE/2.4	480 $\mu W/cm^2$	3260 $\mu W/cm^2$	24 $\mu W/cm^2$
MPE/24	48 $\mu W/cm^2$	330 $\mu W/cm^2$	2.4 $\mu W/cm^2$

The MAE results during the bright light trials found that 33% of the scores went beyond the limits of measurement of the system. Seventeen were CW trials and only three were RP trials. With 1/3 of the trials beyond the limits of measurement it was decided for these trials to use the TTOT scores whose pattern closely parallel MAE scores. The TTOT bright light scores in the field were nearly all complete since the trials lasted for 30 sec which was twice as long as the BLASER trials

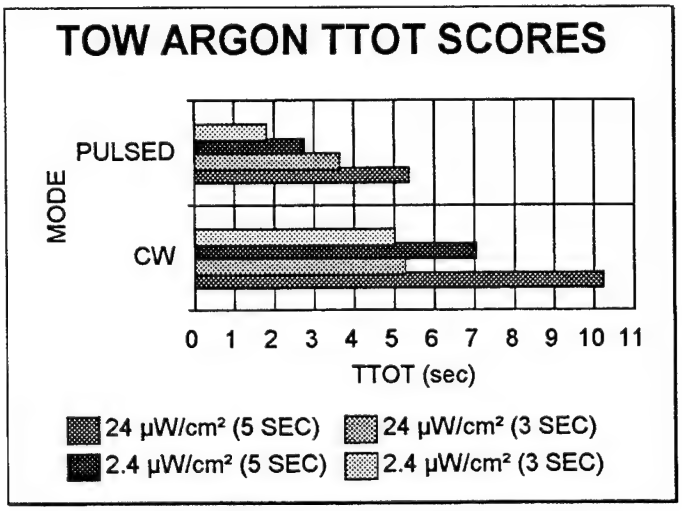

Fig 4 - TTOT scores following exposure to CW or RP argon laser light at 1/10 th or 1/100 th of the MPE for three or five sec.

and gave the tracker enough time to recover from the flash. Fig 4 shows the TTOT results for the bright light trials and Table 6 summarizes the ANOVA results of these data. The pattern of scores in Fig 4 indicates that CW exposures produced longer off-target times than did RP trials and 1/10th MPE trials produced longer off target times than did the 1/100th MPE trials. Five sec exposures produced larger error scores than did the 3 sec exposures. These results are confirmed statistically in Table 7 where the main effects of mode, irradiance level and flash duration were significant. During the dawn/dusk trials it was anticipated that the effects would be even more dramatic than with the earlier BLASER and TOW studies because of the higher irradiance levels. This was found to be true. Of the 64 trials during dawn/dusk condition only 21 remained within measurement of the system.

3.5 - Pursuit tracking performance related to irradiance levels, flash duration, ambient light level and mode.

The developing nature of this work which provided timely information relevant to the understanding of the effects of lasers on vision and performance makes the direct comparison of some of the studies difficult. However, if we use a relational approach to assessing the performance differences among the studies we can show important relationships among these variables. Fig 5 presents TTOT scores for the data points when complete data was determined (i.e., all had target recovery times). These scores were plotted against the log of the ratio of the laser radiance (i.e., the apparent brightness of the laser in Lm/m^{2}sr) divided by the apparent brightness of the ambient light level (in Lm/m^{2}sr). It is clearly seen that as the ratio of the two irradiance levels increase, TTOT scores also increase. The Pearson product moment correlation was $r = 0.59$.

TABLE 7

TOW ARGON ANOVA RESULTS

Source	df	MS	F	P
Mode (A)	1	326.66	12.18	0.01
Error	7	26.82		
Irradiance (B)	1	41.10		
Error	7	16.92		
A X B	1	8.11		
Error	7	20.78		
Duration (C)	1	143.43	7.87	0.03
Error	7	18.23		
A X C	1	0.03		
Error	7	11.37		
B X C	1	4.30		
Error	7	14.36		
A X B X C	1	38.61		
Error	7	21.73		

Note* - Only significant F values are presented.

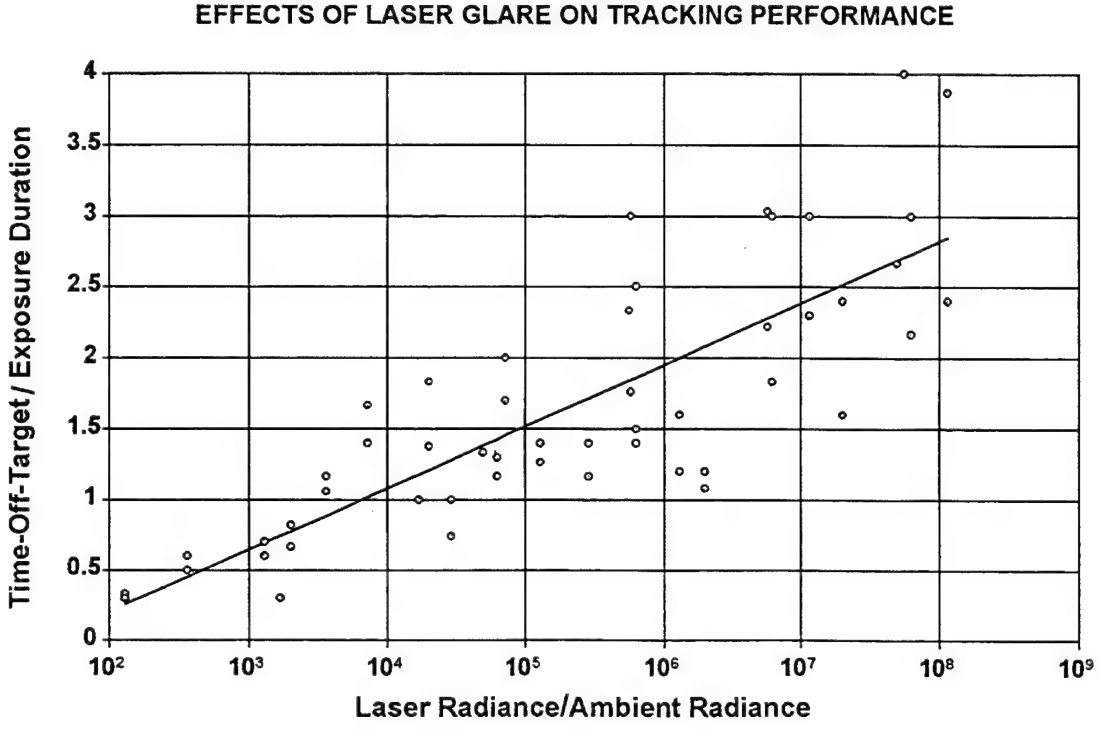

Fig 5 - TTOT scores (+/- one mRad) as a function of the ratio of photometric brightness of the laser and the scene.

We can also plot a distribution of scores (Fig 6), which shows the relationship between laser irradiance (W/cm^2) and ambient luminance (Lm/m^2sr). The ambient light levels extend from bright moon light (10^{-2} - 10^{-3} Lm/m^2sr) through dawn/dusk in the simulator (10^{0} - 10^{-1} Lm/m^2sr) and in the field (10^{1} - 10^{0} Lm/m^2sr) to bright light in the simulator (10^{2} - 10^{3} Lm/m^2sr) and in the field (10^{3} - 10^{4} Lm/m^2sr). The laser irradiances which include a range that extends from nW's (i.e., 10^{-9}) through mW's (i.e., 10^{-3}). The oval circles on the graph represent exposure conditions for studies we conducted and for two accidental night time exposures of pilots. The lower set of three lines on the graph represent a range of laser irradiances which produced disruption of performance for the period of time the laser was on. When the laser was turned off, they immediately reacquired the target. (The upper line was for green lasers, the lower line was for red lasers, and the middle was the average). The upper group of of three lines show the laser irradiance levels which produced TTOT scores that lasted twice as long as the time the laser was on (i.e., a post flash effect). It is apparent that at low ambient light levels it takes relatively little laser energy to disrupt performance. However, to under bright ambient light conditions it takes about 0.5 mW of energy to produce effects which persist beyond time the laser is on.

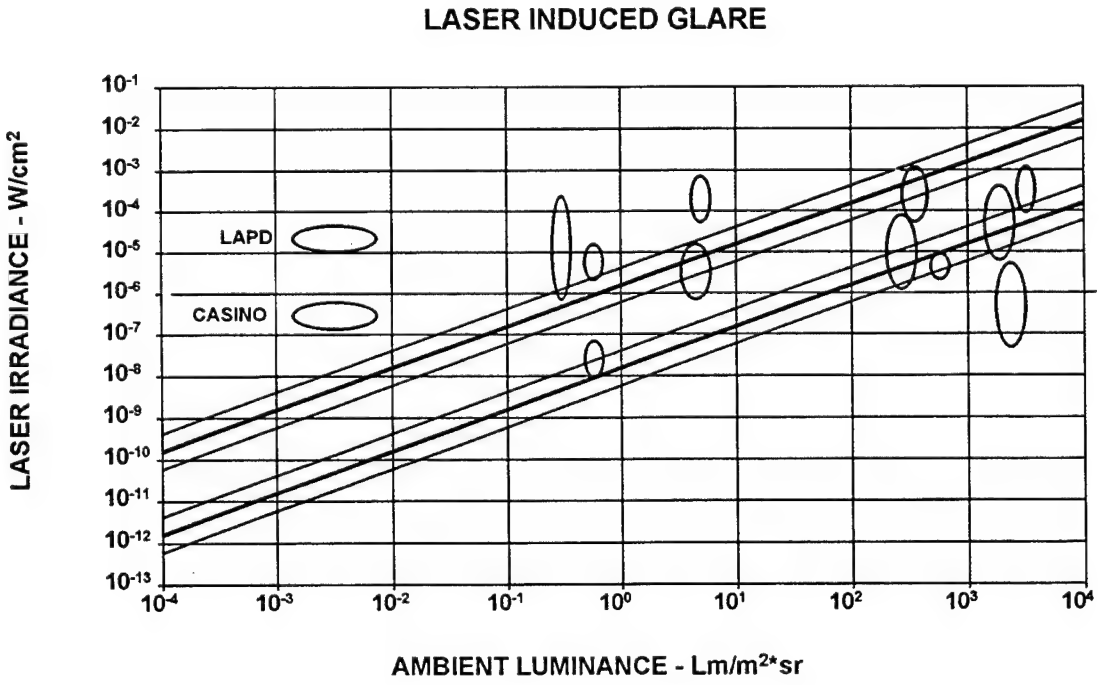

Fig 6 - Laser induced glare effects on performance as a function of ambient light level and laser irradiance levels.

4 - DISCUSSION

From the results noted above several points merit additional comment. First, we found that higher irradiance levels produced larger error scores than did relatively lower irradiance levels. This was true for bright light trials once the irradiance levels approached MPE/10. In the TOW HeNe study where the irradinace level was $1/20^{th}$ of the MPE only mode was found to be significant. In the later studies at MPE/10 or higher a dose response was found. During the dawn/dusk trials all but the lowest irradiance level that was used (i.e., 0.047 $\mu W/cm^2$) produced off-target excursions.

Direct comparison of red vs green lasers for each of the two systems (TOW vs BLASER) was not possible because the parameters in each of the studies changed. One comparison which can be made is between the CW exposures made in the TOW HeNe study and the BLASER Argon study. In both of these studies the CW and RP exposures are made at MPE/10 and MPE/100. Comparison of Figs 2 and 3 indicate that the MAE scores for the argon trials were approximately 2 X larger than were those made with the HeNe laser.

Presentation mode was found to be significant in all three of the studies where the RP condition was presented. While it was thought that the strobing of the RP mode might prove to be more distracting that the CW mode, this was not the case. Apparently during the off period enough of the scene was visible to assist the person tracking to see the target, even up to 30 Hz. In Figs 3 and four where the two argon studies are presented it appears that the average power of the laser rather than the peak power is important. In these figs when the lowest average power for the CW condition is compared with the highest average RP power which are relatively close, the performance scores of the two conditions are nearly alike. This suggest that the average power of the exposure rather than the peak power is most important at sub-damage levels.

Finally, after more than 1500 exposures a visual screen given to the volunteers has not found any change in visual performance following exposure to laser sources up to 40% of the MPE. With some of the volunteers yearly follow-up visual screens have been given annually for up to 14 years and no changes related to laser exposure has been found. The results offer support for the standards presented in ANSI-Z-136.1.

5. REFERENCES

1. E.C. Poulton, *Tracking Skill and Manual Control,* Academic Press, 1974.

2. D.A. Stamper, D.J. Lund, D.M. Penetar, B.E. Stuck, "Project Morning Luster: Pursuit tracking performance decrements following exposure to low-level 632.8 nm laser light in the field," Letterman Army Institute Report No. 203-87, Presidio of San Francisco, CA, 1987 (SECRET).

3. R.R. Levine, D.J. Lund, B.E. Stuck, D.A. Stamper, E.S. Beatrice. "Effects of low-level helium-neon (632.8 nm) laser radiation on human pursuit tracking performance." Letterman Army Institute Report No. 203-85, Presidio of San Francisco, CA, 1985 (SECRET).

4. American National Standards Institute, "American national standard for the safe use of lasers," New York, ANSI Standard Z136.1, 1993.

5. D.A. Stamper, R.R. Levine, P.R. Best, "Effect of practice schedule on two-hand pursuit tracking performance." *Perceptual and motor skills,* 65, pp. 483-492, 1987.

The opinions or assertions contained herein are the private views of the authors and are not to be construed as official or as reflecting the views of the Department of the Army or the Department of Defense.

Human volunteers participated in these studies after giving their free and informed voluntary consent. Investigators adhered to AR 70-25 and USAMRMC Regulation 50-25 on the use of volunteers in research.

SESSION 4

Hazards Assessments from Optical Radiation

Potential ocular hazards from solar exposure during extravehicular activity

James K. Franks, David H. Sliney, and Rodney L. Wood, Jr*

United States Army Center for Health Promotion and Preventive Medicine
5158 Blackhawk Road, APG, MD 21010-5422

ABSTRACT

In earth orbit, the ambient optical radiation environment provided by the sun is not the same as on the surface of the earth. The atmosphere provides a protective layer that is not present in space. The American Conference of Governmental Industrial Hygienists (ACGIH) has published guidelines for exposure to broad-band optical radiation. These guidelines are called Threshold limit values (TLV™). Potential hazards include photochemical and thermal effects on the eye and skin. These guidelines are intended to be used with artificial sources such as arc lamps, however, they may be applied to solar exposure during extravehicular activity so that recommendations may be made to limit the risk of astronauts who are spending more and more time outside the Space Shuttle. Protective filters are discussed that will limit exposure to optical radiation. Permissible exposure times are calculated based on the ACGIH TLVs. Although thermal TLVs may be exceeded, exposures are well below injury thresholds.

Key Words: astronaut, solar exposure, extraterrestrial solar spectrum, "blue-light"

1. PURPOSE

The purpose of this study was to evaluate the potential increased ocular health risk due to removal of a thermal coating from the protective visor during extravehicular activity (EVA), and to make suggestions to minimize the ocular health risk to astronauts.

2. GENERAL

2.1 Background

Personnel at the Lyndon B. Johnson Space Center requested that the U S Army Center for Health Promotion and Preventive Medicine (USACHPPM) provide technical assistance in the evaluation of the potential for increased ocular injury risk to astronauts during EVA. Increased ocular risk may result from exposure to the extraterrestrial solar spectrum after removal of a thermal coating on the protective visor. The solar spectrum ($E_{et}(\lambda)$) must pass through three protective layers. These protective layers are shown in Figure 1.

2.2 Sample"Coupons"

Samples of the sun visor material (sun visor 112 and sun visor 114) were provided by the Goddard Space Flight Center, Greenbelt, Maryland. Samples of the thermally coated and uncoated protective visor (HC) and the "bubble" material (N/HC) were provided by the Deposition Research Laboratory, Inc., St. Charles, Missouri.

2.3 Solar Spectrum

The extraterrestrial solar spectrum[6] used in this study is the American Society of Testing Materials ASTM E 490-73 (Reapproved 1992), "Standard Solar Constant and Air Mass Zero Solar Spectral Irradiance Tables." The spectrum is depicted graphically in Figure 2. Only values of spectral irradiance from 180 nm to 3000 nm were used in this analysis since common glass or plastic materials do not transmit outside this wavelength band.

TLV™ is a registered trademark of the American Conference of Governmental Industrial Hygienists, Cincinnati, OH. Use of a trademarked name does not imply endorsement by the US Army, but is intended only to assist in identification of a specific product.

SPIE Vol. 2974 • 0277-786X/97/$10.00

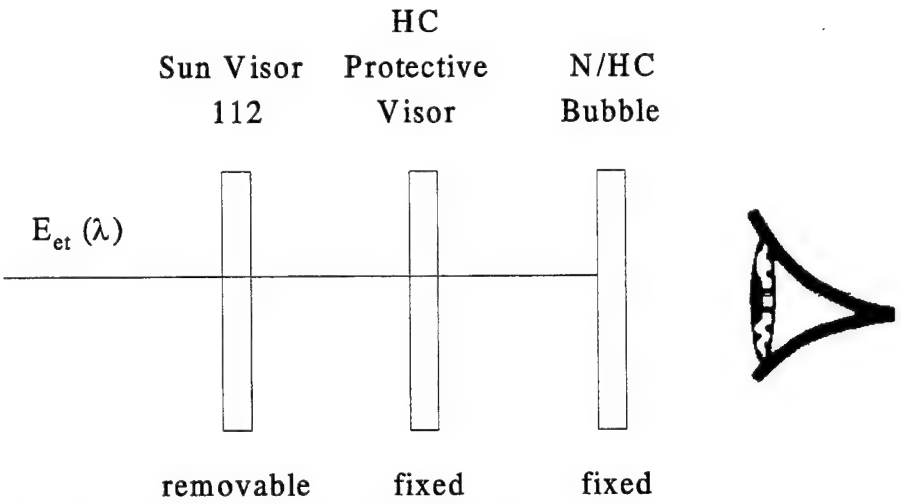

Figure 1. Filter Sequence for Extravehicular Visor.

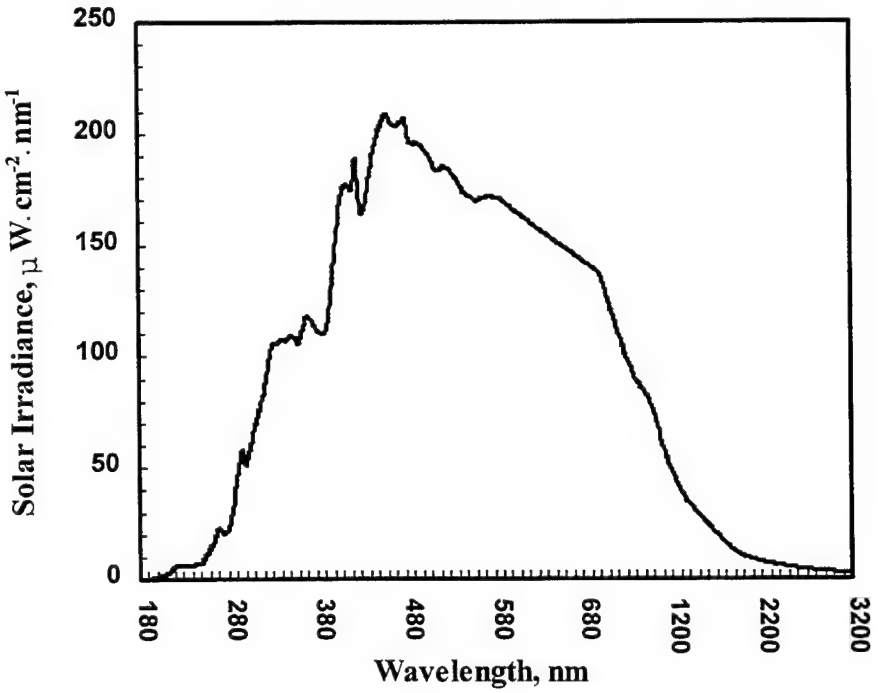

Figure 2. Extraterrestrial Solar Spectrum.

2.4 Instrumentation

Perkin Elmer Lambda 9 UV/VIS/NIR Spectrophotometer Serial No. 1356

2.5 Abbreviations

A table of radiometric terms and units is provided as an Appendix.

3. FINDINGS

3.1 Coupon Spectral Transmission

The spectral transmission of the stack of components that make up the Extravehicular Visor Assembly (EVVA) was determined for two sets of components. A line drawing of the EVVA is shown in Figure 3. Each set of components was identical except for the thermally coated protective visor. The thermally coated protective visor is the current configuration for the EVVA. The subject of this study was to determine the effect of removing the thermal coating on the spectral transmission of the EVVA and then analyze the results using the ACGIH TLV criteria. In addition, the transmitted spectral irradiance of the individual components was also determined. Graphs of the transmitted spectral irradiance are given in Figures 4-5.

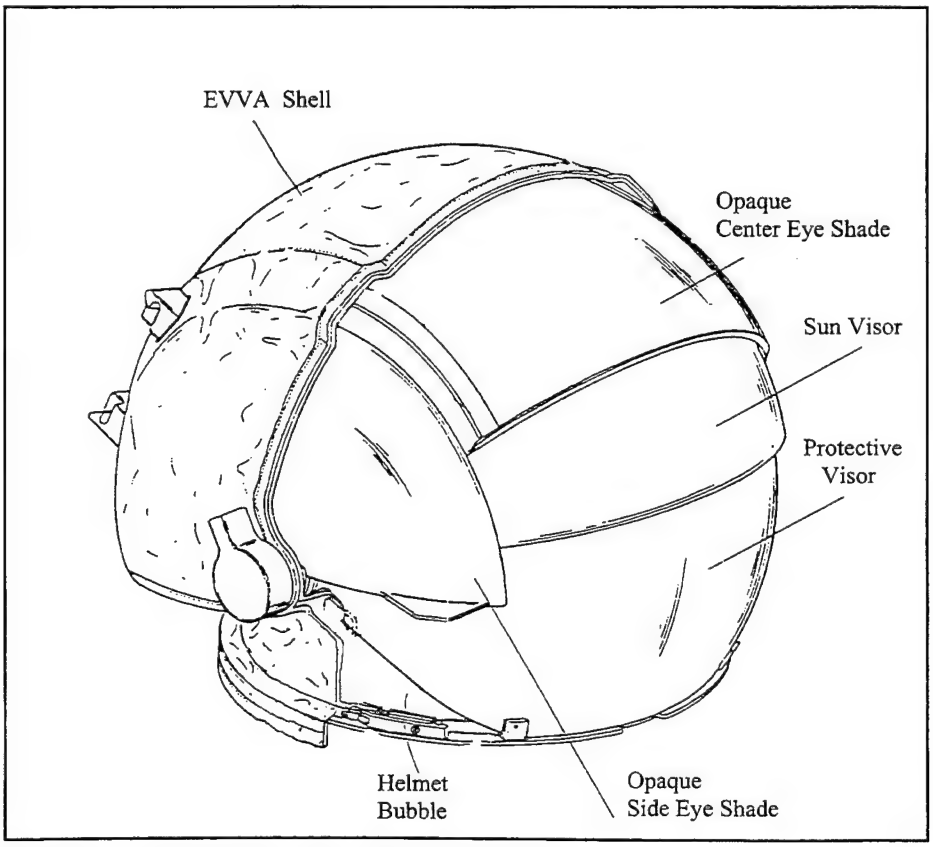

Figure 3. Extravehicular Visor Assembly (EVVA).

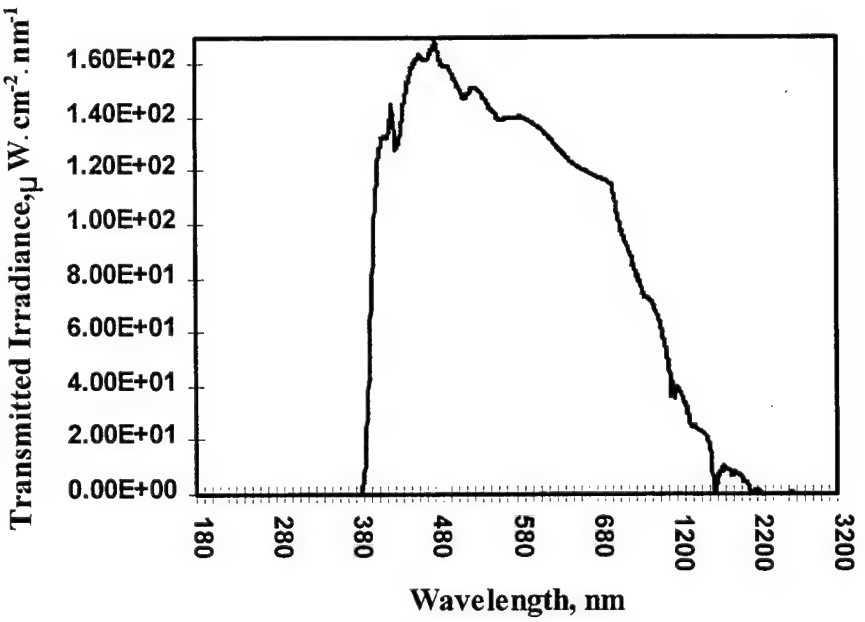

Figure 4. Transmitted Spectral Irradiance Curve of Protective Visor, With Hard Coating (HC) and Helmet Bubble (N/HC) Combination.

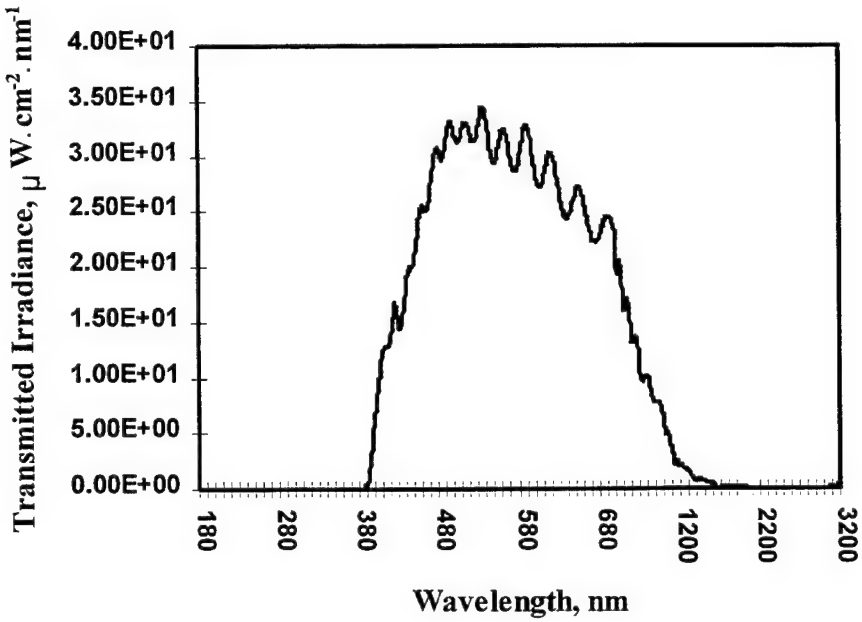

Figure 5. Transmitted Spectral Irradiance Curve of Sun Visor (SN 112), Protective Visor With Hard Coating (HC) and Helmet Bubble (N/HC) Combination.

3.2. Astronaut Solar Exposure and the Threshold Limit Value (TLV)

Weighted ocular exposure values were calculated for astronaut exposure through the nonthermally coated protective visor both with and without the sun visor in position. These exposure values were then compared to those values in the ACGIH TLV[1], and a maximum permissible exposure time (t_{max}) was determined. The results of this analysis are given in the Table.

Table. Permissible Exposure Times for EVVA without Thermal Coat. (In the calculated exposure column, the top line is without a sun visor, and the bottom line is with a sun visor.)

Adverse Effect	Wavelength Range (nm)	TLV	Calculated Exposure	t_{max}
Photokerititis	180-400	3 mJ/cm^2	3.9 x 10^{-8} W/cm^2 1.6 x 10^{-8} W/cm^2	7.8 x 10^4 s 1.9 x 10^5 s
UVA thermally aided cataractogenisis	315-400	1 mW/cm^2	0.43 mW/cm^2 0.035 mW/cm^2	>1000 s >1000 s
"Blue-Light" photoretinitis	400-700	10 mJ/cm^2	9.9 mW/cm^2 1.4 mW/cm^2	1 s 7 s
Retinal thermal injury	400-1400	$5/\alpha t^{1/4}$ W/cm^2•sr (α = 9.31 mrad)	2.1 x 10^3 W/cm^2•sr 320 W/cm^2•sr	4.5 ms 8 s
Thermal Corneal Injury and possible cataractogenisis	770-3000	1.8 $t^{-3/4}$ W/cm^2	43.2 mW/cm^2 3.8 mW/cm^2	143.5 s >1000 s

4. DISCUSSION

4.1 Retinal Injury Mechanisms

There are two predominant retinal injury mechanisms: thermal and photochemical. Photochemical injury is dominant for exposures longer than about 10 s and exhibits no retinal image-size dependence. In this case, blue-violet wavelengths are the most dangerous, and exposures are additive over at least 24 hours. Thermal injury is dominant for exposures less than 10 s, and heat flow away from the retinal image causes an image-size dependence.

4.2 Retinal Exposure

Retinal irradiance (E_r) is related to source radiance (L) by the following equation:

$$E_r = 0.27 L \tau d_e \quad (1)$$

The pupillary diameter is d_e and τ is the spectral absorption/transmission factor for the ocular media. The τ for the solar spectrum is approximately 0.74. For any retinal exposure (400 nm-1400 nm), the pupillary diameter is critical since changing it from 8 mm [dark-adapted and 2-3 mm (daylight)] results in a reduction of 16 in retinal exposure.

4.3. Threshold Limit Values (TLVs)

The TLVs used in this analysis refer to values for ultraviolet, visible and IRA and IRB in the wavelength range of 180 nm to 3000 nm. The TLVs represent conditions under which it is believed that all workers may be exposed without adverse health effects. The values are based upon the best available information from experimental studies. *These values should be used only as guides in the control of exposures to light and should not be regarded as fine lines between safe and dangerous levels.* The TLVs for exposure to light and infrared are given in pages 104-107 of the 1995-1996 TLV book' . The ultraviolet limits are given in pages 119-122. The value or the expression used to calculate the TLV for the different wavelength bands and adverse effects is given in the Table. The linear angular subtense of the solar disc (α) at the earth is 9.31 mrad. This angle is the ratio between the solar diameter and the average distance between the earth and sun. The radiance of the sun is calculated by dividing the extraterrestrial solar irradiance by the solid angle subtended by the sun at the earth. The linear angle is related to the solid angle (Ω) for circular sources by:

$$\Omega = \frac{\pi\alpha^2}{4} \qquad (2)$$

The solid angle subtended by the sun at the earth is therefore 6.8×10^{-5} sr..

4.4 Risks

4.4.1 Retinal Thermal Injury.

The TLV for retinal thermal injury is exceeded within 4.5 ms for viewing without the sun visor. This short time is critical because the aversion response which limits retinal exposure to bright light to about 0.2 s will not limit the exposure to a value less than the TLV. However, Mainster and White[2] have shown that the sun cannot produce a thermal injury, because the 2° C temperature rise in 0.2 s is less than the required 10° temperature change for denaturation of proteins. The 0.2-s limit can be calculated from the expression for the TLV in the Table. The 0.2-s limit is 803 $W/cm^2 \cdot sr$ for an angular subtense of 9.31 mrad. The exposure exceeds the TLV by a factor of 2.6, well within the safety margin of approximately 10 between the TLV and the onset of actual physical damage to the retina. The retinal thermal exposure exceeds the TLV for 0.2 s, but the exposure is not great enough to cause an actual injury. Use of the sun visor will limit 0.2-s exposures to less than the TLV.

4.4.2 Photochemical Retinal Injury

The TLV for photochemical retinal injury is exceeded within 1 s when staring at the sun through the nonthermally coated protective visor, and permissible exposure time increases to 7 s with the addition of the sun visor. This time is the total permissible exposure time in 8 hours. Assuming a "blink reflex" of 0.2 s results in 5 "blinks" (0.2 s x 5 = 1 s) before the TLV is reached. Viewing through the sun visor would permit 35 "blinks" (0.2 s x 35 = 7 s) before the TLV is reached. The photochemical injury threshold, according to Ham[5], is an effective absorbed retinal radiant exposure of 20 J/cm^2. For a 2-mm pupil, the injury threshold will be reached in 14 s, and for a 3-mm pupil, the injury threshold will be reached in 6.3 s. Use of the sun visor would increase these times by a factor of 7. It is unlikely that each exposure would be at the same location on the retina. Other short wavelength visible sources that may expose the astronaut include the solar reflection from the payload bay and any electron beam welding done in space.

4.4.3 Thermal Injury to Cornea and Lens

The TLV for exposure of the cornea and lens to near and mid-infrared radiation (770 nm-3000 nm) is given in the Table. The astronaut exposure is 43.2 mW/cm^2 without the sun visor and 3.8 mW/cm^2 through the sun visor. Because of the blink reflex, it is highly unlikely that the astronaut would be exposed to an average level greater than 10 mW/cm^2 even if exposed occasionally to the 43.2-mW/cm^2 level.

5. CONCLUSIONS

Removing the thermal coating from the protective visor produces only a very minor change in retinal exposure; however, exposure to the extraterrestrial solar irradiance exceeds TLVs under certain conditions. It is unlikely that actual injury thresholds would be exceeded because the eye limits exposure times to about 0.2 s for bright lights. More important is the impact of future more numerous and longer duration EVA missions, since the risk of photochemical injury to the retina is dependent upon the total number of momentary exposures. Therefore, it would seem appropriate that the sun visor always be used during EVA to reduce the risk of retinal injury from photochemical or thermal effects. It would also be appropriate to consider adding additional "blue-light" protection to the protective visor or via other means, i.e., "blue-blocker" sunglass, etc. The level of additional attenuation should consider the length of EVA and what additional sources of "blue light" are exposing the astronaut. Reducing the transmission in the blue end of the visible by an additional 7 to 10 percent will reduce blue-light exposure to approximately that level on the surface of the earth. This should substantially reduce the risk of photochemical injury to the retina.

---

*The views expressed are the personal views of the authors and do not represent an official view of the Department of the Army or the Department of Defense.

REFERENCES

1. American Conference of Governmental Industrial Hygienists, ACGIH, 1995-1996 Threshold Limit Values (TLVs™) for Chemical Substances and Physical Agents and Biological Exposure Indices (BEIs™), Cincinnati, OH (Telephone 513/742-2020).

2. T. J. White, M. A. Mainster, P. W. Wilson, and J. H. Tips, "Chorioretinal temperature increases from solar observation" Bull. Math. Biophys. 33(1), :1-17 (1971).

3. W. T. Ham, Jr., H. A. Mueller, R. C. Williams, and W. J. Geeraets, "Ocular Hazard from Viewing the Sun Unprotected and Through Various Windows and Filters", Applied Optics, Vol 12, No. 9, September 1973.

4. David Sliney and Myron Wolbarsht, "Safety with Lasers and Other Optical Sources", A Comprehensive Handbook, Plenum Press, 1980.

5. W. T. Ham, H. A. Mueller Jr., and D. H. Sliney, "Retinal sensitivity to damage from short wavelength light," Nature, 260:153-155, 1976.

6. ASTM E 490-73a (Reapproved 1992), Standard Solar Constant and Air Mass Zero Solar Spectral Irradiance Tables.

Appendix

Useful CIE Radiometric Units[1,2]

Term	Symbol	Defining equation	SI Unit and abbreviation
Radiant Energy	Q_e	$Q_e = \int \Phi_e dt$	Joule (J)
Radiant Energy Density	W_e	$W_e = \frac{dQ_e}{dV}$	Joule per cubic meter ($J \cdot m^{-3}$)
Radiant Flux (Radiant Power)	Φ_e,P	$\Phi_e = \frac{dQ_e}{dt}$	Watt (W)
Radiant Exitance	M_e	$M_e = \frac{d\Phi_e}{dA} = \int L_e \cos\theta \cdot d\Omega$	Watt per square meter ($W \cdot m^{-2}$)
Irradiance or Radiant Flux Density (Dose Rate in Photobiology)	E_e	$E_e = \frac{d\Phi_e}{dA}$	Watt per square meter ($W \cdot m^{-2}$)
Radiant Intensity	I_e	$I_e = \frac{d\Phi_e}{d\Omega}$	Watt per steradian ($W \cdot sr^{-1}$)
Radiance[3]	L_e	$L_e = \frac{d^2\Phi_e}{d\Omega \cdot dA \cdot \cos\theta}$	Watt per steradian per square meter ($W \cdot sr^{-1} \cdot m^{-2}$)
Radiant Exposure (Dose in Photobiology)	H_e	$H_e = \frac{dQ_e}{dA} = \int E_e \, dt$	Joule per square meter ($J \cdot m^{-2}$)
Radiant Efficiency[4] (of a source)	n_e	$n_e = \frac{P}{P_i}$	unitless
Optical Density[5]	D_e	$D_e = -\log_{10}(\tau_e)$	unitless

1. The units may be altered to refer to narrow spectral bands in which the term is preceded by the word *spectral* and the unit is then per wavelength interval and the symbol has a subscript λ. For example, spectral irradiance E_λ has units of $W \cdot m^{-2} \cdot m^{-1}$ or more often, $W \cdot cm^{-2} \cdot nm^{-1}$.
2. While the meter is the preferred unit of length, the centimeter is still the most commonly used unit of length for many of the above terms
and the nm or μm are most commonly used to express wavelength.
3. At the source $L = \frac{dI}{dA \cdot \cos\theta}$ and at a receptor $L = \frac{dE}{d\Omega \cdot \cos\theta}$.
4. P_i is electrical input power in Watts.
5. τ is the transmission.

LASER SAFETY: THE INFLUENCE OF ATMOSPHERIC SCINTILLATIONS ON THE OCULAR HAZARD DISTANCE

Amir Langus and Moshe Tur

Tel-Aviv University, Faculty of Engineering Department of Engineering
Tel-Aviv, Israel 69978

ABSTRACT

In the presence of atmospheric turbulence the nominal ocular hazard distance may no longer be a safe range for laser inter-beam viewing. Knowledge of the probability density function and standard deviation of the scintillations is essential for proper estimation of laser hazard level. Here we examine the probability of the minimum visible retinal lesion as a function of different forms of the scintillations distribution and standard deviation.

Keywords: laser safety, atmospheric turbulence, retinal lesion, nominal ocular hazard distance

1.INTRODUCTION

The existence of laser eye injuries depends strongly on the amount of the energy that enters into the eye and focuses into the funds. Laser safety regulations are designed to prevent laser injuries. By obeying those regulations, one can be sure that even in an inter-beam viewing case, the inter-ocular energy (IOE) will be far below the energy levels that might produce retinal injuries. Laser safety standards define the Maximum Permissible Exposure (MPE). It is well accepted that if one is exposed to radiant levels lower than the MPE, eye injuries will not occur. Another aspect of the safety standards is the Nominal Ocular Hazard Distance (NOHD). The NOHD is determined by considering the laser total radiant energy output, the beam divergence together with the MPE. The consequences is that if one is located farther than the NOHD, he will be exposed to radiance levels that are smaller than the MPE.

This description of the determination and the implication of the NOHD is correct as long as the beam propagates in a homogenous medium that does not interact with the beam. However, when considering outdoor situations, the laser beam is likely to propagate through the turbulent atmosphere that causes significant fluctuations of the beam intensity around its mean. These so-called scintillations may momentarily result in exposure levels that greatly exceed the MPE even when the average beam exposure is much smaller than the MPE.

Although the scintillation phenomena is well known and explored for at least 40 years, laser safety standards do not specifically consider them. The only reference to scintillations made by the American National Standards Institute for Safe Use of Lasers is in the description of the laser range equation, where it is emphasized that the equation is valid in a non-turbulent medium.

Because the NOHD is nominal and extra safety measures are allowed, it is a common practice to reduce the standard MPE by a factor of 10 and consequently to increase the NOHD by a factor of 3.3. This practice is not based on a study and should be considered as such.

There has been some previous studies on the subject of laser safety and turbulent scintillations. Deitz[1] calculated the probabilities that a radiant exposure will exceed a certain energy density threshold, which he considered as the energy density for a threshold damage to the eye. Deitz neglected that damage to the eye cannot be described as a deterministic process of exceeding a certain threshold. Hermann[2] did a similar analysis calculating the probabilities that a radiant exposure will exceed a safety energy density threshold, which equals the maximum permitted irradiance. He also omitted the stochastic phenomena of laser tissue interaction. Both Deitz and Hermann assumed the scintillation intensity statistics to obey log-normal statistics. A semi experimental work was done by Hill and Sliney[3], in which they estimated the increase of the retinal thermal burn probability due to the accumulated effects of the intensity scintillations for a pupil sized aperture. Smerdon[4] and Smith[5] suggested the idea of a probabilistic approach to laser safety. Under this idea one should consider both the scintillations and laser tissue interaction statistics, among other stochastic elements. However, none of these studies suggested how to modify the NOHD to compensate for the scintillation and to reduce laser hazard back to the risk levels obtained at the NOHD without scintillations.

Recently, we have undertaken a thorough study having the following objectives: estimating the increase in laser hazard from a single Q-switch pulse in the retinal hazard region, due to the turbulent scintillation; suggesting an appropriate correction for reducing laser hazard back to the risk levels obtained at the NOHD without scintillations. All this is done by considering the atmospheric turbulence and laser tissue interaction phenomena. We considered the random properties of laser tissue interaction; the form of the probability function, the mean and variance of the IOE, including beam broadening and beam wandering, and the pupil aperture averaging effect.

In this article we examine the probability of the minimum visible retinal lesion as a function of different forms of the scintillations distribution and standard deviation.

2.THE MODEL

2. 1.Determining a hazard parameter

To be able to express and compare the amount of laser ocular hazard with and without turbulent scintillations a calculable hazard parameter should be defined. We chose to express this parameter as the retinal Minimum Visible Lesion (MVL) probability.

There are several approaches to the MVL. Some[4,5] refer to it as the Minimum Ophthalmoscopically Visible Lesion that they describe as a relatively small ocular damage, though still easily detectable. Its consequences are roughly low vision loss, but yet might be rather significant especially if located in the fovea. Others[6] describe it from an experimental point of view simply as an injury. In those experiments they ophthalmoscopically examined an exposed retinal location for the presence or absence of a visible alteration. Since those injuries were on the boundary of being visually detected, they may be considered as minimum lesions.

It is worth pointing out that the MVL parameters are very well measured and can be reliably used for the calculation of the hazard parameter.

2. 2. Calculating the MVL probabilities

The MVL probabilities can be calculated[4,7] by using the Probit method which was used to analyze the ocular biological effects experiments [6].

$$P_{MVL}(IOE) = \frac{1}{2} + \frac{1}{2}\,\mathrm{erf}\left(\frac{\ln(IOE) - \ln(ED_{50})}{\sqrt{2}\,\ln(slope)}\right) \qquad (1)$$

where:

P_{MVL}: MVL probability.

IOE: the inter-ocular energy calculated as the product of the pupil area [cm^2] with the energy density on the pupil [joules/cm^2].

ED_x: the IOE [joules] having x % probability of causing MVL.

Slope: defined as ED_{84}/ED_{50}, and erf(x) is the error function.

The statistical Probit technique deals with stochastic phenomena that involve a continuous independent (explaining) parameter and a discrete dependent (result, explained) parameter. It is assumed that a specific outcome is the result of a situation in which the independent explaining parameter exceeds a randomly distributed threshold. When the Probit technique is used in ocular laser-tissue interactions it is assumed that each retinal location in each specimen has some kind of energy threshold. If the energy that is focused on a certain retinal location is larger than this energy threshold, a lesion will be found at that location. Otherwise, no lesion will occur. Equation (1) calculates the fraction of retinal locations whose thresholds are smaller than the IOE. The ED_{50} and slope parameters, together with the error function and the natural logarithm indicate that the retinal locations thresholds obey a log-normal distribution, with the ED_{50} to represent these thresholds median, and the slope to represent their standard deviation.

The relatively narrow ED_{50} confidence limits that were experimentally measured[6] indicate that the Probit technique with its implications is quite reliable, at least for the inter ocular energies that were used in those experiments.

Having the appropriate ED_{50} and slope one can predict the MVL probability, hence the hazard parameter for any IOE.

2. 3. Calculating MVL probability for random IOE

To evaluate the MVL probability from laser beam irradiance after propagating through the turbulent atmosphere the fluctuations of the beam intensity should be considered. This can be done by summing the MVL probabilities from a specific fluctuation over all the possible fluctuation values together with their weighting factor [5].

The mathematical expression of this summation is given in equation (2).

$$Pd = \int_0^\infty p_{Sc}(\lambda) * P_{MVL}\left(\langle IOE\rangle * \lambda\right) d\lambda \qquad (2)$$

where:

Pd: the actual MVL probability under random IOE conditions.

<IOE>: the average IOE being equal to the IOE if there were no scintillations.

λ: the scintillation level that is the specific momentary IOE divided by the average IOE. Using equation (1), with the product of <IOE> and λ instead of a deterministic IOE (without scintillations) returns the MVL probability from a specific scintillation level.

$P_{Sc}(\lambda)d\lambda$: the weighting factor, known as the Probability Density Function (PDF), for the specific normalized momentary IOE i.e., the probability that the scintillation level/IOE lies in an infinitesimally small interval (λ , $\lambda+d\lambda$).

2. 4. Parameters and sub models to be defined

From an overall point of view, when discussing the NOHD under turbulent conditions, one should deal with the following parameters and sub models. The first is the average IOE that depends on laser power, distance, beam divergence, atmospheric attenuation and turbulence-induced beam broadening. The second is the ED_{50} and the slope that have a strong wavelength dependence. The third is the scintillation PDF form and standard deviation (including the beam wandering phenomena) as a function of turbulence parameters, distance, wavelength and the pupil averaging effect. The turbulence parameters themselves, i.e., the index of refraction structure constant and the inner scale size of turbulent eddies should also be considered.

All these models and parameters are needed to calculate the MVL probability dependence on distance, for comparing of the MVL probabilities at the NOHD and for proposing an appropriate compensation factor.

As mentioned above, presently we shall discuss the PDF form and the standard deviation value of the IOE.

It is well accepted that under weak turbulence conditions, where the propagation distance is short or the index of refraction structure constant, C_n^2 is small*, the scintillations are weak and obey the log-normal statistics. The scintillations log-normal PDF is supported by the weak turbulent theory [8,9] and has been measured experimentally [3,9]. However, when the propagation distance or the C_n^2 are not small, the scintillations become stronger and the weak turbulence theory does not hold.

There have been many suggestions for the PDF forms for strong scintillations. PDFs such as Rayleigh, Rice-Nakagami, Exponential, Hoyt, m, n, K, as well as log-normal and modulations of one PDF by another were considered [10,11,12]. As of now there is no certain knowledge on the scintillation PDF form.

A similar uncertainty exists regarding the range-dependence of the standard deviation of the scintillations. For the weak turbulence, when the scintillations obey the log-normal statistics, the Scintillations Standard Deviation (SSD) can be calculated with the Rytov approximation. Equations based upon the Rytov approximation predict that the SSD increases without limit as the path length and/or C_n^2 increase. In the real world, however, the SSD does not increase without a limit. With increasing path length or C_n^2 the SSD reaches a peak value and then appears to slowly decrease towards the value of 1. The peak in the SSD value is the most critical value from laser safety considerations. To demonstrate this problem we consider an inter-beam viewing case at the NOHD and a specific C_n^2 that causes the SSD to reach the maximum value. For an inter-beam viewing case at the NOHD, the average IOE is much smaller than the IOE levels that might produce an MVL. The large SSD causes a large probability of having a momentary huge scintillation level. This, in turn, causes a large probability of having a momentary IOE that might produce an MVL. Hence the MVL probability increases together with the SSD value.

2. 5. Sensitivity tests for the IOE PDF and standard deviation value

The basic idea of the sensitivity test is to execute a complete analysis for each of the relevant alternatives, and then to compare the results. If, fortunately, all the final results are close enough, then the analysis is not sensitive to a specific selection among the relevant alternatives. We can select any one of them (the easiest to calculate).

In view of the laser hazard problem together with all the above-mentioned uncertainties, sensitivity tests should be performed using equation (2) for the MVL probability. This is done by substituting the PDF, $P_{Sc}(\lambda)$, with all relevant PDF forms and then using equation (2) with all SSD's values, in the domain where the weak turbulence theory does not hold. Note that most of the attention should be focused on SSD values equal to or larger than 1. If the NOHD is large enough one can expect the SSD value to be equal to 1. Otherwise one should focus on the SSD peak value. In weak turbulence situations, there is no uncertainty and the small scintillations levels are significantly less hazardous.

---

* Actually meaning a situation where the variability in the atmospheric optical refraction index is low.

3. NUMERICAL RESULTS

The results to be presented in this section were evaluated using equation (3) as a function of the IOE that were normalized to the ED_{50} and as a function of the SSD.

$$Pd(\beta,\sigma_\lambda)=\int_0^\infty p_{Sc}(\lambda,\sigma_\lambda)*\frac{1}{2}\left[1+\mathrm{erf}\left(\frac{\ln(\beta*\lambda)}{\sqrt{2}\ln(\mathrm{slope})}\right)\right]d\lambda \tag{3}$$

where:

β= <IOE>/ ED_{50} (i.e., the mean IOE divided by the ED_{50}) is the first influencing parameter. This parameter was chosen to be a causal (explaining) variable in order to bypass geometrical considerations (distance, beam divergence).

σ_λ: the SSD. λ and P_{Sc} are as described in sec. 2.3, and the slope was set to 1.5 (a representative slope value [6]).

Results from the sensitivity tests on the PDF form are presented in Figure 1 for a unity standard deviation. The comparison was done among the log-normal PDF

$$p_{Sc}(\lambda,\sigma_\lambda)=\frac{1}{\sqrt{2\pi\ln(1+\sigma_\lambda{}^2)}\ \mathrm{I}}\exp\left(-\frac{\left(\ln(\lambda)+\frac{1}{2}\ln(1+\sigma_\lambda{}^2)\right)^2}{2\ln(1+\sigma_\lambda{}^2)}\right) \tag{4}$$

the exponential PDF

$$p_{Sc}(\lambda)=\exp(-\lambda) \tag{5}$$

that is valid only for σ_λ=1, and the log-normal modulated exponential PDF

$$p_{Sc}(\lambda,\sigma_\lambda)=\int_0^\infty\frac{1}{\sqrt{2\pi\ln(1+\sigma_\lambda{}^2)}\ z^2}\exp\left(-\frac{I}{z}-\frac{\left(\ln(\lambda)+\frac{1}{2}\ln\left(\frac{1+\sigma_\lambda{}^2}{2}\right)\right)^2}{2\ln\left(\frac{1+\sigma_\lambda{}^2}{2}\right)}\right)dz \tag{6}$$

MVL probabilities for the no turbulence case, i.e., deterministic IOE were calculated using Eq. (4), are also plotted for reference.

$$Pd(\beta)=\frac{1}{2}\left[1+\mathrm{erf}\left(\frac{\ln(\beta*1)}{\sqrt{2}\ln(\mathrm{slope})}\right)\right] \tag{7}$$

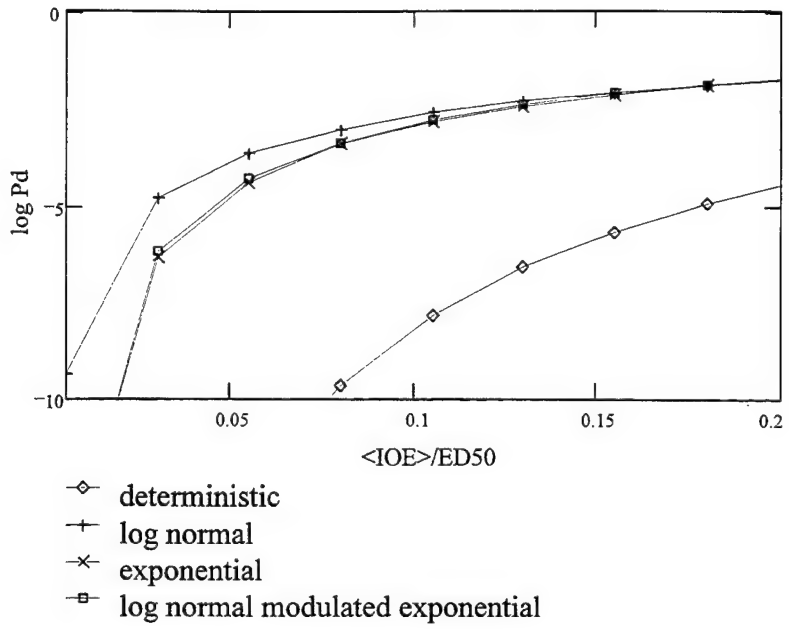

Figure 1- Sensitivity test to the form of the PDF (SSD=1)

In Figure 2 we compare the log-normal PDF with the K-distribution PDF for a standard deviation value of 1.5.

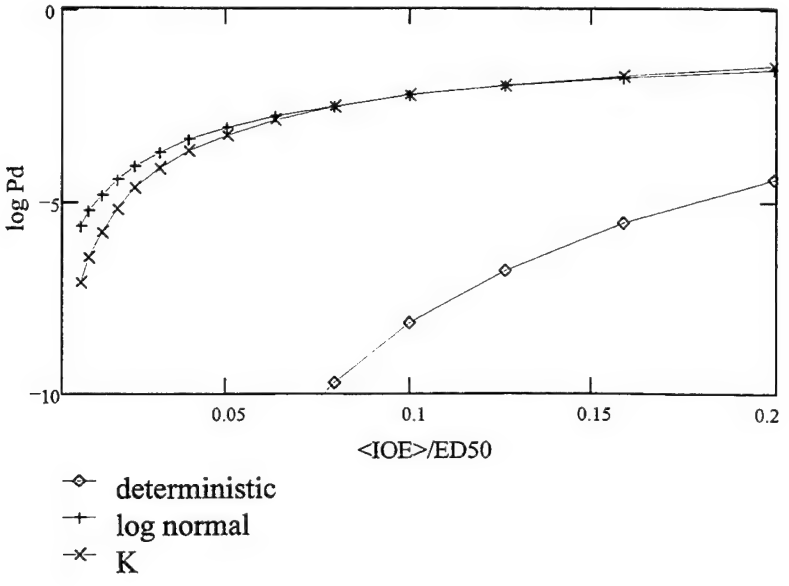

Figure 2- Sensitivity test to the PDF form (SSD=1.5)

From Figure 1 and Figure 2 it is evident that Pd can reach very high and unacceptable values for β=0.1. Also note that while all calculated MVL probabilities are quite close to one another the log-normal one is definitely the worst one, as far as laser safety is concerned. We therefore adopt the log-normal distribution since it is the most appropriate distribution for both weak and strong turbulence.

In Figure 3 - sensitivity test to the SSD value (logarithmic scale) and Figure 4 (linear scale) we present the sensitivity test for the SSD values, using the log-normal PDF. Each figure contains 7 curves, a different curve for each SSD value. The lowest curve (marked with an "x") is for SSD equal to 0, i.e., the deterministic case with no scintillations. The next higher curves is for SSD equal to 0.5, the next one is for SSD equal to 1, etc., each one of the curves was calculated with SSD value that is 0.5 greater than the one below it (the curve marked with a box is for SSD = 1, the SSD value for very large path length).

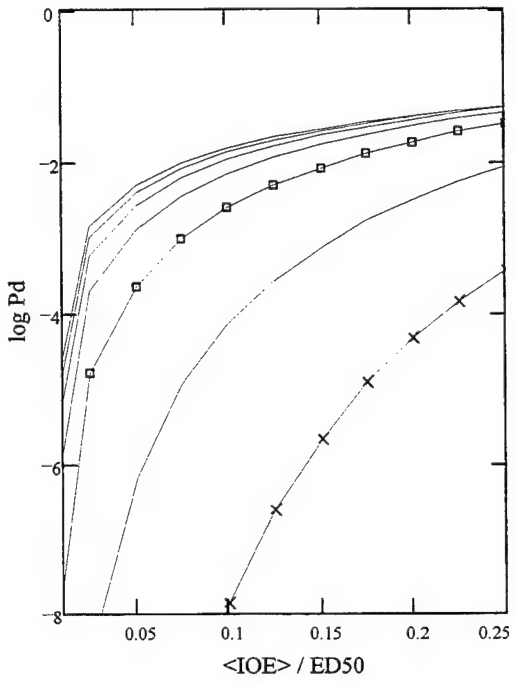

Figure 3 - sensitivity test to the SSD value

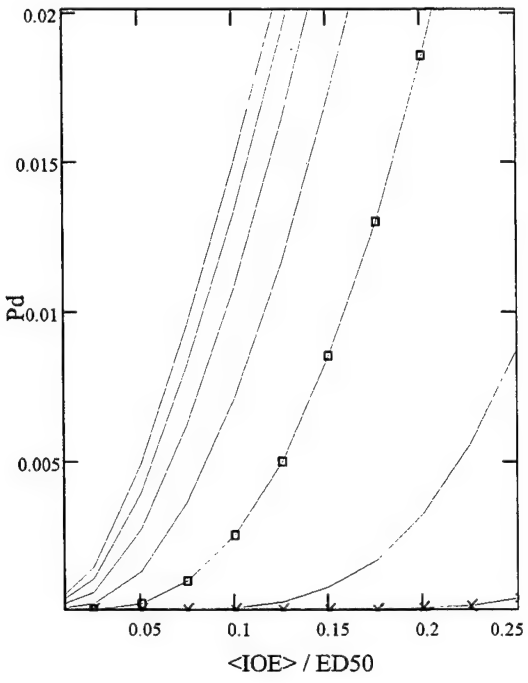

Figure 4 - sensitivity test to the SSD value

It is immediately apparent that there is a saturation in the MVL probability, as the SSD becomes larger. MVL probabilities for SSD values that are greater than 1.5 become very close together; thus MVL probabilities for SSD values larger than 1.5 can be reliably calculated with an SSD value of 1.5.

This result simplifies the range of the uncertainty of the SSD value. The insensitivity of MVL probabilities for an SSD greater than 1.5 almost cancels the problem about the lack of a model for the peak in the SSD value. It can be shown that the Rytov approximation is valid for the calculation of the SSD up to the value of 1.2. From this point on, we can manipulate the SSD value, for example, setting the SSD value to 1.5 or to 1.2, from the point where the SSD equals to 1.2. This will result in a relatively small error in the MVL probability. The error is smaller than a half order of magnitude, which is almost negligible regarding the increase of about 5 orders of magnitude in the MVL probability, due to the scintillations phenomena.

4. DISCUSSION

Here we propose an explanation to the saturation in the MVL probability for large SSD values. This explanation is related to the shape transformation of the log-normal PDF dependence on its SSD value. In Figure 5 we have plotted the log-normal PDF for several SSD values, as described at the legend.

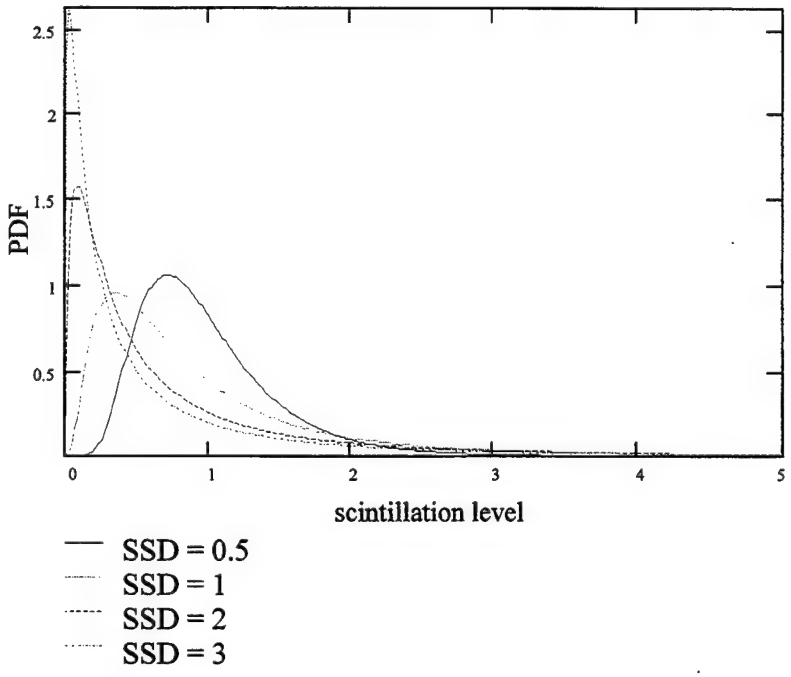

Figure 5 - The dependence of the log-normal PDF form on the SSD

It seems that the log-normal PDF tends to converge to a unique shape as the SSD value becomes large. Hence, for large SSD, a log-normal PDF with a specific SSD can be replaced with one that have another, yet large, SSD. This, in turn, causes the MVL probability to be insensitive to changes in SSD values that are larger than 1.5.

5. CONCLUSIONS

We conclude as follows: If the IOE is $1/10^{th}$ of the ED_{50}, when the eye is exposed to the MPE, then atmospheric turbulence causes the MVL probabilities, at the NOHD, to increase from a rather acceptable low value of 10^{-9} (without turbulence) to the unacceptable unsafe value of about 10^{-4} (Figs. 1-2).

The log-normal PDF is the most appropriate distribution to represent the IOE scintillations for all the SSD values. The log-normal PDF is the true one for weak turbulence and presents an upper bound to all other tested PDFs.

Since the MVL probabilities appear to converge as the SSD increases, accuracy in the SSD value is not needed, as long as the SSD value becomes larger than approximately 1.5. Thus, the SSD expression can follow the Rytov approximation for weak and moderate turbulence up to a value of 1.5, and then decreases slowly to the value of 1 for very strong turbulence. This procedure will result in a relatively small MVL probability error.

In order to propose a correction to the NOHD which includes scintillation phenomena, one should calculate the MVL probabilities as a function of the distance between the laser and an eye looking into the laser, taking into account turbulence-induced beam broadening, the averaging effect of the eye pupil, as well as other relevant biological parameters.

6. REFERENCES

1. H. Deitz, "Probability Analysis of Ocular Damage due to Laser Radiation through the Atmosphere" ,Appl. Opt. 8, 371 - 375 (1969)
2. H. Hermann," Evaluation of the Scintillations Factor for Laser Hazard Analysis ",Appl. Opt. 29, 1287 - 1292 (1990)
3. J. Hill, J. H. Churnside and D. H. Sliney, "Measured Statistics of Laser Beam Scintillations in Strong Refractive Turbulence Relevant to Eye Safety" ,Health Physics, 53, 639 - 647 (1987)
4. S. Smerdon, " A Probabilistic Approach to Laser Safety ", presented at Colloquium Effects Biologiques de Fixceaux Lasers et Normes de Protections. Paris, Nov. 1986.
5. Peter A. Smith." Probability and Risk in Laser Safety" Journal of Laser Applications, 6, 101-107 (1994)
6. J. Lund, and E.S. Beatrice," Near Infrared Laser Ocular Bioeffects ", Health Physics Vol. 56 No. 5 (May) 631 - 636, 1989
7. David Sliney and Myron Wolbarsht; Safety with Lasers and Other Optical Sources, Plenum Press - New York & London, 1980
8. Ishimaru " Wave Propagation and Scattering in a Random Media", Academic Press, New-York, 1978.
9. L. Fante," Electromagnetic Beam Propagation in Turbulent Media", Proc IEEE 63, no. 12, p1669 ,(1975)
10. L. Phillips and L.C. Andrews "Measured Statistics of Laser-Light Scattering in Atmospheric Turbulence", J. Opt. Soc. Am. 81, 1440 - 1445 (1981)
11. H. Churnside and S. F. Clifford "Probability Density of Optical Scintillations in the Turbulent Atmosphere", J. Opt. Soc. Am. A 4, 1923 - 1930 (1987)
12. H. Churnside and R.J. Hill "Probability Density of Irradiance Scintillations for Strong Path-Integrated Refractive Turbulence", J. Opt. Soc. Am. A 4, 727 - 733 (1987)

Laser safety standard for skin at 1540 nm. New experiment and estimations.

Alexei V.Lukashev, Sergei E. Sverchkov, Valery P. Solovyev(*), Boris I.Denker,Victor V. Engovatov(*)

General Physics Institute, 38 Vavilov Str., Moscow 117942, Russia
Phn: (095)-135 3038, Fax: (095)-135 2055, e-mail: lukashev@kapella.gpi.ru
(*) Institute of Biophysics, 46 Zhivopisnaya Str., 123098 Moscow, Russia

ABSTRACT

Radiant exposure of an Er-glass laser(λ=1540 nm) producing 50 percent probability(ED50) of a minimum erythema on porcine skin was measured *in vivo* for laser pulses 100 ns and 2.5 ms pulse duration. ED50 at 24 hours post-exposure was found 3.5 J/cm^2 for short laser pulses and 6.5 J/cm^2 for long ones. The single pulse dose in a chain of repetitive pulses producing minimum erythema were determined for 2^n(n=1-6) pulses. The minimum reaction of skin on laser irradiance were studied for different beam diameter(2-10 mm). The reaction of skin is mostly considered as local super heating. The data obtained in the study are adequate to update safety standards for cutaneous injury.

Keewords: laser safety, skin, Er-glass laser

1. INTRODUCTION

Eye-safe laser systems based on Er glass lasers(λ=1540 nm) have various applications in pilot training facilities. In the previous safety standard (ANSI Z136.1-1986), Table 7(Skin Exposure Limits) had an exception for 1540 nm radiation, permitting 1 J/cm^2 for microsecond to nanosecond pulses. This exception was made, in part, because of high damage threshold that was found by researchers studying ocular damage[1,2]. In the revised Standard (ANSI Z136.1-1993), Table 7 (on Skin) removed the exception for 1540 nm for skin exposure, making it 0.01 J/cm^2 . It means that lasers that are eye-safe may now be skin-hazardous. This great change of the Standard has been done without substantial experimental data on interaction of 1540 nm laser radiation with human skin.

The research reported was undertaken to receive experimental data on minimal reaction(mild erythema) of skin to 1540 nm laser radiation with different pulse duration, number of repetitive exposures and cross section of laser spot.

2. METHODS

In experiments we used 1540 nm Erbium-glass laser radiation produced by an original home-built laser system operating both in free-running and Q-switched regimes. The basic optical setup is described in detail in our paper[3] . The beam shape on the object plane was round with diameter 2-10 mm for free running and 2-4.5 mm for Q-switched modes.

In experiments we used white domestic pigs free of visible pigmentation. Pigs were selected because of histological resemblance of their skin to that of man. The pigs were 1.2-2 months old and weighted 8-16 kg.

One day before the experiment the bristle on the animal's back and sides was removed with hand clippers and then shaved. No visible skin reaction(reddening, cuts, etc.) was observed on the skin at the time of experiments because of hair removing. The depilated area was divided into a grid of squares about 15x15 mm in size. A side of the animal could have up to 90 cells. During experiments we did not used any anesthetic agents, since we assumed possible influence of anesthesia to the skin reaction.

This study had several tasks. It was determination of lesion threshold on the animal skin made during single pulse exposures; determination of dependence of minimal lesion dose upon a number of pulses in multipulse exposure and determination the dependence of minimal lesion dose upon laser beam cross section. All experimental tasks included both free running and Q-switched mode.

SPIE Vol. 2974 • 0277-786X/97/$10.00

The experimental set was started up with preliminary estimation of the ranges and values of dose which produce visible lesions. We started with maximum energy fluence determined by laser output parameters and then decreased the dose by step of 0.5-1 J/cm^2 . Five cells on the animals were exposed by the pulses with the same dose.

The skin reaction data was obtained by visual examination the areas exposed at several minutes, one-hour and at 24 hours post exposure. In general, the one-minute reaction at a given radiant exposure level served as a guide in determining whether increased radiant exposure levels should be given. In general, a very mild erythematous reaction at one-minutes will probably fade at one-hour. This level would represent the lowest level to be used. A definite well demarcated erythematous reaction on the skin at one-minutes will probably be present at one-hour examination.

At one-hour, each area exposed was again visually controlled and photographed. The number of "reactions" (this could be erythema, papules, blanching, etc.) were determined at each exposure level. The burns were categorized independently by two investigators. A similar examination and photographs were done at 24 hours post-exposure. Experimental data were processed by the probit method of Litchfield and Wilcoxon[4]. This data, expressed as a percentage of the reactions observed at each exposure level, was plotted on probability scale and the radiant exposure at the 50 percent probability level was taken as the ED50 level.

In the subsequent experimental sets probability of specific skin response in the range of transient reaction was determined more accurately. To do this we exposed up to ten cells with the same fluence close to threshold range in order to have more accurate statistical data. To obtain truly data and estimate deviation of individual reaction we conducted experimental set on three animals and then the results were averaged.

3. RESULTS

3.1 Damage threshold on pig's skin for single laser pulse.

The statistically processed data for minimal erythema at 1 hour post-exposure are plotted at the Fig 1. ED50 at 1 hour post exposure for 2.5 ms free running laser pulses was found to be 5.7±1.2 J/cm^2. 282 burns were processed. ED50 at 24 hour post exposure 6.5 J/cm^2.

ED50 at 1 hour post exposure for 100 ns Q-switched laser pulses was found to be 3.0±1.1 J/cm^2. 266 burns was processed. ED50 at 24 hour post exposure 3.5 J/cm^2 .

The deviation of individual sensitivity of animals and skin at different places (back, belly) in the both sets was within 15 % of obtained data. The same divergence was also found in the other sets of experiments as multipulse action and dependence on laser spot cross section.

The slope on probability plot(Fig.1) (slope= ED84/ED50=ED50/ED16)[5] is 1.5 for free running and 1.3 for Q- switch. The relatively high value of the slopes are indicative of small increase in dose required for the response to vary from no observed effect to the high probability of observing a response. This may be considered as a reason for assuming threshold character of skin reaction to that laser wavelength.

3.2 Skin damage resulting from exposure to multiple pulses.

The task was to determine dependence of ED50 of minimal erythema upon number of repetitive pulses.

The starting radiant exposure for single pulse was ED60-80(Fig.1) then it was decreased by 0.5 J/cm^2 until ED5-10 exposures. For the series with doubled pulses we started with the fluences a little bit less(5-10%) than with single pulse and decreased fluence as described previously. For the following series we decreased initial radiant exposure and increased number of pulses. In the serie the energy fluence was decreased until lesion probability was 5-10% just after exposure.

The experiments were made with 1, 2, 4, 8, 16, 32, 64 repetitive laser shots to the same area at different radiant exposure of single pulse. The maximum number of 64 pulses at the same place was explained by low repetition rate of the laser(0.1 Hz), the time of this experiment took about 10 min. and the most difficult was to hold the animal unmovable by hands during exposures. In the cases of long overall exposures(16,32,64 pulses) we used cells on the back of the animal close to the spine. With this arrangements the pig could lay down still on the

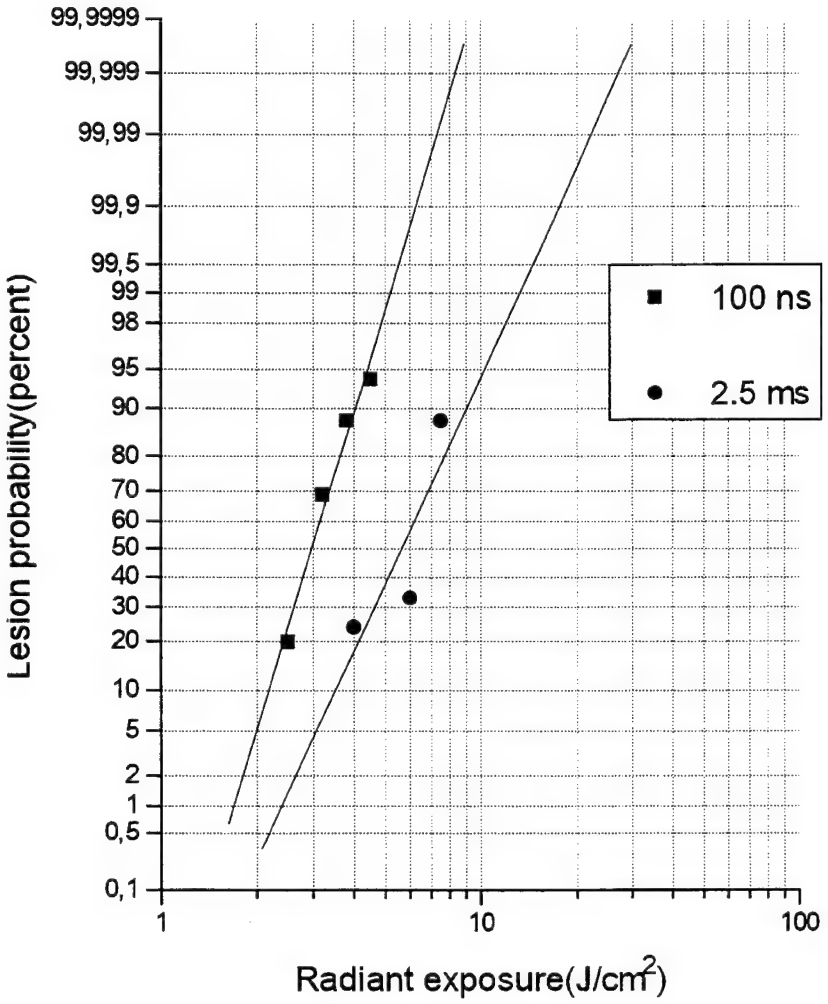

Fig.1. Dependence of the probability of minimal lesion(erythema) on skin caused by 1540 nm laser radiation upon laser energy fluence.

pad in its most natural position for longer time. Since for long multipulse exposure the single pulse energy fluence was well below ED50 there was no visible reaction of the animal to laser shots. Some times during 64 pulses experiments it got asleep. 5-10 cells were exposed to every value of laser fluence.

The value of radiant dose of single pulse for ED50 for free running (τ=2.5 ms, the spot diameter D=6.5 mm) at 1 hour and 24 hour post-exposure are presented in the Table 1.

Table 1.

Number of pulses, N	ED50 at 1h PE, J/cm^2	ED50 at 24h PE, J/cm^2
1	5.4	5.5
2	4.8	4.9
4	3.6	3.8
8	2.8	2.9
16	2.5	2.7
32	1.5	2.0
64	1.0	1.5

In the second set of experiments laser operated in Q-switch (τ=100 ns, D= 3.5 mm). The value of ED50 dose of single pulse at 1 hour and 24 hour post-exposure are presented in Table 2.

Table 2.

Number of pulses, N	ED50 at 1h PE, J/cm^2	ED50 at 24h PE, J/cm^2
1	3.2	3.1
2	2.8	2.9
4	2.4	2.5
8	2.0	2.2
16	1.8	2.0
32	1.7	1.8
64	1.6	1.6

The data are presented in the plots with linear and logarithmic scales(Fig.2). The dependence of overall exposure $E_I = E_{sp}N$ (E_{sp}-energy fluence of single pulse) upon number of pulses N are proportional to $N^{0.58}$ for free running and $N^{0.82}$ for Q-switching mode. In the Fig.3b approximation curves of experimental data are hyperbolas. Extrapolating them to the higher pulse number it is possible to assume that there is minimal exposure dose of single pulse which does not produce visible lesion even in any long series of pulses. It is 0.8 J/cm^2 for free running and 1.1 J/cm^2 for Q-switching.

3.3 Dependence of ED50 upon cross section of laser beam.

During this set of experiment ED50 value of minimal lesion was measured at various laser spot sizes on the animal skin. The maximum spot size was determined by maximum laser energy and energy fluence producing persistent lesion with 60-70% probability. In the case of free running the maximum laser energy was 7J, energy fluence 8 J/cm^2, thus maximum cross section was 0.9 cm^2(d< 11 mm). In the case of Q-switch E_{max} = 0.6 J, energy fluence 5 J/cm^2, S_{max} = 0.12 cm^2(d< 4 mm). The minimum spotsize was about 2 mm, because at spot diameter less than 2.5 mm we found it difficult to distinguish laser lesion due to inhomogenity of porcine skin. For the Q-switch mode we had rather small range of varying laser spotsize.

The results on ED50 of minimal lesions are presented in the Table 3.

Table 3.

	spot diameter d, mm	cross section S, cm^2	ED50 24h PE, J/cm^2
1.Free running			
	10	0.79	6.0
	5.6	0.25	7.0
	2.7	0.057	6.5
	2.0	0.028	6.8
2. Q-switch			
	4.2	0.14	4
	2.6	0.056	3.5

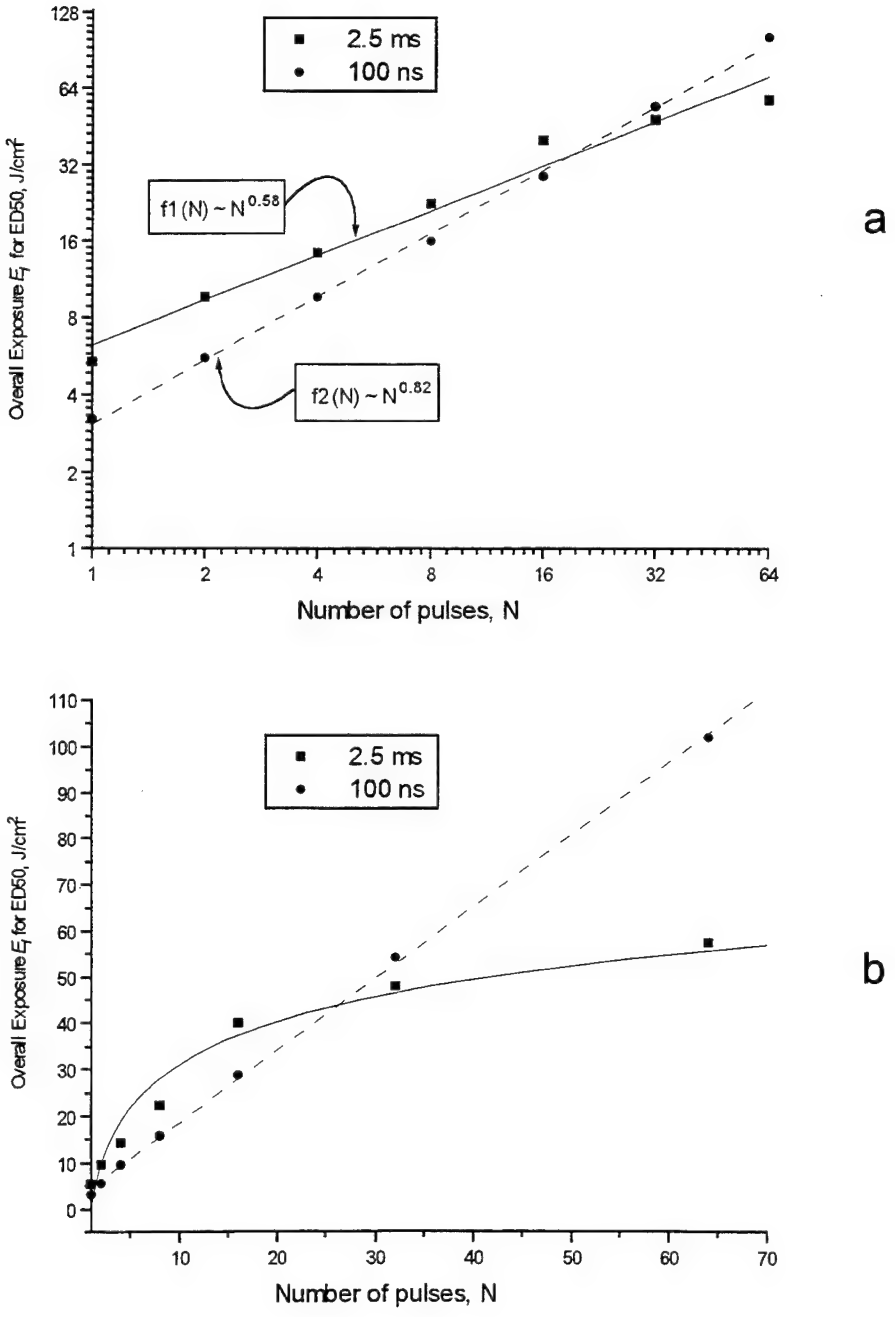

Fig.2. Dependence of overall exposure $E_I = E_{sp}N$, producing minimal lesion in 50% of the cases(ED50) upon number of pulses. **a** - logarithmic scale, **b** - linear scale.

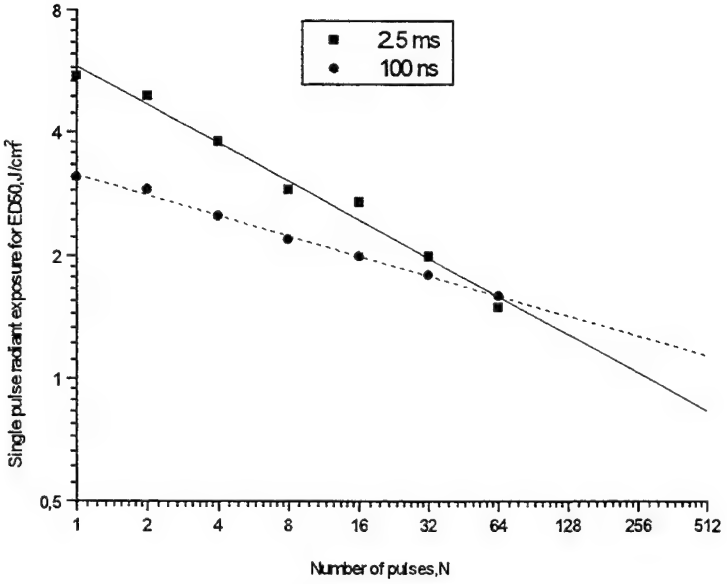

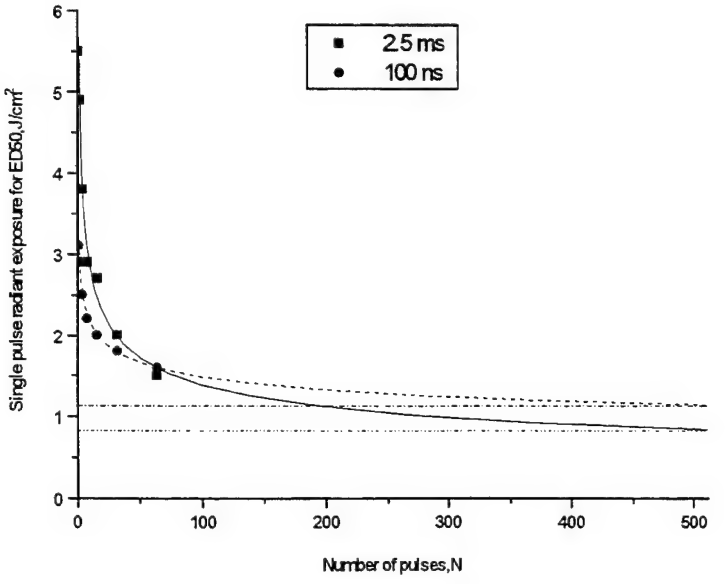

Fig.3. Dependence of single pulse energy fluence in the sequence of N repetitive pulses producing minimal lesion in 50% of the cases (ED50) at 24 h post exposure.
a - logarithmic scale, **b** - linear scale.

We consider that deviation of the obtained data are within the interval of individual and local sensitivity of the animal skin and there was no visual dependence of ED50 upon laser spotsize. The constant value of the ED50 in this experiment is explained by the geometry of the experiment and discussed in the next section.

4. DISCUSSION

The skin response resulting from exposure at 1540 nm is considered to be a result of temperature elevation of the tissue. The clinical description of skin burns at 1540 nm is fairly coincides with that of at 10.6 μm of CO_2 laser[6,7]. The geometry of the experiment and estimation of the cooling of the exposed volume suggests weak influence of heat dissipation in our experiments, especially for short pulses (< 1 μs). The penetration depth h of laser light at 1540 nm to water is about 1 mm(the absorption coefficient $\alpha \approx 10$ cm^{-1} [5,8](Fig.4), in the first approximation we consider that true for the skin too. The smallest laser beam diameter on skin was 2 mm and the largest 10 mm (long pulses: free running). Characteristic cooling time t_c of the layer thickness h could be estimated from formula $h \approx (\chi t_c)^{1/2}$, where χ- thermal diffusivity of water ($\chi = 1.4\ 10^{-3}$ cm^2/s). For water layer 1 mm thick which is equal to penetration of laser light into water t_c is equal 10 sec . The cooling time is much longer than pulse duration for both laser pulses(100 ns and 2.5 ms), only in the latter case some weak heat dissipation could be considered. If again to use water substance as a model for our experiment, the equivalent temperature rise $\Delta T = E_l/(Shc_p)$ is 8^0 C for short and 15^0 C for long pulses at ED50 dose (E_l - laser energy, S - laser beam cross section, c_p - specific heat, $c_p = 4.2$ J/(Kcm^3)). Thus, the absolute temperature of the animal skin is higher than 42-43^0 C which is close to the temperature of protein denaturation. The greater value of ED50 for longer pulses we explained by the influence of heat dissipation during the laser pulse.

The data obtained in our experiments for the skin are in a good agreement with data obtained earlier[1,2,5] for the cornea. In the case of cornea the steepness of lesion probability curve is higher and the ED50 for both short and long pulses are about 10-40% higher. This difference could be because that cornea has higher water content and the structure of corneal and skin melanin as well as their thermo-physical properties are different[9, 10].

If the thermal damage is a valid model for skin injury by laser radiation with wavelength within absorption band of water it is possible estimate ED50 parameter for other wavelength around 1540 nm. It is also possible to determine wavelength band where ED50 is close to that of 1540 nm(Fig.4).

According to estimation made in the previous paragraph the cooling time of the exposed volume is about 10 sec. In the case when repetition rate of the laser is higher than 0.1 Hz the influence of addition of exposure dose of single pulses becomes more pronounced. In our experiments repetition rate was 0.1 Hz and the effect of addition of expose dose should not be so striking. Thus, obtained dependence of integral dose E_I ($E_I = E_{sp}N$) vs. number of pulses is valid only for repetition rate about 0.1 Hz. This dependence should be closer to N^1 (linear addition of radiant exposure of single pulses of the same fluence) for slower repetition rate or faster cooling of the exposed site and maybe decreasing(up to N^0 - constant integral dose equal to the value ED50 of single pulse) for high repetition rate and slow cooling.

The analysis of the data obtained in the experiment revealed that there was no dependence of ED50 parameter upon laser spot cross section within the range of available radiant exposure. This fact could be predicted from the consideration proposed above. Since we consider skin damage to be thermal, the local temperature could be a measure of the damage. Local temperature rise is determined by $\Delta T = E_l/(Shc_p)$, and the rate of cooling is determined by $l_t = (\chi\ \tau_l)^{1/2}$ and dimensions of the experiment. In the framework of our consideration we can assume an increase of heated up volume (dV) due to thermal conductivity and thus decrease of local temperature as the first order approximation.

$$dV = d(Sh) = Sdh + hdS = Shdh/h + 2Shdr/r = V(l_t/h + 2l_t/r)$$

For free running pulses τ=2.5 ms $l_t (\sim 0.02\ mm) << h,r (\sim 1\ mm)$. Thus the absence of dependence of ED50 upon cross section seems rather reasonable. According this estimations one can clearly observe this dependence when r < 0.2 mm.

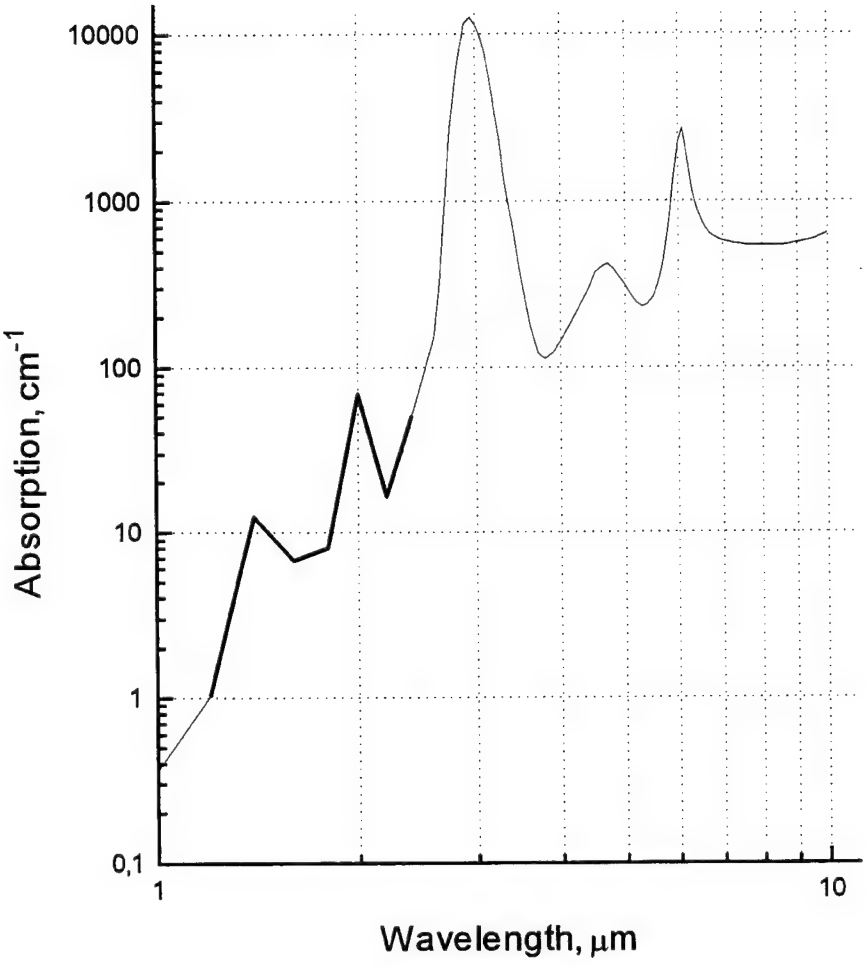

Fig.4. Absorption coefficient of liquid water in the 1-10 μm band[8]. The range where reaction of skin to laser radiation could be predicted based upon results of this work is marked in bold.

5. CONCLUSIONS

In this study we experimentally determined reaction of porcine skin(*in vivo)* to exposure by 1540 nm radiation of Er-glass laser. The ED50 value for minimal lesion was found to be 5.7 J/cm^2 for millisecond and 3.0 J/cm^2 for nanosecond laser pulses.

For multipulse action dependence of ED50 of minimal lesion vs. number of pulses was determined for repetition rate of the laser pulses 0.1 Hz. The dependence of overall dose is proportional to $N^{0.58}$ for free running and $N^{0.82}$ for Q-switch. It was found that there was minimal exposure dose of single pulse which does not produce lesion in multipulse action. It was 0.8 J/cm^2 for free running and 1.1 J/cm^2 for Q-switching. No dependence of ED50 vs. laser beam spotsize was found for beam diameter 2-10 mm.

We believe that data obtained in this work are adequate to update safety standards for cutaneous injury by 1540 nm laser radiation. Additional research of histology of the persistent lesions would be very helpful for more accurate classification of burns and could be used for possible applications of 1540 nm radiation for surface skin operations(cosmetic surgery).

6. ACKNOWLEDGMENT

This work was supported under USAF Contract F61708-94-C-0008 arranged via European Office of Aerospace Research and Development(EOARD). The fulfillment of this work could not be achieved without interest and fruitful discussions with Dr.Mark Rogers(AL,USAF) and David Lund(USAMRD). We also highly appreciate the organizing efforts of Patric Bradshaw (EOARD).

7. REFERENCES

1. Avdeev P.S., Berezin Yu.D., Gudakovskii Yu.P., Muratov V.R., Murzin A.G., Fromzel' V.A. Exprimental determination of maximum permissible exposure to laser radiation of 1.54 μm wavelength, Sov.J.Quantum Electron 8(1),1978:137-139.

2. Lund D.J., Landers M. B., Bresnick G.H., Powell J.O., Chester J.E., Carver C., Ocular hazards of the Q-switched erbium laser, Investigative Ophtalm., 463-470,1970.

3. A. V.Lukashev, V.P.Solovyev, B. I.Denker Morphological and histological changes on skin induced by 1540 nm laser radiation., Proc.SPIE v.2974, paper #2974-07.

4. Litchefield J.T., Wilcoxon F., A simplified method of Evaluting Dose-Effect Experiments. J.Pharmacol.Exp.Ther. 96(2):99,1949.

5. Stuck B.E., Lund D.J., Beatrice E.S. Occular effects of Holmium(2.06 μm) and Erbium (1.54 μm)laser radiation. Health Physics 40(6): 835-846, 1981.

6. Brownell A. S., Parr W. H., Hysell D. K., Dedrick R. S., CO_2 Laser induced skin lesions, Rep. 769, Research in Biomedical Sciences, DA Project No. 3A014501B71R USAML, Fort Knox, Kentucky 40121,1968.

7. Brownell A. S., Parr W. H., Hysell D. K., Skin and Carbon Dioxide Laser Radiation Arch. Environ.Health 18 :437-440, 1969

8. Zolotarev V.M., Morozov V.N., Smirnov E.V. Optical constants of natural and technical substances, Handbook, Ed."Chemistry", Leningrad,1984.

9. Sliney D.N., Wolbarsht M.L. Safety with Lasers and other Optical sources, NY, Plenum Press,1980.

10. Brownell A. S., Stuck B.E. Occular and skin hazards from CO_2 laser radiation, Joint AMRDC-AMC Laser safety team, Frankford Arsenal,Philadelphia, PI

SESSION 5

Treatment and Prevention

Treatment of laser-induced retinal injuries by neuroprotection.

Yoram Solberg, Mordechai Rosner and M ichaelBelkin
The Goldschleger Eye Research Institute, Sheba Medical Center,
Tel-Aviv University, Israel.

ABSTRACT

Retinal laser photocoagulation treatments are often complicated with immediate side-effect of visual impairment. To determine whether glutamate-receptor blockers can serve as adjuvant neuroprotective therapy, we examined the effects of MK-801, an NMDA-receptor antagonist, on laser-induced retinal injury in a rat model. Argon laser retinal lesions were created in the retina of 36 DA rats. Treatment with intraperitoneal injections of MK-801 or saline was started immediately after the laser photocoagulation. The animals were sacrificed after 3, 20 or 60 days and the retinal lesions were evaluated histologically and morphometrically. Photoreceptor-cell loss was significantly smaller in MK-801-treated rats than controls. The proliferative membrane composed of retinal pigment epithelial cells which was seen at the base of the lesion in control retinas, was smaller in the MK-801-treated retinas. MK-801 exhibited neuroprotective and anti-proliferative properties in the retina. Glutamate-receptor blockers should be further investigated for serving as adjuvant therapy to retinal photocoagulation treatments.

KEY WORDS: Glutamate, Laser photocoagulation, MK-801, NMDA, Retina

1. INTRODUCTION

Lasers, which assumed increasing use in the research, industry and military fields, account for growing numbers of occupational eye accidents[5,8]. These ocular injuries which mainly involve the posterior segment of the eye, lead to retinal destruction with large-scale photoreceptor loss and severe visual impairment. Similar visual impairments are often observed when therapeutical retinal laser photocoagulation treatments are considered.

Ophthalmic laser treatments is the standard therapy for many sight-impairing retinal disorders. Diseases that previously resulted in rapid sight deterioration and blindness, are now being treated with laser photocoagulation.

SPIE Vol. 2974 • 0277-786X/97/$10.00

Among these disorders is age-related macular degeneration (AMD), the leading cause of new legal blindness in developed countries.

AMD affects the macula inducing pathological changes in the outer retinal layers. In the advanced stage of the disease, choroidal neovascular elements (CNV) invades the subretinal space, ultimately resulting in the formation of a fibrovascular membrane. The retina over the membrane degenerates and gradually losses its photoreceptor-cells. This eventually leads to severe visual impairment.

The efficacy of argon laser photocoagulation treatment for juxta-foveal CNV in patients suffering from sight-impending AMD has been demonstrated by the Macular Photocoagulation Study[6]: the laser photocoagulation treatments effectively delayed or prevented the deterioration of different visual parameters. However, immediately after the treatment 18% of the eyes exhibited *severe* visual loss. This side-effect is a result of the dynamic laser-induced lesion expansion which involve the destruction of the neurosensory retinal tissue located in the fovea just next to the treated CNV. A presumed neuroprotective therapy which is aimed to save the neurosensory retina from the injurious effects of the laser irradiation, while not impairing its efficacy in destroying the CNV, will protect the patients visual ability and enhance their benefits from the treatment. Glutamate-receptors blockers are promising candidates for such a neuroprotective role.

Glutamate is the major excitatory neurotransmitter in the central nervous system (CNS). It is now well established that glutamate plays a crucial role in mediating neuronal damage in CNS injury[1]. After CNS insult the damaged neurons release large amounts of glutamate, which in turn, by activating its N-methyl-D-aspartate (NMDA) receptor, causes damage to the surrounding neurons by changing their intracellular ionic concentrations. The biochemical cascade that originates in the injured neurons amplifies the initial trauma and eventually causes the damage to spread to the adjacent neuronal tissues[2,3]. It is well documented that NMDA-receptor antagonists (like MK-801) act as neuroprotective agents in a variety of CNS lesions, both ischemic and traumatic[3].

Glutamate, being the main neurotransmitter of the photoreceptor neurons, plays an important role in the normal functioning of the retina and might be involved in the pathogenesis of laser-induced retinal damage and other retinal disorders[4]. This latter possibility is indicated by the vulnerability of retinal neurons to glutamate and NMDA, and by the neuroprotective effect of MK-801 in different retinal injuries. If the pathogenic mechanisms of the spread of neuronal death

following retinal laser injury are indeed mediated, at least partially, by glutamate, it might be expected to be attenuated as a result of the treatment by NMDA antagonists.

In order to test this hypothesis we examined the neuroprotective property of MK-801, a potent non-competitive NMDA-receptor blocker. The drug was evaluated in a pigmented rat model of retinal lesion induced by argon laser irradiation.

2. METHODS

Thirty six inbred pigmented DA rats, 90 days old, were used. This strain has a uniform pigmentation of the posterior segment of the eye, making it particularly useful for retinal laser injury research. The experiments conformed to the ARVO statement for the Use of Animals in Ophthalmic and Vision Research.

The animals were anesthetized by intraperitoneal injections of ketamine (40 mg/kg) and xylasine (8 mg/kg). Six argon laser (Emerald Crystal Focus, U.S.A.) lesions (514 nm, 200 μm, 0.1 W, 0.05 sec), were produced in each eye, two disc diameters from the optic disc. The experimental group (N=18 rats) received intraperitoneal injections of MK-801 (Research Biochemical International, Natick, USA) in normal saline, at a dose of 2 mg/kg, immediately after the laser irradiation. A vehicle-treated control group (N=18 rats) received same volume of saline at the same timing.

The rats were sacrificed 3, 20 or 60 days after laser irradiation (N=6 rats in the treated and in the control groups at each time point) and their eyes were enucleated, sectioned and examined by light microscopy for histopathological changes. To further evaluate the neuroprotective effect of MK-801 in the retinal lesions, a masked-fashioned quantitative morphometric assessment was carried out using a computer-assisted image analysis system (ScanArray3, Galai productions, Migdal-HaEmek, Israel). Two morphometric measurements were performed on each lesion in order to evaluate the severity of the argon laser injuries. The first measured the diameter of the lesion, and the second evaluated the extent of photoreceptor-cell loss.

As the results indicated a neuroprotective and a RPE anti-proliferative effects of the MK-801 treatment, the drug was further tested with a higher dose (3 mg/kg intraperitoneally immediately and 8 hours after the laser irradiation). The lesions in the treated and in the control groups (N=3 for each time point) were processed as described above.

A two-tailed unpaired T-test was used to analyze the significance of differences between the results of the MK-801-treated and the control groups at each time point.

3. RESULTS

Light microscopy revealed histopathological differences between saline controls and the MK-801-treated animals. Three days after laser irradiation, the lesions of the control group showed the following local histopathological changes of the outer retina and of the choroid: at the central area of the lesion there was loss of choriocapillaries and disruption of Bruch's membrane. The RPE showed local proliferation with formation of a fusiform membrane containing macrophagic cells. The outer and inner segments of the photoreceptors were deformed and disrupted and the ONL showed loss of nuclei and the presence of pyknotic nuclei at the periphery of the lesion. The photoreceptor segments and the ONL tapered off toward the center of the lesion, where they were always completely absent. This central area was filled with cellular debris and pigment-laden macrophages. The outer plexiform layer was disrupted, the inner nuclear layer was mildly edematous. The inner plexiform, the ganglion cell layer and the nerve fiber layer were unremarkable.

In MK-801-treated group the retinal response was milder than in the controls. Three days after laser irradiation, the RPE at the base of the lesion showed mild proliferation. Only few macrophages were seen in the area of the disrupted segments and the sub-retinal membranes were less developed. The ONL showed loss of nuclei and the presence of pyknotic nuclei. Mild cystic changes were seen in the inner nuclear layer and the inner plexiform layer, while the ganglion cell layer and the nerve fiber layer were unremarkable.

By 20 days after irradiation, the proliferative membranes in the lesions of the saline-injected rats became multilayered and showed occasional neovascularization. The RPE layer had reformed and was lying on the sub-retinal membrane. The inner nuclear layer was still edematous, and the nerve fiber layer and the inner limiting membrane were folded internally, creating a small internal bulging at the inner retinal surface over the area of the lesion. These bulgings are supposed to be the result of the edema of the inner retinal layers and the traction of the normal retinal layers at the edge of the lesion toward its center. In contrast, the RPE proliferating membranes in the MK-801 treated animals were smaller and less developed with only occasional neovascular blood-vessels. The internal

bulgings seen in the MK-801-treated lesions were similar to those in the controls.

In control retinas, 60 days after irradiation, the sub-retinal membrane had diminished in size, became more fibrotic and contained numerous small blood vessels. The outer and inner segments of the photoreceptors were disrupted only at the central area of the lesion and regenerated at its periphery. Occasional pigment-laden macrophages were seen in the central area at the level of the segments and the ONL. The ONL showed fewer pyknotic nuclei. The internal bulging had not changed its shape as compared to the 20 days old lesions. In the MK-801-treated lesions, the morphological appearance 60 days after laser irradiation resembled that of their control counterparts. However, in the MK-801-treated lesions, the proliferative membranes were still small and undeveloped, and the ONL showed less damage.

In order to further define the effects of MK-801 treatment on laser-induced retinal lesions, a second stage of the study was performed where the drug was delivered twice in a higher concentration (3mg/kg, I.P.).

Three days after laser irradiation, the histologic appearance of the lesions in rats treated by MK-801 delivered twice with a high concentration of 3 mg/kg, resembled their counterparts that received only one dose of 2mg/kg. The only difference detected was the complete absence of the RPE proliferative membrane in any of the lesions. By 20 days after irradiation, again both the control and the treated animals resembled their counterparts in the 2mg/kg stage of the experiment. While the RPE proliferative reaction in the control lesions was organized as a thick multilayered fusiform membrane, only a thin proliferative membrane was seen in part (40%) of the MK-801 treated rats. The same phenomena was observed at 60 days after irradiation where proliferative membranes were absent in most of the treated lesions and when existed were small and undeveloped.

Morphometric measurements of the laser-induced retinal lesions also revealed significant differences between treated and control groups. The mean diameter of the control lesions decreased during the first 20 days after the injury, though not in a significant manner. It also did not change significantly thereafter. The ratio between the numbers of surviving ONL nuclei at the lesioned area and the adjacent normal retina became progressively higher over time in the control lesions. This probably happened as a result of the traction of normal retinal layers at the edge of the lesion toward its center, mainly during the first 20 days ($Pv<0.0001$). Three days after laser irradiation, the mean diameters of the lesions

in the treated and control groups did not differ. However, at 20 and 60 days, the MK-801-treated lesions became significantly smaller than their control counterparts ($P_v<0.001$ and $P_v=0.01$, respectively). Differences in the ratio of surviving photoreceptor cells between MK-801-treated and control lesions were also significant: while at 3 and 20 days after the irradiation, the treated and control lesions had similar ratios of surviving ONL nuclei, at 60 days lesions the ratio of surviving photoreceptor cells was higher in the treated group (by 17.2%; $P_v<0.01$).

4. DISCUSSION

The results of this study indicate that MK-801, a NMDA-receptor blocker, exhibits neuroprotective and anti-proliferative properties in retinal laser lesions. Significant numbers of photoreceptor-cells were salvaged from the laser destruction as shown by the fact that the treated lesions were smaller in diameter than control lesions and that the ratio of surviving ONL nuclei at the area of the lesion was higher (at 60 days). The drug also attenuated the proliferative reaction of the RPE, as indicated by the small size of the sub-retinal membranes in the MK-801-treated retinas. When MK-801 was administered at a higher dose, it failed to rescue more photoreceptor-cells but it did enhanced its anti-proliferative effect on the RPE cells: the membranes were absent in all of the MK-801-treated lesions at 3 days after irradiation and the membranes that eventually did evolved in some of the lesions were small and undeveloped.

Although laser injury to retinal neurons has generally been considered an irreversible phenomenon that cannot be halted or slowed down, new insights into the pathological mechanisms involved in this process have provided a theoretical basis for evaluating various pharmacological strategies to induce neuroprotection.

Most of the available information on neuroprotection come from studies of the CNS following traumatic or ischemic injury. It seems likely that the retina, which is part of the CNS, is also susceptible to these harmful processes and might respond to drugs shown to have neuroprotective properties in the CNS.

Among the most intensively studied pharmacological agents for reducing neurotoxicity during CNS damage are glutamate receptor antagonists. Exposure of neurons to high concentration of extracellular glutamate lead to their death. It is now well established that after CNS injury the damaged neurons release massive amounts of glutamate which interacts with adjacent cells and eventually destroys them. The development of selective NMDA-receptor antagonists has facilitated examination of the role of glutamate in various CNS disorders and demonstrated their neuroprotective properties in these pathological situations.

The neurocytotoxic effect of glutamate, which is mediated through activation of its NMDA receptors, was also demonstrated in the retina both *in-vivo* and *in-vitro*, and the neuroprotective effect of the NMDA blockers was evident in retinal ganglion cells which were involved in the injury. Our study, on the other hand, demonstrated MK-801 neuroprotective effect on photoreceptor-cells. This finding is somehow surprising due to the fact that under normal circumstances photoreceptor-cells do not express NMDA receptors. However, photoreceptor-cells might express NMDA receptors as a result of their exposure to high extracellular levels of glutamate. This phenomena was demonstrated before in the CNS where NMDA receptors were induced in cerebellar granule cells which were exposed to high levels of NMDA. MK-801 might also exert its neuroprotective effect by enhancing the release of growth factors which by themselves promote the survival of the photoreceptor-cells. MK-801 is also known to enhance neuronal survival in an independent manner of its anti-NMDA activity. Nevertheless, the exact mechanisms by which MK-801 exerts its neuroprotective effect on photoreceptor-cell survival is still to be elucidated.

Our study also points to a less recognized property of MK-801, namely its anti-proliferative effect on RPE cells. Treatment with MK-801 (3 mg/kg) blocked the formation of the RPE membranes at 3 days after the insult. Subsequently, at 20 and 60 days after laser-exposure, the membranes did developed, but were seen in only 40% of the treated retinas, and were smaller than in the control retinas. The development of smaller membranes in the treated animals might simply reflect the milder destruction of their external retinal layers by the laser irradiation: the smaller the lesion, the modest the proliferative reaction to it. The anti-proliferative property of MK-801 might be expected from the role of glutamate in RPE metabolism, where *in-vitro* it enhances RPE cell proliferation[7] and the cells' phagocytotic activity, both effects are mediated via a NMDA-receptor-coupled mechanism. Blocking these effects with MK-801 probably resulted in the underdevelopment of the sub-retinal proliferative membranes. However, it is yet to be determined whether this anti-proliferative effect has any clinical implications in different retinal disorders.

On the basis of our results, we suggest that glutamate plays a key role in mediating retinal injury induced by laser irradiation. Antagonism of the glutamate-induced effects at its NMDA receptor significantly improves the outcome of the laser-induced retinal damage. Further studies of glutamate receptor blockers are warranted in order to evaluate their therapeutic potential as accepted therapy for retinal laser injury, both accidental and iatrogenic.

5. REFERENCES

1 Choi DW. Glutamate neurotoxicity and diseases of the nervous system. *Neuron*. 1988;1:623-634.

2 Choi DW. The role of glutamate neurotoxicity in hypoxic-ischemic neuronal death. *Annu Rev Neurosci.* 1990;13:171-182.

3 Danysz W, Parsons CG, Bresink I, Quack G. Glutamate in CNS disorders. *Drug News Presp.* 1995;8:261-273.

4 Kalloniatis M. Amino acids in neurotransmission and disease. *J. Am. Optom. Assoc.* 1995;66:751-757.

5 Stuck BE, Zwick H, Molchany JW, Lund DJ. Accidental human laser retinal injuries from military laser systems. *S.P.I.E.* 1996;2674:7-20.

6 The Macular Photocoagulation Study Group. Krypton laser photocoagulation for neovascular lesions of age-related macular degeneration: Results of a randomized clinical trial. *Arc.h Ophthalmol.* 1990;108:816-824.

7 Uchida N, Kiuchi Y, Yamade M, et al. Glutamate-stimulated proliferation of rat retinal pigment epithelium through NMDA receptor activation and bFGF expression. ARVO Abstracts. *Invest. Ophthalmol. Vis. Sci.* 1996;37:S388.

8 Wolbarsht ML. Permanent blindness from laser exposure in laboratory and industrial accidents. *S.P.I.E.* 1996;2674:21-24.

The effects of methylprednisolone on laser induced retinal injuries

Mordechai Rosner, Marina Tchirkov, Galina Dubinski,
Yoram Solberg and Michael belkin

Goldschleger Eye Research Institute, Tel-Aviv University,
Sheba Medical Center, Tel-Hashomer 52621, Israel

ABSTRACT

Methylprednisolone have been demonstrated to ameliorate retinal photic injury. In the current study we examined its effect on laser induced retinal injury.

Retinal lesions were inflicted by argon laser (0.05 W, 0.1 sec, 200 micrometer) in 36 pigmented DA rats. The treated groups received intra-peritoneally methylprednisolone (160 mg/kg) in saline, injected 3 times a day for 2 days, starting immediately after exposure. The controls received the vehicle on the same schedule. The rats were
sacrificed 3, 20 or 60 days after laser exposure and the lesions were evaluated by light microscopy and morphometric measurements.

Laser injuries were associated with disruption of the outer retinal layers. Three and 20 days after exposure, the loss of the photoreceptor-cell nuclei was significantly milder in the treated groups as compared with controls (39.1 Vs 55.3 % loss, treated and control respectively, 20 days after exposure p=0.00008). There was no difference
60 days after exposure.

In conclusion, methylprednisolone reduced temporarily the photoreceptor cell loss in argon laser induced retinal injury, when treatment was started immediately after laser exposure. There was no long term effect.

Keywords: laser injury, retina, photoreceptors, corticosteroids, methylprednisolone,

2. INTRODUCTION

Although laser induced retinal injury causes visual impairment,1-5 there is no accepted medical therapy for reducing retinal cell death and disruption of architecture following exposure.

An insult to the central nervous system, which the retina is part of, results in excessive release of neurotransmitters such as glutamate, by the damaged neurones. These affect the ionic equilibrium and cause intracellular calcium overload. The calcium overload causes cellular swelling and activation of enzymes that initiate free radical formation.6-9 As a result, cell membranes are damaged and delayed cell□79, death occurs at and around the original injury site. Such a biochemical cascade may enlarge the original damage in the retina resulted from laser exposure or other traumatic or ischemic causes.

Methylprednisolone (MP) has an anti-inflammatory effect, it is cell membrane stabilizer, and in high doses it has an anti-lipid peroxidation effect. We have shown that high dose MP treatment ameliorated light induced injury to the retina in rats.10-11 Corticosteroids are the only□RV, drug being used to treat patients who have retinal njury from accidental ocular exposure to laser radiation, but there have been no systematic studies of the effectiveness of this treatment.

The goal of this study was to examine the effect of treatment with MP on retinal lesions induced by argon laser.

3. MATERIALS AND METHODS

3.1. Animals

Inbred DA pigmented rats (Strain DA\OLa\Hsd, Harlan OLAC LTD. Blackthorn Bicester Oxon. England), that were grown in Tel-Aviv University Animal House, at the age of 60 days, were used as control and treated groups for evaluation of the effect of MP on laser induced retinal lesions. All procedures involving animals

SPIE Vol. 2974 • 0277-786X/97/$10.00

were performed according to the guidelines of the Association for Research in Vision and Ophthalmology Resolution on the Use of Animals in Research.

After anesthetia by ketamin 40 mg/kg and xylasine 8 mg/kg injected intra-peritoneally, the pupils of the rats were dilated by topical Topicamide 0.5% sterile drops (Mydramid, Fischer). A contact lens that has been specially crafted to fit the rat eye was placed on the cornea (using hydroxypropyl methylcelulose 2.5% for contact between the lens and the cornea) to allow better focusing the laser beam on the retina. Retinal lesions were then inflicted by the argon laser.

The rats were treated by MP or by the vehicle as control, and sacrificed with an overdose of pentobarbital sodium 3 days, 20 days and 60 days after the laser exposure. The eyes were submitted for histologic evaluation.

Seventy two eyes of 36 rats were used for the evaluation of the effect of MP on argon laser induced retinal injury. Six rats were used for the study group and 6 rats served as vehicle control group for each of the 3 time points evaluated.

3.2. Laser lesions

Retinal lesions were inflicted using argon laser (Lasertek, Spectra Physics). Six laser lesions were inflicted in each eye, one to two disc diameters from the disc. The settings of the argon laser used were 514 nanometer, 200 micrometers, 0.05 Watts, and 0.1 seconds.

3.3. Methylprednisolone treatment

The MP treatment included intra-peritoneal injections of methylprednisolone sodium succinate (Upjohn) in normal saline, at a dose of 160 mg/kg every 8 hours for 2 days, starting immediately after the laser injury. The control groups received the same volume of vehicle injections at the same timing.

3.4. Histological and morphological evaluation

Histologic changes in control and treated rats which were subjected to retinal laser injury were studied by light microscopy and by morphometric measurements of the retinal lesion. For the histological study, the enucleated eyes were fixed in 1% glutaraldehyde. The posterior segments of the eyes were then dissected, using a surgical microscope, into retinal specimens, each including one retinal laser lesion. The samples were embedded in plastic. The blocks were sectioned serially and stained by toluidine-blue. Sections from the center of the lesions, that included the longest lesion diameter, were picked for histopathologic and morphometric evaluation. The morphometric assessment of the lesions were carried out using an image processing system that included a digitizing pad (Summagraphics, Seymour, CT, USA), a personal computer and suitable custom-made software. A handle with a 45 degree tilted mirror was built to fit the projection microscope. This allowed the projection of pictures of stained retinal sections onto the digitizing pad. Various morphometric measurements were done in order to evaluate the effect of treatment. The borders of the lesions were determined and their diameter was measured. Then, the loss of thickness of the ONL at the area of the lesion as compared with the normal ONL thickness at the normal retina near the lesion was calculated. The area with total loss of ONL at the center of the lesions was also evaluated.

3.5. Statistical evaluation

For statistical evaluation, the calculated mean of measurements of the lesions from both eyes of each animal was the result for that animal. T-test was used to analyze the significance of the differences between the morphometric results of the treated and the vehicle control groups at each time point.

4. RESULTS

4.1. Histologic evaluation of the retinal lesion induced by argon laser

The argon laser retinal lesions seen 3 days after exposure were characterized by disruption of the retinal pigment epithelium, formation of a proliferative plaque and invasion of pigment epithelial cells into the retina. The photoreceptor segments were disrupted and the ONL was tapered toward the center of the lesion, where it was totally lost. The inner retinal layers were intact and edematous in the more severe lesions only. The nerve fiber layer and the inner limiting membrane were folded internally towards the vitreous. By 20 and 60 days after exposure, the pigment epithelial plaque diminished in size.

The lesions of the treated groups and the vehicle-treated groups were similar.

4.2. Morphometric evaluation of the laser induced retinal lesions

The morphometric measurements demonstrated no significant difference between the diameter of the lesions of the control and treated groups at 3, 20 or 60 days after exposure (table 1). However, the area of total ONL loss at the center of the lesion (table 2) was smaller and the loss of ONL thickness at the lesion was significantly milder in the treated group as compared with controls (39.1 Vs 55.3 %, treated and control respectively, 20 days following exposure, p=0.00008 table 3). This difference was not seen at 60 days after exposure.

5. DISCUSSION

As MP was reported to ameliorate non-coherent light induced retinal injury in rats and laser injuries in monkeys,10-12 we evaluated, in the current research, its effect on argon laser induced retinal injuries in pigmented rats. As expected, an ameliorative effect was demonstrated with a high dose MP when started immediately after laser exposure. However, argon laser induced retinal lesions that were evaluated 60 days after laser exposed demonstrated that this effect was only of a short duration.

In conclusion, we found that methylprednisolone reduced photoreceptor cell loss in argon laser induced retinal injury, when treatment is started immediately after laser exposure. However, more research is needed to explain the meaning of the temporary effect seen, and to find out the regime that induce maximal ameliorative effect.

6. ACKNOWLEDGMENT

This study was supported by the U.S.-Israel Binational Science Foundation 91-00225.

Table 1. Effect of MP treatment on the diameter of the retinal lesion induced by argon laser

Time after laser injury (days)	Diameter of retinal lesion (micrometer, mean ± SD)		p (t-test)
	Vehicle treated	MP treated	
3	388.1 ± 34.4	386.7 ± 57.4	0.66
20	345.8 ± 34.1	358.4 ± 30.4	0.26
60	340.1 ± 26.0	346.5 ± 26.4	0.86

Table 2. Effect of MP treatment on the total loss of ONL at the center of the retinal injury induced by argon laser

Time after laser injury (days)	Total loss of ONL at the center of the lesion (micrometer, mean ± SD)		p (t-test)
	Vehicle treated	MP treated	
3	94.6 ± 22.6	89.0 ± 19.0	0.70
20	30.9 ± 10.0	14.5 ± 8.5	0.01
60	22.6 ± 17.2	39.6 ± 12.2	0.12

Table 3. Effect of MP treatment on the loss of ONL thickness at the area of the retinal injury induced by argon laser

Time after laser injury (days)	Loss of ONL thickness at the lesion (% , mean ± SD)		p (t-test)
	Vehicle treated	MP treated	
3	59.4 ± 5.8	50.2 ± 4.9	0.027
20	55.3 ± 1.9	39.1 ± 4.3	0.00008
60	50.1 ± 2.2	48.7 ± 2.3	0.39

7. REFERENCE

1. V. P. Gabel, R. Birngruber, B. Lorenz, G. K. Lang. "Clinical observations of six cases of laser injury to the eye," Health Physics Vol. 56, pp. 705-710, 1989.
2. L. Haifeng, G. Guanghuang, W. Dechang, et al. "Ocular injuries from accidental laser exposures," Health Physics Vol. 56, pp. 711-716, 1989.
3. E. E. Bpoldrey, H. L. Little, M. Flocks, A. Vassiliades. "Retinal injury due to industrial laser burns," Ophthalmology Vol. 88, pp. 101-107, 1981.
4. A. I. Friedmann. "A natural clinical history of a severe accidental retinal laser burn at the posterior pole of the eye," Doc Ophthalmol Vol. 68, pp. 395-400, 1988.
5. J. Mellerio, J. Marshall, B. Tengroth, et al. "Battlefield laser weapons: an assessment of systems, hazards, injuries and ophthalmic resources required for treatment," Laser Light Ophthalmol Vol 4, pp. 41-67, 1991.
6. D. W. Choi. "Cerebral hypoxia: some new approaches and unanswered questions,
" J Neurosci Vol. 10, pp. 2493-2501, 1990.
7. B. K. Siesio. "Mechanisms of ischemic brain damage," Crit Care Med Vol. 16, pp. 954-963, 1988.
8. A. I. Faden. "Pharmacotherapy in spinal cord injury: a critical review of recent development," Clin Neuropharmacol Vol. 10, pp. 193-204, 1987.
9. B. Meldrum, M. Evanse, T. Griffiths, R. Simon. "Ischemic brain damage: the role of excitatory activity and calcium entry," Br J Anaesth Vol. 57, pp. 44-46, 1985.
10. M. Rosner, T. T. Lam, J. Fu, M. O. M. Tso. "Methylprednisolone ameliorates retinal photic injury in rats," Arch Ophthalmol Vol. 110, pp. 857-861, 1992.
11. M. Rosner, T. T. Lam, M. O. M. Tso. "Therapeutic parameters of methylprednisolone treatment for retinal photic injury in a rat model," Res Com Chem Pat Pharmacol Vol. 77, pp. 299-311, 1992.
12. T. Lam, K. Takahashi, J. Fu, M. O. M. Tso. "Methylprednisolone therapy in laser injury of the retina," Graefe's Arch Clin Exp Ophthalmol Vol. 231, pp. 729-736, 1993.

Current therapy for laser-induced retinal injury: overview of clinical and experimental approaches

Steven T. Schuschereba and *David K. Scales

Walter Reed Army Institute of Research, U.S. Army Medical Research Detachment, Brooks Air Force Base, San Antonio, TX; *Wilford Hall Medical Center, Lackland Air Force Base, San Antonio, TX.

ABSTRACT

Adequate treatment strategies do not exist for retinal laser injuries. To gain a better understanding of available treatments, data from a variety of human laser accident cases and relevant experimental work was evaluated. Most laser eye injury cases are not attended by an ophthalmologist for several hours to days after injury and most patients are not treated. Of the few cases receiving treatment; only the FDA approved glucocorticoids are available for use. Their use, however, is still controversial. Experimental animal work during the acute phase of injury indicates that productive efforts have targeted neuroprotection, inflammation (PMNs), ischemia-reperfusion, and lipid peroxidation. Late stage issues for treatment are scarring, retinal hole persistence and expansion, and traction. In summary, treatments for acute and late phase injury are currently inadequate. Preserving existing neural elements should be the top priority in these injuries. We reccomend that relevant treatments begin immediately after injury. Other approaches are necessary to target early and late phase secondary damage events that are entrenched.

Keywords: Laser, retina, macula, injury, neutrophils, edema, macular hole, vitreous hemorrhage, scarring, treatment

1. INTRODUCTION

The proliferation and use of lasers in a wide variety of applications has increased the number of cases of accidental exposure of the retina.[1-22] With further use of laser systems, even greater frequencies of laser-induced retinal injury (LIRI) can be expected. Of the areas within the retina, the fovea is the region of greatest concern because of its importance to central vision. The degree of vision impairment is directly related to the wavelength and the amount of laser energy absorbed within the retina. The extent and nature of the injury is determined by a variety of laser and ocular factors which have been reviewed by Marshall[23] and Mellerio et al.[24]

An emerging problem with repetitively pulsed lasers, is that multiple foci of injury can occur before the eye is averted.[11,22] Previously reported multiple laser exposure injuries of the human retina have resulted in a poor visual prognosis with increasing time after laser injury.[11,17,22] Foveal and near-foveal injuries are the most typical for human laser accidental exposures since the laser beam is more directly engaged by human observers to coincide with direct or near-direct exposure of the fovea. An additional aspect of multiple injuries within the retina is the idea that adjacent injuries involve previously uninjured retina, thus expanding the area of damage.[11,25] Also, since many laser systems are now being used outdoors, the laser beam diameter at extended distances relative to the observer presents special problems. Specifically, if a large beam diameter is appropriately aligned and observed, or if binocular optics are utilized to observe and focus the laser beam energy; bi-lateral injuries can occur.[22]

Rockwell extensively reviewed the literature regarding accidental laser exposures and showed that out of 272 cases, 199 involved the eye and 180 of these cases resulted in permanent changes in

vision.[17] Wolbarsht[26] indicated that the total number of injuries is under represented in the literature because most non-military laser injuries are not reported due to litigation proceedings. Most of the accident case studies show that the Nd:YAG laser is responsible for most of the injuries.[17,22] The trend for overall injury is increasing from 9.6/yr in the previous decade to 14.3 injuries/yr for the last decade ending in 1993.[17]

Location within the retina is perhaps the single most important factor in assessing the severity of injury. Lesions directly in the fovea and in the central retina would be considered most detrimental with the degree of severity falling off as a function of distance from the macula. Also, significant injuries in the papillomacular arcade (zone between the macula and optic nerve) would be considered serious, as nerve fibers coursing toward the optic nerve in this area are usually damaged after moderate to severe LIRI.[27] Injuries in peripheral areas of the retina would be considered less serious.

Retinal responses to LIRI can be classified into three main stages of temporal development: (1) primary damage, which occurs at the moment of injury and involves irreversible photo-mechanical, photo-ionization, photocoagulative, and hemorrhagic damage (this includes the immediate and untreatable damage caused by heat-fixation, photo-mechanical disruption or photoionization processes). Primary damage also involves mechanical shearing, arising from hemorrhage forces, and damage from the superheated gas bubble emerging from the injury site and exiting at the retinal surface; (2) secondary damage, which is produced by complicating processes initiated at the moment of injury. These changes appear rapidly by histology, but may not present clinically for a period of hours to days after injury. Some of these responses include damage related to edema, ischemia/reperfusion, inflammation, and lipid peroxidation; and (3) tertiary or remodeling damage, which occurs weeks to years after injury and involves scar formation and contraction and retinal hole expansion leading to retinal detachments and further loss of vision.

From the treatment perspective, the responses of the retina to LIRI can be divided into two general stages; early and late stage events. Early stage events are referred to as those that can be controlled to prevent permanent and irreversible damage to both normal and initially damaged but viable neural elements. The onset and severity of early stage events are, therefore, critical to neural element survival and outcome of repair. On a time scale, early stage injury may evolve from 0 to 24 h after the injury and is dependent on the extent and severity of injury. Some of the early stage events that are potentially reversible/preventable are: inflammation, ischemia-reperfusion, free radical production, and lipid peroxidation; all of which secondarily destroy neural elements, expand lesion sizes, promote scarring, and complicate visual function recovery. Fundscopic and histologic examples of early stage injury include primary damage such as hemorhaging and secondary damage such as acute inflammation (Figure 1).

Later stage events such as scarring, which can involve vitreo-retinal, chorio-retinal or combinations of these interactions can produce traction, epiretinal membranes, detachments, and permanent defects in the blood-retinal barrier with compromise of vitreo-retinal immune privilege.[28] Excessive scar contraction can also result in retinal detachment, hole formation, and hole enlargement. Late stage events may begin as early as 1-3 h and continue up to months or years after the injury, involving regions and neural elements that were previously uninjured or uninvolved. Late stage damage can also occur via secondary injury processes. Loss of neural elements, especially photoreceptors, results in both lost function and reduced adhesion of the retina to the retinal pigment epithelium, which in turn increases the risk of retinal detachments. Excessive late stage complications, therefore, can ultimately result in total vision loss and possibly loss of the eye. Two general fundus pathology outcomes can occur from early stage severe lesions, when observed over an extended period of time after LIRI in humans; (1) retinal hole development; and (2) extensive scarring and traction (Figure 2). Both entities have been associated with epiretinal membrane (ERM) formation and poor visual prognosis.[9] It is reasonable to speculate that some late stage complications may be prevented by appropriate treatments if administered during the early stage of injury.

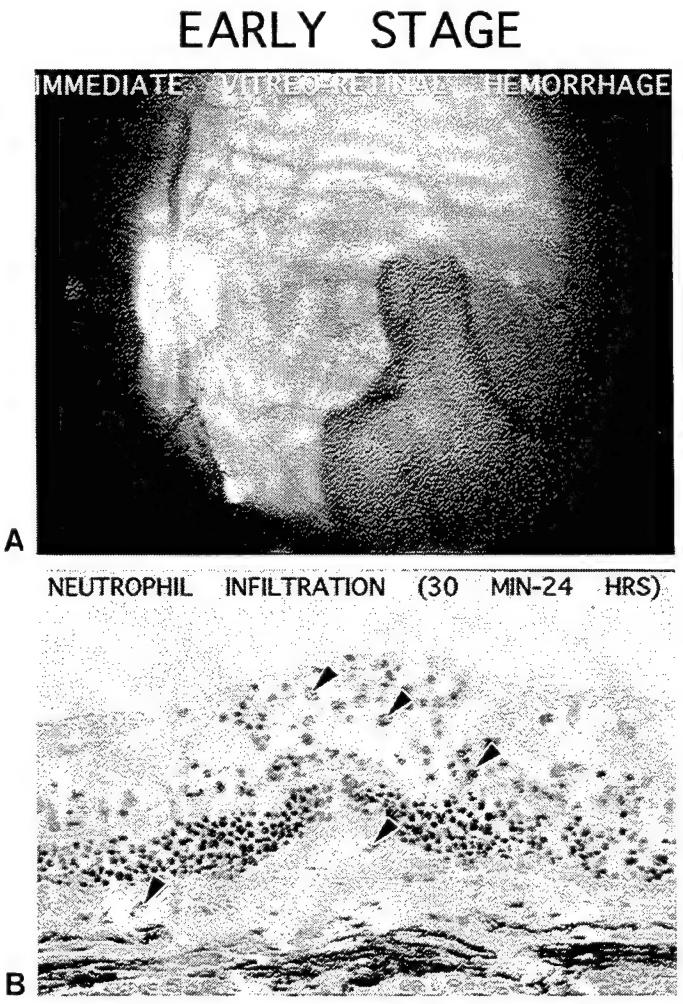

Figure 1. Examples of some of the early stage events that require immediate treatment. A. Vitreous hemorrhage in a macula of non-human primate immediately after injury (primary damage). B. Neutrophils (arrows) enter sites of LIRI in a rabbit retina between 30 min and 24 h after injury (secondary damage). By 24 h after injury, extensive neutrophil and monocyte infiltration is present in an argon laser lesion. Neutrophils in the CNS are known to contribute to extensive secondary damage.

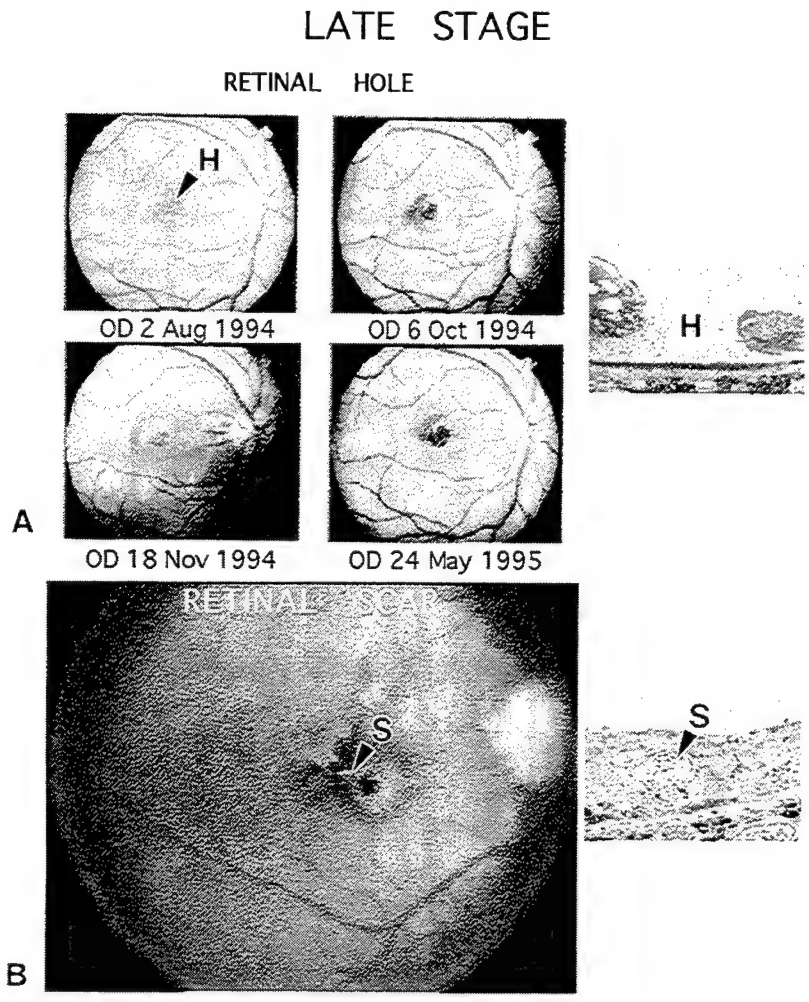

Figure 2. Example of some of the late stage entities that require treatment during the early stages of injury before becoming fully expressed during the late stage (remodeling damage). A. Retinal hole (H) development after Nd:YAG LIRI in a human (non-treated). Histologic section of comparable severity lesion is to right and shows a retinal hole (H) in a 4 mo old Nd:YAG LIRI in a non-human primate. B. Scarring (S) is associated with multiple Nd:YAG LIRIs in a human (non-treated). Histologic section of comparable severity lesion is to right and shows a retinal scar (S) in a 4 mo old Nd:YAG LIRI in a non-human primate.

2. Summary of human laser retinal injuries and treatments provided

It is generally viewed by the medical community that once the retina has been insulted by laser radiation there is very little that can be done by medical management to reverse, halt or slow down degenerative processes.[24] However, recent new advances indicate that potential new treatments may become available.

It is becoming increasingly apparent that important factors in therapy are based on the idea of appropriate timing and use of key agents. Based upon results from brain trauma and spinal cord injury work, the sooner the treatment is provided, the better. Another important aspect that is becoming quite apparent is that no single agent will be sufficient to provide a complete time-course based therapy, but that multiple therapeutics will most likely have to be administered at appropriate times and directed at key targets. It is proposed in this review that the most effective window of treatment for LIRI is within the 0-3 h period. In particular, addressing the acute neutrophil emigration, infiltration, and degranulation responses may be important aspects in limiting severe LIRI (Figure 3). Any treatment after 3 h to limit this response may be of limited value because secondary damage events will have become entrenched and injury to central nervous system (CNS) elements becomes largely irreversible. This treatment window may be more critical for cases with multiple severe injuries in and around the fovea.

A recent review of the literature has resulted in a listing of human LIRI cases and their treatments (see Table I). Only a few of the reports have provided sufficient details to assess aspects of injury and treatment.[9,12,16,17] Table I shows that a majority of the cases occurred from Nd:YAG laser exposure and that the time between initial injury and the first examination by an ophthalmologist is quite variable. Much of the reported literature is not clear with regard to the time from initial injury to the first ophthalmology exam. Also, the treatment regimens applied in many of the cases have not been well documented. Glucocorticoids have been utilized to treat some of the injuries[9,11,14,16,22,29], but most LIRIs have been left untreated.[10,12,15,19,20,21,30] Furthermore, it is unclear if any of the treatments resulted in any benefits[9,12,14]. However, Scales et al[29] recently initiated treatment in one case within 4 h with high dose (30mg/kg) GCs and demonstrated a return to normal visual acuity within 1 mo after a moderate bilateral LIRI. In contrast, this injury was similar to the injury case reported by Hirsch et al[14] where oral Prednisolone treatment was used, but the benefit of treatment was unclear. "Traditional Chinese medicine" treatments have also been utilized, however, the benefits realized were also unclear[13,18,31]. It can then be concluded that the reporting of treatments in the literature for human LIRIs is presently unclear and that further studies are needed to clarify appropriate treatments.

Recently Stuck et al[22] reported on 8 human cases (see Table II) and the format presented from that synopsis is suggested, in part, to assist in documenting the nature of the injuries, treatments, and results of treatments. Additional format suggestions are provided by Ness et al[32] in this volume. National and centralized documentation centers responsible for accurate documentation of LIRIs are currently being developed.[17,32]

2.1. Glucocorticoids

A majority of LIRIs do not receive any pharmacological treatment, and those that do, the treatment is usually glucocorticoid (GC) therapy[9] because GCs are the only FDA approved drugs available to treat CNS injuries. The effectiveness of GC treatment for LIRIs, however, is presently unclear.[14,33,34,35] By better understanding human accidental laser injuries and targeting key factors of injury, better treatment regimens may be developed to treat this emerging problem.

Some GCs are known to slow down certain inflammatory reactions, but they are widely known to inhibit macrophage entry and the phagocytic responses of macrophages and macrophage-like cells such as the retinal pigment epithelium (RPE). They are also known to inhibit glial scar formation. In fact, GCs have been shown to suppress immunity and inhibit wound healing through transcription factor regulation.[36,37] Upon activation of specific transcription factors (such as nuclear factor kappa B, NF-κB), a large number of genes stimulate production of various inflammatory cytokines, adhesion molecules, and other proteins.[38]

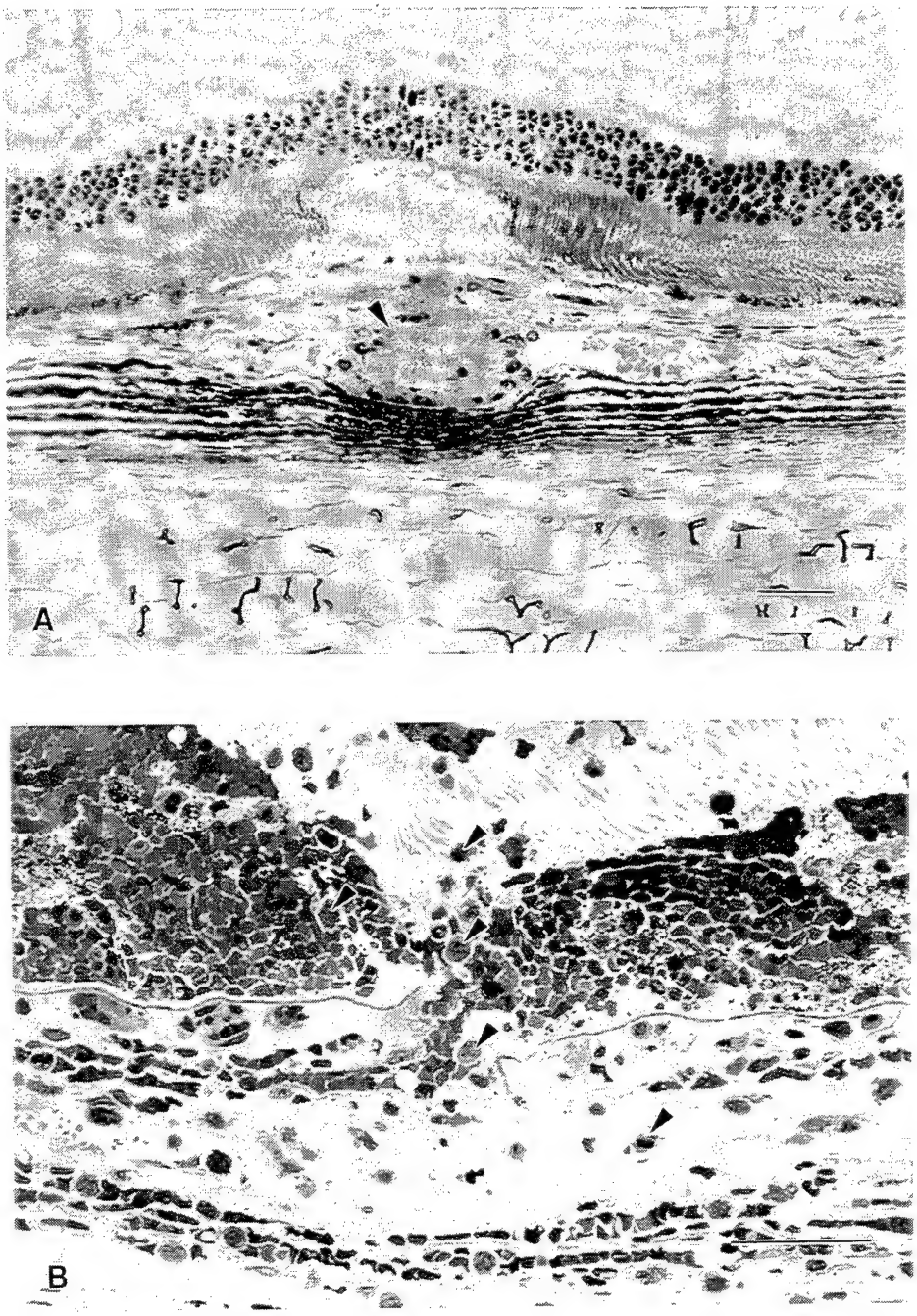

Figure 3. Early PMN response (secondary damage). A. Rabbit lesion 40 min after LIRI. A clot with PMNs is present in the choroid (arrow). B. Human Nd:YAG lesion 4 h after LIRI shows large numbers of PMNs (arrows) in the choroid and retina. Magnification bars = 50 μm.

Table I. Summary of Laser Ocular Injury Cases and Treatments Provided

Reference	# of Cases	Laser	Time to 1st Exam	Treatment
1. Scales et al 1997[29]	1	QS ND:YAG	4 h	MP (30mg/kg + taper/2wk w/80-40mgPOQD Pred
2. Custis et al 1996[21]	1	QSNd:YAG	5d	Surgery @6 mo
3. Stuck et al 1996[22]	8	QSNd:YAG	Var	1/8 DXM
4. Thach et al 1995[20]	5	Nd:YAG	-	None
5. Modarres-Zadeh et al 1995[19]	1	QSRuby	4 h	None
6. Rockwell et al 1994[17]	1 9 9	29% Nd:YAG	Var	None Reported
7. Xu et al 1994[18]	4 8	60% Nd:YAG	Var	Vit,Vasodil, hormones, Ezs Trad. Chin. Med.
8. Rhodes 1993[16]	3 3	Var.	Var.	18/33 w/ various steroids
9. Xu et al 1993[31]	1	Nd:YAG	?	Trad. Chin. Med.
10. Alhalel et al 1993[15]	2	Nd:YAG	?	None reported
11. Hirsch et al 1992[14]	1	Pulsed dye	?	60mg POQD9d Prednisolone
12. Gabel et al 1989[12]	6	QSNd:YAG	Var	None reported
13. Haifeng et al 1989[13]	2 9	19QSNd:YAG	?	ATP, Coenzyme A, Vit A,B,C D, E, Dibazol, Rutin
14. Kearney et al 1987[11]	1	Nd:YAG	?	DXM 10mg-4mgQ6h/48h
15. Manning et al 1986[10]	1	Nd:YAG	~2h	None
16. Lang et al 1985[30]	1	QSRuby	5d	None
17. Wolfe 1985[9]	2 3	Var.	Var.	10/23 treated w/ various steroids

DXM = dexamethasone, MP = methylprenisolone, Prednis. = Prednisolone, and Trad. Chin. Med. = Traditional Chinese Medicine.

Table II. Human Laser Accident Case Data: Evaluations, Treatments, and Visual Acuity Results (After Stuck et al 1996[22])

Case #/ eye	Laser type	Init Exam post Injury	V.A.	Init Injury/ Location	Treatment	Final fundus status / date	Final V.A.
1. C-1/OD	QSNd:YAG	24 h	20/400 20/25 1mo	V-H/ fovea	10mg DXM/d1 4 mg Q 6h/48h	ERM/ scar/ 12 mo	20/40
2. C-2/OD	QSNd:YAG	5 wk	20/50	Opacity/S- fovea	None	cleared/ 10 wks	20/25
3. C-3/OD	QSNd:YAG	24 h	20/200	V-H/ N-T fovea	None	ERM/scar hole/ 18 mo	20/400
4. C-4/OS	QSRuby?	4 h	10/400 20/200 10d	SR-H/ fovea	None	Depig/ ERM/ 5 mo.	/20/400
5. C-5/OS	Nd:YAG-?	5 d	10/400	SR-H/ fovea	None	Depig/ 3 wks	10/400
6. C-6/OS&D	Nd:YAG-?	3wk	20/20 OU	M/punctate S-T fovea	None	Depig/ 11Mo.	20/20 OU
7. C-7/OS	Nd:YAG	24 h	20/200 20/25 3wk 20/17 3mo	Sm V-H S-N fovea	None	Depig/ 2.5 yr	20/17
8. C-8/OD	Nd:YAG	24 h	20/50 20/70 3wk 20/200 3mo 20/400 18 mo	M/V-H N-T fovea	None Surg@6Mo.	Hole.ERM/ 2.5 yr	20/400

Abbreviations: Initial Injury ; V-H = vitreous hemorrhage, SR-H + subretinal hemorrhage, M = multiple injuries, S = superior, and Sm V-H = small vitreous hemorrhage. Locations; N-T = nasotemporal, S-T = superior temporal, and S-N = superior nasal. Final fundus status; ERM = epiretinal membrane, and Depig. = depigmented lesions.

Many of the anti-inflammatories function by preventing the binding of key transcription factors to gene sites. Since GCs are known to inhibit the proliferation of some cells, the repair of the BRB by RPE cells is also delayed.[24] Delay in repair of the BRB then lenghtens the exposure of the retina to molecules normally excluded by an intact BRB. Central nervous system access to molecules normally excluded may have detrimental effects on both survival and repair of neuronal elements.

Bracken et al[39] in a randomized, double-blind, placebo-controlled trial of 487 patients [National Acute Spinal Cord Injury Study-II (NASCIS-II)] showed that a high dose of MP (30mg/kg - MP sodium succinate bolus) followed by 23 h of MP infusion (54.mg/h) was effective up to 8 h, as assessed by a benefit in recovery of motor function at 6 mo. This dose, however, was detrimental if administered after the 8 h window. It was then concluded that after this 8 h window, GCs interfered with neuron regeneration and over the long term there was an increase in infections.

Sapolsky et al[40] indicated that GCs potentiate ischemic injury to neurons. Prendergast et al[34] in a 54 patient study (54 patients/ 29 MP/25 placebo) showed that massive steroids do not reduce the zone of injury in penetrating spinal cord injury and that MP may actually impair recovery of neurologic function. Along similar lines, Hall et al[41] showed that postinjury administration of high doses of MP failed to exert any significant anti-PLA 2 action after spinal cord injury. Results showed that eicosanoid levels (arachidonic acid, PGF2, PGE2, TXA2, and LTs) were not attenuated as previously believed. Recently, Levy et al[35] in a 252 patient study showed that the administration of MP did not significantly improve functional outcomes in patients with gunshot wound injuries to the spine. Since the retina is part of the CNS, and if the pathophysiology of spinal cord and brain trauma can be regarded as being similar to laser retinal trauma; then, valid comparisons and extensions may be made regarding treatment of LIRIs. Most applications of GCs, and in particular MP, appear to be based on possible antioxidant roles. This role, however, has been recently shown to be independent of GC receptor mechanisms, [35] suggesting that a non-GC could duplicate any antioxidant efficacy.

Other effects of GCs are that they suppress immunity, increase infections, and promote cataracts and bone weakening. They also elevate blood pressure, enhance optic nerve damage, and inhibit macrophages, thus suppressing wound healing. Some GCs do not inhibit PMN entry as suggested in some studies and they prevent PMN apoptosis. In combination, these factors may lead to GC-induced leukocytosis.[42,43] In addition, large doses are required for neuroprotection but excessive doses can increase lipid peroxidation and destabilize membranes. The neuronal uptake of GCs has been shown to decrease with time after injury, which argues against their protracted use. Glucocorticoids are also known to exacerbate ischemic lactic acidosis by increasing serum glucose levels, which promote diabetic problems and other complications such as gastric ulceration and a negative nitrogen balance[33]. Generally, there is a maximum treatment window[39] (for MP it is 8 h) and a gradual withdrawal is required.

Some of the positive effects of GC use are that they reduce: inflammation, scarring via antiproliferative effects, O_2 free radical lipid peroxidation, possibly edema, and stabilize blood flow. Fu et al[44] showed that dexamethasone (DXM) was capable of ameliorating photic injury in rats. Lam et al[45] reported that methylprednisolone (MP) therapy, in monkeys 24 h before laser injury with continued lower dose treatment up to 4 days after injury was beneficial; however, severe side effects were also observed from the high dose and extended therapy regimen.

Most ophthalmologists still prefer the use of steroids as acute stage therapeutics for LIRI; however, as increasing evidence indicates, GCs may not be the optimum treatment for LIRIs and caution should be exercised in their use.[39] Clearly, more effective therapeutic regimens need to be evaluated based on well-designed clinical studies.

2.2 Aspirin:

The acetylated form of salicylic acid, aspirin, is the most widely used non-steroidal anti-inflammatory drug (NSAID). The effectiveness of NSAIDs are largely due to their ability to inhibit the synthesis and release of prostaglandins by limiting the production of the cyclooxygenase, prostaglandin H synthase.[46] Non-acetylated forms of the salicylates do not interfere with the prostaglandin synthesis pathway.[47] Evidence for salicylate inhibition of endotoxin-induced tissue factor gene transcription via

NF-κB has also been described[47] and more recently, Cheng, et al[48] described a new hypothesis for salicylate action which involves redox deactivation of iron. If confirmed, this mechanism of action would be significant in limiting lipid peroxidation events. Surprisingly, NSAIDs have not been widely prescribed for the treatment of acute or early stage laser-induced retinal injury.

2.4. Surgery:

Surgical procedures may be required to treat some LIRIs because of the development of secondary complications that threaten previously uninjured retina. Procedures usually involve vitrectomies or excisions to remove proliferating membranes, blood vessels, and scars. In addition, if secondary events lead to detachment, retinal reattachment surgery may be required. Custis et al[21] recently performed one of the first documented surgical procedures to treat a late stage complication after LIRI by successfully alleviating traction; however, hole expansion was not curtailed.

One surgical treatment that may have potential is posterior hyaloid interface detachment surgery. It is believed that if the posterior hyaloid membrane is removed relatively early over a severe injury site, the scaffold for scar proliferation into the vitreous and subsequently traction is eliminated. More studies regarding this type of approach are still needed.

3.0 Review of Experimental treatments for laser injury

The list of potential experimental therapeutics is too extensive and beyond the scope of this discussion but of some of the more promising therapy approaches for the treatment of laser retinal trauma are discussed below. Some of the treatment approaches used in ameliorating light injury may also have application in treatment of mild to moderate laser retinal injury.[54] Drugs approved by the FDA are of more likelihood for immediate use while more experimental approaches will necessitate appropriate evaluations before human use approval.

Work in experimental treatment of LIRIs is presented in Table III. It is clear from the literature that few studies have been undertaken to carefully document appropriate therapeutics for treatment of laser retinal injury. Most studies have involved too few animals and analysis has been conducted on too few lesions. The list of past work on treatments indicates that none of the studies to date have provided conclusive evidence that GC therapy for laser injury is beneficial. Some studies have indicated positive results with dexamethasone (DXM) and triamcinolone to prevent subretinal neovascular membranes[54] while DXM in lower doses, first decreased then increased PGE2 levels by up to 3 fold.[55] Lam et al[45] showed that MP was effective if used as a pretreatment then extended with lower doses up to 24 h; however, use up to 8 h, which is the recommended treatment window (as recommended by the NASCIS-II study)[39], was deemed ineffective. Rosner et al[56] also showed that a high dose of MP in rats rescued photoreceptors after LIRI. In rabbits, high dose MP pretreatment was deemed harmful by 3 h after injury as determined by increased lesion sizes and increased PMN infiltration.[57] Currently, few clear cut therapeutics or regimens can be recommended based on results from the experimental literature but progress is being made in understanding key factors of acute injury. Recent work indicates that treatment of acute inflammatory reactions in moderate to severe lesions must be rapid and appropriately targeted.[57]

3.1 Hemorrhages

Choroidal, sub- and intraretinal, and vitreous hemorrhages or hematomas create problems because of the deleterious effects of trapped blood and the potentiation of ischemia and lipid peroxidation by blood breakdown products. Free reactive iron, which may be released from the cytosol or from hemorrhage breakdown products, is a catalyst for oxygen free radicals.[58] One of the first attempts to address the issue of blood clearance from the vitreous after LIRI was with urokinase, unfortunately, this procedure was deemed unsuccessful, but vitreous fibrosis was curtailed.[59]

Other forms of early surgical intervention for LIRI includes repair of vision threatening retinal detachments and the extraction of trapped hemorrhages from critical areas.

Table III. Review of Experimental Treatments for Laser-Ocular Injury

Reference	Treatment	Therapeutic Endpoint	Result
1. Belkin et al 1983[59] Rabbit	Urokinase	Vit Hem clearance Vit. fibrosis	(-) (+)
2. Ishibashi et al 1985[54] Monkey	DXM(480µg/24h/14d) DXM + TRCL(1mg)	SRN SRN	(+) (+)
3. Deaton et al 1990[94] Goldfish	Hyperthermia/hsp70	Lesion size	(+)
4. Naveh et al 1990[55] Rabbit	DXM (0.5mg/kg) "	PGE_2 levels@7d " " @ 14d	(+) (-)
5. Lam et al 1992[45] Monkey	MP (pre 24h + 24h) MP + 24h " MP + 8 h " (30mg/kg-5.4 mg/hr)	Rescue RPE and Photo " "	(+) (+) (-)
6. Toth et al 1993[49] Cat (Mech. Hem)	tPA	Subret Hem. lysis/removal	(+)
7. Schuschereba et al 1994[69] Rabbit	bFGF	Rescue Photo. BRB repair	(+) (+)
8. Custis et al 1996[22] Human	ERM surgery	Hole enlargement ERM traction	(-) (+)
9. Rosner et al 1996[56] Rat	MP	Rescue Photo.	(+)
10. Solberg et al 1996[82] Rat	MK 801 (3mg/kg) (NMDA chan. blocker)	Rescue Photo	(+)
11. Schuschereba et al 1996[57] Rabbit	HES-DFO (100 mg/kg) MP(30mg/kg) n-saline HES-DFO (100 mg/kg) MP(30mg/kg) n-saline	PMN #s @ 3 h " " " " Lesion size " " " "	(+) (-) (-) (+) (-) (-)

DXM = dexamethasone, MP= methylprenisolone, bFGF = basic fibroblast growth factor, tPA = tissue plaminogen activator, HES-DFO = hyroxyethyl starch-deferoxamine, ERM = epiretinal membrane, PMN = polymorphonuclear leukocyte, TRCL = triamcinolone, and BRB = blood-retinal barrier. Plus and minus indications in result column represent effect on the endpoint.

Procedures utilizing tissue-type plasminogen activator (tPA) to induce fibrinolysis and dissolution of mechanically created subretinal clots were successful but such procedures have not been evaluated in experimental LIRIs.[49] Recently, Thach et al[20] reported that macular holes and subretinal hemorrhages, which were left untreated either by drugs or surgery, showed, in most cases, not to significantly degenerate and that visual acuity also improved slightly over a time course of 13 months. In situations of confined hemorrhage, secondary damage processes run their full course but ideally, therapeutic benefit should be realized if secondary damage processes are appropriately limited. A developing body of literature suggests that free hemoglobin and iron in the CNS, including the retina, participates in destructive lipid peroxidation events.[50,51,52] Removing blood[49] or chelating reactive free iron has been shown to ameliorate early stage CNS injury.[50,57]

3.2 Ischemia/Reperfusion

Ischemic retinal damage associated with laser injury may be one of the most important mechanisms underlying secondary damage associated with severe injury. Ischemic retinal damage may be a key factor in expanding the size of the primary injury. This damage may occur by occlusion of both choroidal and retinal vessels, and by the presence of a focal and large mass of dead retinal tissue, which rapidly contributes to limiting oxygen and glucose transport to marginally injured and adjacent uninjured cells. The injury site itself may contribute to a global decline in retinal metabolic rate and oxygen usage. Upon restoration of blood flow in occluded or constricted vessels, oxygen free radicals are generated and participate in lipid peroxidation.

3.3 Growth factors

The potential for neuronal and nonneuronal cells to recover after traumatic injury seems to be dependent both on the postraumatic ionic/neurotransmitter environment and on the presence of neurotrophic substances such as growth factors. Growth factors support neuronal survival, induce sprouting of neurites, and facilitate the guidance of neurites to their proper synaptic targets. Primary stage retinal trauma can be considered to initiate both cellular and genomic responses that can lead to programmed cell death, similar to what is observed in traumatic brain injury[60] and trophic factors may prevent part of this injury.[61] The best characterized neurotrophic factors include nerve growth factor (NGF), basic fibroblast growth factor (bFGF), brain-derived neurotrophic factor (BNDF), glial derived neuroptrophic factor (GDNF), and neurotrophin-3 (NT-3). Several studies have suggested that neurotrophic factors are synthesized or released after traumatic CNS injury, perhaps to facilitate repair and to stimulate posttraumatic regeneration.[62] In contrast to earlier beliefs, the macrophage in retinal wound healing has recently been shown not to produce bFGF, unless specifically activated.[63,64]

Basic fibroblast growth factor (bFGF) has been described as a multi-functional growth factor that has been implicated in a number of proliferative, regenerative, and survival related events in the central nervous system.[65] Endogenous bFGF levels increased at sites of focal brain injury[66] and retinal injury[67], suggesting regulatory roles in repair. Exogenous delivery of bFGF has been shown to aid injury-related events and to promote neuron survival in the retina.[68,69] Basic FGF has been shown to prevent photoreceptor cell degeneration in light-damaged retinas[70,71] and was also shown to accelerate BRB repair and to rescue photoreceptors after argon laser injury.[69]

Transforming growth factor (TGF) -beta 2, produced by a variety of cells, has been documented to inhibit the growth of many cell types and to stimulate the formation of extracellular matrix and collagen synthesis.[72] Glaser et al[73] has shown a therapeutic benefit in repairing idiopathic macular holes but TGF has not been utilized to repair laser-induced retinal holes.

3.4 Cytokines

Because the BRB is open after laser retinal injury, often for extended periods, it is possible that entry of blood-borne constituents in injured retina may be neurotoxic. Acute PMN entry has been

observed within 24 h of brain injury and correlates directly with the development of postraumatic cerebral edema in rats.[74] Macrophages have been shown to play a major role in wound healing after penetrating brain injury[75] and many of these immunocompetent cells release soluble factors, including cytokines that are known to widely influence posttraumantic neuronal survival and outcome. Taupin et al[76] have shown that IL-1, IL-6, and TNF alpha are upregulated after brain injury and suggest that these cytokines may play a role in the pathophysiologic cascade after trauma. Recent work in a time course RT-PCR study involving a mouse model of LIRI, also showed upregulation of mRNA for IL-1 α, iNOS, and G3PDH and changes in a variety of other cytokines.[95]

Monoclonal antibodies directed against specific antigens represent a unique approach in the blockade of certain molecules. Monoclonal antibodies against TNF-alpha, IL-1, IL-6, IL-8; and the adhesion molecules CD11/CD18 have shown promise as therapeutics.[77]

Interleukin 8 is recognized as a potent neutrophil activator. It is secreted by several cell types such as monocytes, macrophages, endothelial cells, epithelial cells, and fibroblasts.[78] In fact, elevated levels of IL-8 in the airspaces of patients with adult respiratory distress syndrome (ARDS) have been associated with increased mortality. Kurdowska et al[78] demonstrated the pharmacological potential of monoclonal antibodies directed against IL-8 which interfered with such events as IL-8 binding to PMNs, PMN degranulation, and PMN chemotactic activity.

3.5 NMDA antagonists

The release of excitatory amino acid (EAA) neurotransmitters such as glutamate, glycine, and aspartate activate a number of neuronal receptors and cause increased electrical activation of neuronal cells. Such activity usually results in cell swelling, vacuolization, and neuronal cell death. Olney et al[79] proposed the concept of excitotoxicity where overexcitation resulted in eventual cell death. When EAAs are released and activate receptors, there is an increased influx of sodium and calcium ions into the cell through specific membrane channels. Cell death has been proposed to occur through at least two mechanisms: 1) an influx of chloride and sodium leads to acute neuronal swelling and 2) the influx of calcium leads to delayed damage.[80] EAAs are also thought to be liberated during ischemia and hypoxia. Faden et al[51] showed that experimental CNS trauma induces an immediate and profound increase in extracellular EAAs. It is believed that laser-induced retinal injury also involves an excitotoxic component that actively destroys populations of neurons and contributes to diffuse posttraumatic lesion expansion. Pharmacologic antagonists of the N-methyl D Aspartate (NMDA) receptor, which mediate ionic channels, appear to have therapeutic benefit. One of these compounds, MK-801, has been shown to have some benefit but it is also highly toxic. Reports on the use of competitive NMDA antagonists such as CGS-19755 have shown that it is well tolerated by brain-injured patients and indicates a promise for treatment of retinal injury[81]. Solberg et al[82] recently demonstrated that MK-801 has a therapeutic benefit after LIRI in rats.

3.6 Arachidonic acid cascade

Elevations in intracellular calcium will facilitate an attack on the cell membrane by calcium-activated proteases and lipases and produces a variety of pathogenic compounds from a breakdown of endogenous intracellular fatty acids such as arachidonic acid (AA). Activated phospholipase A2, lipoxygenase and cycloxygenase are known to degrade AA into the ecosanoid metabolites thromboxane A2, prostaglandins, and leukotrienes.

Platelet activating factor (PAF) is also produced by the AA pathway. This factor is a potent platelet agonist and activator of neutrophils and monocytes. It is produced by a variety of stimulated inflammatory cells including the neutrophils, basophils, monocytes, platelets, mast cells, and eosinophils.[83] It is also produced by other cells such as vascular endothelium and neurons when membranes are damaged or when inflammation, cell stimulation, or injury activates phospholipase A_2.[84] Neuronally released PAF can produce BRB permeability and vasoconstriction.[85] Faden et al[51] showed that PAF can be upregulated as early as 5 minutes after brain injury. Platelet activating factor

has also been associated with increasing intracellular free calcium levels in cultured neurons, suggesting that it may play an important role in posttraumatic calcium-mediated cell death and perhaps apoptosis. One hour after PAF injection, platelet aggregates have been observed in the lumens of retinal blood vessels and by 2 h numerous PMNs were seen within the vascular walls, demonstrating increased vascular permeability and BRB breakdown.[86]

Use of PAF antagonists was shown to block most of the fluorescein leakage attributed to migrating PMNs. PMNs were observed to enter retinal tissue about 2-4 hr after injection.[86] Frerichs et al[87] showed that by pretreatment with a selective PAF antagonist, nearly all of the brain edema following a Nd:YAG laser injury in the rat was prevented. In addition, PAF acetylhydrolase which breaks down PAF was suggested to have therapeutic potential.[84] In our laboratory the use of the PAF antagonist, BN52021, actually promoted leuckocytosis within moderate to severe LIRI zones.

From the forgoing discussion, the inhibition of neutrophil chemotaxis, adhesion, and migration via PAF antagonism are probably important strategies for augmenting wound healing in laser-injured retina. Better models and therapeutics are still needed to confirm this strategy.

3.7 Ion changes

Calcium: Subarchinoid hemorrhage and cerebral ischemia have been known to produce calcium ion changes which have been reported to underlie delayed cell death. Shapira et al[88] have demonstrated that total brain tissue calcium concentrations were found to be significantly elevated in injured areas. Significant calcium accumulation has also been observed in peripheral populations of laser-injured photoreceptors (unpublished observations).

Schurr et al[89] demonstrated that diltiazem, a L-type calcium channel blocker and MK 801, a noncompetitive N-methyl-D-aspartate (NMDA) receptor antagonist, which functions via calcium channel blocking, provided a synergistic neuroprotective effect against hypoxic CNS damage. This regimen may be useful in treatment of laser-induced retinal trauma.

Magnesium: Magnesium is involved in several critical cellular processes, including glycolysis and oxidative phosphorylation, cellular respiration, and synthesis of DNA, RNA and protein. It also plays an essential role in maintaining mitochondrial and plasma membrane integrity. Reduced cytosolic free magnesium can impair glucose utilization, energy metabolism, and protein synthesis, and can reduce both oxidative and substrate level phosphorylation, thereby, contributing to regional cell death after LIRI.[90] Alterations in intracellular magnesium could potentially contribute to posttraumatic calcium-mediated neurotoxicity or the regulation of regional posttraumatic retinal and choroidal blood flow.

3.8 Heat shock protein induction

When cells undergo rapid increases in temperature sufficient to induce stress (i.e. heat shock) but not cell death, the synthesis of most cell proteins decreases for several hours. A few select proteins, though, are synthesized more rapidly than under normal conditions.[91] These polypeptides are known as heat shock proteins (hsps). Increases in hsp synthesis characterize the heat-shock response. When intracellular concentrations of hsps are increased they are thought to provide protective functions against many noxious stimuli[92] and can protect against the effects of incoherent white light on rat photoreceptors.[93] Deaton et al[94] demonstrated that elevation of hsps in goldfish provided a protective effect against laser-induced photoreceptor damage.

4.0. Discussion/Conclusions

Important interrelationships exist between the photo-mechanical and photocoagulative factors underlying LIRI, the secondary or delayed neurochemical responses to trauma, the remodeling ramifications, and the histologic and funduscopy damage that occurs. In pursuit of understanding the molecular and cellular sequelae of LIRI, it is becoming apparent that many different or distinct types of molecular and cellular events are involved in mediating the posttraumatic pathophysiologic cascade

that results in secondary and tertiary or remodeling damage in the retina. It may be beneficial for future work to examine the timing of this cascade with regard to specific cellular and molecular events as they relate to the initial injury event and to the development of reproducible histologic change, delayed cellular death, and neuronal and visual dysfunction. The characterization of the interrelationships between these diverse secondary injury factors and the specific primary damage factors may provide insight into the timing and use of appropriate therapeutic modalities for treatment of LIRI.

Furthermore, it is clear that adequate therapies for injury are unavailable and that many cases are complicated by not being treated appropriately and quickly enough. Most accidental laser injuries to the retina involve the fovea and a majority result in further and permanent reduction of vision. Histology data from experimental human laser retinal injury indicate that targeting inflammatory responses during the early stage of injury would probably be beneficial. In fact, it would be reasonable to suggest that severe laser retinal injuries receive acute treatment considerations similar to spinal cord injury and head trauma cases. Late stage injuries often involve extensive scarring with previously uninjured retina, which contributes to further vision degradation. If retinal holes persist for more than several weeks after laser injury, then hole closure must be a top priority to limit further vision losses. Retinal holes should be aggressively managed for closure during the early stages of injury because later stage surgical management may be less effective. Collectively, data suggest that early stage treatments should target aspects of neurodegeneration, inflammation, and scarring.

In conclusion, it is clear that a need exists for standardized reporting of injuries and treatments. Furthermore, more definitive experimental studies regarding treatment are needed. Treatment of laser-induced retinal injuries should begin as soon as possible, preferably within the first hour of injury. Some key targets for early phase treatment are; sparing of neural elements, reducing edema, and preventing neutrophil entry and damage. By several hours after injury, key aspects for later stage treatment are minimizing: retinal holes, scarring, and epiretinal membrane formation. Lastly, the use of glucocorticoids to treat LIRIs needs to be carefully evaluated.

5. Disclaimer

In conducting the research described in this report, the investigators adhered to the "Guide for the Care and Use of Laboratory Animals, " as promulgated by the Committee on Revision of the Guide for Laboratory Animal Facilities and Care, Institute of Laboratory Animal Resources, National Academy of Sciences- National Research Council.

The opinions or assertions contained herein are the private views of the authors and not to be construed as official or as reflecting the views of the Department of the Army or the Department of Defense.

Citation of trade names in this report does not constitute an official endorsement or approval of the use of such items.

Human volunteers participated in these studies after giving their free and informed voluntary consent. Investigators adhered to AR 70-25 and USAMRMC Regulation 50-25 on the use of volunteers in research.

6. References

1. Rathkey AS Accidental laser burn of the macula. Arch Ophthalmol. 74:346-348;1965.

2. Apple DJ, Goldberg MF, Wyhinny G Histopathology and ultrastructure of the argon laser lesion in human retinal and choroidal vasculatures. Am J. Ophthalmol 75:595-609;1973.

3. Marshall J, Hamilton AM, Bird AC Histopathology of ruby and argon laser lesions in monkey and human retina. A comparative study. Brit J. Ophthalmol 59:610-630;1975.

4. Gibbons WD, Allen RG Retinal damage from suprathreshold Q-switched laser exposure Health Physics 35:461-469;1978.

5. Boldrey EE, Little HL, Flocks M, Vassiliadis A Retinal injury due to industrial laser burns. Ophthalmol 88:101-107;1981.

6. Glovinsky Y, Regenbogen L, Bartov E, Blumenthal M, Moisseive Y Macular pucker following accidental laser burn. Metab. Pediatr. Syst Ophthalmol 6:355-359;1982.

7. Goldberg MF, Young RSL, Read J, Cunha-Vaz JG Macular hole caused by a 589-nanometer dye laser operating for 10 nanoseconds. Retina 3:40-44;1983.

8. Fowler BJ Accidental industrial laser burn of macula. Ann. Ophthalmol 15:481-483;1983.

9. Wolfe JA Laser retinal injury. Military Medicine 150:177-185;1985.

10. Manning JR, Davidorf FH, Keates RH, Strange AE Neodynium:YAG laser lesions in the human retina: accidental/experimental Contemp. Ophthalmic Forum 4:86-91;1986.

11. Kearney JJ, Cohen HB, Stuck BE, Rudd GP, Beresky DE, Wertz FD Laser injury to multiple retinal foci Lasers Surg Med 7:499-502;1987.

12. Gabel V-P, Birngruber R, Lorenz B, Lang GK Clinical observations of six cases of laser injury to the eye. Health Physics 56:705-710;1989.

13. Haifeng L, Guanghuang G, Dechang W, Guidao X, Liangshun S, Jiemin X, Haibiao W Ocular injuries from accidental laser exposure. Health Physics 56:711-716;1989.

14. Hirsch DR, Booth DG, Schocket S, Sliney DH Recovery from pulsed-dye laser retinal injury. Arch Ophthalmol 110:1688-1689;1992.

15. Alhalel A, Glovinsky Y, Treister G, Bartov E, Blumenthal M, Belkin M Long-term follow up of accidental parafoveal laser burns. Retina 13:152-154;1993.

16. Rhodes JW Laser-induced hemorrhagic lesions: a review of accidental injuries and related experimental findings in animals. Lasers and Light in Ophthalmol. 5: 211-222;1993.

17. Rockwell Jr RJ Laser accidents: reviewing thirty years of incidents: what are the concerns-old and new? J laser Applications 6:203-211;1994.

18. Xu J, Wolbarsht ML Laser injury in China. Lasers Life Sci 6:181-185;1994.

19. Modarres-Zadeh M, Parvaresh MM, Pourbabak S, Peyman GA Accidental parafoveal laser burn from a standard military ruby range finder. Retina 15:356-35;1995.

20. Thach AB, Lopez PF, Snady-McCoy LC, Golub BM, Frambach DA Accidental Nd:YAG laser injuries to the macula Am J. Ophthalmol 119:767-773;1995.

21. Custis PH, Gagliano DA, Zwick H, Schuschereba ST, Regillo CD Macular hole surgery following accidental laser injury with a military range finder. SPIE 2674:166-174;1996.

22. Stuck BE, Zwick H, Molchany JW, Lund DJ, Gagliano DA Accidental human laser retinal injuries from military laser systems SPIE 2674: 7-20;1996.

23. Marshall, J. Structural aspects of laser-induced damage and their functional implications. Hlth Phys. 56: 617-624;1989.

24. Mellerio, J. Marshall, J., Tengroth, B., Anderberg, B. and Wolbrascht, M. Battlefield laser weapons: an assessment of systmes, hazards, injuries and opthalmic resources required for treatment. Laser Light Ophthalmol. 4:41-67;1991.

25. Dastgheib K, Bressler SB, Green WR Clinicopathologic correlation of laser lesion expansion after treatment of choroidal neovascularization. Retina 13:345-352;1993.

26. Wolbarsht ML. Permanent blindness from laser exposures in laboratory and industrial accidents. SPIE 2674:21-24; 1996

27. Frisch, G.D., Shwaluk, P.D., and Adams, D.O. Remote nerve fiber bundle alterations in the retina as caused by argon laser photocoagulation. Nature. 248:433-435;1974.

28. Hooper P, Bora NS, Kaplan HJ, Ferguson TA, Inhibition of lymphocyte proliferation by resident ocular cells. Cur Eye Res 10:363-372;1991.

29. Scales DK. 1997 (Personal Communication)

30. Lang GK, Lang G Naumann GOH "Akzidentelle bilaterale asymmetrische rubin-laser-maulo-pathie" Klin. Mbl. Augenheilk. 186:366-370;1985.

31. Xu J, Zhou S, Chen Z. Macular burn induced by accidental Nd:YAG laser exposure Lasers in the Life Sciences 5:285-290;1993.

32. Ness J, et al SPIE 1997 (this volume)

33. Hall ED, Yonkers PA, Taylor BM, Sun FF. Lack of effect of postinjury treatment with methylprednisolone or tirilazad mesylate on the increase in eicosanoid levels in the acutely injured cat spinal cord. J Neurotrauma 12: 245-256;1995.

34. Prendergast MR, Saxe JM, Ledgerwood AM, Lucas CE, Lucas WF. Massive steroids do not reduce the zone of injury after penetrating spinal cord injury. J Trauma 37: 576-580;1994.

35. Levy ML, Gans W, Wijesinghe HS, SooHoo WE, Adkins RH, Stillerman CB Use of methylprednisolone as an adjunct in the management of patients with penertrating spinal cord injury: outcome analysis. Neurosurgery 39: 1141-1149;1996.

36. Scheinman, R.I., Cogswell, P.C., Lofquist, A.K. Baldwin Jr. A.S. Role of trascriptional activation of IkB alpha in mediation of immunosuppression by glucocorticoids. Science 270:283-286;1995.

37. Auphan, N., DiDonato, J.A., Rosette, C., Helmberg, A., Karin, M. Immunosuppression by glucocorticoids: inhibition of NF-kB activity through induction of IkB synthesis. Science 270:286-290;1995.

38. Grilli M., Chiu JJ.-S., Lenardo, M.J. NFκB and Rel: Participants in a multiple transcription regulatory system Internat. Rev. Cytol. 143:1-61;1993.

39. Bracken MB, Shepard MJ, Collins WF et al., A randomized, controlled trial of methylprednisolone or naloxone in the treatment of acute spinal-cord injury. N Engl J Med 322:1405-1411;1990.

40. Sapolsky RM Pulsinelli WA. Glucocorticoids potentiate ischemic injury to neurons: therapeutic implications. Science 229:1397-1400; 1985.

41. Hall ED The neuroprotective pharmacology of methylprednisolone. J Neurosurg 76:13-22;1992.

42. Liles C, Dale DC, Klebanoff SJ. Glucocorticoids inhibit apoptosis of human neutrophils Blood 86:3181-3188;1995.

43. Cox G. glucorticoid treatment inhibits apoptosis in human neutrophils. Separation of survival and activation factors. J. Immunol 154:4719-4729;1995.

44. Fu, J., Lam, T.T. Tso, M.O.M. Dexamethasone ameliorates retinal photic injury in albino rats. Exp Eye Res. 54:583-594;1992.

45. Lam TT, Takahashi K, Fu J, Tso MOM. Methylprednisolone therapy in laser injury of the retina. Grafe's Arch Clibn Exp Ophthalmol 231:729-736; 1993

46. Weissmann, G. Aspirin. Sci Am. 264:84; 1991.

47. Oeth, P., Mackman, N. Salicylates inhibit lipopolysaccharide-induced transcriptional activation of the tissue factor gene in human monocytic cells. Blood. 86:4144-4152;1995.

48. Cheng, I.F., Zhao, C.P., Amolins, A., Galazka, M., Doneski, L. A hypothesis for in the in vivo antioxidant action of salicylic acid. Biometals 9:285-290;1996.

49. Toth CA, Benner JD, Hjelmeland LM, Landers III MB, Morse LS. Ultramicrosurgical removal of subretinal hemorrhage in cats Am J. Ophthalmol 113:175-182; 1992.

50. Panter SS, Faden AI Biochemical changes and secondary injury from stroke and trauma. In: Principles and practice of restorative neurology, Eds, RR Yooung and PJ Delwade, Butterworths, NY 1992, pp32-52.

51. Faden AI, Demediuk P, Panter SS, Vink R. The role of excitatory amino acids and NMDA receptors in traumatic brain injury. Science 244:798-800;1989.

52. Schuschereba ST, Clifford CB, Vargas JA, Bunch D, and Bowman PD: Morphologic alterations in rat retina after hypervolemic infusion of cross-linked hemoglobin. Biomat Art Cells Art Org 18:299-307,1990

53. Organisciak, D.T., Winkler, B.S. Retinal light damage: Practical and theoretical considerations. Prog. Retinal Eye Res. 13:1-29;1994.

54. Ishibashi T, Miki K, Sorgente N, Patterson R, Ryan SJ, Effects of intravitral administration of steroids on experimental subretinal neovascularization in subhuman primate Arch Opthalmol 103: 708-711;1985.

55. Naveh N, Weissman C. Corticoid treatment of laser retinal damage affects prostaglandin E2 response. Invest. Ophthalmol Vis Sci 31:9-13;1990.

56. Rosner M, Tchirkov M, Dubinski G, Naveh N, Tso MOM. Methylprednisolone ameliorates laser induced retinal injury in rats. Invest Ophthalmol Vis Sci 37:S694; 1996.

57. Schuschereba ST, Cross ME, Pizarro JM, Ujimori V, Nemeth TJ, Bowman PD, Stuck BE, Marshall J. Pretreatment with hydroxyethyl starch-deferoxamine but not glucocorticoids limits neutrophil infiltration in acute retinal laser injury. Invest Ophthalmol Vis Sci 37:S695;1996.

58. Hallaway PE and Hedlund BE: Therapeutic strategies to inhibit iron-catalyzed tissue damage. In: Lauffer RB (ed.) Iron in Human Disease. pp 476-508. Boca Raton, FL: CRC Press 1992.

59. Belkin M, Lund DJ, Beatrice ES Urokinase treatment of fresh laser irradiation-induced vitreous hemorrhage. Ophthalmologica 187;152;1983

60. Rink AD, Fung K-M, Perri BR, Lee VM, trojanowski JQ, Gennarelli TA, Neugebauer E, McIntosh TK Programmed cell death after traumatic brain injury J. Neurotrauma 12:137;1995.

61. Granerus M, Engstrom W. Growth factors and apoptosis. Cell Proliferation 29:309-314;1996.

62. Gomez-Pinilla PG, Lee JW-K, Cotman CW Basic FGF in adult rat brain : Cellular distribution and response to entorhinal lesion and fimbria-fornix transection J. Neurosci 12:345-355;1992.

63. Ogata N, Matsushima M, Takada Y, Tobe T, Takahashi K, Yi X, Yamamoto C, Yamada H, Uyama M. Expression of basic fibroblast growth factor mRNA in developing choroidal neovascularization. Cur Eye Res 15:1008-1018;1996.

64. DiPietro LA, Wound healing: the role of the macrophage and other immune cells. Shock 4:233-240;1995.

65. Lewis, G.P., Fisher, S.K., ANderson, D.H. Fate of biotinylated basic fibroblast growth factor in the retina following intravitreal injection. Exp. Eye Res. 62:309-324;1996.

66. Finklestein, S.P., Apostilides, P.J., Caday, C.G., Prosser, J., Philips, M.F., Klagsburn, M. Increased basic fibroblast growth factor (bFGF) immunoreactivity at the site of focal brain wounds. Brain Res. 460:252-259;1988.

67. Wen R, Song Y, Cheng T, Matthes MT, Yasumura D, LaVail MM, Steinberg RH. Injury-induced upregulation of bFGF and CNTF mRNAs in the rat retina. J. Neurosci 15:7377-7385;1995.

68. Lewis, G.P., Erickson, P.A., Guerin, C.J., Anderson, D.H., Fisher, S.K. Basic fibroblast factor: a potential regulator of proliferation and intermediate filament expression in the retina. J. Neurosci. 12:3968-3978;1992.

69. Schuschereba ST, Bowman PD, Ferrando RE, Lund DJ, Quong JA, and Vargas JA. Accelerated healing of laser-injured rabbit retina by basic fibroblast growth factor. Invest. Ophthalmol Vis Sci 35:945-954;1994.

70. Faktorovich, E.G., Steinberg, R.H., Yasumura, D., Matthes, M.T., La Vail, M.M. Basic fibroblast growth factor and local injury protect photoreceptors from light damage in the rat. J. Neurosci. 12:3554-3567:1992.

71. LaVail, M.M., Unoki, K., Yasumura, D., Matthes, M.T., Yancopoulos, G.D., Steinberg, R.H. Multiple growth factors, cytokines, and neurotrophins rescue photoreceptors from the damaging effects of constant light. Proc. Natl. Acad. Sci. U.S.A. 89:11249-11253; 1992.

72. Sporn MB, Roberts AB, Wakefield LM, and de Crombrugghe B Some recent advances in the chemistry and biology of transforming growth factor-beta. J.C. Biol. 105:1039-1045;1987.

73. Glaser BM, Michels RG, Kuppermann BD, Sjaarda RN, Pena RA Transforming growth factor -β_2 for treatment of full-thickness macular holes. Ophthalmol. 99:1162-1173;1992.

74. Schoettle RJ Kochanek PM, Magaaree MJ, Uhl MW, and Nemento EM Early polymorphonuclear leukocyte accumulation correlates with the development of posttraumatic cerebral edema in rats. J Neurotrauma 7:207-217;1990.

75. Giulian D, Chen J, Ingeman JE, George JK, Noponen M. The role of mononuclear phagocytes in wound healing after traumantic injury to adult mammalian brain. J. Neuroscience 9:4416-4429;1989.

76. Taupin V, Toulmond S, Serrano A, Benavides J, Zavala F. Increase in IL-6, IL-1, and TNF levels in rat brain following traumatic lesion: Influence of pre- and posttraumatic treatment with Ro5 4864, a peripheral-type (p-site) benzodiazepine ligand J Neuroimmunol 42:177-186; 1993.

77. Choi M, Rabb H, Arnaout MA, Ehrlich HP. Preventing the infiltration of leuckocytes by monoclonal antibody blocks the development of progressive ischemia in rat burns. Plast Reconstru Surg 96:1177-1185;1995.

78. Kurdowska, A., Miller, E.J. Cohen, A.B. An anti-interleukin 8 monoclonal antibody tha interferes with the binding of interleukin 8 to cellular receptors and the activation of human blood neutrophils. Hydbridoma 14:225-233;1995.

79. Olney, J.W., Ho, O.L., Rhee, V. Cytotoxic effects of acidic and sulpher-containing amino acid on the infant mouse central nervous system. Exp. Brain Res. 14:61-76;1971.

80. Choi, D. Ionic dependence of glutamate neurotoxicity. J. Neurosci. 7:369-79;1987.

81. Stewart, L. Bullock, R., Jane, M. Teasdale, G.M. The cerebral hemodynamic and metabolic effect of CGS 197555 in humans with severe head injury. J. Neurotrauma 10:S104;1993.

82. Solberg Y, Belkin M, Rosner M MK-801 has neuroprotective effect in retinal laser lesions Invest Ophthalmol Vis Sci 37:S694; 1996

83. McManus 86 McManus, L.M. Pathobiology of platelet-activating factors. Pathol. Immunopathol. Res.5:104-117;1986.

84. Bazan, N. A signal terminator. Nature 374:510-502;1995.

85. Frerichs, K.U, Feuerstein, G.Z Platelet-activating factor: key mediator in neuroinjury? Cerebrovasc. Brain Metab. Rev. 2:148-160;1990.

86. Smith, D., Lee, E.K., Saloupis, P., Davis, J.K., Hatchell, D.L. Role of neutrophils in breakdown of the blood-retinal barrier following intravitreal injection of platelet-activating factor. Exp Eye Res. 59:425-432;1994.

87. Frerichs, K.U., Lindsberg, P.J., Hallenbeck, J.M. and Feuerstein, G.Z. Platelet-activating factor and progessive brain damage following focal brain injury. J. Neurosurg. 73:223-233;1990.

88. Shapira Y, Yadid G, Cotev S. Shohami E. Accumulation of calcium in the brain following head trauma. Neurol Res. 11:169-171;1989.

89. Schurr, A., Payne, R.S, Rigor, B.M. Synergism between diltiazem and MK801 but not APV in protecting hippocampal slices against hypoxic damage. Brain Res. 684:233-236;1995.

90. Vink R, and McIntosh TK. Pharmacological and physical effects of magnesium on experimental traumatic brain injury Magn Res 3:163-169;1990.

91. Lindquist S, and E.A. Craig EA The Heat Shock Proteins Ann. Rev. Genet. 22:631-677, 1988.

92. Pelham HRB. Heat Shock Proteins, Coming in from the Cold, Nature 332: 776-777, 1988.

93. Barbe MF, Tytell M, D.J. Gower, DJ, and Welch WJ Hyperthermia Protects Against Light Damage in the Rat Retina. Science 241, 1817-1820, 1988.

94. Deaton MA, Odum DG, Dahlberg AM, Lester P, Cowan BL, Lund DJ. Increased synthesis of heat shock proteins and partial protection of the retina against the damaging effects of argon laser irradiation. Lasers in the Life Sciences 3:177-185;1990.

95. Schuschereba ST, Bowman PD, V. Ujimori V, Hoxie S, Cross ME, and Lund DJ Cytokine mRNA synthesis in mouse retina after laser injury by reverse transcriptase polymerase chain reaction (RT-PCR). In Laser-Inflicted Eye Injuries: Epidemiology, Prevention, and Treatment. Bruce E. Stuck, Michael Belkin, and Abraham Katzir. Editors, Proc. SPIE 2674:146-156; 1996.

The *Shalon* Ballistic, Sun, Wind, Dust and Laser Goggles

Michael Belkin

Goldschleger Eye Research Institute, Tel Aviv University,
Tel Hashomer 52621, Israel

ABSTRACT

We designed, manufactured and field-tested new combat protection goggles which endow their users with optimal protection against ballistic injuries as well as against dust, sand and wind. A laser protection filter can be snapped on the ballistic goggles. Filters can be provided for any required wavelength.

The goggles are of a warp-around shape ensuring peripheral as well as frontal protection. It is "one size fit all" design with the least possible clearance between eye and lens so as to cause minimal interference with the use of optical equipment such as binoculars. There is an integral insert for prescription lenses inside the goggles. The head bands are self locking and putting the goggles on and off with or without a helmet on is easy.

Key words: eye protection, laser protection, eye injuries, combat, polycarbonate, visual fields, goggles.

This item of protective equipment attempts to overcome optimally the deficiencies noted in all the old type of ballistic goggles, as well as to provide the possibility of laser protection.

The Shalon goggles are based on the design concept of a basic platform that provides ballistic, dust, sand and wind protection. The primary eyepiece is made of 4 mm thick polycarbonate that can prevent almost all relevant ballistic eye injuries. Its V_{50} is over 1200 feet/sec when tested with a 2 grain projectile. The eyepiece will stop

all shrapnel-type missile of any size. The potential injurious agents which are not likely to be stopped completely are rifle and other high-velocity bullets.

The polycarbonate eyepiece is a spherical injection molded lens which meets exact optical specification. The mold is so designed that the eyepiece induces negligible parallax in any direction of gaze. The optical power at any point on the lens is less than 0.125D, the horizontal prism imbalance is less then 0.18D base-in, both in horizontal and vertical meridians and less than 0.75D base-out in the horizontal meridian. The astigmatism is less than 0.0825D and there is no visible distortion. The same optical specification apply to the various filters that can be attached to the goggles. The visible light transmission of the goggles, integrated between 380 and 740 nm, is over 85%. There is less than 1% UV transmission (between 280 and 380 nm) and then is no more than 2% haze. The polycarbonate lenses are hard-coated to prevent scratching.

The lens is incorporate in a frame made of two elements - a rigid plastic frame with flexible lateral ends with the strap retainers and a pliable elastomere frame with corrugate temporal zones to fit different facial sizes and contours. This design enables the goggles to be "one size fit all" as well as comfortable. The lens and frame are of a "warp around" design ensuring both frontal and peripheral protection. The design also ensures perfect dust protection even under the most inclement conditions.

Another feature of the eyepiece - frame ensemble is the lack of limitation of the normal visual field. The constriction of the visual filed by older goggles is one of the main causes of their inacceptance. The Shalon goggles were tested extensively on the Esterman program of the Humphrey field analyzer and found not to inpede the visual field in the primary direction of gaze and minimally in the secondary directions.

The goggles are designed with a minimal vertex distance between the apex of the cornea and the eyepiece. This feature enables the use of optical instruments such as binoculars with the goggles in place protecting the eyes. The interference of old-fashion goggles with the visual field of optical equipment was one of the chief causes of their inacceptance.

The Shalon goggles are well ventilated by ports with a labyrinth design within the plastic frame. Thus adequate ventilation is provided with no dust penetration without the use of maintenance-requiring dust filters. Another cause of non-use by the

customers' was fogging inside the goggles. This is overcome by the inside surface of the eyepiece being coated with antifogging material.

For ametropes there is a specially designed prescription lens holder behind the eyepiece with attachment to the nose bridge. Even with high minus lenses no optical aberrations over 0.25D are engendered.

The retaining straps were also designed to afford the user with optimal flexibility and convenience of use. There is both a headband suspension to be used under the helmet and an over-the-helmet strap. Both systems allow the soldier to remove and re-wear the goggles easily and freely while using any type of helmet.

Laser Protection

The laser protection problem is solved by adding means for attaching a frontsert laser filter. The goggles have a socket which accepts the appropriate secondary frontsert filter which has an attachment prong that snaps into the socket. The attachment and removal of the forntsert filter can be easily and rapidly performed by the soldier in the filed. The line of contact between the main eyepiece and the frontesert is dust-proof. This arrangement makes it possible to provide the soldier with any number of laser protective filters to protect against laser radiation in any part of the spectrum.

The overall laser protection concept is similar in principle to the chemical/biological warfare protection practices, i.e. the protection is used only when indicated, so as not to interfere with the soldier's combat duties when not threatened by laser irradiation. It must be remembered that all laser filters blocking part of the visible spectrum interfere considerably with soldiers' vision especially at twilight and dawn.

Any configuration of laser protection can be provided according to expected laser usage on the battlefield. All filters conform to the same standards as the primary lens.

A sunshield filter can be attached in front of the polycarbonate eyepiece instead of the laser filter. The goggles underwent rigorous field testing in armored and infantry units and were found to serve very satisfactory with almost complete troop acceptance. They are now the regular combat eye protection of the Israeli military.

SESSION 6

Laser Safety in Medicine

Institutional safety certification of a research class IV laser for clinical photodynamic therapy

Jon A. Schwartz, Sharon L. Thomsen, Erle Janssen,
Sharon Erickson, Daniel E. Supkis, Jr.

Laser Biology Research Laboratory
University of Texas/M.D. Anderson Cancer Center, 17
1515 Holcombe Blvd., Houston, Texas 77030

ABSTRACT

In preparation for photodynamic therapy (PDT) clinical trials, a research class IV argon ion-pumped dye laser (Coherent Innova 90/CR-599) was modified to allow delivery of laser radiation from the Laser Biology Research Laboratory (LBRL) to a surgical operating room (OR) located one floor below and over 50 meters away. Optical fibers and coaxial cable, protected by flame retardant conduit, were fed from the LBRL to the OR. A remote control box was constructed to allow physician control of the laser output from the OR. A Safety-Off and Output-Power Control were included in the control system. Safety issues involved calculations of maximum permissible exposure of OR staff to optical radiation, the classification of the laser output in the OR and dealing with the placement of relatively high-flux carrying optical fiber placed in utility chases. Operational considerations involved the calculation and measurement of optical transmission losses, the procedure for relaying operational status between the OR and laser facility and the necessity of conducting practice runs with the laser and OR staff.

Keywords: photodynamic therapy, laser safety, eye safety, threshold limit value (TLV)

1. INTRODUCTION

Photodynamic therapy involves the prolonged exposure of a patient's visceral lumina or skin surface to relatively high power, generally class IV, laser irradiation. This necessarily involves considerations of laser safety[1], particularly eye safety, for the patient and clinic staff. These safety issues overlap operational considerations in cases where the PDT treatment facility is separate from the laser facility.

For some medical facilities, particularly research facilities where many different types of treatment are being tested, or where lasers have been purchased for research work that must make a transition to clinical trials, it may not be possible to have a dedicated PDT laser within the treatment room. In such cases it is typical to try to make a research laser, located in a remote laboratory, act as the light source for PDT. This raises control and communication issues as well as coordinated safety issues for two different sites.

SPIE Vol. 2974 • 0277-786X/97/$10.00

One advantage that accrues to such an arrangement is that the electrical, mechanical, plumbing issues can be kept away from the patient treatment room and handled essentially as they are in any laboratory facility. The main safety issues revolve around the transmission of class IV laser light through utility chases of a patient care facility and the delivery of class IV laser light into a patient care room. The laser eye safety within the laser room and the patient treatment room have to be handled as a simultaneous event. Control of the laser will originate within the laser room, be handed over to the clinician at some point, and then relinquished back to the laser room after the procedure.

2. SYSTEM OVERVIEW

The use of a research laser for clinical purposes allows for flexibility, i.e., the ability to do a wide variety of different procedures, but research lasers are typically more complicated to operate and contain more optional hardware than dedicated clinical lasers. Scientific lasers generally allow for ease of access to optics and electronics and have a large number of controls for output power, wavelength tuning, modes of operation, etc. This is a drawback in clinical settings where unnecessary control options can easily lead to mistakes and confusion, and where repeatability is more important than versatility. Reliable operation of a scientific laser system really requires a competent laser technician. Even experienced laser nurses are not trained to work in a mode where they do extensive manipulations of lasers. Simpler, clinical lasers are available, but may not provide the flexibility that running several different research protocols require, or may not be available at the outset of clinical trails. Additionally, a large laser system will typically have to be in a fixed position owing to the need for specialized electrical and water handling requirements. This is the situation we will address in this paper. Figure 1) shows a schematic of the major components of a separated PDT facility. Functionally, we divide the overall facility into a laser facility, a treatment facility, and the interconnecting utility chase.

Optical fiber permits high-power laser light to be transmitted over distances of up to 100 meters or so from one site to many. In general, it is not a good idea to try to maintain multiple PDT treatment rooms if patient scheduling can at all be accommodated for a single room. Optical fiber makes it deceptively easy to deliver laser light to any number of rooms, but in practice the laser can be delivered to only one room at a time anyway. Additionally, each laser treatment room has to be equipped with all of the appropriate laser warning signs and door interlocks and these must be coordinated with the laser personnel who need to be able to activate the appropriate room's interlocks. The question has to be asked: Is the facility willing to maintain duplicate remote control boxes, duplicate sets of laser eyewear, duplicate power meters and such? If not, then there really is no point in equipping more than one treatment room per laser system.

The installation of a PDT facility needs to be under the guidance of an institutional laser safety committee that includes: 1) the clinicians and nurses who will to advise on how the system is to be used by the staff with patients, 2) the laser safety officer who assumes overall responsibility

for the safe operation of the laser, and 3) the engineers who must arrive at a solution for meeting the needs of the others. This is really just a formal way of emphasizing that the users and safety people need to concur on what the PDT system is to do and how it should be installed and operated.

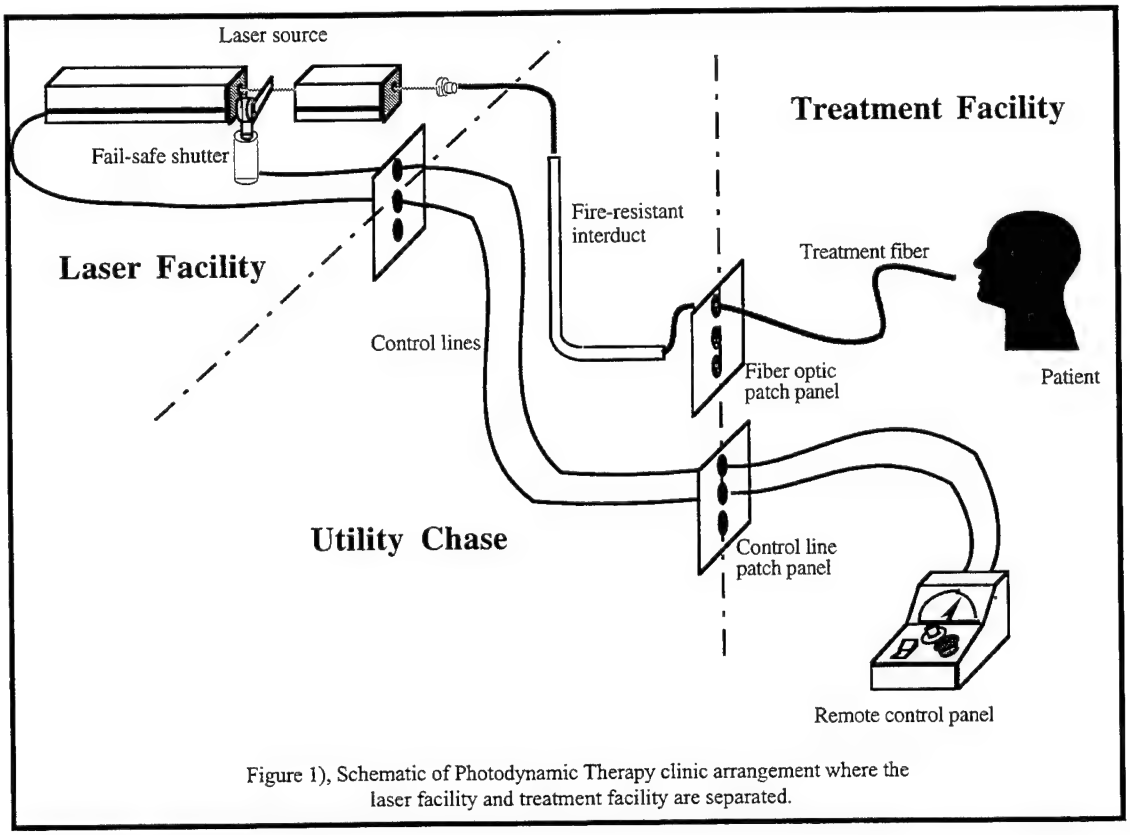

Figure 1), Schematic of Photodynamic Therapy clinic arrangement where the laser facility and treatment facility are separated.

3 SAFETY ISSUES; INSTALLATION

3.1 Communication

In a situation where the laser source and the clinical procedure room are separate there is a need for the clinic personnel to inform the laser personnel about: 1) the anticipated procedure start and stop times, 2) the approximate power settings required, 3) the wavelength required (if that is not standard), 4) which clinic room is to be used if there are multiple rooms available, and 5) to inquire about problems if the laser output changes unexpectedly. The laser personnel need to inform the clinic personnel when the laser is ready (dye systems typically have to be cooled down and to run for a few minutes before the power and mode structure stabilize). This situation requires that the clinic procedure room and laser room be able to communicate without interruption. The best way would be to have an intercom system between the two rooms, or an institution-approved walkie-talkie. A phone line is also useful, but clinics also need to call for orderlies, drugs, pathology reports, etc., so a continuously open telephone line is not practical.

Also not practical in the near term is the use of cellular phones since these have been shown to cause interruption in delicate electronic systems such as those used in clinics and operating rooms.

3.2 Laser control

There are two distinct phases in the clinical use of a remotely located laser: the preparatory and the therapeutic. The preparatory phase is under the control of the laser operator who must assure that the laser system is operating as planned. The therapeutic phase is under the control of the clinic personnel who must verify the power output and stability of the system and control the laser on/laser off function into the clinic room. The two situations call for communication as discussed above and require the ability to hand over control of the laser from local (the laser room) to remote (the clinic). A remote control box, as shown in Fig. 1) is needed to permit the clinician to control the laser. Laser personnel must be available to give laser control to the clinician and take back control when the clinician is finished with the laser.

No physician wants to depend on waiting for the laser operator to receive a message to de-activate the laser, or have to pull the fiber from the patient suddenly in order to terminate a procedure in some emergency. This means that dedicated control lines will have to be run from the laser to each clinic room and the appropriate connections verified prior to treatment. As mentioned elsewhere, these control lines should not be run with, or in intimate contact with the optical fiber that is carrying the photodynamic light. One can run 50Ω coaxial lines for laser systems equipped for analog remote control, or shielded, twisted-pair for digital remote control. In both cases, pre-amplification at the remote end or regeneration at the laser end may be necessary depending on the distance separating the two rooms.

PDT procedures typically are long enough that a foot pedal is not practical. A switch with a non-red illuminated "ON"" indicator will normally be used on the remote control box, remembering that red indicators will not be readily visible to anyone wearing eyewear designed to block red PDT radiation. The switch, and an "Emergency Off" button, should operate some fail-safe device on the laser such as a spring-loaded shutter as illustrated in Fig. 1).

3.3 Fire protection and firewall penetration.

The several watts of power required for PDT contained within an optical fiber is capable of causing a fire should the fiber break unexpectedly. For example, 1 W transmitted in a 600 μm diameter fiber yields a fluence of 354 W/cm^2 within the fiber. Clinic personnel should be in a position to identify breaks in the treatment fiber in the clinic procedure room, and the laser operator should be able to identify breaks that occur in the laser room. For separated systems as illustrated in Fig. 1) the optical fiber will have been pulled between the two rooms creating the possibility of a fracture in the optical fiber that could, with use, develop into an actual break.

Attention, then, needs to be paid to the rated pull strength of the jacket of the optical fiber before purchase. After installation, an optical time domain reflectometer (OTDR) can be used to identify any discontinuities in the fiber's loss profile. Installing, and pulling the optical fiber through a fire-resistant, plenum-rated raceway or "interduct" is recommended for several reasons: 1) on the off chance that a fracture in the fiber fails and turns into a break, the interduct will prevent anything in the vicinity of the break from igniting, 2) the fiber will be partially protected from fires from other sources, 3) a fire-resistant interduct will maintain the integrity of any fire walls that inevitably have to be penetrated, and 4) perhaps most cogently, the fiber will be protected from damage by the multitude of other cables and conduits that are always being installed and removed from utility chases.

Since one purpose of the interduct is to prevent a sudden failure of the optical fiber from causing any additional damage, the remote-control lines for the laser should be run external to the fiber interduct. This has the effect of isolating control of the laser from problems caused by the laser.

3.4 Eye safety issues.

The ANSI Z136.3-1996 standard[2] defines a continuous-wave laser emitting in the 400-700 nm regime as class IV if it emits 0.5 W or more. Most PDT applications, then, will involve class IV laser radiation entering the clinic treatment room, and the safety precautions (signage, access control, etc.) have to reflect this. For example, 1 W transmitted through a 600 μm diameter, step-index fiber has a fluence of 354 W/cm^2 within and at the exit of the fiber. Thus, the optical fiber carrying PDT levels of optical radiation counts as class IV equipment and has to be sustained as such.

Any time different laser wavelengths are used in a facility, care must be taken to provide eyewear that covers all of the laser radiation spectrum. Just as important, and much more likely to be a problem, is that, if a number of wavelengths are available, the clinic staff must be provided with eyewear for each specific procedure. Severe eye injuries have resulted to clinicians who were given incorrect eyewear.

Figure 2) shows a comparison of the optical density (OD) of laser eyewear typically used for protection from Krypton and HeNe lasers. Both offer good protection in the red where most PDT excitation is done. The Krypton eyewear offers 0.5 OD more absorption at the 633 nm

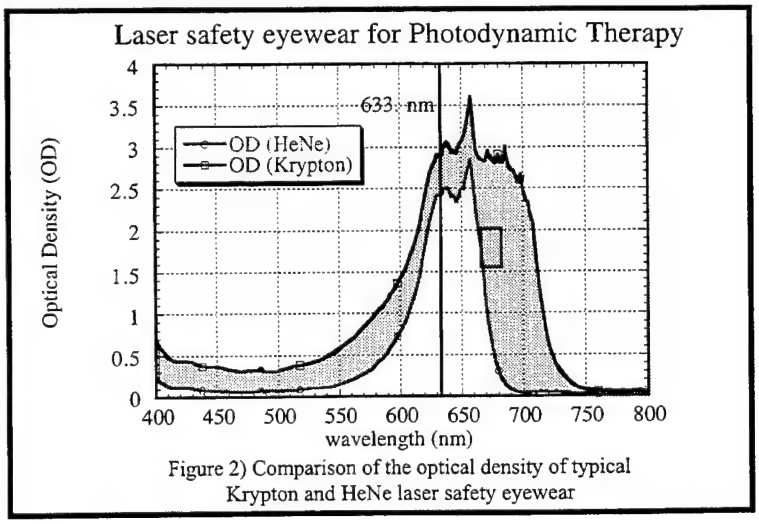

Figure 2) Comparison of the optical density of typical Krypton and HeNe laser safety eyewear

line typically used for porphyrin-based PDT and, in fact, has an OD >2.5 over the range 620-700 nm. This renders red indicator lamps effectively invisible; they appear un-illuminated. The HeNe eyewear covers a much narrower band, and is hence less versatile, but red indicator lamps can still be seen, albeit at reduced intensity. Audible alarms should be considered where red indicators such as on anesthesiology monitors denote some emergency condition. As illustrated in Fig. 3), HeNe eyewear with an OD of 2.4 at 633 nm should be adequate for most PDT procedures.

Similar bandpass filters need to be installed on the eyepieces of other optical equipment such as the endoscopes or bronchoscopes used to place PDT optical fibers, unless the PDT fiber insertion will be done exclusively by camera.

3.5 Treatment room access

Since the laser facility personnel control the time at which the laser is energized and to which room the laser is directed, these personnel need to have the control switch that activates the laser warning signs on the appropriate clinic rooms. The clinic staff will also have the control box in the treatment room to enable the laser for test, calibration, and treatment. Laser warning signage at the clinic treatment room should be illuminated from the laser facility and note the wavelength and power levels possible per ANSI Z136.3-1996.

4 SAFETY ISSUES - OPERATIONAL

4.1 Trained personnel.

Laser training courses are offered through a number of organizations and companies. Any personnel working extensively with lasers of any sort and, particularly, supervisory personnel should be availed of these courses. Clinic personnel training must include a successful practice run with the laser on to familiarize personnel with: 1) procedures of laser control, 2) the character of the irradiation, and 3) the appearance of the clinic room, particularly control panels and indicator lights when viewed through the laser safety eyewear. Another factor, difficult to quantify or test for is insight. Inevitably, a situation will arise in the clinic that is not covered by established procedure. Airway and anesthesia complications have been known to happen, and laser power settings have been known to drift. In such situations, prior training and familiarity with the equipment is essential, but so too is an understanding of how the laser beam is blocked and how light travels in optical fiber and what observed effects can and cannot be caused by particular equipment.

Figure 3) shows the Threshold limit values for ocular exposure for 1Watt emitted from a step-index optical fiber having a numerical aperture of 0.37. The graph assumes normal boresight exposure from the fiber that emits light with a Gaussian transverse distribution.

The Threshold Limit Values (TLV)[3] for ocular exposure for a cw laser operating at 633 nm is illustrated by the cross-hatched region of Fig. 3). Superimposed on this graph are irradiances produced by 1 W emitted from a flat termination of a 600 μm diameter optical fiber having a numerical aperture of 0.37. Equation (1) is used to determine the ocular irradiance at distances of 10, 25, and 50 cm from the fiber tip.

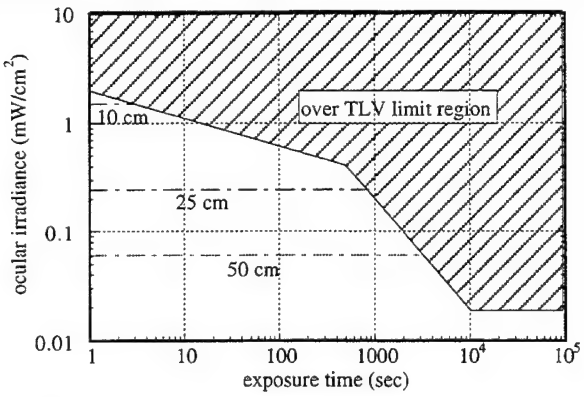

Figure 3) Permitted ocular exposure from an optical fiber pointed directly at an eye protected by a filter of OD2.4 from a distance of 10, 25, and 50 cm. (1 W output from fiber, 633 nm)

$$Irradiance = \frac{P}{A}\left(mW/cm^2\right) = \frac{P \bullet T \bullet 4.075}{A}\left(mW/cm^2\right) \quad (1)$$

where: P = power (mW) exiting from fiber terminus

T = optical transmission of the safety eyewear, (0.00398 @ 633 nm)

4.075 = peak-to-average intensity for a Gaussian beam profile

A = area subtended by the laser beam (cm^2) $= \left(\frac{\pi}{4}\right)\theta^2 r^2 \left(cm^2\right)$

and where: θ = beam divergence from the optical fiber (radians) = 0.37

r = distance from fiber terminus to eye (cm)

5. SUMMARY

Safety planning at the time of operational installation planning has to be done in order to prevent foreseeable unsafe conditions from arising and to obviate the need for expensive retrofitting of hardware later. A priori considerations of safety will greatly reduce the cost of installing and operating a PDT facility. As in all other activities, however, safe operations can be carried out only as long as all of the staff are trained and conscientious about following procedures. In addition, they need to understand underlying principles sufficiently to know when written procedure doesn't cover a new situation and must be superseded in the interests of safe operation.

6. ACKNOWLEDGMENTS

The authors gratefully acknowledge the Department of Energy which provided funding for equipment used in the installation of the PDT facility at M.D. Anderson, (grant #DE-FG03-

95ER61971/A001) and Mr. Ron Davis of Communications & Computer Services at M.D. Anderson Cancer Center for providing safety equipment technical information.

7. REFERENCES

[1] D.H. Sliney and S.L. Trokel, "Medical Lasers and Their Safe Use". Springer-Verlag New York, Inc., ISBN 0-387-97856-9, 1993.

[2] American National Standard for Safe Use of Lasers in Health Care Facilities, ANSI Z136.3-1996, The Laser Institute of America, Orlando, FL 32826, 1996.

[3] Threshold Limit Values (TLVs) form Chemical Substances and Physical Agents and Biological Exposure Indices (BEIs), ACGIH Worldwide, ISBN: 1-882417-11-9, pp. 96-103, 1995-1996.

Laser safety considerations for a mobile laser program

Mary Flor

TransOne Advanced Mobile Healthcare Technologies
Abbott Northwestern Hospital, Minneapolis, Minnesota 55407

ABSTRACT

An increased demand for advanced laser technology, especially in the area of cutaneous and cosmetic procedures has prompted physicians to use mobile laser services. Utilization of a mobile laser service allows physicians to provide the latest treatments for their patients while minimizing overhead costs. The high capital expense of laser systems is often beyond the financial means of individual clinicians, group practices, free-standing clinics and smaller community hospitals. Historically rapid technology turnover with laser technology places additional risk which is unacceptable to many institutions. In addition, health care reform is mandating consolidation of equipment within health care groups to keep costs at a minimum. In 1994, Abbott Northwestern Hospital organized an in-house mobile laser technology service which employs a group of experienced laser specialists to deliver and support laser treatments for hospital outreach and other regional physicians and health care facilities. Many of the hospital's internal safety standards and policies are applicable to the mobile environment. A significant challenge is client compliance because of the delicate balance of managing risk while avoiding being viewed as a regulator. The clinics and hospitals are assessed prior to service to assure minimum laser safety standards for both the patient and the staff. A major component in assessing new sites is to inform them of applicable regulatory standards and their obligations to assure optimum laser safety. In service training is provided and hospital policies and procedures are freely shared to assist the client in establishing a safe laser environment. Physician and nursing preceptor programs are also made available.

Keywords: Policies, procedures, mobile laser, laser safety, laser safety officer, regulatory standards, ANSI, TransOne.

1. Policies and Procedures

The laser safety policies and procedures of the hospital have been extended to include all activities of the mobile laser service thorough a unifying document as follows:

TransOne Advanced Mobile Health care Technologies

Title:	Guidelines and Protocol, Laser Treatment Policy and Procedure
Source:	TransOne Program Manager
Approval:	Administrative Director of Outpatient Services
Rationale:	To ensure safe and appropriate care of mobile program patients receiving treatments through TransOne mobile laser services.

SPIE Vol. 2974 • 0277-786X/97/$10.00

Policy: TransOne Mobile Systems Specialists shall comply with all laser policies and standard operating procedures as established by Abbott Northwestern Hospital. TransOne Mobile Systems Specialists shall comply with laser technician competency standards established by Abbott Northwestern Hospital.

Limitations: It is the responsibility of each mobile client facility to establish credentialing standards for the physician(s) who with to provide laser treatments utilizing equipment provided by TransOne. The physicians shall select laser settings (power, duration, treatment mode) and determine the manner of treatment desired. It is the responsibility of each mobile client facility to comply with applicable regulations and standards as established by JCAHO, OSHA, ANSI or other governing bodies.

2. CONTRACT/SITE ASSESSMENT

As of this writing, the formal laser mobile service contract is still under legal review. The critical components of this contract will include defining the mobile laser service duties and limitations, client responsibility, physician credentialing, billing arrangements, liability coverage, and scheduling. This contract reflects key concerns identified from our site visits.
The site assessment worksheet serves as an assessment vehicle to determine client readiness and safety issues. In addition to basic client information (name, address, etc.), the assessment sheet includes:

Contacts:
- Physicians/Nurse/Scheduler
- Nurse Supervisor
- Safety Officer/Laser Safety Officer
- Medical Staff Office
- Administrator
- Engineering/Security

Assessment/ Requirements:
- Physicians: Specialty/Wavelength Credentials
- Laser Education for staff, including
- Basic Physics, Safety and Tissue Interaction
- Pre and Post Procedure Education
- Laser Policies and Procedures

When the assessment is complete, we assist the facility to comply with the requirements of federal regulators such as OSHA and the standards established by ANSI and JCAHO. It is clearly communicated that it is the facility's responsibility to meet these requirements and that we are an available resource. When the site assessment is completed, and the facility has reviewed and agreed to the terms of the service contract, it is clearly understood through verbal notice and documented who has what responsibility. For example, it is the facility's responsibility to credential their physician for wave-length specific laser use. It is the mobile laser service's responsibility to verify that the physician has established laser priveledges. Additional examples of the mobile laser services responsibilities include maintenance of all lasers in safe working order and providing trained and competent laser specialists.

3. QUALITY ASSURANCE

3.1 QUALITY INDICATORS

The TransOne mobile laser service reports to and fully participates in the Quality Monitoring (QM) program of Abbott Northwestern Hospital. After one year's experience we have recognized that quality indicators utilized in a hospital environment are often not applicable to the mobile laser services provided because there is no direct patient care provided by the laser specialist. We are currently evaluating alternative QM indicators and are developing a satisfaction survey for our clients to fill out after each visit. Included in this survey will be questions specific to measure safety compliance by the laser specialist. These surveys will be reviewed and recorded by the QM Committee.

3.2 DOCUMENTATION

The mobile laser service staff is responsible for all documentation regarding the laser procedure. This document reflects the recommendation from ANSIZ136.3-1996. The document is provided in triplicate; one copy each for the patients chart, facility's log book, and the mobile laser service logbook.

ACKNOWLEDGMENTS

This report was prepared with the cooperative efforts of Paul Plumb, TransOne Program Manager.

REFERENCES

1.American National Standard for the Safe Use of Lasers in Health Care Environment. Z136.3 -1996, The Laser Institute of America, Orlando, 1996.

Laser initiated decomposition products of indocyanine green (ICG) and carbon black sensitized biological tissues

John M. Kokosa and Andrzej Przyjazny

GMI Engineering & Management Institute, Flint, MI 48504

Kenneth Bartles

Oklahoma State University, Stillwater, OK 74078

Massoud Motamedi

University of Texas Medical Branch at Galveston, Galveston, TX 77550

Donald C. Hayes and David B. Wallace

MicroFab Technologies, Inc, Plano,TX 75074

Christopher Frederickson

University of Texas at Dallas, Richardson, TX 75083

ABSTRACT

Organic dyes have found increasing use as sensitizers in laser surgical procedures, due to their high optical absorbances. Little is known, however, about the nature of the degradation products formed when these dyes are irradiated with a laser. Previous work in our laboratories has shown that irradiation of polymeric and biological tissues with CO_2 and Nd:YAG lasers produces a host of volatile and semivolatile by-products, some of which are known to be potential carcinogens. This work focuses on the identification of the chemical by-products formed by diode laser (805 nm) and Nd:YAG (1.06 μm) laser irradiation of indocyanine green (ICG) and carbon black based ink sensitized tissues, including bone, tendon and sheep's teeth. Samples were mounted in a 0.5-L Pyrex sample chamber equipped with quartz optical windows, charcoal filtered air inlet and an outlet attached to an appropriate sample trap and a constant flow pump. By-products were analyzed by GC/MS and HPLC. Volatiles identified included benzene and formaldehyde. Semivolatiles included traces of polycyclic aromatics, arising from the biological matrix and inks, as well as fragments of ICG and the carbon ink components. The significance of these results will be discussed, including the necessity of using appropriate evacuation devices when utilizing lasers for surgical procedures.

Keywords: indocyanine green, carbon black, dyes, laser, chemical by-products, benzene, formaldehyde

1. INTRODUCTION

The use of lasers for surgical applications has found broad acceptance, due to its many advantages, including precision and speed. However, there are also potential disadvantages to using lasers for surgery, including ocular damage, the possibility of bacterial or viral transmission through the plume, and the generation of hazardous chemical products during the laser initiated decomposition of tissue.[1-5] Ocular damage has been minimized through the use of appropriate light filtering goggles and viral/bacterial transmission has been managed through the use of smoke evacuation devices. Chemical by-product hazards , evidenced by the smell associated with laser tissue cutting, have also been reduced through the use of efficient smoke evacuation devices. Thus, most of the potential hazards to operating personnel have been eliminated or reduced through the use of appropriate safety measures. The question of potential harm to patients by the formation of hazardous chemicals is still to be resolved, however.

Ott, for instance, has shown that smoke formed during laser surgery within the peritoneal cavity, is quickly absorbed into the patient's bloodstream, causing elevated methaemoglobin levels.[6] There is one additional practical problem associated with the use of lasers: the efficiency of laser light absorption. Lasers produce light in various regions of the spectrum, ranging from the ultraviolet (excimer lasers, 180 - 350 nm) to the near infrared (Nd:YAG, 1.06 μm) to the mid infrared (CO_2, 10.6 μm). Unfortunately, no single laser wavelength is suitable for all biological tissues, due to varying water content, chemical make-up and the susceptibility to thermal damage.[1] One method, becoming increasingly popular for enhancing the absorption of the laser energy, is to apply a dye to the tissue surface. The dye chosen has a maximal absorption of light close to the operating wavelength of the laser. Thus, reduced laser energy operating levels are possible, with increased ablation efficiencies while reducing potential hazards from the laser beam and decomposition products. Indocyanine green (ICG) is one dye which has been used successfully as a photoenhancer for tissue welding.[7,8] ICG seems well suited for microsurgical procedures, since it possesses low toxicity and high optical absorbance at ~800 nm, where most biological tissues are relatively transparent. However, little is known about the degradation products of ICG, and their potential toxicity, when exposed to laser light.[9,10] The current study resulted from a desire to use ICG and a carbon black based dye as photoenhancers in microsurgical procedures utilizing a diode laser (805 nm) and a Nd:YAG laser (1.06 μm). The relative hazard, due to chemical by-product formation, posed by the interaction of the laser light with these dyes and the tissue was unknown. A study was therefore undertaken to determine the amounts of representative hazardous chemicals present in the resulting smoke plumes produced when dye enhanced tissues were irradiated.

2. MATERIALS AND METHODS

2.1 Tissue samples

The laser surgical procedures to be studied included cutting of the bones of the middle ear, ablation of spinal discal material, and removal of superficial dental caries. The middle ear bone was represented in this study by a chicken bone, coated with a dried 3% solution of ICG and cut with a Surgimedics Diomed 805 nm diode laser. The spinal discal material was represented by a similarly ICG coated pig tendon, again cut with the diode laser. The dental material was represented by sheep's teeth, coated with a proprietary carbon black based injet formulation dye and cut with an Americal Dental Technologies, Incisive Technologies Division Pulse Maser 1000U Nd:YAG medical laser (1.06 μm). In addition, reference samples were prepared by coating standard microscope slides with thin coatings of the ICG and carbon inks.

2.2 By-product collection

The samples were weighed immediately before and after laser cutting. Each sample was mounted in a 500-cc cylindrical Pyrex chamber (Figure 1) equipped with a quartz window, an activated carbon filtered air inlet (SKC Inc. charcoal sampling tube), and a sample collection tube. Air was drawn from the chamber into the collection tube at a constant velocity using a calibrated sampling pump (SKC Inc.). Volatile and semivolatile chemical by-products were first collected on activated charcoal tubes and ORBO-43 tubes (Supelco, Inc.), respectively. These tubes were then solvent extracted (CS_2) and analyzed by gas chromatography/mass spectroscopy (GC/MS). The solvent extraction technique, however, was not found to be sensitive enough and was subsequently replaced with an adsorption/thermal desorption tube (200 cc/minute collection) for analysis of both volatile and non-volatile components. Aldehydes were analyzed by collection on Supelco dinitrophenylhydrazine (DNPH) coated silica gel tubes at a sampling rate of 1 L/minute.

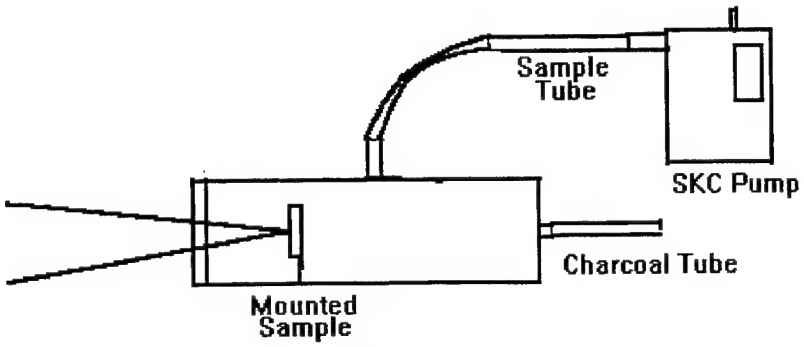

Figure 1. Sampling chamber used for sample irradiation and by-product collection

2.3 Laser operating parameters

The optic fibers for the diode and Nd:YAG lasers (400 μm diameter) had laser beam divergences such that it was necessary to use a quartz double condensing lens system (Figure 2) to focus the beam within the chamber. Actual spot size on the sample was 800 μm, decreasing the laser power density by 75%. Also decreasing laser power density was a 3% light reflection loss at each lens and window surface. The Nd:YAG laser was operated in the pulsed mode, 280 mJ at 25 Hz with approximately 5 W delivered to the sample. The diode laser was also operated in the pulsed mode, at a 0.5 second duration and a 0.1 second interval between pulses with ~ 6 W delivered to the sample. The sample chamber was mounted on an XY table and the sample then moved through the beam at a rate of 0.22"/second.

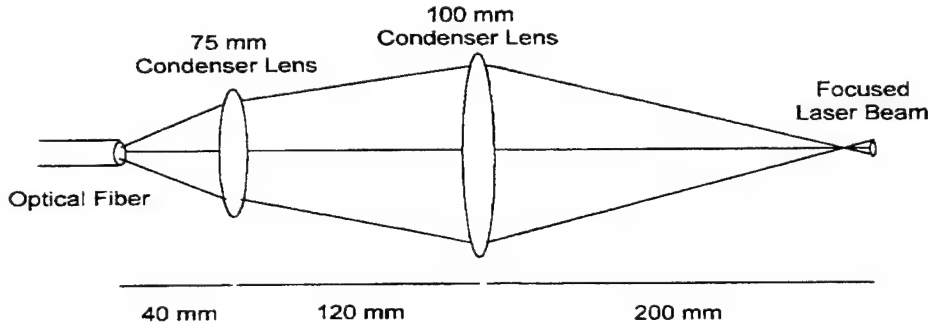

Figure 2. Condensing lens used to focus laser beam from the optical fiber onto the sample in the chamber

2.4 Aldehyde analyses

Aldehyde by-products were collected on Supelco DNPH sample tubes and analyzed by high performance liquid chromatography (HPLC). Two blanks were obtained for each set of samples collected by drawing an equivalent volume of air through the chamber onto the tube, with a sample mounted in the chamber. Each DNPH tube was eluted with 5.0 mL of HPLC grade acetonitrile into a 5-mL volumetric flask, and a portion subjected to HPLC analysis. The HPLC instrument used was a Waters 616 system with a Waters 996 photodiode array detector set at 360 nm and a 717 autosampler. The separation column was a Waters Nova-Pak C18 (150 mm x 3.9 mm, 4 μm diameter packing). Themobile phase flow was 1.0 mL/minute. Solvent A was acetonitrile : tetrahydrofuran : water, 30 : 10 : 60; solvent B, acetonitrile : water, 60 : 40. The gradient program used was 0 % B for 1 minute, followed by a linear gradient to 100% B over 10 minutes, and held at 100% B for 15 minutes. Under these conditions, separations were obtained for all but two aldehyde/ketone DNPH derivative standards (Supelco, Inc.): methacrolein and 2-butanone (Figure 3). Retention times for each standard are given in Table 1.

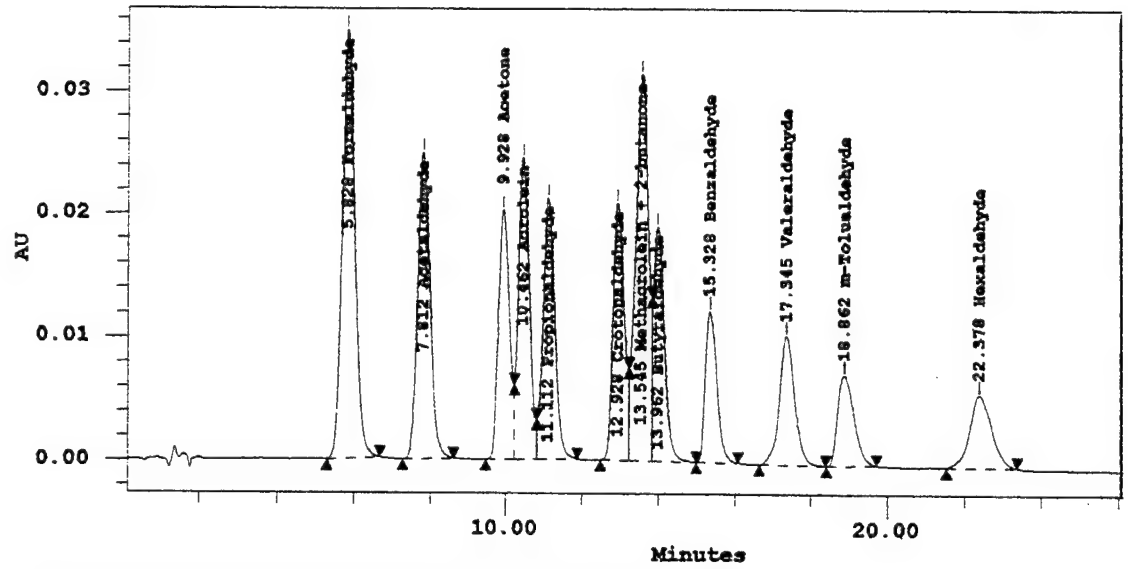

Figure 3. HPLC separation of aldehyde and ketone DNPH derivatives

Aldehyde/Ketone	HPLC Retention Time (min)
Formaldehyde	5.828
Acetaldehyde	7.812
Acetone	9.928
Acrolein	10.462
Propionaldehyde	11.112
Crotonaldehyde	12.928
Methacrolein + 2-Butanone	13.545
Butyraldehyde	13.962
Benzaldehyde	15.328
Valeraldehyde	17.345
m-Tolualdehyde	18.862
Hexaldehyde	22.378

Table 1. HPLC retention times for aldehyde/ketone DNPH standards in Figure 3

2.5 Volatile/semivolatile hydrocarbon analyses

Analysis for volatile and semivolatile hydrocarbons used a modification of the National Institute of Occupational Safety and Health (NIOSH) method 2549.[11] This involved trapping the by-products in a 4 inch x 1/4 inch diameter stainless steel adsorption tube (inner surface coated with Silcosteel, Restek, Inc) consisting of a three-layer adsorbent medium: Carbotrap C (300 mg), Carbotrap (200 mg) and Carbosieve S-III (125 mg) (Supelco, Inc). Two blanks were collected for each set of samples. Each tube was spiked with 1 µL of a methanol solution containing 181 ng of decafluorobiphenyl, which acted as an internal standard. Quantitative standards were obtained for benzene, toluene, ethylbenzene, o-, m, p-xylene (BTEX standards, Supelco, Inc) by injecting 1 µL methanol standards onto the trap. Semivolatile polycyclic aromatic hydrocarbon standards were also run separately to obtain their respective gas chromatographic (GC) retention times. The tube was mounted in a Tekmar 4000 purge and trap (PNT) device, modified to allow thermal desorption at 300 °C and interface line operation at 200 °C. Sample

tubes were purged for 1 minute with helium to remove air and methanol and then thermally desorbed at 20 cc/minute at 300 °C onto a Hewlett-Packard 5990 Series II GC interfaced to a HP - 5971A benchtop mass spectrometer (MS). The GC was operated with the split-splitless inlet purge on, 20 cc/minute, and septum purge 2 cc/minute. The PNT transfer line was connected through the inlet septum and supplied 20 cc/minute, the GC inlet an additional 2 cc/minute. With a column flow rate of 0.5 cc/minute, the split ratio was therefore 40 : 1. The chromatography column used was a HP-5, 25 m x 0.2 mm i.d. with a 0.25 µm column coating. GC oven parameters were as follows:10 °C for 4 minutes, ramped at 6°C/minute to 100°C, held at 100°C for 4 minutes, then ramped at 20 °C to 300 °C and held at 300 °C for 1 minute. MS acquisition began 6 minutes after initiation of desorption. A typical BTEX analysis, with a concentration of 400 ng for each BTEX component and 181 ng for decafluorobiphenyl is shown in Figure 4. The components and retention times for the BTEX mixture are given in Table 2.

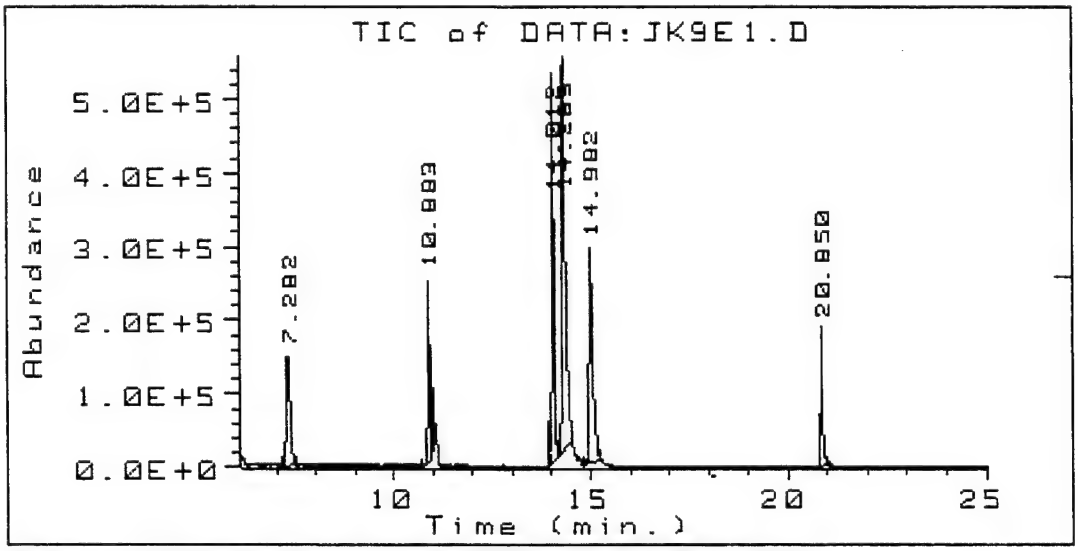

Figure 4. GC/MS total ion chromatogram for BTEX mix and decafluorobiphenyl

Component	Amount	Retention Time (min)
Benzene	400 ng	7.282
Toluene	400 ng	10.883
Ethylbenzene	400 ng	14.012
m-, p-Xylene	400 ng each	14.289
o-Xylene	400 ng	14.982
Decafluorobiphenyl	181 ng	20.850

Table 2. Components and retention times of BTEX and internal standard (GC/MS)

3. RESULTS

Previous analyses of laser generated by-products of biological samples indicated that a complex mixture of chemicals would be found in the samples studied in this work.[1,3] This was indeed the case. A typical example of a GC/MS trace for a carbon black ink coated tooth cut with the Nd:YAG laser is shown in Figure 5. Components include benzene, toluene, the xylenes and naphthalene (retention time 21.762 min). A typical HPLC trace for aldehydes and ketones obtained from a bone sample using the diode laser is shown in Figure 6.

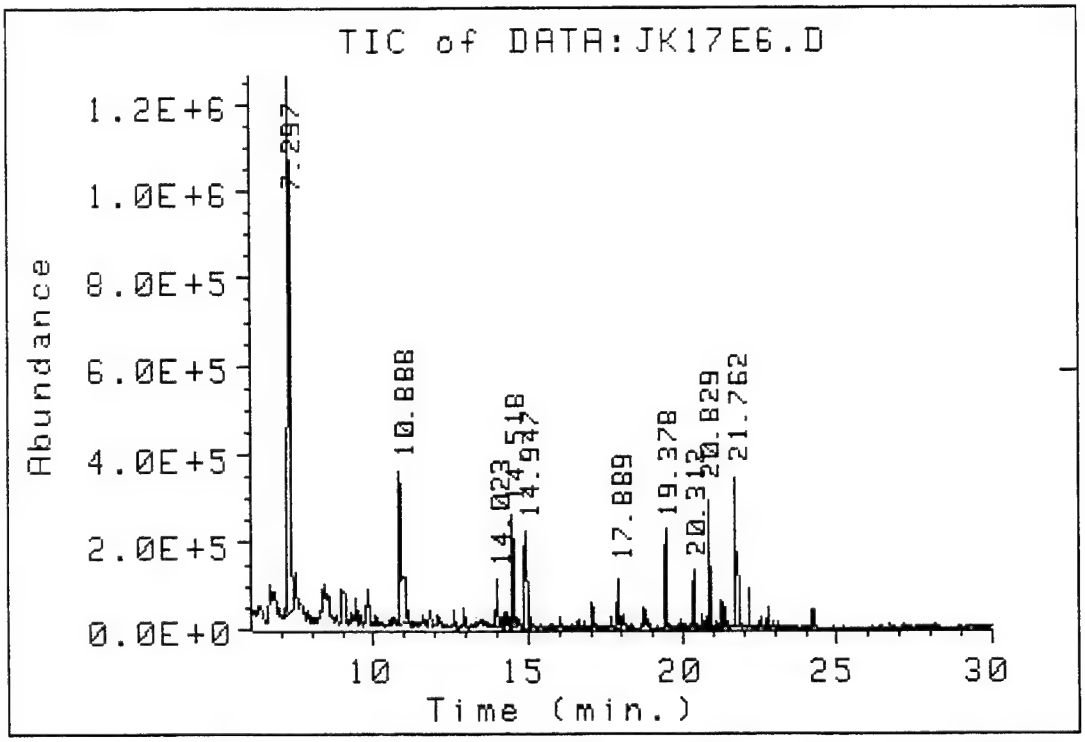

Figure 5. GC/MS chromatogram for hydrocarbon by-products obtained by Nd:YAG laser cutting a carbon black ink coated tooth

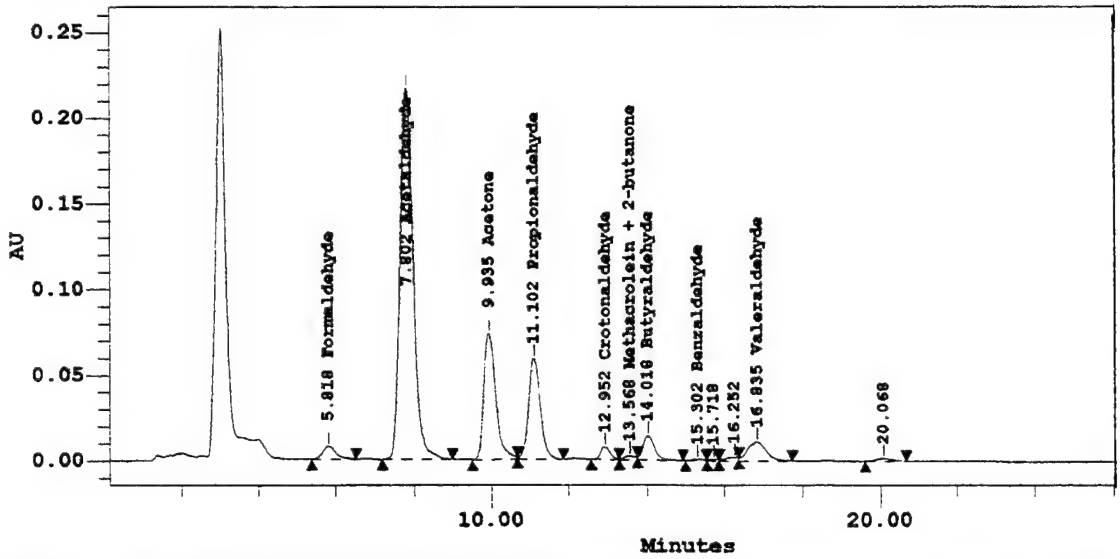

Figure 6. HPLC chromatogram for aldehyde and ketone DNPH derivatives obtained by diode laser cutting ICG coated bone

Table 3 summarizes the results obtained for the analyses of benzene and formaldehyde formed by cutting ICG and carbon ink coated slides with the diode and Nd:YAG lasers (average of two samples each), cutting bone and tendon samples coated with ICG and carbon ink with the diode laser (average of two samples each), and cutting teeth coated with carbon ink with the Nd:YAG laser (average of four samples).

Sample	Benzene ng/mg	(ppm/mg)	Formaldehyde µg/mg	(ppm/mg#)
slide/C*/D**	65	(0.02)	3.0	(2.4)
slide/I***/D	510	(0.16)	0.1	(0.08)
slide/C/N****	---	------	0.4	(0.4)
bone/C/D	572	(0.18)	3,6	(2.9)
bone/I/D	110	(0.03)	Not Detected	(Not Detected)
tendon/C/D	1.1	(5×10^{-4})	0.2	(0.2)
tendon/I/D	2.2	(3×10^{-5})	Not Detected	(Not Detected)
teeth	146	(0.04)	0.4	(0.32)

* carbon based ink, ** diode laser, ***ICG ink, **** Nd:YAG laser, # based on a volume of 1 L

Table 3. Average amounts of benzene and formaldehyde formed during cutting of tissues

For comparison, the complete listing of aromatic hydrocarbon and aldehyde/ketone compounds obtained from a tooth (GC/MS trace represented in Figure 5) and bone (HPLC trace in Figure 6) are listed in Tables 4 and 5.

Aromatic Hydrocarbon	GC/MS Retention Time (min)	Amount Detected (ng)
Benzene	7.297	1643
Toluene	10.890	319
Ethylbenzene	14.023	40
m-, p-Xylene	14.518	153
o-Xylene	14.947	170
Decafluorobiphenyl	20.829 (internal standard)	181

Table 4. Aromatic hydrocarbons obtained from one tooth sample (GC/MS trace Figure 5). Total material removed, 13.8 mg.

Aldehyde/Ketone	HPLC Retention Time (min)	Amount Detected (ng)
Formaldehyde	5.818	962
Acetaldehyde	7.802	39900
Acetone	9.935	17600
Acrolein	10.462	Not Detected
Propionaldehyde	11.102	12500
Crotonaldehyde	12.952	1240
Methacrolein + 2-Butanone	13.568	256
Butyraldehyde	14.018	3400
Benzaldehyde	15.302	277
Valeraldehyde	16.835	5610
m-Tolualdehyde	18.862	Not Detected
Hexaldehyde	22.378	Not Detected

Table 5. Aldehydes and ketones obtained from one bone sample (HPLC trace Figure 6). Total material removed, 5.2 mg.

4. DISCUSSION OF RESULTS

The significance of the results obtained in this study must be looked at in the context of the limitations of the experimental data and the relative hazards of the chemicals analyzed. The purpose of this study was to provide a measure of the potential hazards which laser generated decomposition products might pose to laser operating personnel and patients. However, conditions employed for laser cutting were meant to mimic, but not duplicate, conditions to be employed during actual surgical or dental procedures. In fact, actual surgical or dental laser operating conditions to be finally employed will be modified, if possible, to minimize by-product hazards. Thus, the laser systems will be operated at a minimum energy level, with good gas evacuation systems, to reduce the laser plume and by-product concentrations. In addition, the photoenhancing inks employed will be dispensed as measured microdrops, immediately before a laser pulse, decreasing the total amount of ink interacting with the laser beam.

With these differences between actual surgical/dental procedures and the experimental conditions utilized for this work, what is the significance of the types and amounts of the chemicals detected as health hazards for laser operating personnel and patients? Table 6 lists the NIOSH, OSHA and ACGIH permissible limits for the chemicals determined in this study.[11-13] Note that these limits pertain to allowed limits for the laser operating personnel only, and do not pertain to patients. In fact, there are no established exposure limits for patients, and such limits would be different for different operating procedures, if they did exist. Of the chemicals in this list, two deserve close attention, benzene and formaldehyde. Both have very low worker exposure limits, since they are suspect carcinogens. Both of these chemicals were found in measurable quantities in all of the smoke samples analyzed (Table 3), and this is also true for laser decomposition studies previously carried out by us.[1,3] The question is whether or not these quantities represent a true hazard, or are so small that they can be ignored. This depends on how one looks at the data. Atmospheric levels, measured in parts per million (ppm) or mg/m^3, are certainly lower than even the NIOSH limits, even if a smoke evacuator were not used, given the tiny amounts of material vaporized during a microsurgical or dental procedure, presuming the laser operator is not close enoough to the site to enhale the fumes directly. But, how about the patient? Given Ott's study of the effect of peritoneal cavity laser surgery, it may not be necessary for the patient to breath the vapors in order to suffer ill effects from them.[6] This leads to the conclusion that, despite the very small amount of material produced during these studies, a smoke evacuation system will be mandatory for these types of microsurgery or dental procedures, to protect the patient.

Chemical	OSHA Limits (ppm)	NIOSH (ppm)	ACGIH (ppm)
Formaldehyde	3; C* 5; P** 10/30 min	0.016; C 0.1, Carc***	C 0.3 Suspect Carc
Acetaldehyde	200	18, Carc	100 STEL****
Acrolein	0.1	0.1; 0.3 STEL	0.3 STEL
Crotonaldehyde	2	2	2
Valeraldehyde	---	50	50
Benzene	1; 5 STEL	0.1, C 1ppm/15 min, Suspect Carc	10, Suspect Carc
Toluene	200; C 300; P 500	100; STEL 150	50
Ethylbenzene	100	100, 125 STEL	100
o-, m-, p-Xylene	100	100; 150 STEL	100; 150 STEL

* Ceiling concentration, ** maximum permissible, instantaneous, *** Carcinogen, ****short-term (15 min) exposure limit

Table 6. Permissible hazardous chemical atmospheric limits allowed for workers

5. CONCLUSIONS

Small quantities of potentially hazardous chemicals are formed when diode and Nd:YAG lasers are used, in conjunction with a photoenhancing dye, to cut biological materials. Results indicate that the photoenhancing dyes do not contribute significantly to the by-product concentration, compared to the products formed by decomposition of the biological materials. Use of an appropriate smoke evacuation device in conjunction with this laser ablation technique is mandatory, in order to protect the patient from potential harm by these by-products.

6. ACKNOWLEDGEMENTS

This work was supported by National Institutes of Health grants 2 R44DE10687-02A1 and 2R44 GM50602-02. The authors wish to thank Mr. Gary Thieme, GMI, for assistance with the laser studies, Professor David Parker, GMI, for assistance with the laser optics, Surgimedics, the Woodlands, TX, for providing the diode laser used in this study, and American Dental Technologies, Incisive Technologies division, San Carlos, CA, for providing the Nd:YAG laser used in this study.

7. REFERENCES

1. J. M. Kokosa and M. Benedetto, "Probing plume protection problems", *J. Laser App.*, Vol. 4, pp. 39-49, 1992.

2. M. S. Baggish, B. J. Poiecsz, D. Jaret, P. Williamson and A. Refei, " Presence of human immunodeficiency virus DNA in laser smoke", *Lasers Surg. Med.*, Vol. 11, pp. 197-203, 1991.

3. J. M. Kokosa and J. Eugene, "Chemical composition of laser-tissue interaction smoke plume", *J. Laser App.*, Vol. 1, pp. 59-63, 1989.

4. R. H. Clark, J. M. Ismer, R. F. Donaldson and G. Jones II, "Gas chromatographic-light microscopic analysis of excimer laser photoablation of cardiovascular surgery: ablation products and photoacoustic spectrum of cardiovascular wall", *Cir.. Res.*, Vol 60, pp. 429-437, 1987.

5. N. P. J. Walker, J. Mathews and S. W. B. Newsom, "Possible hazards from irradiation with the carbon dioxide laser", *Lasers Surg. Med.*, Vol. 6, pp. 84-86, 1986.

6. D. Ott, " Smoke production and smoke reduction in endoscopic surgery: preliminary report", *End. Surg.* Vol. 1, pp. 230-232, 1993.

7. S. D. DeCoste, W. Forinelli, T. Flotte and R. R. Anderson, "Dye-enhanced laser welding for skin closure", *Laser Surg. Med.*, Vol. 12, pp. 25-32, 1992.

8. M. C. Oz, J. P. Johnson, S. Paranzi, R. S. Chuck, C. C. Marboe, L. S. Bass, R. Nowygrod and M. R. Treat, "Tissue soldering by use of indocyanine green dye-enhanced fibrogen with the neear infrared diode laser", *J. Vasc. Surg.*, Vol. 11, pp. 718-725, 1990.

9. D. Dimikov, L. S. Bass and M. R. Treat, "Thermal breakdown properties of indocyanine green", *Proc. SPIE*, Vol. 2395, pp. 486-489, 1995.

10. J. F. Zhou, M. P. Chin and S. A. Schafer, "Aggregation and degradation of indocyanine green", *Proc. SPIE*, Vol. 2129, pp. 495-505, 1994.

11. *First supplement to NIOSH manual of analytical methods (NMAM)*, 4th Edn., 1996.

12. *Threshold limit values for chemical substances and physical agents and biological exposure indices for 1993-1994*, ACGIH, Cincinnatti, OH, 1993.

13. *OSHA analytical methods manual*, 2nd Edn. Part 1, Organic substances, Vol. 1-4, 1990.

Laser Safety in Dentistry

Harvey Wigdor
Dental Section Chief
Ravenswood Hospital Medical Center

Wenske Laser Center
Chicago, Illinois

ABSTRACT

One of the major causes of anxiety in the dental clinic is the dental handpiece(drill). Because dentists wish to provide a method which can replace the drill there has often been a premature use of the laser in dentistry. Various lasers have been introduced into the clinic before research has shown the laser used is of clinical benefit. Any new treatment method must not compromise the health of the patient being treated. Thus a method of evaluating the clinical abilities of dentists and their understanding the limitations of the laser used must be developed. Dentists must be trained in the basic interaction of the laser on oral tissues. The training has to concentrate on the variation of the laser wavelength absorption in the different tissues of the oral cavity. Because of the differences in the optical properties of these tissues great care must be exercised by practitioners using lasers on patients.

Key Words: Laser, Dentistry, Safety

INTRODUCTION & DISCUSSION

The intent of this paper is to discuss the present status of lasers in dentistry with a brief history of where they have been. Discussion will include some concerns why we in dentistry are is such a precarious place with respect to lasers and how changes now can prevent some of the potential harm that inappropriate laser use in dentistry can bring to our patients.

The vision of lasers in dentistry began just about the time of the development of the ruby laser in the early 1960's. The researchers of that time theorized that a laser could be used to fuse the deep pits and fissures of the chewing surfaces of teeth which would reduce the incidence of decay. It was unfortunate that the heat generated by the ruby laser caused too much damage to the teeth so it was discarded as a viable method. Since the early 1960's there has been only a fleeting interest in lasers for dentistry this however changed within the last five years. In 1988 there was an introduction of a laser which was directed to only the dental market. It was a 3 watt pulsed Nd:YAG laser which was given the name American Dental Laser(ADL).

At the time of it's introduction there were very few applications and the development of applications and indications was left up to the dentist who owned the machine. This led to a flurry of anecdotal reports written by dentists who in the confines of their private offices developed a scientific network providing absolutely no basis for the use of this laser. Since there was an initial interest in lasers among dentists and

SPIE Vol. 2974 • 0277-786X/97/$10.00

ADL sold some lasers other laser manufacturers entered this market. At the present time there are no less than thirteen different kinds of lasers available to dentists marketed as dental lasers. These lasers vary in wavelength and include CO_2, Argon, Nd:YAG, Ho:YAG and just entering the marketplace is the Er:YAG lasers. Some very good research has been done with the lasers mentioned above but this research is very limited and does not provide enough information to suggest using lasers in ways advocated by some clinicians today(1,2,3,4,5,7,12,13,14,15,16,17&20). The Food and Drug Administration (FDA) has, to date, limited it's clearance to simple soft tissue applications because there has not been enough research both in the laboratory and clinically to prove safety and effectiveness beyond cleared applications.

The status of dental lasers and their safe use is based on a number of issues these include good controlled research, unbiased education of the practitioners using the lasers, continuing education requirements and possible periodic examination leading to a method of credentialling of dental laser users. These actions are necessary because of the way dental care is provided to patients. Most dentists are independent practitioners and do not have any governing body reviewing their care of patients. This is quite different from hospitals where departments of surgery review credentials of lasers users and monitor their use.

The underlying quest of all laser researchers, manufacturers and dentists is to find a laser that can replace the dental handpiece which will remove decay in a way that is less frightening. To this end a number of dental laser manufacturers have overstepped the FDA clearance process by suggesting that their laser can be used in place of a dental drill. It must be understood that to date no laser has been cleared by the FDA for dental hard tissue treatment or removal. This clearance has not been granted because the research that is needed has not been done which proves that lasers are safe and effective.

The lack of sufficient controlled research is why lasers have not been embraced by the dental community as a new method of treatment. This lack of research is also the fundamental reason why dental lasers are in the precarious place they find themselves presently. Any lecturer, practitioner, manufacturer and most importantly salesman can make a claim about a particular laser either pro or con and because the information is not fully known the claim can neither be refuted nor proven true.

This leads to another problem which is the educational process presently used to train dentists. It is essential that any educational process in laser training be unbiased and have as a goal to educate dentists in general laser use and safety and not meant to be a sales pitch to sell a laser. Most laser courses now are given by manufacturers and ultimately are intended to lead to a sale of the laser by the company giving the laser course. It would be a fantasy to believe one laser company would teach participants that maybe another laser might be better for a certain treatment and most importantly treatment with the other laser just might be in the best interest of the patient. The intent of a good educational process is to educate the users in basic information so than the users can make the decision which laser would be the best for a certain indication.

The ultimate goal should be improved treatment with lasers of our patients What follows is an outline of suggested actions that could lead to the goal stated above i.e., efficient, safe and effective use of lasers in dentistry.

Research

The basis for all laser treatment in humans must be in line with existing research that proves that the treatment is safe and effective. Indicated methods must not be based on financial gain and/or improved reputation of the user. The use of the scientific method should not be ignored by laser researchers and practitioners and all research must be scrutinized for its scientific merit. An additional intent of this research is to review the parameters of a specific lasers and find those parameters for optimal use of a specific condition. The FDA has established guidelines which are meant to protect patients and must be followed. The FDA must also be considered an advocate for the safe use of lasers. Changes in stated guidelines will be based on controlled research proving lasers are of value by the results of this research.

Education

There is a great need at present for an educational process that will inform dental practitioners of lasers use and potential use in the future. This education initially should be only didactic covering the areas of basic laser physics, laser safety and tissue effects of lasers without "hands on" training. The variability of wavelength and its effect on tissue is the essential component necessary that needs to be understood by any practitioner using a laser. It is when this information is known that a dentist can make an informed decision about the ideal treatment for a specific condition. It should also be understood that a specific treatment may not be restricted to one wavelength. Changing parameters of different wavelengths may have similar effects on tissues.

It is imperative that there is an integration of current research in any educational process, only than can the most up-to-date information be imparted on the profession.

A thorough understanding of laser basics should preclude clinical application instruction. The education process must be evaluated on a regular basis and be unbiased It should also have no ties with the laser manufacturing sector.

Credentialling of Use

1. Establishing Standards

To make sure that there is a uniform understanding of the guidelines that will regulate laser use in dentistry standards must be developed. As the knowledge expands in this field there must be flexibility to incorporate this new technology.

a. Governing Agency

To insure the safe use of lasers a body which can be either private or governmental must be developed. The intent of this agency is to provide licensing boards with the information necessary to regulate safe laser usage. This body should also add legitimacy to these standards.

b. Education Standards

Education of laser users must be uniform, with its main intent to provide an unbiased laser training of lasers users. This training should be divided into didactic and clinical components where the practitioner must show proficiency in the didactic component before progressing to the clinical training.

c. Continuing Education Standards

All laser users must be required to attend continuing education courses. With this area of clinical dentistry expanding at such a fast pace it is imperative that users maintain their proficiency on a regular basis.

All practitioners that use lasers for surgery must be keep abreast of new advances in laser research, use lasers only in FDA cleared applications and keep the interest of their patients in mind. Only when there is a concerted effort by dental researchers and practitioners to understand lasers and their potential use can patients be assured of safe and effective treatment.

BIBLIOGRAPHY

1. Stern R.H., Sognnaes, R.F., Laser Beam Effect on Dental Hard Tissues, J Dent Res 43 (Suppl. to No. 5):873, Abstract 307, 1964.

2. Lobene, R.R., Bhussry, B.R., Fine, S., Interaction of Carbon Dioxide Laser Radiation with Enamel and Dentin. J Dent Res 47:311-317, 1968.

3. Borggreven, J.M.P.M., van Dijk, J.W.E., Driessens, F.C.M., Effect of Laser irriadition on permeability of Bovine Dental Enamel. Arch Oral Biol 25:831-832, 1980.

4. Yamamoto, H., Sato, K., Prevention of Dental Caries by Acousto-optically Q-switched Nd:YAG Laser Irradiation. J Dent Res 59(2):137, 1980.

5. Hibst, R., Keller, U., Experimental Studies of the Application of the Er:YAG Laser on Dental Hard Substances: 1 Measurement of Ablation Rate. Lasers Surg Med, 9:338-344, 1989.

6. Pick, R.M., Picaro, B.C., and Silverman, C.J., The Laser Gingivectomy. The Use of the CO2 Laser for the Removal of Phenytoin Hyperplasia. J Periodontol 56(8):492-496, 1985.

7. Kuroda, S., Fowler, B.O., Compositional, Structural, and Phase Changes in-vitro Laser-Irradiated Human Tooth Enamel. Calcif Tissue Int 36:361-369, 1984.

8. Melcer, J., Chaumette, M.T., Melcer, F. Dejardin, J., Hasson, R., Merard, R., Pinaudeau, Y., Weill, R., Treatment of Dental Decay By CO2 Laser Beam : Preliminary Results. Lasers In Surgery and Medicine 4: 311-321, 1984

9. Melcer, J., Latest Treatment in Dentistry by Means of the CO2 Laser Beam. Lasers in Surgery and Medicine 6: 396-398, 1986.

10. Abt, E., Wigdor, H.A., Lobraico, R., Carlson, B, Harris, D., and Pyrcz, R.; Removal of Benign Intraoral Masses Using the CO2 Laser. JADA 115(11): 729-31, 1986.

11. Wigdor, H.A., Harris, D., Carlson, B. and Abt, E.; Dental Applications of the Laser. Newsletter of Midwest Bio-Laser Institute, 1987.

12. Wigdor, H.A.,Lobraico, R, Abt, E., Carlson, B., Harris, D. and Pyrcz R.; The Use of the CO2 Laser to Remove Dental Decay. Laser Institute of America Proceedings (ICALEO) Vol.64,153-162,1988.

13. Harris D, Wigdor, H.A., The Q-Switched Nd:YAG as a Dental Drill, Newsletter of Midwest Bio-Laser Institute, 1987.

14. Zachariasen, K., Barron, J., Boran, T.; Carbon Dioxide Laser Effects On Dental Hard Tissues. Laser Institute of America Proceedings (ICALEO) Vol.64,163-169,1988

15. Dederich D.N., Zakariasen, K.L., Tulip, J; Scanning Electron Microscopic Analysis of Canal Wall Dentin Following Nd:YAG Laser Irradiation. J of Endodontics, 10(9):428-431, 1984.

16. Pini, R., Salimbeni, R., Vannini, M., Barone, R., Laser Dentistry: A New Application of Excimer Laser in Root Canal Therapy. Lasers Surg Med, 9:352-357, 1989.

17. Wigdor, H.A.; The Use Of The HeCd And Argon Lasers To Cure Dental Composites When Compared With White Light Sources. SPIE Proceedings Vol. 1200 372-378 , 1990.

18. Dederich, D.N.; Laser/Tissue Interaction. Magazine of Alpha Omega Dental Fraternity, 84:4, 33-36, 1991

19. Willenborg G. C.; The Future of Lasers in Clinical Dentistry. Laser Institute of America Proceedings (ICALEO) Vol.64,170-183 ,1988.

20. Bahcall, J., Howard, P., Miserendino, L., Walia, H.; Preliminary Investigation of the Histological Effects of Laser Endodontic Treatment of the Periradicular Tissues in Dogs, J of Endodontics, Vol.18, No.2 47-51,1992.

21. Miserendino, L., Abt, E., Harris, D., and Wigdor, H., Recommendations For Safe and Appropriate Use of Lasers in Dentistry In The Face of Rising Concerns, J of Laser Applications, Vol 4 No.3 16-17, 1992.

22. For Safe Use of Lasers in Health Care Facilities, American National Standards Institute ANSI Z136.3-1988.

Materials and Constructions to Improve the Laser Resistance of Medical Equipment

Hans-Jochen Foth

Department of Physics, University of Kaiserslautern,
Erwin-Schrödinger-Straße, D-67663 Kaiserslautern, Germany

ABSTRACT

In laser surgery power densities of 10^3 W/cm^2 are used for tissue vaporisation or 10^6 W/cm^2 and more for photoablation. These densities are harmful to endotracheal tubes or other devices which are used in a close distance to the laser beam. The laser resistance of endotracheal tubes was measured under the exposure of various lasers in the UV, the visible and the IR wavelength range. The laser induced temperatures of the tube materials were measured by an IR camera. It is discussed which physical processes of light material interaction cause heat and how this heat deposition is compensated by cooling processes to keep the temperature rise in an acceptable range. The experimental observation can be well described by the physical properties of the materials and their composition.

Key words: Laser Safety, Laser Surgery, Endotracheal Tubes, Protection Mechanism

1 INTRODUCTION

Laser safety covers not only the risk of direct laser tissue interaction but also indirect risks which are induced when the power of the laser beam ignites burnable materials. Especially this second point is important in the field of laser surgery when tubes are placed in natural or artifical openings of the human body.

In the upper aerodigestive tract tumor resection is nowadays successfully performed with CO_2 laser beams with powers of 20 W and more. The beam is delivered by an adjustable mirror arm, where in the last step a tiny mirror brings the beam on a straight path to the area of surgery. This path has a length of appr. 40 cm. A common version for the supply of the patient with oxygen and narcotic gases is to use an endotracheal tube. Since the inner diameter of the trachea is small and the path of the laser beam quite long an accidental exposure of the tube can not be excluded. Laser induced ignition of endotracheal tubes is seen as the most serious accidence in the field of laser surgery.

2. Experimental Setup and Results

2.1 Endotracheal Tubes

Two different types of endotracheal tubes were studied in detail.

2.1.1 Compound Tube

The compound tube ("Laertubus", Rüsch, Waiblingen, Germany) is build by a tube of ivory colored rubber, with a wall thickness of 1 to 2 mm. Two channels in the thickest part of the tube wall are the two lumens for cuff inflation. At a length of 170 mm the rubber tube is surrounded by an ondulated silver foil, which itself is covered by a 0.7 mm thick layer of white polyacetate foam ("Merocel^{R} foam"). This foam was moistened before the tubes were irradiated by the laser beam. At the distal end this tube is equiped with two flexible cuffs: The inner cuff is formed of a yellow rubber membrane and the outer cuff fabricated by a white rubber membrane. The inner cuff can be inflated by air or sterile saline solution, while the outer cuff has to be inflated by sterile isotonic saline solution.

2.1.2 Metallic Tube

The metallic tube ("Laser-Flex^{TM}", Mallinckrodt, Glens Falls, Inc. USA) is fabricated by a 0.09 mm thin stainless steel ribbon to form a helically convoluted tube. At the distal end , this tube has two cuffs formed by polyvinyle chloride (PVC). The lower cuff is discribed as the sealing cuff and the upper as the barrier cuff. Both cuffs have to be infleted by sterile isotonic saline solution. The two PVC conduits for the cuffs are disposed inside the metal tube to protect them against direct laser exposure.

2.2 Experimental setup

Two different types of experimental investigations had been carried out. In a first series the resistance against laser radiation was determined, i.e. the time was measured until a serious destruction was induced. In a second series the temperature rise inside and outside of the tubes was observed by an IR camera.

2.2.1 Laser Resistance

The tubes were mounted and then exposured at the outside perpendicularly by laser radiation with wavelengths in the UV, visible and IR. The time until serious damage took place was measured by a stop watch or by photo sequencies obtained by 3 or 5 exposures per second. Further details of these experiments had been described in earlier papers [1].

2.2.2 Temperature Rise

The tubes were fixed in a stable mount and irradiated at the outside perpendicularly by the beam of a medical CO_2 laser (Sharplan 20 c). Continious radiation was used with a power up

to 20 Watts as well as pulses in the "super pulse" mode with pulse lengths of 70 µs, peak power of 250 Watt and an average power of 7 Watt. The laser beam was delivered by a mirror arm and focussed by ZnSe lens with 125 mm focus length to spot size of 0.2 mm diameter. Thus the irradiance was $6.4 \cdot 10^4$ W/cm^2 in the cw mode and $8 \cdot 10^5$ W/cm^2 in the super pulse mode. The laser system is supplied with a gas flow which is usually used to protect the optical surfaces against pollution. It was observed that this gas flow works as an additional cooling process for the endotracheal tubes; therefore measurements were carried out with and without this gas flow.

The surface temperatures was recorded free of contact by an infra red camera (AVIO 2000). The spectral window of the camera from 3 to 5.4 µm ensured that the laser radiation at the wavelength of 10.6 µm did not falsify the measurements. The emission factor was set to 0.8 for both tubes; this value was checked by temperature measurements performed by thermo coubles. To monitor the inner surface temperature of the tubes a window was cut into the tube walls. This was performed by taking care that the conduits remained unperturbed.

2.3 Experimental Results

2.3.1 Laser Resistance

The experimental results are summarized in Table 1. Due to the wide range of the applied power densities, from 10^3 - 10^{11} W/cm^2, different degrees of damages were observed. The Merocel^R foam covering of the compound tube vaporised easily at power densities of more than 600 W/cm^2, leaving an exposed silver foil. However this variation was limited to the spot of impact. When the diameter of the laser spot was small, less than or in the range of 1 mm, the foam vaporised with generation of small clouds of smoke and water dust. At power densities of 700 W/cm^2 and irradiating a larger area, which was done with the cw CO_2 laser, a small flame was observed. The lower layers of the tube were not damaged, i.e. the silver foil and the rubber were unaffected.

The damage threshold of the compound tube was found to be at $3.2 \cdot 10^6$ W/cm^2. It appeared to be undependent of the laser wavelength.

The metallic tube was destroyed in all experiments. The exposure time until a hole occurred was correlated to the power density: at 2000 W/cm^2 (cw CO_2 laser) it took 3 seconds, at 0.8 10^6 W/cm^2 (pulsed CO_2 laser) 1.3 seconds to perforate one wall and 2.3 seconds until also the second wall was perforated. In all experiments the PVC conduits inside of the metallic tube were heated up to temperatures above the point of melting or ignition. In several experiments, this destruction inside of the tube was not visible while looking at the laser induced alterations at the outside of the tubes. The full damage was observed after splitting the tube with a diamond saw.

The laser resistance of the cuffs was measured in the same way. The rubber membranes of the compound tubes were seen to be much more stable, by a factor of two to 20, than the PVC cuffs of the metallic tube. Details are described in the literature [2].

Type of Laser	Type of Tube	Number of Tests	Power Density [W/cm^2]	Observation
CO_2, cw	Compound	8	$2.6 \cdot 10^3$	no hole within 5 s*
	Metal	3	$2.5 \cdot 10^3$	flame, hole after 2 s
CO_2, pulsed	Compound	2	$1.6 \cdot 10^6$	no hole within 120 s*
	Metal	2	$0.8 \cdot 10^6$	hole after 1.3 s, penetration after 2.3 s
Holmium	Compound	14	$2 \cdot 10^6$	no hole within 60 s*
			$3.2 \cdot 10^6$	4 s: hole when fiber is pushed
	Metal	3	$2 \cdot 10^6$	hole in less than 10 s
Nd/YAG	Compound	16	$2 \cdot 10^3$	no hole within 10 s*
	Metal	6	$2 \cdot 10^3$	hole after 1 s, penetration after 4.3 s
Nd/YAG freq. doubl.	Compound	10	$28 \cdot 10^9$	no hole within 40 s
			$185 \cdot 10^9$	15 s: hole in silver foil
				30s: crater in rubber 1.3 mm deep
				60 s: crater in rubber 1.8 mm deep
			$300 \cdot 10^9$	15 s: crater in rubber 2.5 mm deep
				30 s: rubber perforated
	Metal	7	$27 \cdot 10^9$	no hole within 120 s
			$185 \cdot 10^9$	15 s: crater, no hole; 30 s: hole
			$3 \cdot 10^{11}$	15 s: crater; 30 s: hole
Ar^+	Compound	2	$1.5 \cdot 10^6$	no hole within 120 s*
	Metal	2		10s: no hole but destroyed PVC conduits
Excimer	Compound	8	$4.7 \cdot 10^9$	hole in ~ 12 s, perforation in 36 s
			$5.5 \cdot 10^9$	hole in 7 s, perforation in 20 s
	Metal	6	$4.7 \cdot 10^9$	hole in 26 s, perforation in 40 s

§Penetration: Laser beam exits at the rear side of the shaft
*Experiment was stopped after this time

Table 1: Summary of the experimental results on the laser resistance of the tubes shafts

2.3.2 Temperature Rise

Fig. 1 shows the result of the temperatures measured at the outside of the metallic and the compound tube while the tube were exposured with a laser pulse of 1 s duration and 20 W. While the temperature of the metallic tube rises up to 240 °C the measured temperature at the surface of the compound tube stood below 140 °C, which was the temperature of the cloud of water dust leaving the surface. The temperatures inside of the tubes are shown in Fig. 2. Again a 20 W pulse was used. After 5 s the exposure was stopped in case of the metallic tube, since the temperature has rised up to 280 °C. This was in clear contrast to the observation with the

compound tube where the inside temperature reached 38 °C after 20 s exposure time and stood stable at this value until the exposure was stopped after 60 s.

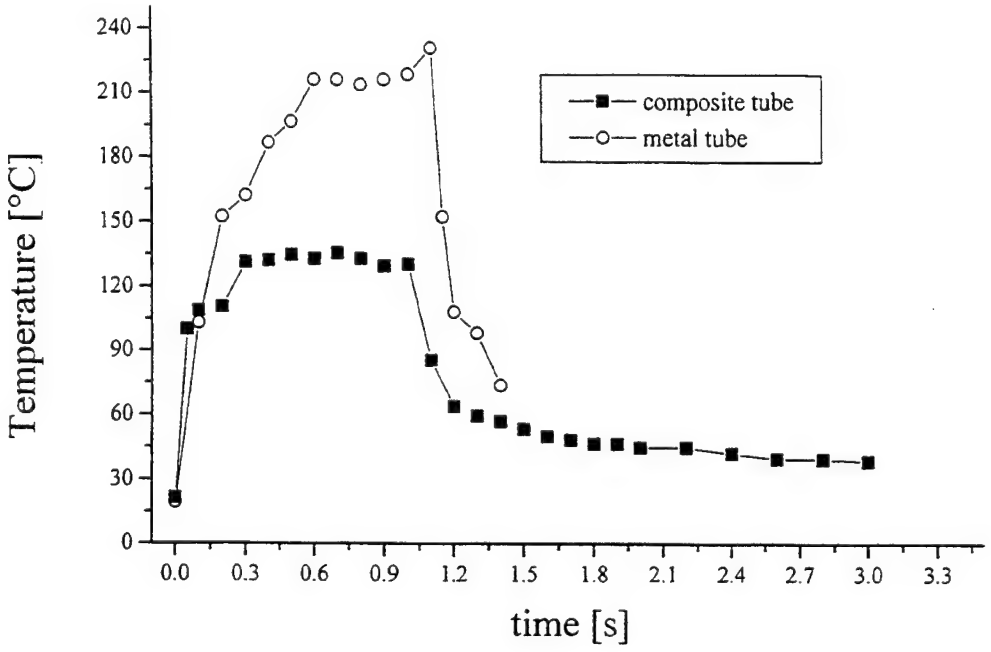

Fig. 1: Temperature rise measured inside of endotracheal tubes; CO_2 laser, 20 W, exposure time 1 s

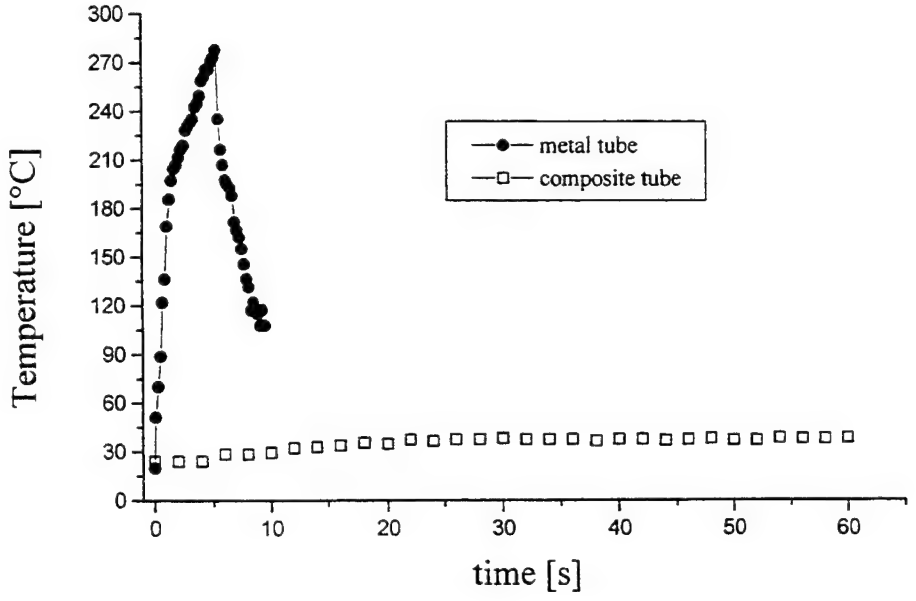

Fig. 2: Temperature rise measured inside of endotracheal tubes; CO_2 laser, 20 W, exposure time 5 s for the metallic tube and 60 s for the compound tube.

3 Discussion

Looking from a global standpoint it is not very difficult to find laser resistant materials; for example bricks are used for beam stopps for high power laser beams. However for clinical equipment, like endotracheal tubes, the demand of laser resistance is only one condition among others, like the mechanical flexibility or a smooth surface for biological acceptance or the avoidance of toxic evaporations generated by laser induced heating.

Power densities used in laser surgery range from several hundred Watts per square centimeter for coagulation up to 10^6 W/cm^2 for tissue ablation; values of the same range are used for material processing as shown in Table 1. This points out that laser power densities neccessary to induce specific laser tissue interactions are already harmfull to technical surfaces, i.e. it needs special prepared and selected materials to avoid laser induced damage.

Power Density	Laser Tissue Interaction	Material Processing
10^3 W/cm^2	Coagulation	Soldering
10^4 W/cm^2	Vaporization	Transformation Hardening
10^6 W/cm^2	Ablation	Welding
10^7 - 10^8 W/cm^2		Drilling
10^{11} W/cm^2	Disruption	Shock Hardening

Table 2: Comparison of power densities used for laser tissue interaction and material processing

As indicated in Table 2 it is not a simple task to achieve laser resistance; therefore the different processes of laser light interacting with material are described in more detail.

When a laser beam reaches a material surface,it gets reflected or scattered at the surface or transmitted into the material. Inside the material the beam gets absorbed and scattered, while a remaining part may exit the material at the opposite side.

The intensity of the incidented laser beam is indicated by I_0 the fraction of this intensity reflected or scattered at the surface is given by

$$I_R = R \cdot I_0$$

and

$$I_S = S \cdot I_0.$$

Thus this part of the intensity which is transmitted into the material is calculated to

$$I_M(0) = I_0 - I_R - I_S = (1 - R - S)\cdot I_0$$

This intensity is decreased by absorption and scattering when the beam propagates to the depth x inside of the material

$$I_M(z) = I_0(0)\cdot\exp(-\alpha\cdot x)$$

α is the coefficient of attenuation, which is the combination of scattering and absorption. For the discussion here it is unimportant by which process inside of the material the beam gets decreased. Whenever the absorption factor is larger than the scattering, the photons will get absorbed, which means, the deposition of energy into the material differs only in the spatial distribution. Assuming the material has the thickness d the totally transmitted intensity is

$$I_T = (1 - R - S)\cdot\exp(-\alpha\cdot d)\cdot I_0$$

That amount of the intensity which is absorbed in the material is calculated by combining all equations described so far

$$I_A = (1 - R - S)\cdot(1-\exp(-\alpha d))\cdot I_0$$

Since this amount of intensity heats up the material its value should be as small as possible. This can be obtained in two ways:

a) The first bracket (1 - R - S) could be very small, which means R + S should be close to 1; S close to 1 would mean a high reflexion which invoves the risk of strong uncontrolled reflexion. This has to be avoided since it may hurt surrounding tissue. Therefore the best way is to select R very small and the coefficient of scattering S close to 1.

b) The second bracket (1- exp(-ad)) should be small. Since this expression can be approximated by $\alpha\cdot d$, it is obvious that the thickness d or the attenuation coefficient α should be very small, i.e. one should select thin and transparent tubes.

Version a is followed by the construction of several kinds of endotracheal tubes. Especially metals with a rough and ondulated surface structure come close to this postulated optimum. However it can not be avoided totally that a fraction of the laser beam is transmitted into the material and finally absorbed.

In practice also Version b is limited. The CO_2 laser radiation at a wavelength of 10.6 µm is strongly absorbed in many solid polymers by excitation of vibronic bands; on the other hand a thin wall would lead to an unstable mechanical construction with the tendency to collapse or crack. Furthermore a tube with thin wall would have a small heat capacity.

Therefore one has to accept the boundary condition that laser energy is absorbed and finally transferred to the heat Q, which is calculated by the absorbed laser intensity I_A per area A and the exposure time τ,

$$I_A = \text{Absorped Power/ Area} = E \cdot \tau / A$$

The heat Q can be expressed as the product of the heat capacity c and the temperature rise ΔT

$$E = Q = c \cdot \Delta T$$

Now the question has to be answered, which is the best construction to accepted the largest amount of heat Q without destruction. There are at least two ways to achieve this goal:

a) One should use high temperature materials, i.e. materials which are mechanically and chemically stable when be heated up. In other words chemical reactions, especially with air oxygene, and phase transitions like melting or getting soft should start at high temperatures; again metals seems to fulfil this condition in the best way especially stainless steel.

b) One should use devices with a large heat capacity, which keeps ΔT small at a specific amount of heat Q

The heat capacity c is determined by the specific heat c_S of the material and the mass m_h which is heated up.

$$c = c_S \cdot m_h$$

The mass m_h is determined by the heat transport in the material. As more heat is distributed as more mass is heated up.. Heat transmission is performed by heat conduction, heat convection and radiation. While the last one is not important an important factor in the temperature range up to several 100° C, the other two factors are important. Heat conduction depends on the material, it varies from 33000 W/(cm·K) for diamond, 427 for silver, 15 -21 for stainless steel to 0.7 - 1.4 for glass. The most efficient way for heat transport is convection especially when a phase transition is involved, i.e. a liquid is vaporized at the hot side and condensated at a cooler area. Heat pipes, which are used to cool high power semiconductors are working in this way. Also the cooling mechanism of the compound tube is based on convection, here by vaporizing water which involves a heat of vaporisation of 2258 J/g. Capillary forces in the foam guide water from areas far off the laser spot to the heated spot and ensure that this area is not dehydrated. For the numbers given in table 3 only the amount of water in the surface area of 1 cm^2 was used; since the reservoir of water available for cooling is much larger the real heat capacity is much higher.

	Metallic Tube	Compound Tube
At the Surface		
Material	Stainless Steel	Moistened Foam, Silver Foil
Specific Heat Conduction	15 -21 W/(m·K)	427 W/(m·K) (silver)
Heat Capacity per 1 cm^2	0.162 J/K	0.188 J/K + 101,6 J (vaprization)
Energy for a Temperature Rise: 20° - 100° C	13 J	117 J
To the Inside		
Specific Heat Conduction	15 -21 W/(m·K)	2.2 W/(m·K) (rubber)
Thickness	0.15 mm	2 mm
Heat Conduction	1 - 1.4 10^5 W/K	1.1 10^3 W/K
Critical Temperature	160° C	400° C

Table 3: Comparison of the heat transport and the heat capacities of the metallic tube and the composite tube.

The results of this discussion are summarized in Table 4. The second column shows the optimum of all different factors, while the columns three to seven show how good these values are reached by the different constructions of endotracheal tubes. Obviously all the uncovered polymers have a low heat capacity and a low heat conduction; furthermore their absorption coefficients at the wavelength of 10.6 µm are large, they get heated up to critical temperatures in a short time by a laser power of 10 or 20 Watts. Within this group teflon (PTFE) has the highest ignition point; nevertheless it should be carefully used, since the avaporations caused by laser pyrolysis are extremely toxic.

Protecting the polymer tubes by wrapping them by metallic tapes or foils does not improve the heat capacity but brings up the risk of uncontrolled reflexions as shown in the 5th column.

Only two columns come close to the neccessary conditions. The metallic tube is build up by thermally high resistant material with a melting point at 1500° C. A weak point is the low heat conduction und heat capacity which leads to a hot spot at the location of impact. These critical points are much better solved in the construction of the compound tube. The heat conduction of silver is 20 times larger than that of stainless steel and the cooling due to the moistened foam results in a high amount of energy which is neccessary to heat 1 cm^2 from 20° C to above of 100° C.: 117 J, which is 9 times larger than in the case of the stainless steel tube.

A critical point is the transmission of heat to the inside of the tube. A construction by a homogenious material gives an isotropic propagation of heat; heat conduction at the surface is

the same as to inner part of the tube. The inner part of the composite tube consists of rubber which has a low heat conduction. With the thickness of the wall of 2 mm the heat conduction is $1.1 \cdot 10^3$ W/K which is 100 times lower than the heat conduction in the stainless steel tube. The differences of these two in heat capacity and heat conduction explains the temperature rises observed at inner surface. While the temperature inside of the stainless steel tube rised up to several hundred degree Celcius within seconds, the temperature inside of the composite tube stood constant at 38° C during the exposure of one minute.

Another serious point is the inner construction of the stainless steel tube. The conduits for the cuffs are guided inside the tube to protect against direct laser exposure, which works suffiently unless the tube wall got heated up. A critical temperature of the metallic tube is reached at least at 160° C when PVC gets soft. At higher temperatures the PVC conduits start to desintegrate and even ignite. Critical temperatures of the rubber material of the composite tube are at 400° C where after 30 s rubber shows first thermal destruction. Not only this value is significantly higher than 160° C, furthermore the cooling mechanism by evaporation of water keeps the system on a much lower temperature level.

Item	Optimum	PVC	Teflon	Poly-ethylene	PVC + Foil	Metallic Tube	Compound Tube
Toxic Evaporations	small	-	- -	+	-	++ (outside) - (inside)	++
Reflexions	small	+	+	+	- -	**0**	+
Scattering	large	**0**	**0**	**0**	- -	+	+
Absorption $\alpha \cdot d$	small	-	-	- -	**0**	+	+
Critical Temperature	large	- -	+	- -	-	+	+ +
Heat Capacity	large	- -	- -	- -	-	-	+ +
Heat Conductivity: at the surface to the inside	large small	- - + +	- - + +	- - + +	+ +	- - - -	+ + + +

Table 4: Conditions which should be fulfilled by a laser resistant endotracheal tube in comparison to the properties various polymers and tube constructions

4 SUMMARY

It had been pointed out which mechanisms lead to laser induced heating and which physical processes can be used to avoid heating of delicate parts. The points had been discussed at the example of the laser resistance of endotracheal tubes. While scattering at the surface is the best way restrain absorption of laser energy in the material, the temperature rise is determined by the heat capacity and the heat transport in the material. Herein an anisotropic heat conduction protects the device much better than an isotropic conduction. The heat should be distributed on the surface and not transmitted to the inside, especially when parts are located inside which are sensitive against higher temperatures. These are the reasons why the compound tube has a much higher laser resistance than the metallic tube.

ACKNOWLEDGEMENT

The author likes to thank Dirk Meyer for the support by measuring the temperatures and Prof. Weiß (Dept. of Electric Engineering) for borrowing the IR camera.

REFERENCES

[1] H.-J. Foth, D. Meyer, A. Baker-Schreyer, W. Bergler, K. Hörmann and J. Ungemach, Endotracheal Tubes for Laser Surgery: Temperature Rise and Clinical Experiences, in Brown at al. Medical Applications of Lasers III, SPIE 2623: 522 - 529 (1996)

[2] H.-J. Foth, Laser Resitance of Endotracheal Tubes, Laser und Optoelektronik 26(6): 53 - 60 (1994)

Addendum

The following papers were announced for publication in this proceedings but have been withdrawn or are unavailable.

[2974-01] **Diagnostic criteria for laser-induced visual impairment**
B. E. Stuck, H. Zwick, D. K. Scales, J. W. Ness, Walter Reed Army Institute of Research; M. Belkin, Tel Aviv Univ. Goldschleger Eye Research Institute (Israel)

[2974-15] **Visual function recovery based on infrared-range laser use**
I. N. Ushkova, N. Y. Mal'kova, L. A. Pokeovskaja, Institute of Industrial Hygiene and Occupational Diseases (Russia); Yu. D. Berezin, S.I. Vavilov State Optical Institute (Russia)

[2974-31] **Update on regulations, standards, and practice guidelines on management of airborne contaminants resulting from laser and electrosurgical procedures**
P. J. Smalley,Technology Concepts International

Author Index